Gold uptake and tolerance in Arabidopsis

Andrew Taylor

PhD Thesis

University of York, Department of Biology

September 2011

Abstract

Gold is a precious metal with a variety of industrial uses. The gold mining process is often incomplete, and discarded mine tailings contain quantities of gold uneconomical for conventional extraction. Previous work has indicated the potential to use plants for gold phytoextraction from these sites. Additionally, it has been demonstrated that gold nanoparticles can form within the tissues of live plants. These small particles have many uses in catalysis and medical applications but are expensive to synthesise chemically. Plants have the potential to be used as a low cost method of gold nanoparticle manufacture.

Whilst gold uptake and nanoparticle formation in plants has been studied, little research has investigated mechanisms of gold uptake. The aims of this study were therefore to characterise gold uptake and nanoparticle formation in the model plant species *Arabidopsis thaliana* and subsequently investigate the transcriptional response to gold to identify mechanisms of uptake and tolerance.

A number of approaches were used to investigate the gold tolerance and uptake by Arabidopsis. Growth studies determined that gold is toxic to plants and inhibits plant growth. Methods were developed to investigate and measure gold uptake in a variety of conditions. Arabidopsis was found to remove gold from soil and contained similar concentrations to those in previously tested species. Gold uptake from liquid media was also investigated. These studies determined that Arabidopsis contained significant quantities of gold in the root tissues, some of which was translocated to aerial tissues.

Electron microscopy analysis showed that gold nanoparticles form in the roots of Arabidopsis plants in a variety of growth conditions. However, gold nanoparticles were never observed in the aerial tissues of Arabidopsis but were found in the aerial tissues of alfalfa, demonstrating a difference between these two species. Gold nanoparticles were not taken up by Arabidopsis seedlings, an interesting observation because of the potential impacts of increasing numbers of nanoparticles present in the environment.

A microarray study of the transcriptional response of Arabidopsis to gold identified approximately 800 genes upregulated more than two-fold in the presence of gold. Many of these are normally upregulated in a general response

to stress including cytochromes P450 and glucosyl transferases, further demonstrating the toxicity of gold to plants. Over 800 genes were downregulated more than two-fold in response to gold, including various aquaporins and transition metal transporters. Many of the most downregulated genes are controlled by the FIT1 transcription factor. FIT1 is involved in the Arabidopsis response to iron, suggesting that gold interacts in this pathway.

COPT2 (encoding a copper transporter) was one of the most downregulated genes in the presence of gold (24-fold). The other five members of the *COPT* family did not have altered expression in the presence of gold. A putative Arabidopsis *COPT2* knockout mutant was obtained and tested for increased gold tolerance. No obvious phenotypic differences were observed when *copt2-1* and wild-type seedlings were compared, suggesting that COPT2 is not involved in plant gold tolerance.

This work is the first investigation of the transcriptional response of plants to gold and indicates targets to further study for involvement in gold uptake and tolerance.

Table of Contents

List of Figures

List of Tables

Acknowledgements

I would like to thank the following people for all of their help and support during my PhD:

Professor Neil Bruce, for his supervision, advice and direction. His group has been an enjoyable place to work.

Dr Liz Rylott for all the help, constructive advice and time given to discuss my research.

Dr Chris Anderson at Massey University, a collaborator who gave guidance and constructive discussion whilst completing this work.

The Burgess family, whose kind sponsorship has provided me with financial support.

I would also like to thank:

The Bruce group, who were always there to provide help and advice. Special thanks go to Chong, Federico, Helen, Florian, Will, Hazel, Joe and Astrid.

David Lindsey and Helen Burrell in the Department of Chemistry for use of their equipment.

Professors Pratibha Gai and Edward Boyes in the Nanocentre for assistance with chemical analysis of my electron microscopy.

Staff in the Technology Facility. Naveed Aziz and Celina Whalley for processing my microarray samples and data. Meg Stark and Karen Hodgkinson for their time and effort in preparing electron micrographs.

My family and friends for supporting me and distracting me from science whenever it was needed.

And Louise Ridley.

Author’s declaration

I declare that I am the sole author of this work and that it is original except where indicated by reference in the text. No part of this work has been submitted for any other degree to any other institution.

Chapter 1 Introduction

1.1 Gold

Gold is a d-block transition element and is the least reactive metal in the periodic table (Massey et al. 1973); oxygen does not react with gold, even at high temperatures. This makes it suitable for the wide range of uses described below. Additionally, gold is resistant to acids: aqua regia, a mix of three parts hydrochloric acid to one part nitric acid, is the only acid known to dissolve gold. Gold is also soluble in some cyanide solutions, a property which is important in the mining process described below. The chemical properties of gold are outlined in Table 1.1.

Table 1.1 Properties of gold

Name	Gold
Symbol	Au
Atomic number	79
Atomic mass	196.97
Standard state	Solid at 298 K
Melting point	1 337 K
Boiling point	3 129 K
Density	19 300 kg/m3

Historical evidence shows that gold has been in use by humans for at least the last 5000 years and as such is likely to have been the first metal to be utilised by humans (Massey et al. 1973). Gold has a high monetary value and is widely traded on international markets with a large amount of gold stored in reserves around the world, mainly by the world's largest economies. These high prices are maintained by its rarity. To date approximately 145 000 tonnes have been mined globally (Anderson 2004), an amount which would fill a volume smaller than 8 000 m^3. The 2 500 tonnes mined annually is tiny (0.002%) compared to the amount of steel produced by the US alone (125 000 000 tonnes per year).

The low chemical reactivity of gold and some of its other properties make it an element with many applications (Figure 1.1). The precious nature, colour and malleability of gold mean that the main use of gold is jewellery. In addition to this, a large amount of gold is used for medical purposes. As a non-corrosive and

malleable metal, gold finds use in dentistry, with a large proportion of gold mined every year used for this purpose. The high conductivity of gold and its non-corrosive nature means that it is also used in many electrical components. Further to this, gold is used in nanoparticle form. These particles, which are between 1 and 100 nm in at least two dimensions (Aitken et al. 2006), have various uses including catalysis and in medical applications. The uses of gold nanoparticles are further discussed in Section 1.5.2.

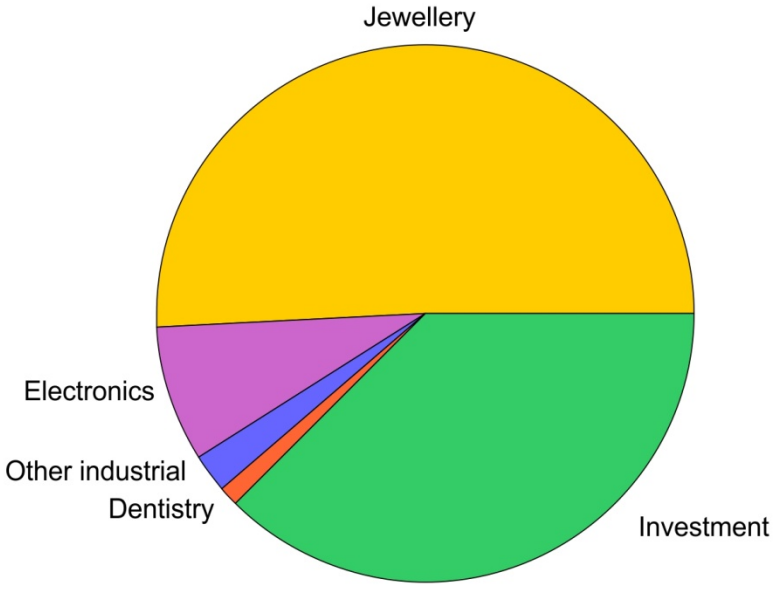

Figure 1.1 Gold use
The five main uses of gold in 2010 as a proportion of the total gold demand. Data from the World Gold Council.

Gold has low average concentration within the Earth's crust of approximately 2 ng/g (Pitcairn et al. 2006), and is primarily found at high concentrations in specific locations. Various methods to mine gold exist, however, the main method used currently is the cyanidation process (Anderson 2004). Here, crushed ore is treated with cyanide compounds to dissolve the gold using the reaction outlined in Figure 1.2. This dissolved gold is subsequently precipitated prior to purification. This is an expensive process and is also harmful to the environment; large amounts of toxic waste remain at the end of the process (Korte et al. 2000).

$$4Au + 8CN^- + O_2 + 2H_2O \longrightarrow 4[Au(CN)_2]^- + 4OH^-$$

Figure 1.2 The dissolution of gold by cyanide

1.2 Plant transition metal transport

1.2.1 Plants and metals

Metals play an important role in plant nutrition and many are essential plant nutrients. Potassium, magnesium and calcium are macronutrients and higher amounts are required in comparison to other essential metals (Marschner 1995). Copper, iron, manganese, molybdenum, nickel and zinc are all determined to be essential micronutrients for higher plants (Hänsch and Mendel 2009). Additionally, aluminium, cobalt and sodium are beneficial to plant growth and are thought to be essential for some, but not all, species (Pilon-Smits et al. 2009).

Metals have a wide range of functions in plants. These roles include structural stabilisation by calcium (Demarty et al. 1984), the activation of a number of enzymes by potassium (Suelter 1970) and the possible role of cobalt in herbivore defence (Ohnishi et al. 1990). Transition metals are often essential for protein function and are involved in many cellular processes. Copper and iron are required in a range of important systems and are essential for respiration, photosynthesis and nitrogen assimilation and metabolism (reviewed by Hänsch and Mendel (2009)). These two metals are essential for the correct function of a number of proteins. Examples include the use of iron in cytochromes P450, aldehyde oxidases and ferredoxins whereas copper is an essential component in a number of oxidases and in plastocyanins.

The essential nature of these metals means that when these metals are absent, growth is reduced and deficiency symptoms occur (Marschner 1995). Conversely, toxicity can occur when metals are present at high concentrations (Schutzendubel and Polle 2002). It is therefore essential that plants have mechanisms to take up these metals and also detoxify them when in excess.

1.2.2 Transition metal transporters in plants

Due to the importance of transition metals in plants, the transition metal transporters have been extensively studied. There are six main families of transition metal transporters in Arabidopsis: Natural resistance associated macrophage proteins (NRAMP), ZRT, IRT-like proteins (ZIP), heavy metal ATPases (HMAs), yellow stripe1-like (YSL) proteins, cation diffusion facilitator (CDF) and copper transport (COPT) proteins. These families have a varied number of members and varying numbers of transmembrane domains and are described in greater detail in Chapter 4 and Table 1.2.

Table 1.2 The main transition metal transporter families in Arabidopsis

Transporter Family	Numbers in Arabidopsis thaliana	Number of transmembrane domains
ZIP	15	8
NRAMP	6	12
HMA	8	8
YSL	8	12-15
CDF	12	6
COPT	6	3

Although individual proteins from within these families of metal transporters have been characterised, knowledge is limited for many of these genes. Substrate specificities are not known for many of these proteins, neither are their cellular locations. However, from those that have been characterised, it is evident that there is diversity of function, metal specificity and cellular location for these proteins, both within, and between families. It is also possible that some of the proteins are functionally redundant. Details of the characterisation of some of these transporters are reviewed by Colangelo and Guerinot (2006) and Krämer et al. (2007) and are described in more detail in Chapter 4.

Of the six families described here, four are described as metal uptake proteins, and two are metal efflux proteins as reviewed by Colangelo and Guerinot (2006). The HMA and CDF families are involved in metal efflux from the cytoplasm. These proteins are important in the movement of metals into organelles including the chloroplast, xylem and vacuole. The NRAMP, ZIP, COPT and YSL proteins are all involved in uptake into the cytoplasm. This includes the transport of metals into the roots from external sources, across plasma membranes, or into the cytoplasm from organelles.

1.2.3 Metal hyperaccumulation

Metal hyperaccumulators are plants which can accumulate metals at concentrations orders of magnitude higher than those in non-hyperaccumulating plants. These were first defined as plants which contained more than 1 000 µg/g nickel (dry weight) (Brooks et al. 1977). Since this, hyperaccumulators have been identified for a number of metals (as well as the non-metals arsenic and selenium). The current accepted concentrations of different metals at which plants are defined as hyperaccumulators are outlined in Table 1.3. So far, it has been determined that there at least 500 known metal hyperaccumulator species which belong to a wide range of families (Table 1.3) (McGrath and Zhao 2003; Sheoran et al. 2009). Most hyperaccumulators identified to date are nickel hyperaccumulators.

Two of the most studied metal hyperaccumulators are *Thlaspi (Noccaea) caerulescens* and *Arabidopsis halleri*. These are both examples of zinc hyperaccumulators and part of the reason for the research in these organisms is that they are closely related to *Arabidopsis thaliana* which is used extensively as a model plant species for molecular genetic studies. Both *T. caerulescens* and *A. halleri* have therefore been used to investigate the molecular mechanisms of metal hyperaccumulation by comparison with *A. thaliana* (Section 1.2.4).

Table 1.3 Number of metal hyperaccumulators
The number of plant species known to hyperaccumulate different metals, and the concentration of each metal a plant is required to contain to be classified as a hyperaccumulator. For those with the number of hyperaccumulators classed as n/a, metal solubilisation is required for accumulation to occur. Table adapted from (Sheoran et al. 2009).

Element	Number of known hyperaccumulators	Lower limit of hyperaccumulation (mg/kg)
Arsenic	5	1000
Cadmium	2	100
Cobalt	30	1000
Copper	34	1000
Gold	n/a	1
Lead	n/a	1000
Manganese	11	10,000
Nickel	320	1000
Selenium	20	100
Silver	n/a	1
Thallium	1	100
Uranium	n/a	1000
Zinc	16	10,000

Hypotheses as to why plants hyperaccumulate metals include increased metal tolerance, drought resistance and the possibility that the increased uptake has no benefit. However, increased resistance to herbivory is a hypothesis which is gaining support although with varied results, as reviewed by Boyd (2007). Some studies have shown that herbivores often choose ‘low metal’ over ‘high metal’ plants to eat (Jiang et al. 2005; Jhee et al. 2006). Additionally herbivores feeding on ‘high metal’ plants can have reduced fitness (Behmer et al. 2005; Coleman et al. 2005). Conversely, it has been demonstrated that increased metal content could promote tolerance to herbivory, rather than defending against it (Palomino et al. 2007). It is therefore possible that high metal concentrations promote herbivory tolerance alongside reducing herbivore fitness.

1.2.4 Molecular mechanisms of metal hyperaccumulation

Genetic techniques have allowed the study of the molecular mechanisms of metal hyperaccumulation, and many of the metal transport proteins described above have been putatively shown to be involved in both increased uptake, and increased tolerance. Crossing hyperaccumulating and non-hyperaccumulating plants that are closely related has demonstrated that tolerance and hyperaccumulation are independent with different genes responsible for each trait (Macnair et al. 1999).

Microarray technology has been successfully employed to compare the model plant species, *A. thaliana*, with a closely related zinc hyperaccumulator, *A. halleri* (Becher et al. 2004; Weber et al. 2004; Chiang et al. 2006). Amongst those genes with higher expression in *A. halleri* than *A. thaliana* were genes closely related to *A. thaliana* ZIP, HMA, NRAMP and CDF genes. These genes encode metal transporters and as such are likely to be at least partly responsible for zinc hyperaccumulation. Further to this, NAS3 (a nicotianamine synthase) was more highly expressed in *A. halleri* (Becher et al. 2004). Nicotianamine synthase protein levels were also found to be high in *A. halleri* roots (Weber et al. 2004). Nicotiamine is a metal chelator and is thought to be important in long distance metal transport (Takahashi et al. 2003) and so is also likely to be involved in zinc hyperaccumulation.

T. caerulescens has also been investigated using microarray technology to identify mechanisms of metal hyperaccumulation and compared to both *A. thaliana* and non hyperaccumulating *Thlaspi arvense* (Hammond et al. 2006; Van de Mortel et al. 2006). These studies found higher expression of metal transporters in *T. caerulescens*. These results are similar to those of *A. halleri*, in that members of similar groups are more highly expressed in the hyperaccumulator than the non-hyperaccumulator, also suggesting that multiple metal transporters are involved in hyperaccumulation. As with *A. halleri, NAS* genes were highly expressed in *T. caerulescens* compared to the non hyperaccumulator, suggesting again, that increasing metal mobility is partly responsible for hyperaccumulating ability.

1.2.5 Engineering metal uptake and tolerance

Knowledge of the molecular mechanisms of metal uptake and hyperaccumulation led to the idea that hyperaccumulation and metal tolerance can be engineered in plants. Increasing the expression of metal transporters has been shown to increase both metal uptake and tolerance. Overexpression of NRAMP1 in *A. thaliana* increased tolerance to high iron concentrations (Curie et al. 2000) and overexpression of the zinc transporter MTP1, increased zinc tolerance and uptake (van der Zaal et al. 1999). Changing the protein sequence of the iron transporter IRT1 altered substrate specificity (Rogers et al. 2000). IRT1 has a broad specificity, and iron and manganese transport were inhibited completely by alterations.

Genes other than metal transporters can also be overexpressed to increase uptake and tolerance to metals. Examples of this include metallothioneins, which have high affinity to metal ions. These proteins have been overexpressed in plant species to increase cadmium tolerance and uptake (Misra and Gedamu 1989; Pan et al. 1994; Hasegawa et al. 1997). Additionally, phytochelatins, which play an important role in metal tolerance, have been overexpressed in several studies, including in tobacco (Gisbert et al. 2003). These plants had increased tolerance to the presence of lead and cadmium, and accumulated higher concentrations of these metals.

Metal uptake and tolerance can be increased by introducing genes from other species with important functions. The first example of this technique was the introduction of the *merA* gene into *A. thaliana* (Rugh et al. 1996). This mercuric iron reductase increased plant tolerance to mercury ions, by reducing the ions into less toxic metallic mercury. Initial studies using these plants found that expression of *merA* increased tolerance to growth in the presence of gold. Methylmercury tolerance was also increased by the introduction of *merB*, an organomercurial lyase which catalyses the conversion of methylmercury to mercury ions, in addition to *merA* (Bizily et al. 2000). The plants expressing both of these genes were able to grow on higher methylmercury concentrations and accumulate more within the plant tissues. Tolerance and uptake of lead and cadmium have both been increased, by expressing the yeast protein YCF1 in *A. thaliana* (Song et al. 2003). This protein transports the metal into the vacuole, thereby detoxifying it. Further to this, arsenic tolerance and hyperaccumulation

have been engineered in *A. thaliana*. Plants coexpressing the *E. coli* genes ArsC (arsenic reductase) and γ-ECS (γ-glutamylcysteine synthetase) showed increased tolerance to arsenic and accumulated more arsenic than wild-type plants (Dhankher et al. 2002). ArsC reduces arsenic to arsenite, which can then be trapped in complexes with γ-glutamylcysteine, thus increasing arsenic resistance (Dhankher et al. 2002).

1.3 Metal phytoremediation

Phytoremediation is the use of plants to remove pollutants from the environment. This is a technique that can be used to remediate both organic and inorganic pollutants. There are four main strategies by which phytoremediation can be carried out: stabilisation, extraction, volatilization and degradation (Pilon-Smits 2005). For the purposes of this work, only phytoextraction is discussed below.

1.3.1 Metal phytoextraction

Phytoextraction is the use of plants to extract contaminants from the soil and isolate them in the plant tissues, so that they can be removed from the environment when the plants are harvested. This technique has the potential to be used for the phytoremediation of metal contaminated areas, or used for phytomining. There are two strategies for phytoextraction of metals from soils. The first is to use hyperaccumulator species to naturally extract the metal. The second is to induce metal uptake chemically through increasing the availability of the metal to the plants, and this technique can be employed using hyperaccumulating or non-hyperaccumulating species.

The use of hyperaccumulators has been largely discussed for the phytoextraction of nickel. *Berkheya coddii* and *Alyssum bertolonii* are two species which have been studied to assess their potential for nickel phytoextraction (Robinson et al. 1997a; Robinson et al. 1997b; Keeling et al. 2003; Li et al. 2003). These species were found to be effective at accumulating the metal and produced enough biomass for remediation of nickel to be economically viable. *Berkheya coddii* has also been used to investigate the uptake of palladium and platinum at the same time as nickel, although plant concentrations of palladium and platinum were low, suggesting that phytoextraction of these would not be commercially viable (Nemutandani et al. 2006).

Cobalt phytoextraction has been investigated using similar species to those used to study nickel phytoextraction. Cobalt can be taken up for phytoextraction using nickel hyperaccumulators from the *Alyssum* genus, *Nyssa sylvatica* and *B. coddii* (Malik et al. 2000; Keeling et al. 2003). Field trials using *B. coddii* found that it could be used for phytoextraction of nickel and cobalt. However, when both metals were present, the metal concentration in the plant decreased (Keeling et

al. 2003). Further to this, it has been demonstrated that nickel and cobalt can be successfully coextracted by *Alyssum* species (Li et al. 2003).

The ability of the cadmium hyperaccumulators in the genus *Thlaspi* (specifically *Thlaspi caerulescens*) has been investigated for potential to phytoextract this metal from contaminated soils (Lombi et al. 2000; Schwartz et al. 2003). However, the low biomass, and poor agricultural traits of *Thlaspi* species can limit the commercial potential of these species. Cadmium phytoextraction has therefore also been investigated in non-hyperaccumulating species (rice, soybean and maize) because of the high biomass, improved agricultural characteristics and ease of harvesting (Murakami et al. 2007). The coextraction of cadmium and zinc has been investigated using *T. caerulescens* and *Arabidopsis halleri* with *T. caerulescens* able to accumulate more cadmium than zinc (Brown et al. 1995; Hammer and Keller 2003; McGrath et al. 2006).

Chemically induced phytoextraction has been studied for lead. The soil solubility of lead is low, and although some hyperaccumulators of lead have been reported (Baker et al. 2000), lead availability can be increased by the addition of chemicals. The application of chelating agents such as EDTA (and related compounds), as well as citrate, were shown to increase both metal uptake and root to shoot translocation (Blaylock et al. 1997; Huang et al. 1997; Vassil et al. 1998). Further to these studies, the uptake by plants of other non-essential metals has been enhanced. Examples include caesium, cadmium, gold and uranium (Anderson et al. 1998; Huang et al. 1998; Lasat et al. 1998; Lombi et al. 2001). Studies have also focused on using chemicals to increase the uptake of essential metals and those which have hyperaccumulators. These include, copper, zinc and nickel (Lombi et al. 2001; Chiu et al. 2005; Meers et al. 2005). Zinc, copper and cadmium accumulation were increased in various non-hyperaccumulating species using EDTA, nitrilotriacetate and sulfur (Kayser et al. 2000; Lombi et al. 2001). This accumulation was compared to uptake by a hyperaccumulator of these metals and was found to be less effective. This therefore suggests that phytoextraction using hyperaccumulators (if they exist) is preferential to induced hyperaccumulation for both metal concentration in the plant and because chemical treatment is not required. Using chemicals to solubilise metals leads to increased metal run off, which causes environmental damage and if there is increased metal content in water supplies, health problems (Lombi et al. 2001).

1.3.2 Phytomining

Phytomining is a form of phytoextraction but uses the technique to extract metals in order to harvest them for commercial gain, rather than for environmental cleanup. However, these two aims are not mutually exclusive. It is thought that nickel, thallium, cobalt and gold have the potential to be phytomined (Robinson et al. 1997a; Anderson et al. 1998; Robinson et al. 1999; LaCoste et al. 2001; Sheoran et al. 2009). The gold mining process (described in Section 1.1) is often incomplete and, as such, tailings contain gold at low concentrations which are uneconomical to be extracted conventionally at current gold prices (Sheoran et al. 2009). Due to the increasing price of gold, novel methods of extracting the gold in discarded tailings are becoming more attractive. A large number of natural hyperaccumulators of nickel and cobalt have been identified (Section 1.2.3). However, as there are no known natural hyperaccumulators of gold and only one identified for thallium (*Iberis intermedia*), chemical induction of hyperaccumulation is required for the hyperaccumulation of these metals. In addition to these four metals, the potential of silver phytomining has been discussed (Sheoran et al. 2009), however, little research has looked at silver uptake for phytomining purposes, and it is likely to require chemical induction.

The first experiments to determine whether gold uptake using plants could be economically viable were carried out using *Brassica juncea* (Anderson et al. 1998). Although work has been carried out studying gold uptake in plants without the use of chemicals (Section 1.4.2), studies concentrating on the phytomining of gold have involved the use of chemicals to solubilise the gold in the growth substrate and make it available for plants to take up (Section 1.4.1). Initial studies demonstrated that the gold concentration within plant material would have to be close to 17 µg/g for the process to become economically viable with the gold price at the time (Anderson et al. 1998; Anderson et al. 1999). In the time since these initial studies were carried out, the price of gold has increased approximately five-fold, making gold phytomining a more favourable prospect.

Factors which influence the effectiveness of gold phytomining include the gold concentration in the substrate, which can have a marked effect on uptake along with other substrate properties including pH and the chemical used to solubilise the gold. Unsurprisingly, recent theoretical work suggests that quick growing, high biomass species would be the most economically advantageous (Harris et

al. 2009). Additionally, it has been suggested that plant gold concentrations around 3 µg/g (dry weight) could be high enough to generate around £600 of gold per hectare (Sheoran et al. 2009).

1.4 Gold uptake in plants

There are two categories of studies into gold uptake in plants. In the first of these, chemicals were used to solubilise gold and induce gold uptake. The focus of these studies was to quantify gold uptake. Those in the second category were carried out without chemical solubilisation of gold and mainly focus on the formation of gold nanoparticles within the plant tissues.

1.4.1 Chemically induced gold uptake

The studies described in this section were carried out with the aim of quantifying gold uptake from both natural and artificial gold ores. These experiments were carried out using a variety of plants grown in different environmental conditions and using different chemicals to solubilise the gold. A summary of these data and experimental methods is presented in Table 1.4.

Gold solubilisation to facilitate uptake was first described using *Brassica juncea* grown in a variety of gold ores using ammonium thiocyanate to solubilise the gold (Anderson et al. 1998). A maximum of 19.34 µg/g (dry weight) of gold was measured, demonstrating higher gold concentrations than were in the substrate (3.45 µg/kg). Further to this, it has been demonstrated that ammonium thiosulfate, sodium thiocyanate, cyanide, sodium or potassium cyanide are also able to induce gold accumulation (see Figure 1.3 and Table 1.4). Unsurprisingly, increasing the concentration of these compounds increases gold uptake due to increased gold availability (Piccinin et al. 2007). Using these methods, gold accumulation has also been described in a wide range of species including *Zea mays*, *Berkheya coddii,* carrots, red beet, onion, radish and a range of plant species native to Australia (see Table 1.4).

A) Reaction of gold with cyanide

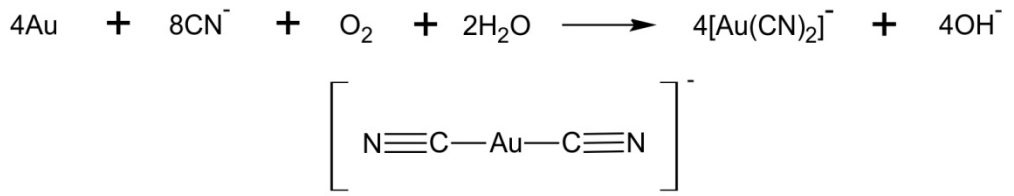

B) Reaction of gold with thiocyanate

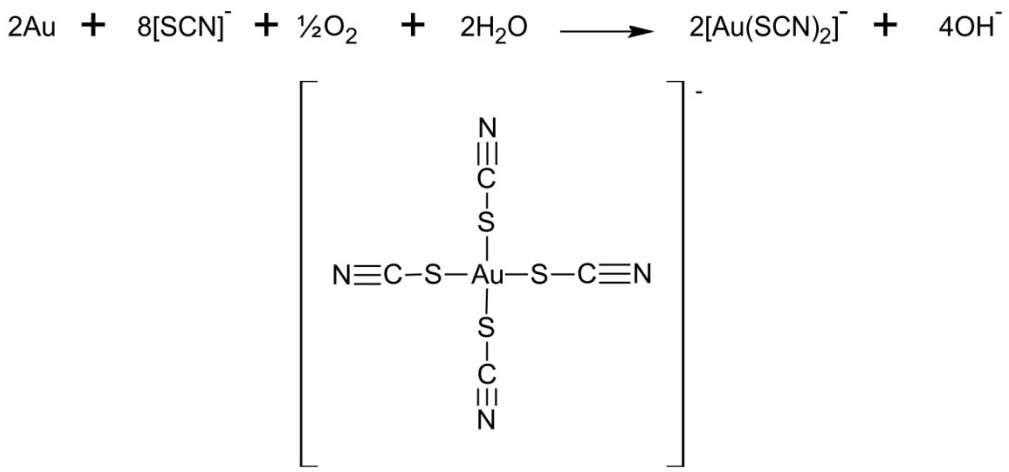

C) Reaction of gold with thiosulfate

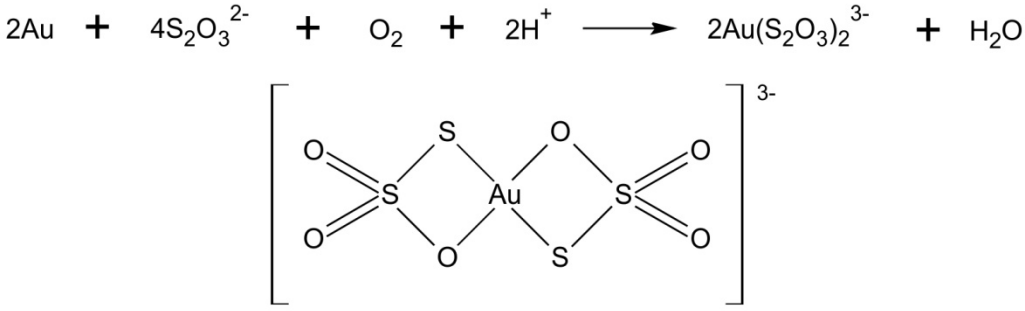

Figure 1.3 Chemicals able to induce gold accumulation and their reactions with gold

The reactions of gold with A) cyanide, B) thiocyanate, and C) thiosulfate. The resulting gold complex is indicated.

The data outlined in Table 1.4 show large variation in the gold concentrations accumulated by different plants. In part, this could be due to the substrate gold concentration and also in part to the concentration of chemicals used to increase gold solubility. However, even when experimental conditions are controlled, species differences suggest that plant physiology is important in gold uptake. In some cases, plant gold concentrations were comparable to the substrate

concentration suggesting equilibrium between the substrate and plant. In other examples, there was more gold in the plants than in the substrate (approximately 50 times in some cases).

Table 1.4 Summary of gold uptake experiments

Concentrations of gold (mg/kg dry weight) taken up from ores of different concentrations by various different plant species. References refer to: 1. Anderson et al. (1998), 2. Anderson et al. (1999), 3. Msuya et al. (2000), 4. Lamb et al. (2001), 5. Anderson et al. (2005b), 6. Piccinin et al. (2007), 7. Marshall et al. (2007), 8. Haverkamp et al. (2007).

Plant	Ore concentration (mg/kg)	Chemical	Plant concentration (mg/kg)	Ref
Brassica juncea	3.45	Ammonium thiocyanate	9-19.34	1, 2
Chicory	0.56	Ammonium thiocyanate	0.07-1.19	1, 2
Impatiens sp.	3.45	Ammonium thiocyanate	3.09	1, 2
Arrhenatherum elatius	3.45	Ammonium thiocyanate	0.07-1.43	1, 2
Brassica juncea	5	Ammonium thiocyanate	2.13-57.32	1, 2
Carrot tops	3.8	Ammonium thiocyanate	3.16	3
Carrot roots	3.8	Ammonium thiocyanate	48.3	3
Onion tops	3.8	Ammonium thiocyanate	12	3
Onion roots	3.8	Ammonium thiocyanate	13.8	3
Red beet tops	3.8	Ammonium thiocyanate	6.5	3
Red beet roots	3.8	Ammonium thiocyanate	5	3
Salad radish tops	3.8	Ammonium thiocyanate	10.6	3
Salad radish roots	3.8	Ammonium thiocyanate	113	3
Oriental radish tops	3.8	Ammonium thiocyanate	5	3
Oriental Radish roots	3.8	Ammonium thiocyanate	102	3
Carrot tops	3.8	Ammonium thiosulfate	12.9	3
Carrot roots	3.8	Ammonium thiosulfate	89	3
Onion tops	3.8	Ammonium thiosulfate	21.5	3
Onion roots	3.8	Ammonium thiosulfate	2.6	3
Red beet tops	3.8	Ammonium thiosulfate	4.1	3
Red beet roots	3.8	Ammonium thiosulfate	3.2	3
Brassica juncea leaves	5	Potassium cyanide	326	4
Brassica juncea stems	5	Potassium cyanide	46	4
Brassica juncea roots	5	Potassium cyanide	88	4
Brassica juncea leaves	5	Sodium thiocyanate	15	4
Brassica juncea stems	5	Sodium thiocyanate	62	4

Plant	Ore concentration (mg/kg)	Chemical	Plant concentration (mg/kg)	Ref
Brassica juncea roots	5	Sodium thiocyanate	172	4
Burkheya coddii leaves	5	Potassium cyanide	97	4
Burkheya coddii stems	5	Potassium cyanide	94	4
Burkheya coddii roots	5	Potassium cyanide	36	4
Burkheya coddii leaves	5	Sodium thiocyanate	0.31	4
Burkheya coddii stems	5	Sodium thiocyanate	0	4
Burkheya coddii roots	5	Sodium thiocyanate	49	4
Chicory	5	Potassium cyanide	164	4
Chicory	5	Sodium thiocyanate	31	4
Brassica juncea	0.64	Ammonium thiocyanate	5.3	5
Brassica juncea	0.64	Sodium cyanide	35.9	5
Brassica juncea	0.64	Potassium cyanide	35.1	5
Zea mays	0.64	Ammonium thiocyanate	1.2	5
Zea mays	0.64	Sodium cyanide	17.2	5
Zea mays	0.64	Potassium cyanide	15.3	5
Sorghum bicolor	1.75	Cyanide	5.7	6
Trifolium repens cv. Prestige stems	1.75	Cyanide	26.87	6
Trifolium repens cv. Prestige leaves	1.75	Cyanide	4.16	6
Trifolium repens cv. Tribute stems	1.75	Cyanide	19.08	6
Trifolium repens cv. Tribute leaves	1.75	Cyanide	2.71	6
Microlaena stipoides	1.75	Cyanide	4.12	6
Austrodanthonia caespitosa	1.75	Cyanide	21.64	6
Bothriochloa macra stem	1.75	Cyanide	4.65	6
Bothriochloa macra leaves	1.75	Cyanide	23.78	6
Eucalyptus polybractea sterms	1.75	Cyanide	11.11	6
Eucalyptus polybractea leaves	1.75	Cyanide	1.8	6
Acacia decurrens stems	1.75	Cyanide	14.79	6
Acacia decurrens leaves	1.75	Cyanide	5.31	6
Brassica juncea	48	Potassium cyanide	760	7, 8

1.4.2 Non-induced gold uptake

In addition to the experiments described above, research has been carried out to study the uptake of gold from controlled growth substrate without the use of chemicals to solubilise gold. In general, these experiments studied the formation of gold nanoparticles within the plant tissues rather than quantifying gold uptake. These studies have been carried out in a range of species; *B. juncea*, *Chilopsis linearis*, *Cucumis sativus*, *Helianthus annuus*, *Lolium multiflorum, Medicago sativa*, *Origanum vulgare*, *Sesbania drummondii* and *Trifolium pratense* (Gardea-Torresdey et al. 2002a; Gardea-Torresdey et al. 2005; Rodriguez et al. 2007; Sharma et al. 2007; Bali and Harris 2010; Starnes et al. 2010).

Although gold uptake by plants had previously been observed, no work had studied gold uptake in a controlled environment until Shacklette et al. (1970). Plants which had been cut to remove the roots could take up gold solutions easily although when the roots were still present, gold uptake was reduced. This showed that the gold in the rootless plants was taken up with water. Additionally, gold uptake was increased with the addition of cyanide because of the increased gold solubility.

It was found that a number of the plant species tested that could take up gold were also cyanogenic and therefore were able to produce cyanide compounds which would act to solubilise the gold ($Au(CN)_2^-$) and so increase uptake (Girling and Peterson 1980). Gold translocation to the shoots was reduced when transpiration was compromised and root uptake was unaltered. This shows that transpiration is important for gold translocation, but not for uptake into the root tissues, further emphasising the results of Shacklette et al. (1970). Girling and Peterson (1980) also studied the effects of metabolic inhibitors (including 2,4-dinitrophenol and sodium azide) on gold uptake, finding that these inhibitors reduced uptake, indicating that plant metabolism might be involved in gold uptake.

More recently, there has been an increase in studies which have explored gold uptake by plants. Gold uptake has been demonstrated in *M. sativa* (alfalfa) grown on solid artificial growth medium, containing 1.6 mM gold (Gardea-Torresdey et al. 2002a). Although the amount of gold taken up was not quantified, gold was present in the roots and shoots of the plants, showing that gold had moved into

the aerial tissues from the roots. The formation of gold nanoparticles was also demonstrated and the authors hypothesise that nanoparticle formation is external, and that gold is taken up as nanoparticles and translocated through the plants. This hypothesis is not consistent with the other studies described here. Formation and uptake of gold nanoparticles within plants is discussed below (1.5.3 and 1.5.4).

Gold uptake from controlled growth media, tested in a variety of species in different conditions, has found that uptake is species dependent (Starnes et al. 2010). Unsurprisingly, in all species tested, gold uptake increased when treated with higher gold concentrations and increased exposure time (Rodriguez et al. 2007; Sharma et al. 2007; Bali et al. 2010).

Bali et al. (2010) recently studied gold uptake in alfalfa and in *B. juncea* in a variety of different conditions in an attempt to explain some of the factors involved in plant gold uptake. In both species, as predicted from earlier studies, increasing gold concentration in the growth substrate led to increased concentration within the plants. Additionally, uptake also increased with time, although the increase was small, showing that most of the uptake of the gold from the media happens within the first 24 hours. This research also found an important effect of pH, with increases in uptake at lower pH and an optimum at pH 3, however this may be due to increased gold binding to external root surfaces at lower pH as is discussed below (Section 1.4.5). Gold uptake in barley was also increased by a reduction in pH from 8.0 to 3.6 (Girling and Peterson 1980).

1.4.3 Molecular mechanisms of gold uptake in plants

Although the research described above has looked at gold uptake in various plant species, no data have been published which elucidate the mechanisms of gold uptake within plants. It has been suggested that metal transport proteins may be involved in transporting gold across membranes (Bali et al. 2010). Further to this it has been hypothesised that the transport is active (Gardea-Torresdey et al. 2002a). More recently, these authors have suggested that translocation through the plant occurs through the water transport pathway (Sharma et al. 2007). The most logical hypothesised mechanism is that metal transporters used for essential metals are able to transport gold without having evolved to do so.

1.4.4 Molecular mechanisms of gold uptake and tolerance in other taxa

Recent microarray data have elucidated the transcriptional response of the metal tolerant bacterium *Cupriavidus metallidurans* to gold (Reith et al. 2009). The upregulated genes were found to include a gene cluster involved in hydrogen peroxide oxidative stress resistance and genes involved in the detoxification of copper ions. Two of the upregulated genes were *CupR* and *CopA*. CupR is a DNA-binding transcriptional activator orthologous to *E. coli* CueR and *S. enterica* GolS. CopA is a P-type ATPase, shown to be a copper transporter, suggesting it has a role in the efflux of copper from the *C. metallidurans* cells. P-type ATPase proteins are also found in plants (see Section 1.2.2). These two genes had previously been found to be upregulated in response to gold in *C. metallidurans* and *E. coli* (Stoyanov and Brown 2003; Checa et al. 2007; Jian et al. 2009).

1.4.5 Mechanisms of gold binding to plant material

Binding of gold to the surface of plants exposed to the gold-containing medium is thought to be important in uptake (Bali et al. 2010). Binding is also important in gold nanoparticle formation by plant tissues (described in Section 1.5.3). Studies of gold binding to plants have focused on binding to plant "biomass," a term that refers to dried plant material which is subsequently ground. This term and usage are used below, although experimental methodology in the studies may vary.

Gold binding has been investigated in a variety of species and a number of factors which might influence gold binding have been studied. Increasing temperature led to increased gold binding in alfalfa biomass presumably due to increased reaction rates at this higher energy (Gardea-Torresdey et al. 2000). Gold binding is also dependent on pH, with increased binding at lower pH (Gardea-Torresdey et al. 2000; Gardea-Torresdey et al. 2002b; Gamez et al. 2003; Romero-Gonzalez et al. 2003; Armendariz et al. 2004). As the pH decreases, the increase in H^+ ions results in protonation of the plant biomass (Gardea-Torresdey et al. 2000; Armendariz et al. 2004). In the research described, the gold complex used was $AuCl_4^-$. It therefore follows that as the positive charge of the biomass increases, more $AuCl_4^-$ can bind.

Various residues are thought to be involved in gold binding including amine and sulfhydryl residues which have increased protonation at low pH (Gardea-Torresdey et al. 2000) and carboxyl groups (Romero-Gonzalez et al. 2003; Lopez

et al. 2005a; Lopez et al. 2005b). When hop (*Humulus lupulus*) biomass was esterified to block carboxyl groups, binding was found to be pH independent, suggesting that there was no increasing positive charge and confirming the importance of both pH and carboxyl residues on gold binding (Lopez et al. 2005b).

1.4.6 Gold toxicity

The toxicity of gold to plants has also been investigated. *Chilopsis linearis* root growth was inhibited in the presence of gold above 0.8 mM (Rodriguez et al. 2007). This was also seen for both the roots and shoots of *Sesbania drummondii* grown in liquid medium containing 1mM gold, but not below this concentration (Sharma et al. 2007). Gold ions inhibited alfalfa growth in liquid culture above 250 µM gold and inhibited *A. thaliana* grown on solid medium above 100 µM gold (Binder et al. 2007; Starnes et al. 2010).

One potential mechanism for gold toxicity is the inhibition of aquaporin function. Aquaporins are a group of proteins which are able to transport a wide range of molecules including water. A fuller description of this group of proteins is found in Chapter 4. It has been shown that plant aquaporin function can be inhibited by gold (Niemietz and Tyerman 2002). Aquaporin function is also blocked by mercury and has been shown to cause toxicity (Zhang and Tyerman 1999). This process is likely to be due to the covalent blocking of cysteine residues and the sulfhydryl groups within them (Preston et al. 1993; Niemietz and Tyerman 2002). Further to this, it has been suggested that gold disrupts disulfide bonds or displaces other metals and as such may disrupt proteins (Van Assche and Clijsters 1990; Best and Sadler 1996; Rodriguez et al. 2007). Additionally, research with other metals and organisms demonstrates that electrostatic interactions, oxidative stress and free radicle formation might also be important factors in gold toxicity (Halliwell and Gutteridge 1984; Messer et al. 2005).

1.5 Gold nanoparticles

Gold nanoparticles are small particles of gold which have at least two dimensions between 1 and 100 nm; they may form a multitude of shapes, including spheres, rods and many irregular shapes (Aitken et al. 2006). The colour of light that gold nanoparticles reflect is determined by the size of the particles. This colour changes from red to purple as the nanoparticle size increases (Figure 1.4.)

Figure 1.4 Colours of spherical gold nanoparticles
Nanoparticles are those used in Chapter 3 for uptake studies and shown here as an indication of colour. Nanoparticles were obtained from Nanopartz (Colorado, US). Sizes are nanoparticle diameters as determined by the manufacturer. The nanoparticles were at concentrations (particles per mL) as follows: 7 nm, 1.36×10^{13}; 18 nm, 7.03×10^{11}; 48 nm, 3.46×10^{10}; 108 nm, 3.8×10^{9}.

1.5.2 Uses and production of gold nanoparticles

The properties of gold nanoparticles differ from those of the bulk metal, which is generally thought to be unreactive, and as such, these nanoparticles are useful industrial products with high commercial value.

Gold nanoparticles are useful catalysts for a number of different reactions. These include the catalysis of organic reactions in chemical synthesis (reviewed by Hashmi and Rudolph (2008)). Further to these reactions, oxidation reactions have been found to be catalysed by gold nanoparticles (Abad et al. 2005; Hughes et al. 2005; Turner et al. 2008). The catalytic oxidation of carbon monoxide to produce electricity might have an application in fuel cells, a potentially lucrative application (Kim et al. 2004b).

The optical properties of gold nanoparticles have also led to the development of techniques to use the particles in detection and sensing systems (Elghanian et al. 1997; Himmelhaus and Takei 2000). Gold nanoparticles can also be used in oncology treatments by conjugating the particles with antibodies targeted to markers for cancerous cells (El-Sayed et al. 2005).

The delivery of chemicals and other products to cells can be facilitated by gold nanoparticles and as such, they have important uses in medicine in addition to the optical uses described above. They have been used in the delivery of drugs (De Jong and Borm 2008), and in delivery of oligonucleotides for the modification of gene regulation within cells (Rosi et al. 2006). Additionally, it has been demonstrated that gold nanoparticles can be used to disrupt cancerous cells by stimulating nanoparticles with near infra-red light which increased nanoparticle temperatures capable of causing tissue damage (Hirsch et al. 2003). Additionally, if gold nanoparticles are coated in specific molecules they are able to disrupt the fusion of HIV molecules (Bowman et al. 2008). The medicinal uses of gold nanoparticles are therefore varied and have potential for use in other future applications.

Gold nanoparticles are generally produced using reduction reactions from gold(III) salts. There are two main synthesis methods which are widely used. The first is the Turkevich method which uses the reduction by citrate at 100 ºC (Turkevich et al. 1951; Frens 1973). Further to this, a two-phase process is also widely used, which uses organic reduction of the gold nanoparticles (Brust et al. 1994).

1.5.3 Biological production of gold nanoparticles

Although there are chemical methods of synthesis, more recently, the production of gold nanoparticles using dead plant tissue or plant extracts along with production using other biological methods has been investigated. Further to this, the production of gold nanoparticles within living plant tissue has also been studied. These biological methods of gold nanoparticle formation are described in this Section.

1.5.3.1 Production of gold nanoparticles within plants

Many of the studies described above (Section 1.4.2), where plants were treated with gold explored the formation of gold nanoparticles within the living plant tissue. The germination and growth of alfalfa on media containing gold led to the formation of gold nanoparticles which were found to be distributed throughout the plant (Gardea-Torresdey et al. 2002a). These nanoparticles ranged from 2-20 nm in size and were thought to be reduced to gold(0) externally and subsequently transported into and through the plant. However, this seems unlikely as more recent studies suggest that the nanoparticle formation is intracellular (Sharma et al. 2007). Nanoparticles are also likely to be deposited on the root surface, as indicated by purple roots (Sharma et al. 2007)

Nanoparticles have been found in a variety of sizes within plant tissue. As mentioned above, particles were 2-20 nm diameter in alfalfa, a similar size (5-20 nm) to those found when *S. drummondii* was treated with gold (Sharma et al. 2007). These were smaller than when both alfalfa and *B. juncea* were tested: nanoparticles were in the range 20-100 nm (Gardea-Torresdey et al. 2002a; Bali and Harris 2010). In these cases, nanoparticles were found within the roots and gold(0) was found in the aerial tissues. In other species, nanoparticles have been found to be smaller than those described in alfalfa; those in all tissues of *C. linearis* have diameters ranging from 0.5 to 2 nm with an average of 1 nm (Gardea-Torresdey et al. 2005; Rodriguez et al. 2007). These data show that the plant species may be important in determining both nanoparticle size and distribution.

In addition to the importance of the plant species used, other factors such as gold concentration, treatment time, pH and temperature were studied to determine their effects. Altering the gold concentration plants were treated with did not affect nanoparticle size (Rodriguez et al. 2007) and the time of exposure was a not factor in size or shape (Starnes et al. 2010). Starnes et al. (2010) found that although there were some differences in the size and shapes of nanoparticles for different times, the majority of nanoparticles were spherical with an average diameter of approximately 20 nm. pH plays a large role in nanoparticle shape and size. Increased pH led to a shift of the size distribution to a smaller diameter and significantly increased the number of hexagonal nanoparticles present. Further to this, decrease in pH did not affect the size of the nanoparticles but did increase

the number of triangular nanoparticles present. Increases in temperature led to the formation of smaller nanoparticles and increased the number of hexagonal nanoparticles whereas the reduction in temperature led to an increase in nanoparticle size and an increase in the number of rectangular particles. Treatment in the dark did not have effects on shape but did reduce the size of the nanoparticles, although plant gold concentrations were not determined and so in dark conditions, plants may have contained less gold due to reduced transpiration. It is therefore evident that a number of factors are all important in determining the size and shape of nanoparticles which form within plants.

Three hypotheses could explain where nanoparticles are formed and how they are subsequently distributed. The first of these, proposed by Gardea-Torresdey et al. (2002a), is that gold(III) ions are reduced to gold(0) in the growth substrate or on the root surface. These are subsequently taken up by the roots and distributed throughout the plant. The second hypothesis is that the gold ions are taken up and nanoparticles form within the plant roots prior to distribution throughout the plant (Sharma et al. 2007). Alternatively, the gold ions would be taken up into the plant cells and distributed around the plant. Nanoparticles would then form *in situ* and not move from the location in which they form. It is possible that all three of these hypotheses could be involved.

1.5.3.2 Other plant-based methods of gold nanoparticle production

In addition to the formation of gold nanoparticles within live plants, nanoparticle formation on dried and ground dead plant biomass has also been investigated. The formation of nanoparticles in the presence of plant material has been described in various species and was generally studied alongside how gold binds to plant tissue. Accumulation of gold(III) on biomass from alfalfa, oat and hops has been described (Gardea-Torresdey et al. 2000; Armendariz et al. 2004; Lopez et al. 2005a; Lopez et al. 2005b). These studies demonstrate that gold(III) binds to the biomass where it is subsequently reduced to form gold(0) nanoparticles. This reduction is likely to involve cysteine, methionine and carboxyl groups (Gardea-Torresdey et al. 2000; Lopez et al. 2005a).

The reduction of gold(III) on the plant biomass can lead to nanoparticles of various shapes and sizes. Nanoparticle sizes have been found to be different depending on the pH. Lowering the pH increased nanoparticle size (Gardea-

Torresdey et al. 2000; Armendariz et al. 2004). It also appears that large gold nanoparticles are able to form from the coalescence of smaller particles (Gardea-Torresdey et al. 1999).

Further to these experiments, plant extracts have also been used in the synthesis of gold nanoparticles (Shankar et al. 2004a; Shankar et al. 2004b; Shankar et al. 2005; Narayanan and Sakthivel 2008). Plant extracts were from boiled leaf material in contrast to the dried and ground plant material described above. Using these extracts, it has been demonstrated that the size of the nanoparticles can be controlled by the conditions under which the particles are grown, including the concentration of the extract used. Reduction of gold(III) to gold(0) was rapid, and both shape and size were variable (Shankar et al. 2003).

1.5.3.3 Other biological methods of gold nanoparticle production

The synthesis of nanoparticles using biological methods is not restricted to higher plants. Gold nanoparticle formation has been observed using a variety of microorganisms and algae. Although algae are often classified in the plant kingdom, they are sufficiently distinct from the higher plants described above to be included here. Gold nanoparticle formation has been observed on the surface of algal cells. In *Chlorella vulgaris*, gold binding was found to be rapid, with a subsequent slow reduction to gold nanoparticles (Greene et al. 1986; Hosea et al. 1986). Gold binding was found to be greatest at pH 2, an observation which is the same for plants as described above (Section 1.5.3.1) (Darnall et al. 1986). This increased binding at low pH is due to the increased positive charge on the cell surface, which allows greater binding of negatively charged $AuCl_4^-$. Since then, various other algae have been shown to bind gold and form nanoparticles (Romero-Gonzalez et al. 2003; Chakraborty et al. 2009).

Fungi and yeast bind $AuCl_4^-$ on the cell surface which is subsequently reduced to form nanoparticles (Mukherjee et al. 2001; Mukherjee et al. 2002; Lin et al. 2005). Additionally, bacteria also bind and reduce $AuCl_4^-$, including *E. coli*, the metal tolerant *Capriavidus metallidurans*, actinomycete species and filamentous cyanobacteria (Ahmad et al. 2003b; Lengke et al. 2006a; Lengke et al. 2006b; Du et al. 2007; Deplanche and Macaskie 2008; Reith et al. 2009). This is not an exhaustive list and many other bacterial species have been shown to form nanoparticles. Nanoparticle synthesis is not exclusively extracellular, and studies

have shown intracellular gold nanoparticle formation, for example in *C. metallidurans*, *Shewanella algae* and species of *Rhodococcus* (Ahmad et al. 2003a; Konishi et al. 2006; Reith et al. 2009).

The reduction of gold(III) to gold(0) is closely related to the binding of the gold to the biological material. This has also been identified in the species described here. Gold binding in the alga *C. vulgaris* has been shown to bind gold whether the cells are alive or dead, indicating that binding is not a biological function (Darnall et al. 1986). As with the plant studies described above, various chemical groups on the surfaces of cells have been shown to be involved in gold binding and subsequent reduction to gold(0). Carboxyl, amino and sulfhydryl groups are thought to be important in binding prior to reduction in various species (Darnall et al. 1986; Ahmad et al. 2003b; He et al. 2007). The aldehyde groups of reducing sugars may also be involved in gold binding (Lin et al. 2005). Sulfur containing groups are important, with gold(I)-sulfur complexes important in binding and reduction (Lengke et al. 2006a; Lengke et al. 2006b; Reith et al. 2009).

After binding, it has been hypothesised that reduction of gold(III) to gold(0) is carried out by, possibly NADH-dependent, reductases (Mukherjee et al. 2002; Ahmad et al. 2003b; He et al. 2007; Husseiny et al. 2007).

1.5.4 Nanoparticle uptake and toxicity in plants

The recent large expansion in nanoparticle use (Section 1.5.2) means that the environmental and toxicological impacts of nanoparticles are important areas for study. The uptake of gold nanoparticles has been studied in various species. There is evidence that gold nanoparticles can be taken up by plants and subsequently biomagnified in the food chain (Judy et al. 2010). Additionally, it has been demonstrated that gold nanoparticles are able to transfer from water to plants and subsequently travel through the food chain (Ferry et al. 2009). Translocation of nanoparticles through the food chain has previously been observed with other nanoparticles including silver and titanium dioxide (Zhao and Wang 2010; Zhu et al. 2010). Gold nanoparticles were found to be taken up by, and have inhibitory effects on the growth of lettuce seedlings (Shah and Belozerova 2009). However, it has been recorded that gold nanoparticles increased both germination and root lengths in lettuce and cucumber (Barrena et

al. 2009). The toxicity of gold nanoparticles therefore requires further understanding to determine the effects on different plant species.

The uptake and toxicity of metallic nanoparticles has been demonstrated in a variety of species. Uptake of silver nanoparticles has previously been studied, with uptake observed in *Cucurbita pepo* (courgette) (Stampoulis et al. 2009). This caused a reduction in biomass and transpiration and further studies have shown that germination and shoot growth are reduced in various species (Barrena et al. 2009; El-Temsah and Joner 2010; Musante and White 2010). It is possible that the reduction in biomass when treated by silver nanoparticles is due to the disruption of cell division (Kumari et al. 2009).

Uptake of copper nanoparticles has also been studied in various species, including *C. pepo, Phaseolus radiatus* and *Triticum aestivum* (Lee et al. 2008; Shah and Belozerova 2009; Stampoulis et al. 2009; Musante and White 2010). As with the silver nanoparticle studies, copper nanoparticles inhibit plant growth with plants exhibiting smaller roots, shoots and overall biomass. Aluminium nanoparticles do not have an effect on the growth of *Phaseolus vulgaris* or *Lolium perenne* (Doshi et al. 2008). However, aluminium and zinc nanoparticles have been shown to almost entirely stop root growth in some species, but not in others (Lin and Xing 2007). Together, these studies show that the presence of metallic nanoparticles is not always detrimental to plant growth and may be dependent on the plant species, the nanoparticle sizes and concentrations and on the metal the particle contains.

The mechanisms of metal nanoparticle uptake and toxicity are currently unknown. For metallic nanoparticles most of those reported to be taken up by plants also have transporters for the metal ion, including copper and iron (Rico et al. 2011). However this does not necessarily indicate that the two are related because the differences in nanoparticle and ion size and chemistry mean that the mechanisms for ion and nanoparticle uptake are likely to be different.

Factors important in toxicity have been discussed. Metallic nanoparticles are likely to have a large effect on the plant root surface by altering the root surface chemistry (Rico et al. 2011), especially considering that silver nanoparticles have been shown to accumulate on root surfaces (Harris and Bali 2008). Additionally metallic nanoparticles might interact with pores and channels within the root

surface leading to blockages and thus causing toxicity (Asli and Neumann 2009). This is likely to be a contributing factor in any gold nanoparticle toxicity due to the ability of gold to inhibit aquaporin function (Niemietz and Tyerman 2002). Further to this, oxidative stress is likely to be a contributing factor in nanoparticle toxicity as reactive oxygen species have been identified in various cells after treatment with nanoparticles (MacCormack and Goss 2008).

Further to these studies, the formation of gold nanoparticles within live plants has also been investigated. These works are described in Section 1.5.3.1.

1.6 Thesis aims

The broad aim of this study is to investigate and describe gold uptake in *Arabidopsis thaliana* along with investigating the response of Arabidopsis to gold treatment. Gold uptake has been studied in numerous species, often with the addition of chemicals to increase gold uptake. The potential to use plants to take gold up from ores commercially has been explored and research suggests that it may be possible to use live plants or dead plant biomass as a tool for producing gold nanoparticles. However, the mechanisms of uptake have never been identified or researched.

A main aim of this work is therefore to elucidate possible mechanisms of gold uptake or gold tolerance. The genetic response to gold will be investigated using microarray technology to reveal which genes have altered transcript numbers in response to gold treatment. This will aim to identify a gene or group of genes which are possibly involved in gold tolerance and target genes will be selected for further study. These studies will be performed using the model plant species *Arabidopsis thaliana*. None of the research so far has studied either gold uptake or gold tolerance in *Arabidopsis thaliana*. Prior to the investigation of gene expression changes in response to gold it is therefore important to characterise gold uptake and nanoparticle formation in Arabidopsis.

Chapter 2 Methods

2.1 Reagents and suppliers

Unless otherwise stated, all reagents and supplies were obtained from: Sigma-Aldrich (Poole, UK), New England Biolabs (NEB) (Hertfordshire, UK), Thermo Fisher Scientific (Loughborough, UK), Invitrogen (Paisley, UK), Promega (Southampton, UK), Qiagen (Crawley, UK), Fermentas (York, UK) and VWR (East Grinstead, UK). Gold nanoparticles were supplied by Nanopartz (Colorado, US). The compost used in this work was Levington F2 compost sourced from Scotts (Suffolk, UK). Water used for all solutions and media was purified using an Elga Purelab Ultra water polisher (Elga Labwater, High Wycombe, UK) and sterilized by autoclave if necessary. For reactions involving RNA, molecular grade nuclease-free water was used. All primers used throughout this work were synthesised by Sigma-Aldrich (Poole, UK).

2.2 Plant growth

Unless otherwise stated, wild-type seeds were the *Arabidopsis thaliana* (Arabidopsis) Columbia-0 (Col-0) ecotype. These were initially obtained from the Nottingham Arabidopsis Stock Centre (NASC); stock number N1093.

2.2.1 Seed sterilisation

Two methods were used to sterilise seeds to stop bacterial and fungal growth when growing Arabidopsis on sterile growth media.

2.2.1.1 Bleach sterilisation

One Klorsept tablet (Medentech, Wexford, Ireland) was added to 14 mL of water and 0.05 % Tween 20. This solution was added to 95 % ethanol in a 1:9 ratio (bleach solution : ethanol). The bleach solution was used to sterilise seeds for five minutes with shaking. Seeds were subsequently washed six times with 95 % ethanol and air dried.

2.2.1.2 Chlorine gas sterilisation

Seeds were dry sterilised with chlorine gas in an airtight container for four hours. Chlorine gas was produced by the addition of 3 mL of concentrated hydrochloric acid to 100 mL of Chloros bleach solution.

2.2.2 Plant growth media used in this work

Two types of plant growth media were used in this work. Murashige and Skoog medium and Richards medium (as named by Kumari et al. (2008)). The components of these media are detailed below (2.2.2.1 and 2.2.2.2).

2.2.2.1 Murashige and Skoog medium

Murashige and Skoog basal salt medium (Sigma) contained the following components: 20.6 mM NH_4NO_3, 18.8 mM KNO_3, 3 mM $CaCl_3$, 1.5 mM $MgSO_4$, 1.25 mM KH_2PO_4, 0.2mM Na_2 EDTA, 0.1 mM $FeSO_4 \cdot 7H_2O$, 0.1 mM H_3BO_3, 0.1 mM $MnSO_4 \cdot 4H_2O$, 30 µM $ZnSO_4 \cdot 4H_2O$, 5 µM KI, 1 µM $Na_2MoO_4 \cdot 2H_2O$, 0.1 µM $CuSO_4 \cdot 5H_2O$, 0.1 µM $CoCl_2 \cdot 6H_2O$, 2 mg/L glycine, 100 mg/L *myo*-Inositol, 0.5 mg/L nicotinic acid, 0.5 mg/L pyroxidine hydrochloride and 0.1 mg/L thiamine hydrochloride (Murashige and Skoog 1962).

Generally, half strength Murashige and Skoog medium (½MS) was used throughout this work. The pH was altered to 5.7 using NaOH. When solid media were required, ½MS was supplemented with 8 g/L agar (½MS(A)). In some experiments, ½MS was supplemented with 20 mM sucrose (½MS(S)). All media batches were autoclaved prior to use.

2.2.2.2 Richards medium

Richards medium contained the following components; 5 mM KNO_3, 2.5 mM KH_2PO_4, 2 mM $MgSO_4$, 2 mM $Ca(NO_3)_2$, 12.5 µM Fe-EDTA, 70 µM H_3BO_3, 14 µM $MnCl_2$, 0.5 µM $CuSO_4$, 1 µM $ZnSO_4$, 0.2 µM $NaMoO_4$, 10 µM NaCl, 0.01 µM $CoCl_2$ (Haughn and Somerville 1986; Richards et al. 1998; Kumari et al. 2008). The pH of this medium was altered to pH 5.75 using NaOH and was autoclaved prior to use.

2.2.3 Supplements to plant growth media

$KAuCl_4$ and $AuCl_3$ were dissolved at 100 mg / mL (0.5 M) in water and filter sterilised (0.45 µm). If the pH of the $KAuCl_4$ or $AuCl_3$ were to be adjusted to pH 5.7, the pH was adjusted using 1 mM NaOH and the gold concentration was adjusted to 5 mM (1 mg/mL). The pH 5.7 solution was subsequently filter sterilised (0.45 µm). KCl was produced at 1 M (pH 6) and filter sterilised (0.45 µm). 0.1 mM ammonium thiocyanate (NH_3SCN) was filter sterilised (0.45 µm). Copper was added as $CuSO_4$ from a filter sterile 30 mM stock solution. The sterile supplements described here were subsequently added to autoclaved plant media.

2.2.4 Germination

Sterile seeds were stratified in the dark for three nights at 4 ºC, unless stated otherwise. Seeds were germinated on ½MS(A) under a 16 hour constant light (80 $\mu mol.m^{-2}.s^{-1}$), 8 hour dark cycle at 20 ºC.

2.2.5 Bulk seed propagation

Seeds were propagated by growing plants in F2 compost in greenhouse conditions, under at least 16 hours of light per day. Plants were dried prior to harvesting of seeds.

2.3 Electron microscopy

Freshly sampled plant tissues were fixed and subsequently sectioned by the Technology Facility staff (University of York). Samples were fixed in 2.5 % (v/v) glutaraldehyde, 4% formaldehyde (v/v) in 50 mM phosphate buffer for 3.5 hours and washed twice with 100 mM phosphate buffer. A secondary fix of 1% osmium tetroxide in 50 mM phosphate buffer (on ice) was carried out for 40 minutes and material was washed twice with 50 mM phosphate buffer. Samples were subsequently dehydrated through an acetone series (25, 50, 70, 90 and 2 x 100 %) for thirty minutes each. Dehydrated samples were infiltrated with Spurrs resin (Agar Scientific) (25, 50 and 75 %) in acetone for thirty minutes each and subsequently with 100 % Spurrs resin for two hours with overnight polymerisation at 70 ºC. Sections were then cut at 1 µm and stained with toluidine blue for light microscopy before 70 nm sections were cut for transmission electron microscopy

(TEM). Sections were placed on 200 or 400 mesh thin-bar Athene grids (Agar Scientific) and stained with saturated uranyl acetate in 50 % ethanol for ten minutes and Reynolds lead citrate for ten minutes. Once sectioned, samples were viewed and photographed using a Tecnai 12 Bio Twin TEM operating at 120 kV.

2.3.1 Electron microscopy microanalysis

To determine the chemical composition of putative nanoparticles observed in electron micrographs, microanalysis was carried out on the samples. This was carried out at the University of York Nanocentre with the assistance of Professor Pratibha Gai and Professor Ed Boyes. Embedded sections were viewed using a high resolution transmission electron microscope. Energy-dispersive X-ray spectroscopy (EDX) was used to determine the emission spectrum of the samples. These data were analysed using an Oxford INCA analysis system.

2.4 Molecular Biology in Arabidopsis

2.4.1 DNA extraction from Arabidopsis

DNA was extracted from Arabidopsis using an Extract-N-Amp plant PCR kit (Sigma-Aldrich) according to the manufacturer's instructions. Briefly, DNA was extracted from leaf tissue excised using a 0.2 mL microcentrifuge tube lid. Leaf tissue was incubated in 50 µL of extraction solution at 95 ºC for ten minutes prior to the addition of 50 µL of dilution solution to neutralise the reaction. REDextract-N-Amp PCR reaction mix was used to carry out PCR amplifications of the extracted DNA.

2.4.2 Agarose gel electrophoresis

DNA fragments were separated by size via agarose gel electrophoresis. Gels contained 1 % agarose and 200 µg/L ethidium bromide, buffered in 40 mM 2-amino-2-hydroxymethyl-1,3-propanediol (Tris)-HCl, 18 mM glacial acetic acid and 1 mM ethylenediaminetetraacetic acid (EDTA). As a molecular marker, a 1 kb DNA ladder (NEB) was used (0.5 µg per well). DNA was separated using an electrical current at 80 - 120 V and visualised using ultraviolet light.

2.4.3 RNA extraction from Arabidopsis

Plant tissues were harvested and snap frozen in liquid nitrogen. Tissue was homogenised using a pestle and mortar using liquid nitrogen to prevent thawing. Plant RNeasy kits (Qiagen) were used to extract RNA from the tissue (approximately 100 mg) according to the manufacturer's instructions. An on-column DNA digestion was carried out using RNase-free DNase (Qiagen) as per the manufacturer's protocol. RNA was quantified using a Nanodrop ND-1000 Spectrophotometer (Thermo Scientific) at 260 nm.

2.4.4 Reverse transcription of plant RNA

The cDNA was synthesised from total RNA using M-MLV reverse transcriptase (Promega). 1 µg of RNA, 1 µL of 10 mM oligo-$dT_{(12\text{-}18)}$ (Invitrogen) and 1 µL dNTP mix (10 mM each dNTP) were incubated at 65 ºC for 5 minutes. Reverse transcription buffer, 2 µL of 0.1 M DTT and 40 units of RNaseOUT (Invitrogen) were added on ice and incubated at 42 ºC for 2 minutes. Reverse transcriptase (200 units) was added and incubated at 42 ºC for two hours prior to enzyme inactivation at 70 ºC for 15 minutes. RNase H (NEB) was used to remove all RNA after the reaction and the PCR product was cleaned up using a Wizard PCR clean-up system (Promega) according to the manufacturer's instructions. cDNA was quantified using a Nanodrop spectrophotometer (Thermo Scientific) at 260 nm.

2.4.5 Real-Time (quantitative) PCR

Real-time (quantitative) PCR (qPCR) was used to compare the expression levels of different genes. cDNA was produced from RNA (as outlined in Section 2.4.4) to be used in qPCR reactions. For all reactions, the experiment was performed using an ABI Prism 7000 Sequence Detection System (Applied Biosystems, Warrington, UK). Reaction mixes contained 5 µL of cDNA (0.5, 5 or 50 ng), 2 µL of primers (each primer at 10 µM), 5.5 µL of nuclease free water and 12.5 µL of Power SYBR green PCR master mix (Applied Biosystems, Warrington, UK). Reactions were carried out in a sealed 96 well plate which were centrifuged at 5000 x g for two minutes. All qPCR reactions were carried with the following cycle conditions; two minutes at 50 ºC, ten minutes at 95 ºC, followed by 40 cycles of 95 ºC for 15 seconds and 60 ºC for one minute.

Primers for qPCR were designed using Primer Express Version 3 (Applied Biosystems) and were synthesised by Sigma Aldrich (Haverhill, UK). Primers were tested for efficiency prior to use for testing relative gene expression. Standard curves were generated for each primer using cDNA at 10, 1, 0.1 and 0.01 µg/µL with three technical replicates. The primer efficiency PCR reaction was carried out as for relative quantification described above with an extra dissociation step in the PCR reaction. This step involved heating to 95 ºC for 15 seconds followed by 60 ºC for 30 seconds and 95 ºC for a further 15 seconds.

In all qPCR reactions *ACTIN2* expression was used as a constitutive control to normalise the data as widely reported in the literature (Herbette et al. 2006; Franklin and Whitelam 2007; Wan et al. 2008). Primers for *ACTIN2* are outlined in Table 2.1.

Table 2.1 qPCR primers for *ACTIN2*
Primers in the forward and reverse direction are denoted by F and R respectively.

Gene	Primer name	Sequence
ACTIN2	ACTINF	TACAGTGTCTGGATCGGTGGTT
	ACTINR	CGGCCTTGGAGATCCACAT

Chapter 3 Characterisation of gold uptake in *Arabidopsis thaliana*

3.1 Introduction

3.1.1 Plant uptake of gold

Although uptake of a range of metals has been studied in plants, and biological mechanisms for uptake of many of these have been elucidated, the means of gold uptake by plants are poorly understood. Research published so far has placed the emphasis of the studies on quantifying gold accumulation in plant tissues from ores using chemicals to solubilise the gold or on the use of plants to produce gold nanoparticles. Any biochemical mechanisms involved in uptake and sequestration are still largely unexplained.

The ability to accumulate gold from soil and gold ores has been quantified in a range of species including *Brassica juncea*, *Zea mays* and *Berkheya coddii* (Anderson et al. 1998; Lamb et al. 2001; Anderson et al. 2005b; Haverkamp et al. 2007; Marshall et al. 2007) as well as various root crops (Msuya et al. 2000). In addition to this, research has been carried out on a range of species native to Australia (Piccinin et al. 2007). In all of these studies, gold accumulation was induced by the addition of chemicals. Ammonium thiocyanate and potassium cyanide are the two main chemicals used to solubilise gold and make it more available for uptake. See Table 1.4 in Chapter 1 for a summary of this research.

The use of plants to produce gold nanoparticles has been investigated in *Medicago sativa* (alfalfa), *B. juncea*, *Sesbania drummondii*, *Chilopsis linearis*, *Cucumis sativus*, *Organum vulgare*, *Trifolium pratense*, *Lolium multiflorum* and *Helianthus annuus* (Gardea-Torresdey et al. 2002a; Gardea-Torresdey et al. 2005; Rodriguez et al. 2007; Sharma et al. 2007; Bali and Harris 2010; Starnes et al. 2010). The mechanism for nanoparticle formation within plants is unknown, however studies have shown that in alfalfa, gold(III) ions were reduced in the plant growth media prior to uptake (Gardea-Torresdey et al. 2002a). More recent research has suggested that the gold nanoparticles form within the root cells and are then transported through the plant to the aerial tissues (Sharma et al. 2007). Alternatively, nanoparticles may form in plant tissues after the uptake and translocation of gold ions (Gardea-Torresdey et al. 2005; Marshall et al. 2007;

Rodriguez et al. 2007; Starnes et al. 2010). Studies of silver nanoparticle formation in plants also found that ions are taken up through the roots and then reduced to nanoparticles within the plant (Harris and Bali 2008; Haverkamp and Marshall 2009).

3.1.2 Aims of this chapter

One of the main aims of this project was to investigate the genetic responses of plants to treatment with gold. *Arabidopsis thaliana* is an ideal model species to use for this as there is a large range of genetic tools and mutants available (Meinke et al. 1998; Somerville and Koornneef 2002). Additionally, Arabidopsis is small, fast growing and a member of the family Brassicaceae; a number of studies on gold accumulation have already been performed in other *Brassica* species. Metal uptake and tolerance has already been extensively studied in Arabidopsis for various transition and p-block metals (Section 1.2). To characterise the genetic response, a microarray approach was used. Prior to this, a thorough characterisation of the phenotypic effects of gold on Arabidopsis was undertaken.

The effects of gold on the germination and growth of Arabidopsis, gold accumulation and nanoparticle formation are presented in this Chapter.

3.2 Methods

3.2.1 Measurement of gold concentration

3.2.1.1 Measurement of gold concentration in liquid samples

Liquid samples from plant growth media or plant extracts (see Section 3.2.1.2) were analysed for gold concentration using flame atomic absorption spectroscopy (AAS). A Hitachi Z-5300 Polarized Zeeman Atomic Absorption Spectrophotometer at 242.2 nm was used. Samples were measured against a standard curve determined using gold atomic absorption standards (Sigma) at 1, 5, 10, 20 and 50 µg/mL. At these concentrations, the absorbance and gold concentration exhibited a linear relationship, a typical standard curve is shown in Figure 3.1. For all concentrations above this, samples were diluted to between 5 and 50 µg/mL.

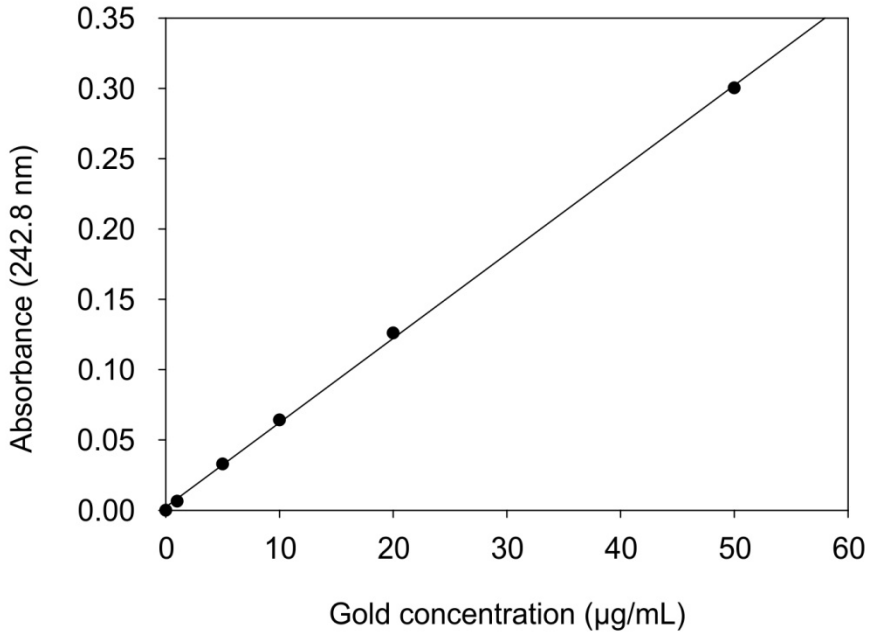

Figure 3.1 Atomic absorption standard curve
Representative atomic absorption standard curve using gold atomic absorption standard solution (Sigma) on a Hitachi Z-5300 Polarized Zeeman Atomic Absorption Spectrophotometer at 242.8 nm.

3.2.1.2 Measurement of gold concentration in plant samples

Gold concentrations in plant tissues were measured as described below. For a full explanation of the method development, see Section 3.3.1.

Plants were harvested and, if required, roots and shoots separated. Plant tissues were dried at 60 ºC prior to measurement of dry mass. Dry samples were ashed at 550 ºC for six hours using a Carbolite AAF 11/7 furnace (Carbolite, Hope, UK). Aqua regia (3:1 (v/v) 12 M hydrochloric acid : 15.6 M concentrated nitric acid) at a volume of 2.5 mL was added to the ashed samples at 60 ºC and 7.5 mL of water added. These samples were analysed via AAS as for liquid samples (Section 3.2.1.1).

A sample of plant material was supplied to use as a standard with a known gold content by Dr Chris Anderson (Massey University, New Zealand). The concentration of gold in this material was 15.3 µg/g as determined by fire assay (Anderson et al. 2005a). For every set of extraction procedures (ashing, acid treatment and measurement) 0.1 g of this material was also treated as a control for the extraction.

3.2.2 Transfer of Arabidopsis seedlings to gold

Sterile Arabidopsis seeds were imbibed and stratified as described in Section 2.2.4. Seeds were subsequently pipetted onto sterile filter paper strips placed on ½MS(A) and grown vertically in growth room conditions (Section 2.2.4). After seven days, the seedlings were transferred on the filter paper onto ½MS(A) plates containing $KAuCl_4$ at 0, 0.125, 0.25, 0.375 or 0.5 mM at either pH 5.7, or with uncontrolled pH (see Table 3.2). Seedlings were grown on the media containing gold for a further 24 hours in growth room conditions.

3.2.3 Germination studies

Imbibed and stratified Arabidopsis seeds (Section 2.2.4) were pipetted onto ½MS(A) plates containing $KAuCl_4$ at 0, 0.125, 0.25, 0.375 and 0.5 mM (at pH 5.7). Seeds were also germinated on ½MS(A) plates containing $AuCl_3$ at 0, 0.125, 0.25, 0.375 and 0.5 mM (at pH 5.7) or KCl at 0, 0.125, 0.25, 0.375 and 0.5 mM (at pH 5.7). Seedling growth was measured over eight days. Root lengths were measured for thirty biological replicates. Mean root lengths were compared

using one-way analysis of variance (ANOVA) followed by a test for least significant difference.

3.2.4 Hydroponic plant growth

For liquid culture experiments, seeds were germinated and grown on ½MS(A) for seven days. Seedlings were transferred to 100 mL conical flasks containing 20 mL ½MS(S). After further growth under a 16 hour constant light (10-20 $\mu mol.m^{-2}.s^{-1}$), 8 hour dark cycle at 20 ºC with shaking at 100 rpm, media were replaced with $KAuCl_4$ at 0, 0.125, 0.25, 0.375 or 0.5 mM (pH 5.7 or uncontrolled pH). For the experiments with dead plants, the plants were killed by autoclaving prior to the treatments. The growth medium was supplemented with sugar to compensate for the decreased gas exchange and consequent disruption to photosynthesis due to the leaves being submerged. Lower levels of light compared to standard growth room conditions (Section 2.2.4) were used to minimise plant stress.

3.2.5 Plant growth on sieves

For studies looking at the translocation of gold from the roots to the shoots of plant material, Arabidopsis seeds were germinated and grown on metal sieves on stands to allow root tissue to be submerged in liquid without the aerial tissue being in contact with the liquid. The stands are shown in Figure 3.2. Sieves were autoclaved in 580 mL preserve jars (Weck, Illinois) sealed with metal clips. To germinate the seeds on the sieves, the sieve component of the stand was coated with ½MS(A) (12 g/L agar). Sterile and stratified (Sections 2.2.1 and 2.2.4) Arabidopsis seeds were pipetted onto the sieves and seeds were germinated in growth room conditions (Section 2.2.4) and seedlings were grown for 30 days. Seedling roots were grown into 125 mL of ½MS. Liquid growth media were replaced with 0, 1 or 2.5 mM $KAuCl_4$ (pH 5.7) for 20 hours. Plant tissue was harvested after 20 hours and roots and shoots were carefully separated. The gold content of the root and shoot tissues was measured (Section 3.2.1.2) and tissue samples were analysed via transmission electron microscopy (Section 2.3).

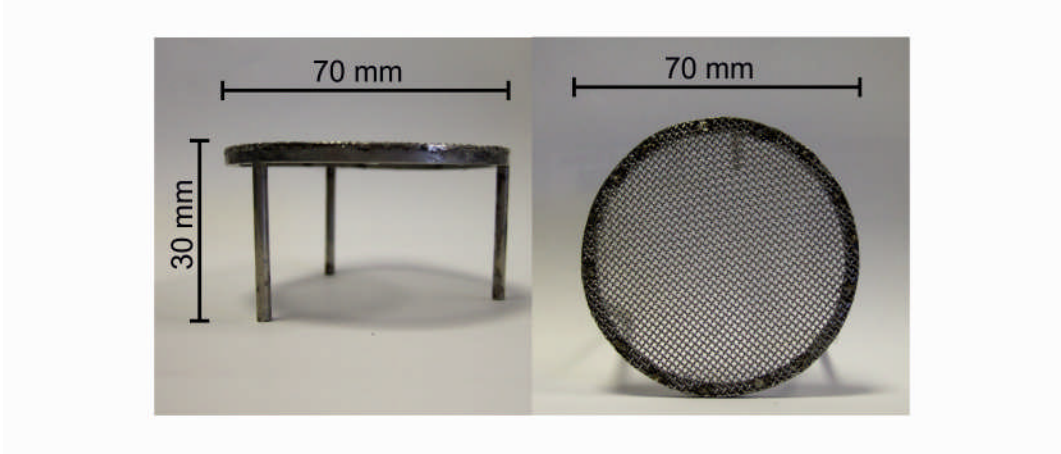

Figure 3.2 Dimensions of stainless steel sieve stands
Sieves were produced at the University of York from stainless steel in the dimensions outlined. Stainless steel mesh (hole diameter is 1 mm) was welded to the top.

3.2.6 Growth of Arabidopsis in gold treated soil

Aqueous gold solutions ($KAuCl_4$, 0.5 mM, pH 5.7) were applied to 65 g of sand in 2 L polypropylene tubs, with shaking to allow even gold distribution in the sand. Liquid was allowed to evaporate at room temperature, the sand and gold were mixed and 585 g of F2 compost was added (soil water content was determined prior to mixing to ensure all replicates were identical). Tubs were shaken for 24 hours to ensure even gold distribution throughout soil. Treated soil was then added to pots in 30 g aliquots. Plants were germinated and grown in growth cabinets (Sanyo, Leicestershire, UK) with 180 µmoles.m^{-2}.s^{-1} white light in a 12 hour photoperiod, with temperatures of 20 ºC during the light and 18 ºC in the dark. Seeds were germinated under propagator lids for five days to increase seedling establishment. After seven weeks, plants were treated with water or 0.5 or 50 g / kg soil of ammonium thiocyanate. Plants were grown for a further seven days and regularly watered. After seven days, aerial and root tissues were separated. Root tissues were washed in water to remove soil bound to the roots. The gold content of aerial and shoot tissue was then measured as described above (Section 3.2.1.2). Mean gold content of the treatments was calculated and these were compared using a Kruskal-Wallis test followed by a Mann-Whitney U test.

3.2.7 Growth of alfalfa in soil

Alfalfa seeds (Unwins, UK, commercially sourced) were sterilised by chlorine gas sterilisation (Section 2.2.1.2) and germinated on ½MS(A) for 5 days as described in Section 2.2.4. These were subsequently transplanted to soil containing $KAuCl_4$ (50 mg/kg) which had been treated as described in Section 3.2.6. These plants were subsequently grown in a growth cabinet as described in Section 3.2.6 for eight weeks. Root and shoot tissues were harvested separately and the gold concentration was measured. Aerial samples were taken and analysed using electron microscopy (Section 2.3).

3.2.8 Nanoparticle uptake experiments

Alfalfa seeds were stratified in water in the dark (4 ºC) for two nights and germinated in growth room conditions as described in Section 2.2.4. After growth for five days, individual seedlings were floated on 250 µL of ten different treatments in a 96 well plate with seedling roots submerged. Treatments were as follows: water, 0.25 mM gold, 7, 18, 48 or 108 nm gold nanoparticles. Nanoparticle treatments were either at 0.25 mM gold or 3.65×10^8 nanoparticles per mL. Sizes are as described by the manufacturer (Nanopartz, Colorado, US). Seedlings were treated for 24 hours with shaking at 150 rpm to ensure nanoparticles remained in suspension.

After 24 hours of treatment, roots were fixed and sectioned for electron microscopy as outlined in Section 2.3. Nanoparticle samples were embedded on a 200 mesh thin-bar Athene grid (Agar Scientific) and analysed via electron microscopy.

3.3 Results

3.3.1 Development of an assay to measure gold concentration

Anderson et al. (2005a) tested the efficacy of the following methods for measuring gold content in plant tissue: fire assay followed by inductively-coupled plasma optical emission spectrometry (ICP-OES), flame atomic absorption spectroscopy, graphite furnace atomic absorption spectroscopy, inductively-coupled plasma mass spectroscopy (ICP-MS) and X-ray fluorescence. The research found that flame atomic absorption spectroscopy was a suitable method for measuring the gold concentration of plant tissue. For all of the methods tested by Anderson et al. (2005a) plant samples were dried at 70 ºC and ground. These samples then underwent further treatments prior to testing. For flame atomic absorption analysis, ground samples were ashed at 550 ºC for 14 hours and subsequently treated with 5 mL of aqua regia. The resulting liquid was then suitable for analysis via flame atomic absorption spectroscopy.

The study described above formed the basis for developing a method to measure plant gold concentration used throughout this work. Work by Dr Chris Anderson (personal communication) had shown that the ashing time could be reduced to six hours at 550 ºC. These conditions were therefore used in the following experiments and throughout this work. To determine the best method for treating the samples after ashing, samples were digested with 2.5 mL of either aqua regia or concentrated hydrochloric acid. Acid was added at room temperature or at 60 ºC. Water was subsequently added to dilute the samples within two minutes of acid addition or after one hour. The samples used for this experiment were of known gold concentration (15.3 mg/kg) and had been tested by fire assay, a standard method for determining gold concentration (Anderson et al. 2005a).

The results from these tests (Figure 3.3) show that in all cases the addition of aqua regia was the best acid to use to dissolve the gold as the results obtained in this study compared most closely to the published concentration. Aqua regia dissolves gold facilitated by the combination of the two acids (Figure 3.4). The nitric acid component oxidises gold to Au^{3+}. Following this, the hydrochloric acid provides chloride ions which react with Au^{3+} forming $AuCl_4^-$. It is evident from the above results that hydrochloric acid alone will dissolve some gold due to some of

the free chloride ions available. However, aqua regia is a more suitable method for dissolving the gold present after ashing the samples.

Acid	Time	Temp	Concentration (µg/g)	SD
Aqua regia	Immediate	Room	11.2	3.9
HCl	Immediate	Room	7.4	2.3
Aqua regia	Immediate	60 ºC	21.6	3.9
HCl	Immediate	60 ºC	3.9	1.9
Aqua regia	1 hr	60 ºC	17.6	3.4
HCl	1 hr	60 ºC	5.9	3.0

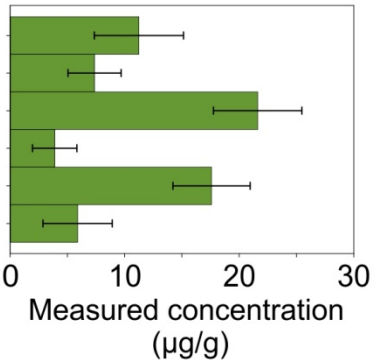

Figure 3.3 Comparison of different gold extraction methods
Concentrations of gold in the same tissue sample extracted using different methods. Two different acids were used (aqua regia or concentrated hydrochloric acid) at either room temperature or 60 ºC. The acid was added for one hour prior to dilution with water, or diluted immediately. Data are the means from three replicates and error bars represent the standard deviation from the mean.

$$Au_{(s)} + 3NO_{3\,(aq)}^{-} + 6H_{(aq)}^{+} \longrightarrow Au_{(aq)}^{3+} + 3NO_{2\,(g)} + 3H_2O_{(l)}$$

$$Au_{(aq)}^{3+} + 4Cl_{(aq)}^{-} \longrightarrow AuCl_{4\,(aq)}^{-}$$

Figure 3.4 Reaction of aqua regia and gold during extraction from plant material

The results outlined in Figure 3.3 also show that the temperature of the aqua regia is important in the process. The accuracy of the measured gold concentration was closest to the published data (Anderson et al. 2005a) when the aqua regia was added at 60 ºC. It is also evident that the time the aqua regia was added for, prior to the dilution of the reaction with water, was not important. From these results, the conditions chosen to treat the ashed samples prior to the measurement of gold content were the addition of aqua regia pre-heated to 60 ºC followed by the addition of water within five minutes of the addition of aqua regia. Although the concentration measured was slightly larger than the published fire assay standard, the concentration was corrected using the data outlined below. This corrected concentration was measured at 16.1 µg/g, a concentration similar

(and within the standard deviation of the experiment) to the fire-assay determined concentration.

In order to verify that this method was suitable for plant material with a range of gold concentrations, dry Arabidopsis material was dosed with a known amount of gold (0.1 to 5 000 µg/g). These gold treated tissues were then ashed and treated using the method outlined above. The liquid samples were subsequently analysed by flame atomic absorption spectroscopy (Table 3.1). At the highest concentrations (50 µg/g to 5 000 µg/g) the measured gold content of the plants was similar to that which was predicted. The slightly higher concentrations recorded are due the evaporation of aqua regia during the addition to the ash.

Table 3.1 Gold recovery from plant tissues with known gold concentrations

Concentrations and percentage recovery of gold from dry Arabidopsis plant tissue which had been treated with different amounts of gold. Gold was extracted from the plant tissue as described in Section 3.2.1.2.

Plant material gold concentration (µg/g)	Measured Concentration (µg/g)	Concentration difference (µg/g)	Percentage recovery (%)
0	0	0	
0.1	2.1	2.0	2099.9
1	2.5	1.5	251.5
5	6.8	1.8	135.9
10	13.4	3.4	133.9
50	57.0	7.00	114.0
100	106.4	6.4	106.4
5 000	5238.1	238.1	104.8

At the lowest gold concentrations (less than 5 µg/g), the concentrations detected appeared much higher than the concentrations that were added. This is probably due to the sensitivity of the spectrophotometer used as the concentrations were only around 2 µg/g higher than they should have been, although this gives a large difference in the proportion recovered. From these data, it was concluded that the methods described were suitable for analysing the gold content of plants at concentrations above 5 µg/g with reasonable accuracy and above 50 µg/g with greater precision. Below these concentrations, the atomic absorption spectrophotometer was not sensitive enough and measured concentrations were not accurate. Throughout this study, this method was used to determine the gold concentration of the plant tissue.

3.3.2 Gold uptake from solid media

To study whether plants could take gold up from solid media, seedlings were grown as described in Section 3.2.2 on filter paper in a vertical orientation. Seven-day-old seedlings were subsequently transferred to ½MS media containing $KAuCl_4$ at 0, 0.125, 0.25, 0.375 or 0.5 mM. As the concentration of gold in the growth medium increases, the pH of the medium decreases (Table 3.2).

Table 3.2 pH of ½MS plus $KAuCl_4$ at different concentrations
pH of the liquid was calculated using liquid media using a Hanna pH210 Microprocessor. These were subsequently confirmed for ½MS(A) plates using pH paper (Sigma, pH 0-6).

Gold concentration (mM)	pH
0	6.0
0.05	5.7
0.1	5.4
0.15	4.8
0.2	4.4
0.25	4.1
0.3	4.0
0.35	3.9
0.4	3.8
0.45	3.8
0.5	3.7

Two days after transfer to gold, the roots were examined for phenotypic changes (Figure 3.5). As the gold concentration of the media increased, the colour of the roots changed to increasing intensities of purple. Without gold, the roots remained white in colour and at 0.5 mM they were a deep purple. This purple colouration suggests that the gold has been reduced from the gold(III) in the media to gold(0) and gold nanoparticles have formed externally and/or internally within the roots. The formation of nanoparticles within the seedlings is explored in Section 3.3.2.2. The colour of the growth media also changed to a purple colour within 24 hours (Figure 3.5) suggesting that the some of the gold(III) added to the media had also been reduced to gold(0).

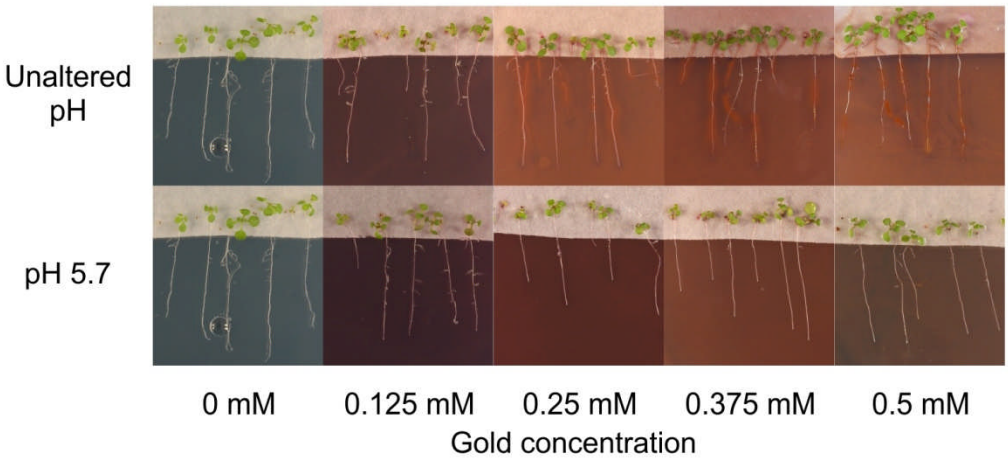

Figure 3.5 Gold uptake from solid media
Seven-day-old Arabidopsis seedlings two days after transfer to ½MS(A) plus $KAuCl_4$ at different concentrations (0, 0.125, 0.25, 0.375 and 0.5 mM) with unaltered pH or at pH 5.7.

In order to assess whether the pH of the media (described in Table 3.2) had an effect on the root colouration and the formation of nanoparticles, the experiment described above was repeated using media at the same concentrations (0, 0.125, 0.25, 0.375 and 0.5 mM), but adjusted to pH 5.7 with NaOH (the pH of the ½MS media without gold) (Figure 3.5). When the pH was at pH 5.7, the roots remained white at all concentrations tested, showing a difference compared to when the pH was not controlled. This suggests that nanoparticles did not form on the root surface, or within the plant, a hypothesis examined below (Section 3.3.2.2). The media the plants were transferred to also changed colour in a similar manner to when the pH was not buffered at pH 5.7.

3.3.2.2 Electron microscopy of plants transferred to gold

Samples from the 0.5 mM treatments in both pH conditions and the no gold treatments described above (Section 3.3.2) were fixed and sectioned as described in Section 2.3. Roots of seedlings that had been transferred to gold (pH 3.7) contained discrete gold nanoparticles (Figure 3.6). These particles were not visible in the roots of the samples which were transferred to media which did not contain gold (Figure 3.6c-d). Gold nanoparticles were distributed throughout the root tissue in both the epidermal cells (Figure 3.6a) and in the cells of the central root cortex (Figure 3.6b). The nanoparticle distributions and sizes were different within these two tissue types. Within the epidermal cells, the nanoparticles were various shapes and sizes with a large number of particles

with a rod-shaped profile. The particles in this tissue ranged from between 35 nm (which was the width of a rod) to 950 nm (the length of a rod). Spherical particles were all within this size range. In contrast to these findings, the nanoparticles in the central root cortex were smaller (between 18 and 271 nm). The shapes of the nanoparticles in the cortex were also diverse, although appeared to contain fewer particles with rod-shaped profiles than in the epidermis.

Electron micrographs from roots of seedlings transferred to media containing gold at pH 5.7 (Figure 3.7) show that gold nanoparticles were present in both the epidermis and cortex of the root tissue. This is complimentary to the data for the plants transferred to media containing gold at pH 3.7 (Figure 3.6). The nanoparticles in the epidermis (Figure 3.7a) were approximately 18 nm to 153 nm diameter. They were however, more sparsely distributed than for the comparative sample from plants transferred to media with gold at pH 3.7 (Figure 3.6a). The nanoparticles present in the root cortex (Figure 3.7b) were between 5 and 112 nm in diameter with those associated with the xylem spherical in profile. These were at a similar spatial density when compared to the corresponding sample at pH 3.7 (Figure 3.6b). Although gold nanoparticles were visible within the cells of the root tissues, comparing the cells between the different treatments did not show any major differences in root architecture.

No gold nanoparticles were visible in any of the aerial tissue from plants transferred to media with gold at uncontrolled pH, media containing gold at pH 5.7 or media containing no gold (Figure 3.8). Black spots visible in some of the chloroplasts (see Figure 3.8a for an example) are not nanoparticles but are plastoglobules. These are electron dense particles made from lipoproteins, which are often found in the chloroplasts of Arabidopsis (Brehelin et al. 2007).

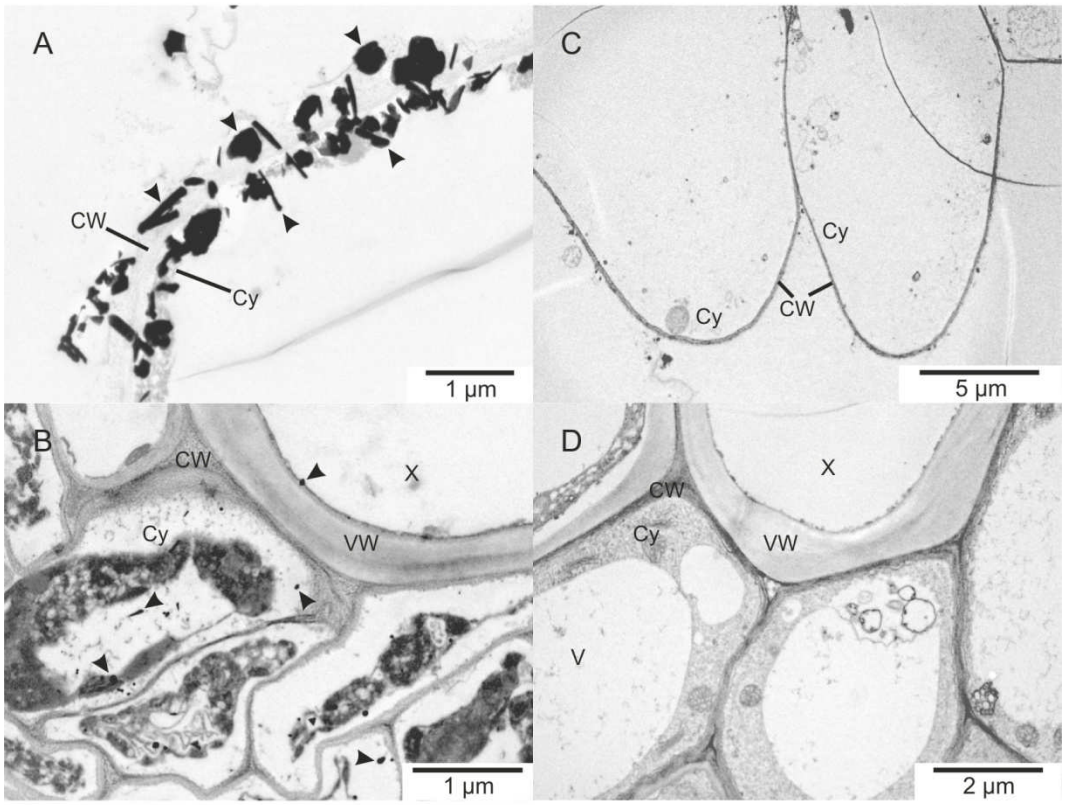

Figure 3.6 Electron micrographs of roots transferred to media containing $KAuCl_4$ with uncontrolled pH

Transmission electron micrographs of roots from seven-day-old Arabidopsis seedlings 48 hours after transfer to ½MS(A) plus 0.5 mM $KAuCl_4$ (A and B) or a ½MS(A) control (C and D). The pH of the media was not controlled (see Table 3.2). A and C) root epidermis tissue and B and D) root central cortex. Samples were fixed and sectioned as described in Section 2.3. Key; CW, cell wall; Cy, cytoplasm; V, vacuole; VW, vessel wall, X, xylem. Example nanoparticles are indicated by arrows.

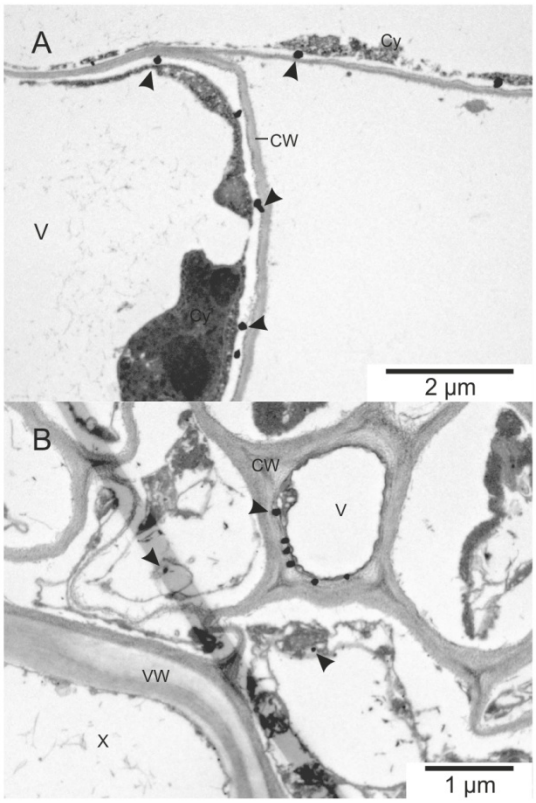

Figure 3.7 Electron micrographs of roots transferred to media containing $KAuCl_4$ at pH 5.7

Transmission electron micrographs of roots from seven-day-old Arabidopsis seedlings 48 hours after transfer to ½MS(A) plus $KAuCl_4$ buffered at pH 5. A) root epidermis tissue and B) root central cortex. Samples were fixed and sectioned as described in Section 2.3. Key; CW, cell wall; V, vacuole; VW, vessel wall, X, xylem. Example nanoparticles are indicated by arrows.

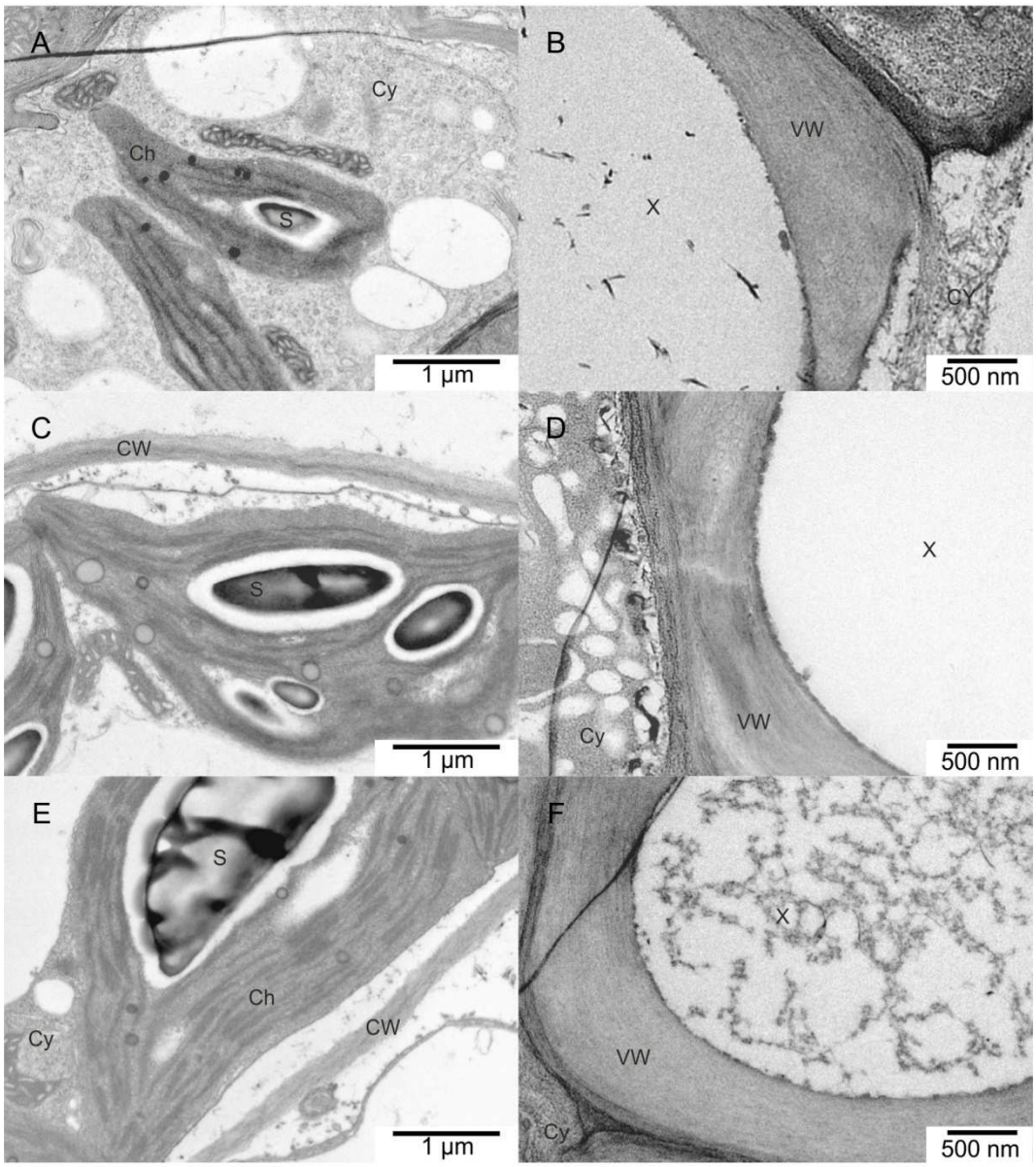

Figure 3.8 Electron micrographs of aerial tissue from plants transferred to solid media

Transmission electron micrographs of aerial tissue from seven-day-old Arabidopsis seedlings 48 hours after transfer to ½MS(A). The plants were transferred to ½MS(A) (A and B) or ½MS(A) supplemented with 0.5 mM $KAuCl_4$ with no pH control (C and D), or 0.5 mM $KAuCl_4$ at pH 5.7 (E and F). Samples are either chloroplast tissue (A, C and E) or xylem tissue (B, D and F). Samples were fixed and sectioned as described in Section 2.3. Key; Ch, chloroplast; CW, cell wall; Cy, cytoplasm; S, starch; VW, vessel wall, X, xylem.

3.3.3 Germination studies

3.3.3.1 Growth on $KAuCl_4$

To determine whether gold affects the germination and growth of Arabidopsis, seeds were grown as described in Section 3.2.3. The seeds were imbibed and stratified for three nights and subsequently germinated on ½MS(A) supplemented with gold at 0, 0.125, 0.25, 0.375 and 0.5 mM at pH 5.7 so that pH did not affect the results. Increasing the gold concentration did not affect the germination frequency or germination time of the seeds; 100 % of seeds germinated in all five treatments. As the gold concentration increased, root growth decreased (Figure 3.9 and Figure 3.10) and after eight days, the roots of the plants germinated on $KAuCl_4$ were significantly shorter than the no gold control ($p<0.001$). The roots of seedlings grown in the presence of 0.25 mM gold were less than half the length of the no gold control. The growth of seedlings showed a negative correlation with gold concentration; higher gold concentrations led to shorter root lengths.

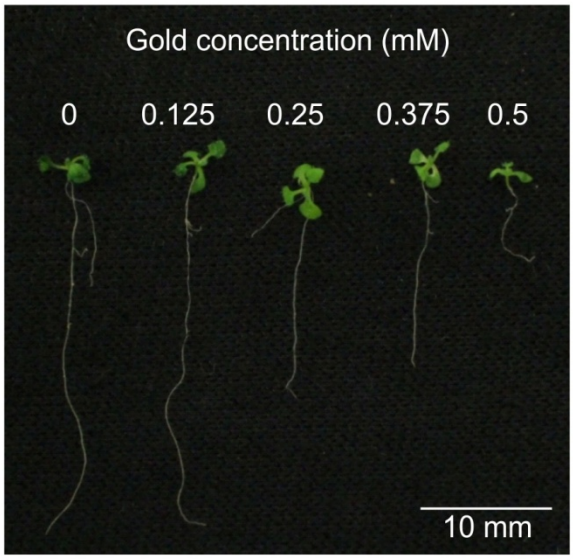

Figure 3.9 Arabidopsis grown on $KAuCl_4$
Arabidopsis seedlings after germination and growth for eight days on ½MS(A) supplemented with $KAuCl_4$ (pH 5.7) at 0, 0.125, 0.25, 0.375 and 0.5 mM.

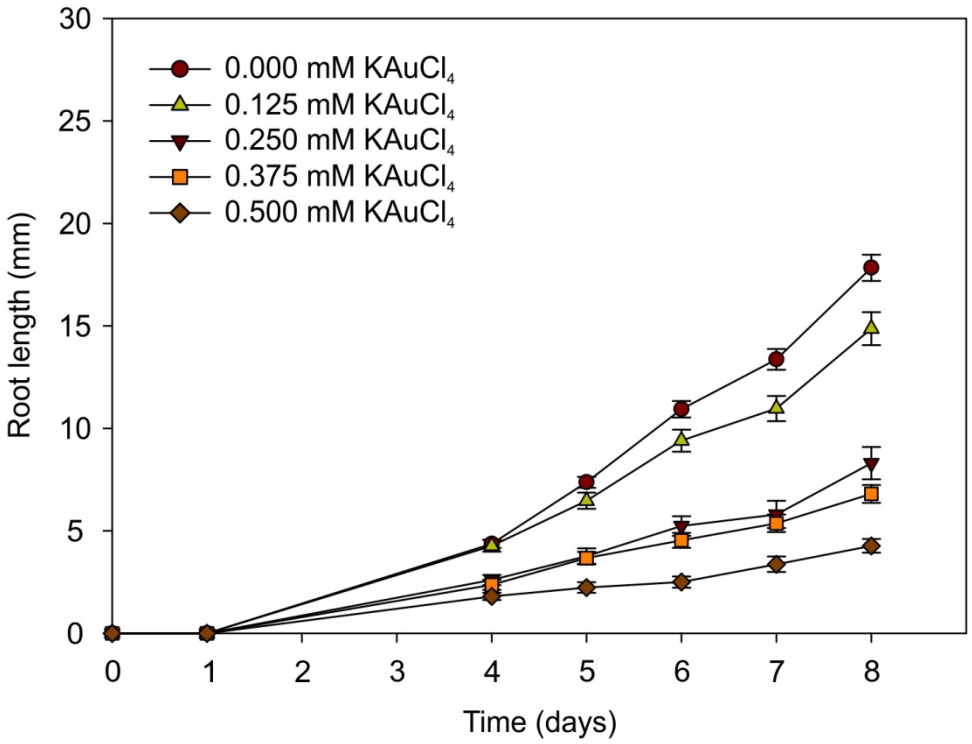

Figure 3.10 Growth of Arabidopsis seedlings on $KAuCl_4$
Root lengths of Arabidopsis seedlings germinated and grown on ½MS(A) plus different concentrations of $KAuCl_4$ (0, 0.125, 0.25, 0.375 and 0.5 mM) at pH 5.7. Lengths were measured over eight days. Data points represent the mean root length from 30 biological replicates and error bars represent the standard error of the mean.

3.3.3.2 Growth on $AuCl_3$

The results described above (3.3.3.1) indicate that gold inhibits Arabidopsis root growth. However, as gold is not the only component of the $KAuCl_4$ compound, the potassium and chlorine components were investigated to determine whether the effects seen were due to gold alone. To test the effect of the potassium, Arabidopsis seeds were germinated and grown on ½ MS agar supplemented with $AuCl_3$. Seeds were stratified and germinated as described above on agar supplemented with $AuCl_3$ at 0.125, 0.25, 0.375 and 0.5 mM to compare the growth with the growth on $KAuCl_4$. Seedlings were grown for eight days (Figure 3.11). As with the growth of Arabidopsis seedlings in the presence of $KAuCl_4$ (Figure 3.10), increasing the concentration of gold in the media led to slower growth over eight days. As the concentration increased, the root lengths were significantly shorter than those grown at lower $AuCl_3$ concentrations ($p<0.01$). The final root lengths were similar to those described for when plants were grown

on $KAuCl_4$. These data therefore show that the potassium component of the $KAuCl_4$ was not responsible for the reduction in seedling growth.

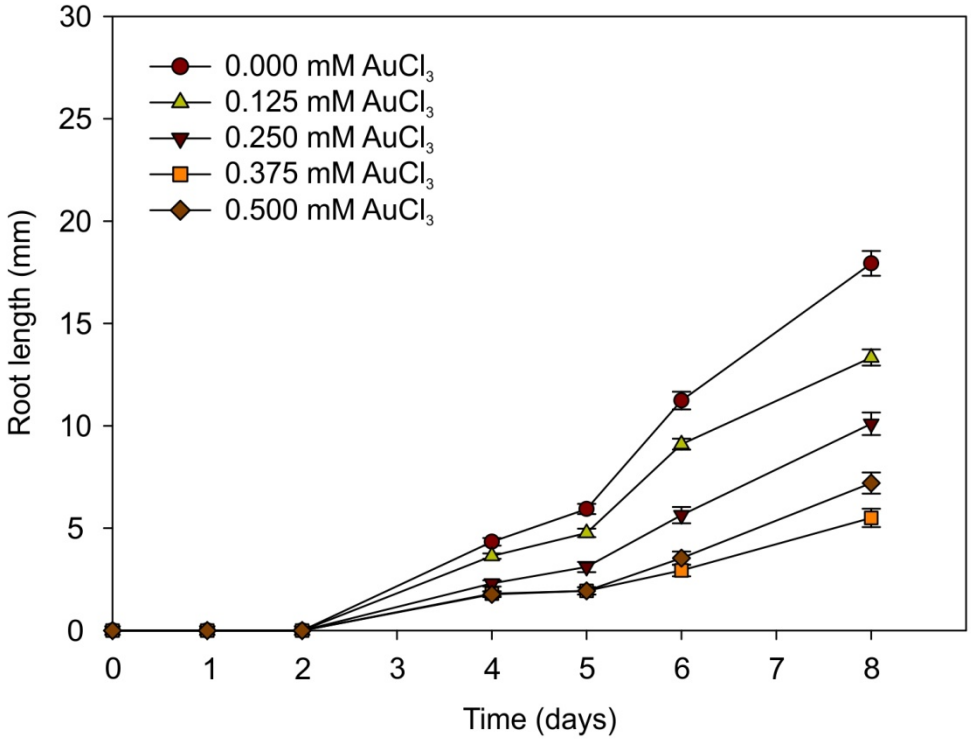

Figure 3.11 Growth of Arabidopsis roots on $AuCl_3$
Root lengths of Arabidopsis seedlings germinated and grown on ½MS(A) plus different concentrations of $AuCl_3$ (0, 0.125, 0.25, 0.375 and 0.5 mM) at pH 5.7. Lengths were measured over eight days. Data points represent the mean root length from 30 samples and error bars represent the standard error of the mean.

3.3.3.3 Growth on KCl

To determine the effects of the chlorine ions in both the $KAuCl_4$ and $AuCl_3$ compounds on the growth of gold, seeds were germinated as described above (Section 3.2.3) on ½MS(A) supplemented with KCl at 0, 0.5, 1, 1.5 and 2 mM. These concentrations were comparable to the concentrations of chlorine in the $KAuCl_4$ at the five different concentrations as described in the previous Sections (3.3.3.1 and 3.3.3.2). Seedlings were grown for eight days (Figure 3.12).

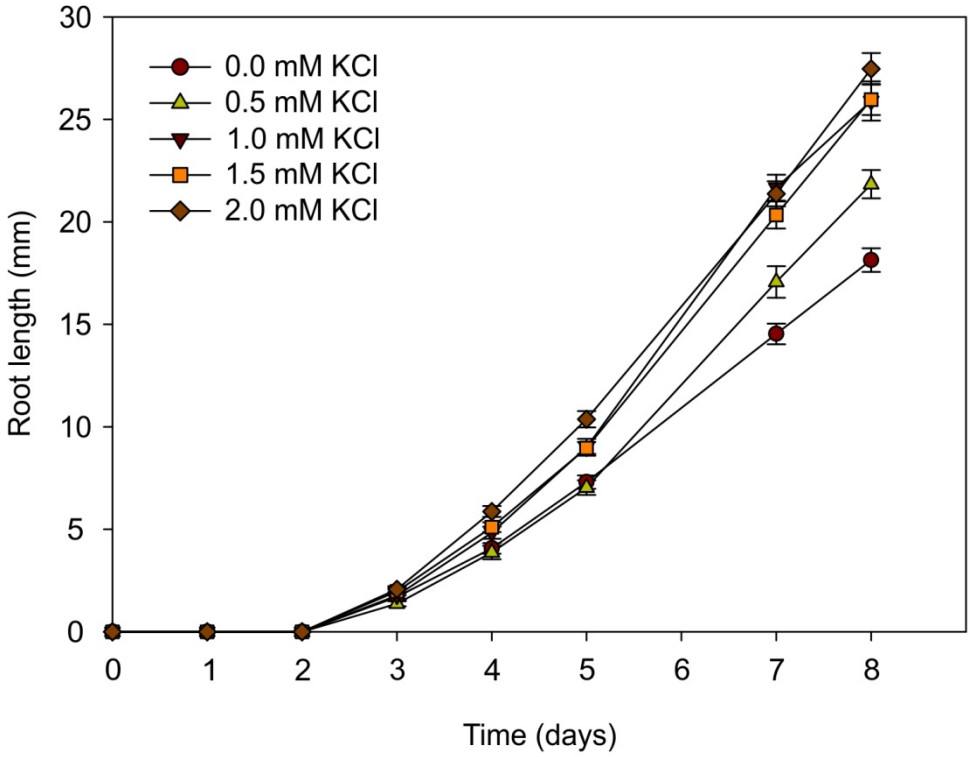

Figure 3.12 Growth of Arabidopsis on KCl
Root lengths of Arabidopsis seedlings germinated and grown on ½MS(A) plus different concentrations of KCl (0, 0.5, 1, 1.5 and 2 mM) at pH 5.7. Lengths were measured over eight days. Data points represent the mean root length from 30 samples and error bars represent the standard error of the mean.

The addition of KCl to the media led to an increase in the root lengths of Arabidopsis seedlings in comparison with seedlings grown on ½MS(A) without additional KCl. All treatments had significantly longer roots than when no supplemental KCl was added to the ½MS(A) ($p<0.001$). Roots of seedlings grown with 0.5 mM KCl were significantly longer than those without additional KCl. Roots of seedlings grown at 1, 1.5 and 2 mM KCl were not significantly different in length although they were significantly longer than those for the 0 and 0.5 mM KCl treatments. These data show that the potassium and chlorine in the $KAuCl_4$ and $AuCl_3$ were not responsible for the shorter root lengths at increasing $KAuCl_4$ or $AuCl_3$ concentrations.

3.3.3.4 Chemical analysis of $KAuCl_4$

The experimental data outlined above all strongly suggest that it is gold that is responsible for the toxicity and not potassium or chlorine. However, the manufacturer's (Sigma) information states that $KAuCl_4$ is 98 % pure. To determine whether the impurities in $KAuCl_4$ were responsible for the toxicity observed, a sample of $KAuCl_4$ was sent for analysis of inorganic metal impurities via ICP-OES (inductively-coupled plasma-optical emission spectrometry) by Medac Ltd (Egham, Surrey). The results of the analyses are outlined in Table 3.3.

Table 3.3 Chemical analysis of $KAuCl_4$
Main components and contaminants of $KAuCl_4$ from Sigma Aldrich. Analysis was ICP-OES carried out by Medac Ltd. Concentrations were determined for a 0.5 mM solution of $KAuCl_4$.

Element	Results	Concentration in 0.5 mM Au solution (nM)
Au	50.33 %	
K	6.93 %	
Ag	4 ppm	6.4
Al	8 ppm	50.8
B	4 ppm	63.4
Ca	69 ppm	294.8
Co	94 ppm	273.4
Cu	6 ppm	16.2
Fe	3 ppm	9.2
Hg	2 ppm	1.7
Mg	4 ppm	28.2
Na	45 ppm	335.2
Ni	6 ppm	17.5
P	3 ppm	16.6
Pt	21 ppm	18.4
Ru	1 ppm	1.7
Sb	14 ppm	19.7
Se	13 ppm	28.2
Si	2 ppm	12.2
W	4 ppm	3.7
Zn	72 ppm	188.6
All other elements	<1 ppm	

Cobalt and zinc were found to be the highest contaminants at 94 and 72 ppm respectively. When these values were extrapolated to the concentrations in the (0.5 mM) $KAuCl_4$ media, cobalt was 273 nM and zinc was 188 nM (Table 3.3). Readjusting all of the impurities for the molar concentrations found that sodium and calcium were the highest concentrations (335 and 295 nM respectively). All

other elements were lower than these. At the concentrations listed in Table 3.3, the contaminants are unlikely to affect root growth.

3.3.3.5 Electron microscopy of seedlings germinated on gold

Roots from seven-day-old Arabidopsis seedlings that had been germinated and subsequently grown on media containing $KAuCl_4$ at 0.5 mM (Section 3.3.3.1) were fixed and sectioned according to the methods outlined in Section 2.3 (Figure 3.13).

No gold nanoparticles were found in roots of seedlings grown in the presence of 0.5 mM $KAuCl_4$ (Figure 3.13). All features visible in the roots of this tissue were also found in the control sample which was grown without the gold supplement in the media. This result contrasts sharply to those for which Arabidopsis plants were transferred to gold in the same conditions (Section 3.3.2 and Figure 3.7), in which gold nanoparticles were identified within the roots of the seedlings.

The aerial tissues of all treatments did not contain gold nanoparticles (Figure 3.14). Small black spots visible within the chloroplasts in these samples are plastoglobules, and occur within both the treated and untreated samples (see Section 3.3.2.2). This result compares to that for the transferred material (Figure 3.8) in that no nanoparticles were found in either of these two treatments.

Although the root architecture in the two electron micrographs of the root tissue appears to be similar (Figure 3.13), the chloroplasts in the aerial tissue differed (Figure 3.14). The chloroplasts in the samples grown in the presence of $KAuCl_4$ did not contain as much starch as those that were grown on ½MS(A) alone.

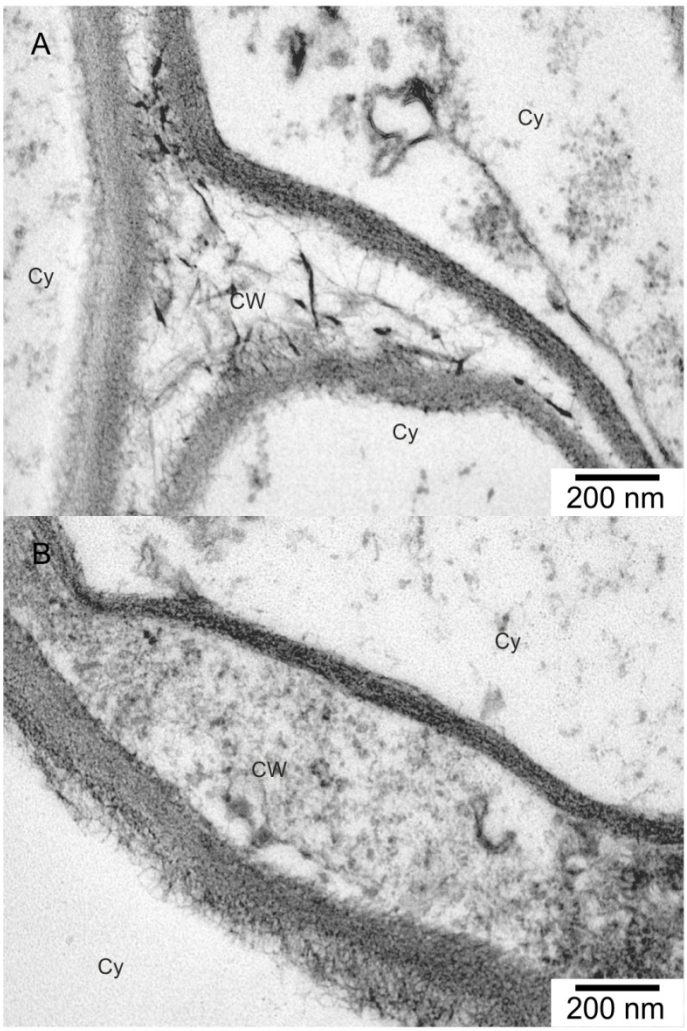

Figure 3.13 Electron micrographs showing the effects of gold on roots during germination

Transmission electron micrographs of root tissue from seven-day-old Arabidopsis seedlings germinated on A) ½MS(A) or B) ½MS(A) supplemented with 0.5 mM $KAuCl_4$ at pH 5.7. Samples were fixed and sectioned as described in Section 2.3. Key; CW, cell wall; Cy, cytoplasm.

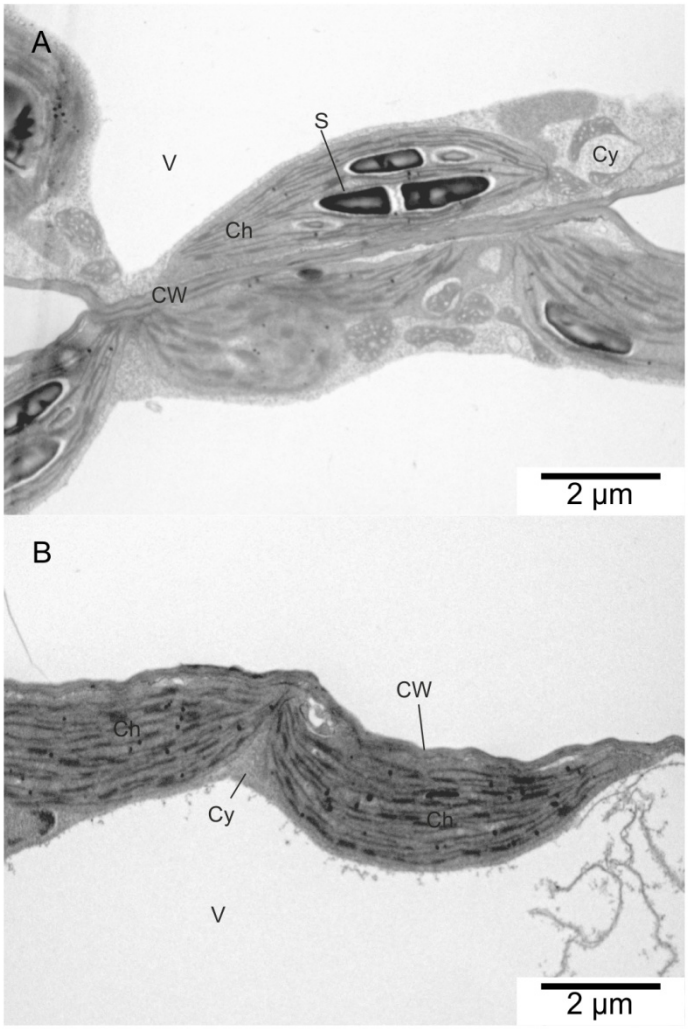

Figure 3.14 Electron micrographs showing the effects of gold on aerial tissue during germination

Transmission electron micrographs of aerial tissue from seven-day-old Arabidopsis seedlings germinated on A) ½MS(A) or B) ½MS(A) supplemented with 0.5 mM $KAuCl_4$ at pH 5.7. Samples were fixed and sectioned as described in Section 2.3. Key; Ch, chloroplast; CW, cell wall; Cy, cytoplasm; S, starch; V, vacuole.

3.3.3.6 Growth on higher $KAuCl_4$ concentrations

To determine the effects of increasing the $KAuCl_4$, Arabidopsis seeds were germinated and grown as described above on ½MS(A) plus $KAuCl_4$ at 0, 0.5, 1, 1.5 and 2 mM (pH 5.7) for seven days (Figure 3.15 and Figure 3.16). As has been described above (Section 3.3.3.1), the presence of $KAuCl_4$ caused the inhibition of Arabidopsis growth. Again, germination time and frequency were not affected. However, at the highest gold concentration (2 mM), root growth was

severely inhibited. In addition to this, at 2 mM, there was no development of aerial tissue.

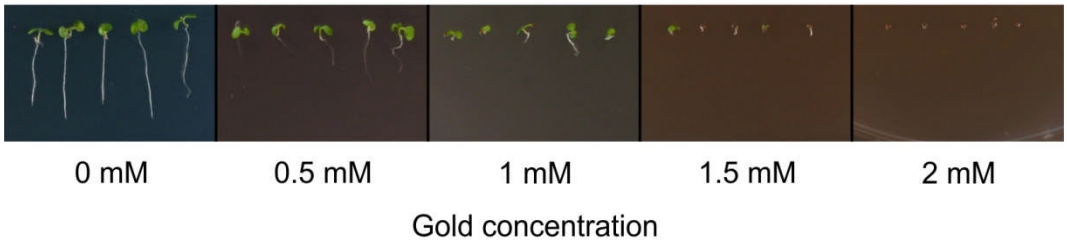

Figure 3.15 Arabidopsis seedlings grown on $KAuCl_4$
Seven-day-old Arabidopsis seedlings germinated on ½MS(A) plus $KAuCl_4$ at 0, 0.5, 1, 1.5 or 2 mM (pH 5.7).

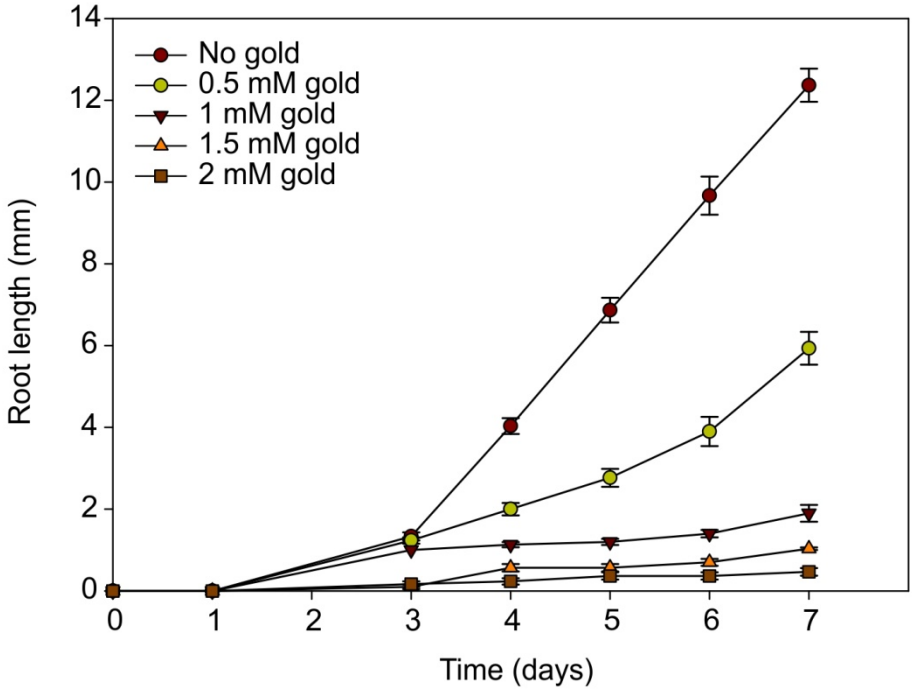

Figure 3.16 Growth of Arabidopsis seedlings on $KAuCl_4$
Root lengths of Arabidopsis seedlings germinated and grown on ½MS(A) plus different concentrations of $KAuCl_4$ (0, 0.5, 1, 1.5 and 2 mM) at pH 5.7. Lengths were measured over seven days. Data points represent the mean root length from 30 samples and error bars represent the standard error of the mean.

3.3.4 Gold uptake from hydroponics (submerged)

Arabidopsis seeds were germinated on ½MS(A) for seven days and subsequently transferred to sterile 100 mL conical flasks containing 20 mL of ½MS(S) as described in Section 3.2.4. Fourteen-day-old plants were treated with 0, 0.125, 0.25, 0.375 or 0.5 mM $KAuCl_4$ at pH 5.7. In order to investigate the binding of gold to plant material, some plants were autoclaved prior to treatment with $KAuCl_4$. Plant samples were harvested 24 hours after treatment and the gold concentration was measured as described in Section 3.2.1.2.

After 24 hours of treatment, live plants had a collapsed structure which was more severe as gold concentration increased (Figure 3.17). Gold concentrations within the plants increased as treatment concentration increased (Figure 3.18). This was also the case for dead plant material, although the autoclaved plants contained less gold than the live plants.

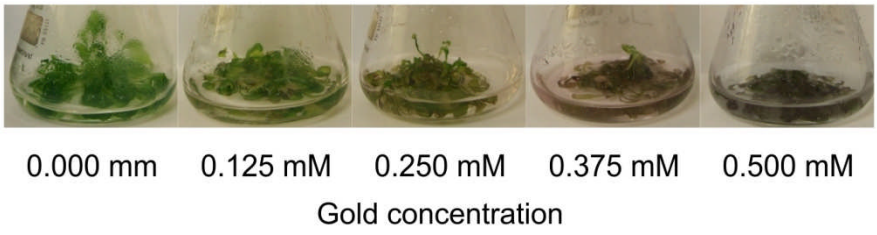

Figure 3.17 Hydroponically grown plants after treatment with gold.
Two-week-old Arabidopsis plants 24 hours after treatment with 0, 0.125, 0.25, 0.375 or 0.5 mM $KAuCl_4$ (pH 5.7).

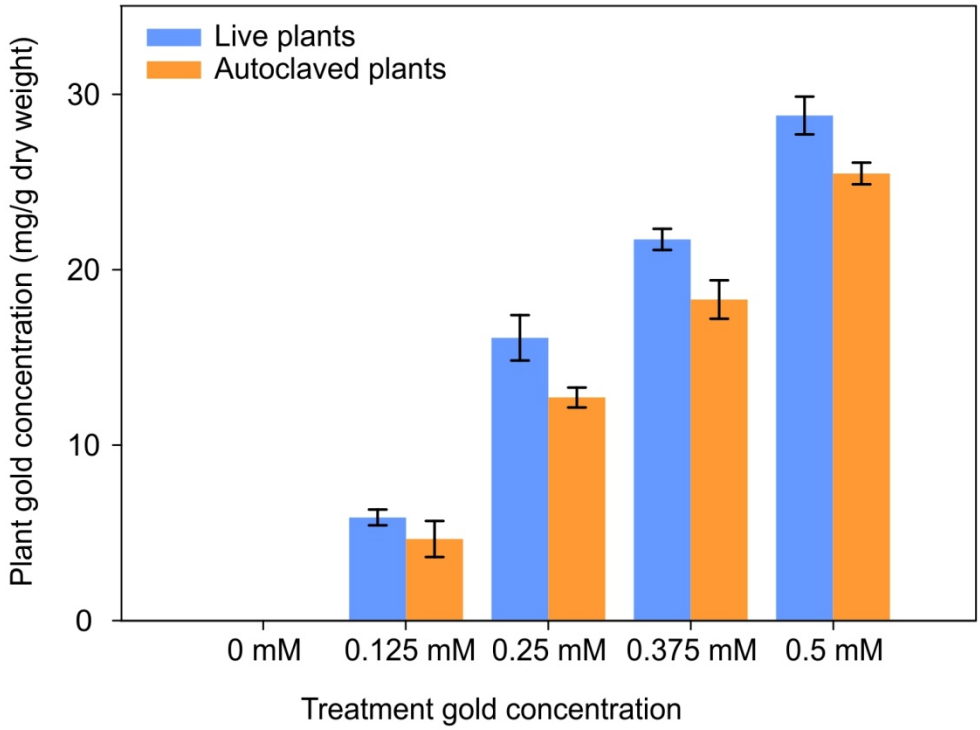

Figure 3.18 Gold uptake from hydroponically grown Arabidopsis plants
Gold concentrations in Arabidopsis plants grown for 14 days prior to 24 hours treatment with 0, 0.125, 0.25, 0.375, 0.5 $KAuCl_4$ (pH 5.7). Plants were either live or autoclaved to kill the plants. Results are the mean from four replicates and error bars represent the standard error of the mean.

3.3.5 Gold uptake and translocation in liquid culture

Arabidopsis seeds were germinated on sieves (as outlined in Section 3.2.5). After five weeks of growth, the liquid was replaced with water containing gold at 0, 1 or 2.5 mM gold for 20 hours (Figure 3.19). Root tissue for both treatments appeared to be healthy, although it was purple in colour suggesting that the gold(III) present in the media had been reduced to gold(0), possibly forming nanoparticles within the plant tissues. The aerial parts of the plants remained healthy and no colour changes were observed.

Root and shoot tissues were subsequently harvested and the gold content was analysed (Section 3.2.1.2). The gold concentration in the roots of both samples (Figure 3.20) was higher than in the shoots. This shows that although gold was translocated through the plant from the roots to the aerial parts, the majority remained in the roots. There were similar gold concentrations in the same tissues for the different samples, suggesting that in the 1 mM $KAuCl_4$ treatment, the plants had taken up the maximum that they could. In the 2.5 mM $KAuCl_4$ sample,

there was slightly more in the roots and slightly less in the shoots compared to the 1 mM $KAuCl_4$ sample. This led to a higher root to shoot ratio for the 2.5 mM $KAuCl_4$ sample (Table 3.4).

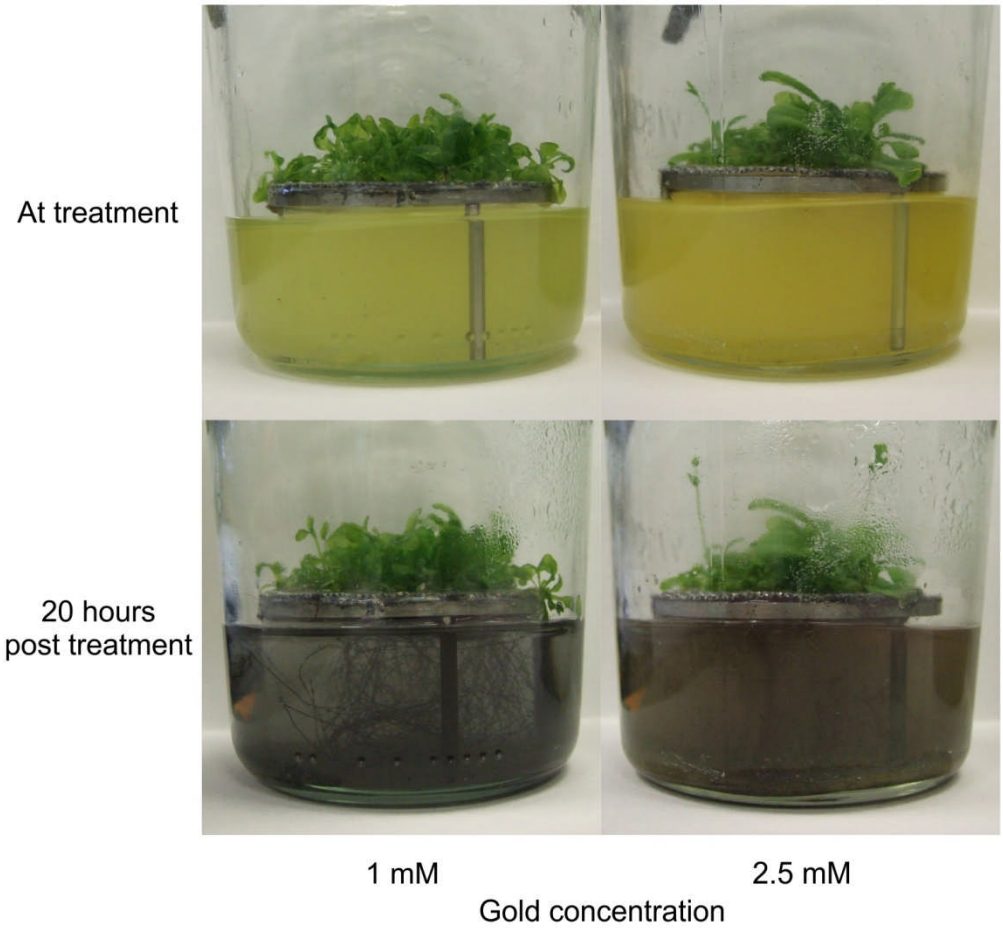

Figure 3.19 Sieve grown Arabidopsis plants after treatment with gold
Five-week-old Arabidopsis plants dosed with either 1 or 2.5 mM $KAuCl_4$ (pH 5.7). Images show the two treatments both at the time of treatment, and 20 hours after treatment.

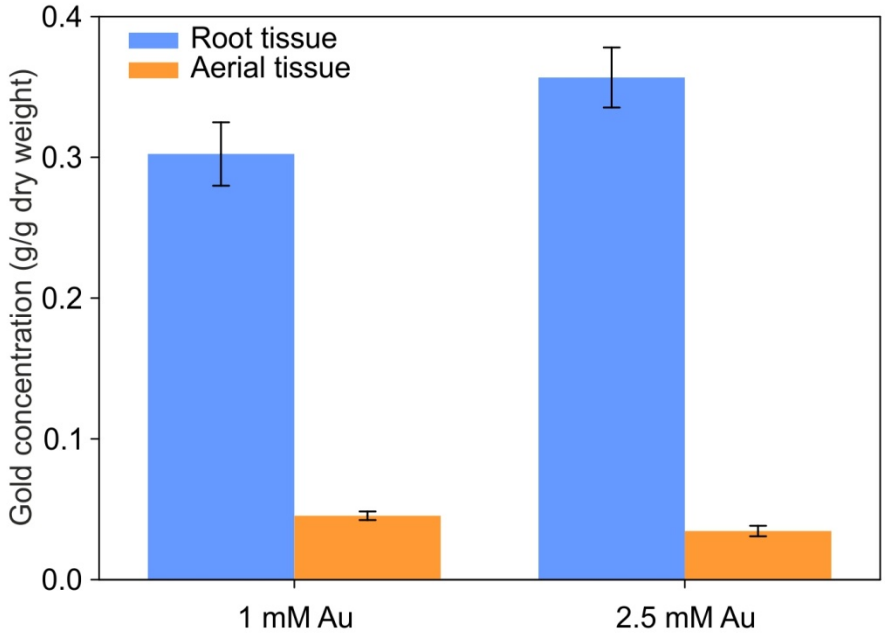

Figure 3.20 Gold concentrations in root and shoot tissue from sieve grown plants

Five week old Arabidopsis plants were treated with 1 or 2.5 mM $KAuCl_4$ (pH5.7). Root and shoot tissues were harvested and the gold concentration measured (as described in Section 3.2.1.2). Values are the mean concentration from three replicates and error bars represent the standard error of the mean.

Table 3.4 Gold concentration and root/shoot quotients from liquid culture

Gold concentration (dry weight) in the root and aerial tissues from five-week-old Arabidopsis plants dosed with 1 or 2.5 mM $KAuCl_4$ (pH 5.7) for 20 hours. Data are the means from three replicates.

	Gold concentration (mg/g)		
Treatment	**Root**	**Shoot**	**Root/shoot quotient**
1 mM Au	302.4	45.3	6.67
2.5 mM Au	356.7	34.5	10.35

3.3.5.2 Electron microscopy of sieve grown Arabidopsis

To determine whether gold nanoparticles could be seen within Arabidopsis as had been seen previously (Section 3.3.2.2), root and shoot tissues from no gold control and the material treated with 1 mM gold were fixed and sectioned. They were subsequently analysed using transmission electron microscopy (Figure 3.21 and Figure 3.22).

Gold nanoparticles were found throughout the tissues of the Arabidopsis roots. Nanoparticles were identified in the epidermis (Figure 3.21b) and in the central root cortex (Figure 3.21c). The particles within the root cortex indicate that gold had moved through the plant and had not only remained in the tissue in contact with the gold. There were also particles associated with the outside of the root tissue (Figure 3.21a). These were not in the epidermal layer but instead were outside of the plant structure, suggesting that there was external gold nanoparticle formation. This might explain the colour change of the roots to purple (Figure 3.19). The diameter of the profiles of the external particles ranged in size from 4 nm to 88 nm. These were larger than those in the epidermal tissue which ranged from 2 to 17 nm. Within the cortex, the nanoparticle profiles were 4 nm to 63 nm in diameter. All particle profiles seen in this experiment were spherical. This contrasts with the experiments described above (3.3.2.2), where nanoparticles of various shapes were identified.

Electron microscopy of the leaf tissue (Figure 3.22) indicated that no nanoparticles formed in the aerial tissue of the plants, even with the high concentration of gold seen (almost 45 mg/g dry weight). Nanoparticles were not visible in the epidermis of the leaf tissue or within the central vein of the leaf, suggesting that the gold(III) had not been reduced to gold(0) in these tissues.

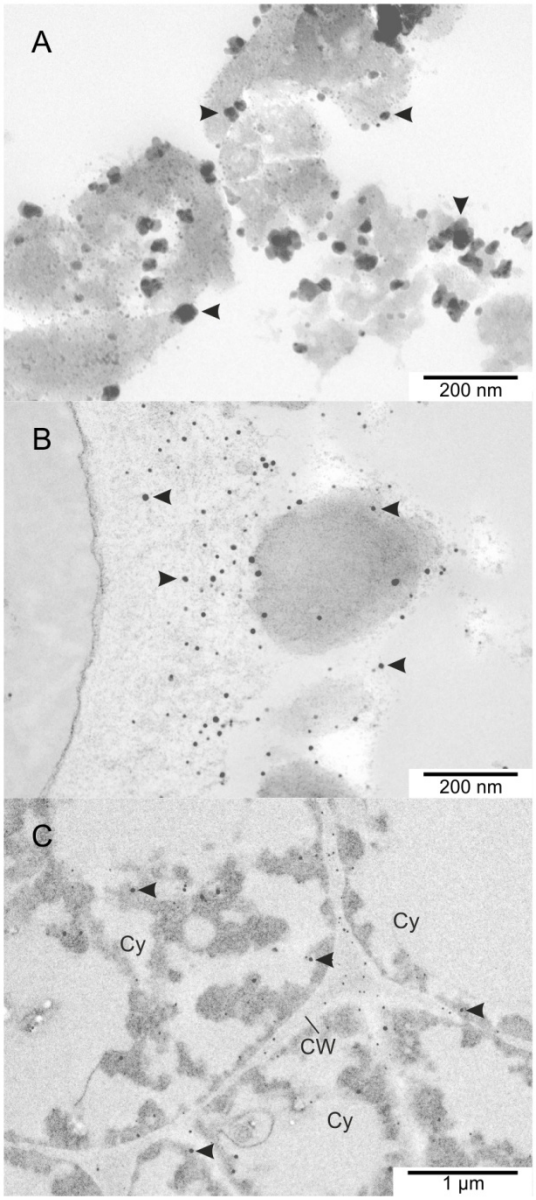

Figure 3.21 Electron micrographs of root tissue from sieve experiment
Transmission electron micrographs of root tissue from five-week-old Arabidopsis plants grown on sieves and dosed with 1 mM gold (pH 5.7). Micrographs represent A) outside the root tissue, B) epidermis tissue and C) root cortex tissue. Samples were fixed and sectioned as described in Section 2.3 without lead citrate staining. Key; CW, cell wall; Cy, cytoplasm. Example nanoparticles are indicated by arrows.

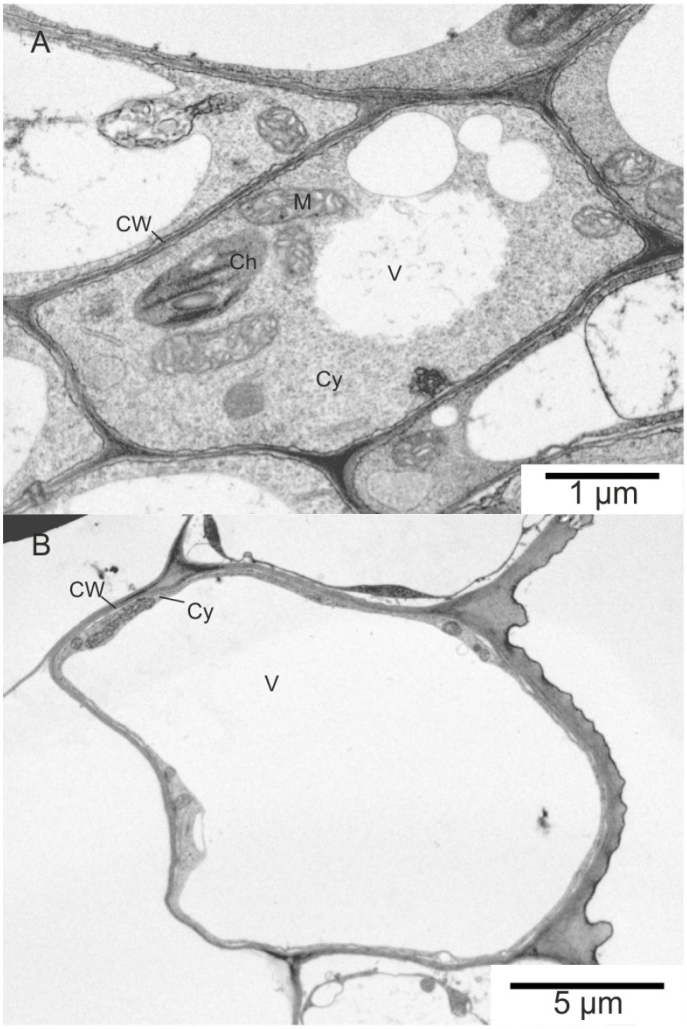

Figure 3.22 Electron micrographs of aerial tissue from sieve experiment
Transmission electron micrographs of aerial tissue from five-week-old Arabidopsis plants grown on sieves and dosed with 1 mM gold (pH 5.7). Micrographs represent two separate locations within leaf tissue A) epidermis, B) leaf vein cell. Samples were fixed and sectioned as described in Section 2.3, without lead citrate staining. Key; Ch, chloroplast; CW, cell wall; Cy, cytoplasm; M, mitochondrion; V, vacuole.

3.3.5.3 Microanalysis of gold nanoparticles

An electron micrograph section of the root from the 1 mM $KAuCl_4$ treatment (see Section 3.3.5 and Figure 3.21) was used to identify an area of putative gold nanoparticles. The chemical composition of the nanoparticles was determined using EDX as described in Section 2.3.1 (Figure 3.23). Peaks were identified and assigned by the software running an Oxford INCA analysis system. Peaks present at approximately 2.1, 9.7 and 11.5 keV were identified as gold. Other minor peaks were also identified at approximately 1.7, 2.3 and 2.9 keV. Bombarding the sample with electrons leads to the promotion of different electrons to higher energy states. Electrons from higher states then fall to the level of the promoted electron, emitting an X-ray. Different electrons may be promoted, and different electrons fall back into the available energy states emitting X-rays with different energies. This was the cause of the detection of gold at multiple energies in this experiment.

Copper was also identified at 8 keV (with smaller peaks at 0.9 and 8.9 keV). The presence of copper in the sample was because the sample was embedded on a copper grid to support the sample and X-rays are transmitted as background interference. Lead citrate was used to stain for the TEM sections and explains the presence of lead in the sample (at 2.3 and 10.6 keV). These data show that the putative nanoparticles observed in the electron micrographs are gold.

In order to confirm this, the electron diffraction pattern of the nanoparticles was analysed (Figure 3.23). As gold exhibits a face centred cubic crystal structure, the d spacing (the distance between atoms) was calculated using the equation outlined below, where *a* is the lattice parameter (4.08 Å for gold) and *h*, *k* and *l* are Miller indices.

$$d = \frac{a}{\sqrt{h^2 + k^2 + l^2}}$$

Calculating the d spacing for the d_{111} and d_{200} gave an expected ratio of 1.15 between the diffraction rings. The ratio between the diffraction rings in Figure 3.23 is 1.15, further confirming that the nanoparticles were gold. This evidence in combination with the EDX results described above shows that the particles visible in the electron micrographs are gold nanoparticles.

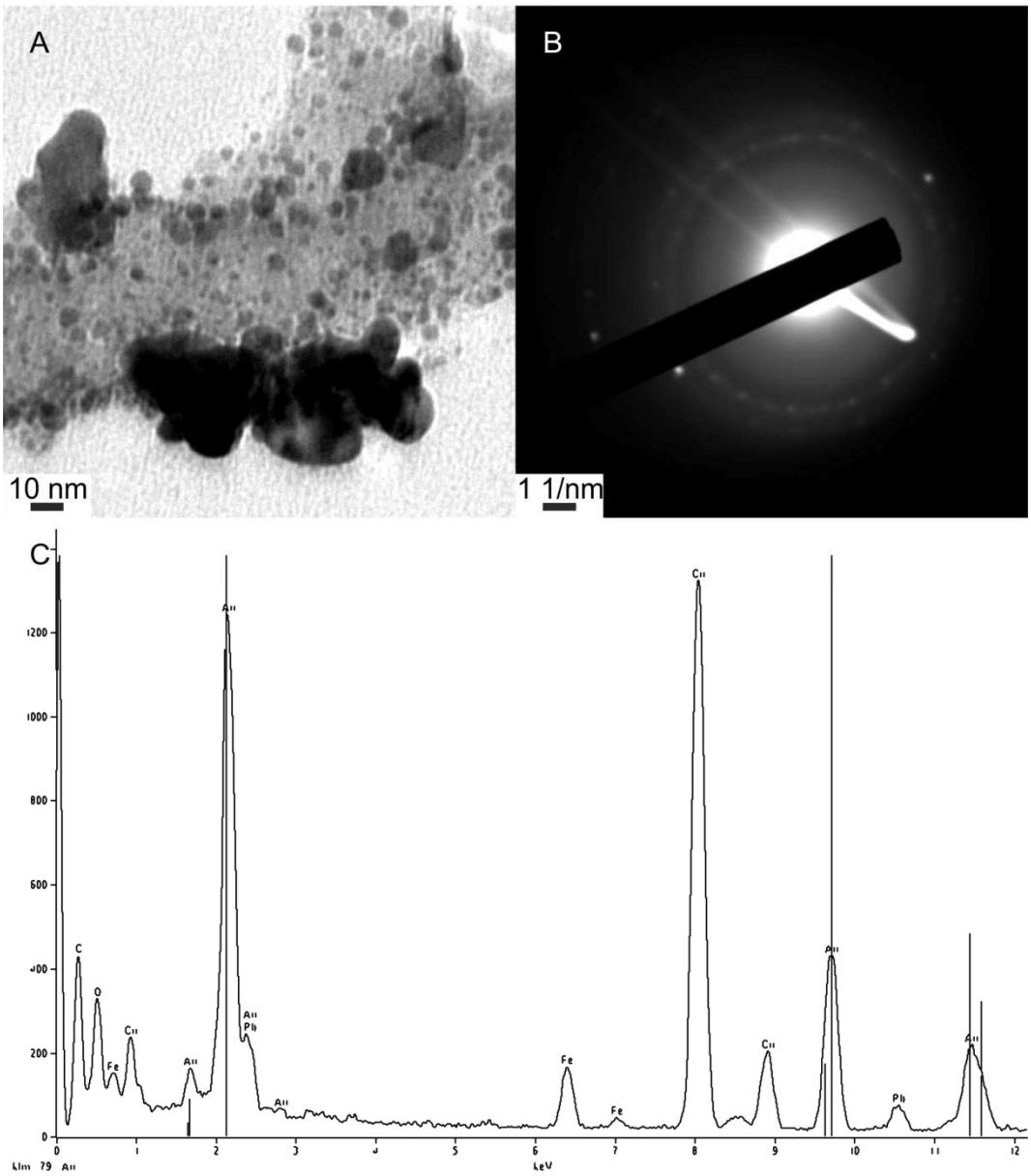

Figure 3.23 Microanalysis of gold nanoparticles
A) Nanoparticle cluster from the roots of plants treated with 1 mM gold (Section 3.3.5.2). B) Electron diffraction rings. C) EDX trace of the sample.

3.3.6 Gold uptake from soil

Previous work by other groups has found that gold is taken up from soil (see Section 3.1.1). This uptake can be increased by the addition of thiocyanate compounds to the soil which increases the solubility of gold. Arabidopsis plants were grown as described in (3.2.6) for eight weeks. After eight weeks, plants were treated with water or ammonium thiocyanate for one week (Figure 3.24). Root and shoot tissues were subsequently harvested and analysed for gold concentration (Figure 3.25 and Table 3.5). As would be expected, increasing the gold concentration resulted in an increased amount of gold in the plant tissues. For the samples without thiocyanate, the gold concentration in the roots was similar to that in the soil, showing that the plants did not accumulate gold above the concentration they were exposed to. Root concentrations were significantly higher than the shoot concentrations (3.7 and 6.4 fold for 5 and 50 mg/kg samples respectively) ($p<0.01$). Upon the addition of ammonium thiocyanate, the amount of gold in the shoots increased significantly ($p<0.01$). Upon the addition of ammonium thiocyanate, the root/shoot ratios decreased (3.7 to 2.7 fold and 6.4 to 1.8 fold in the 5 and 50 mg/kg samples respectively), although significantly more gold was located in the roots than in the shoots ($p<0.01$). Addition of ammonium thiocyanate increased the total amount of gold in the plants from 6.9 to 13.6 µg/g in the 5 mg/kg samples and 74.5 to 116.3 µg/g in the 50 mg/g samples. Thus, the addition of ammonium thiocyanate increased total gold uptake and translocation from roots to shoots in Arabidopsis.

The addition of ammonium thiocyanate was toxic to the plants (Figure 3.24) when compared to the plants grown on gold alone.

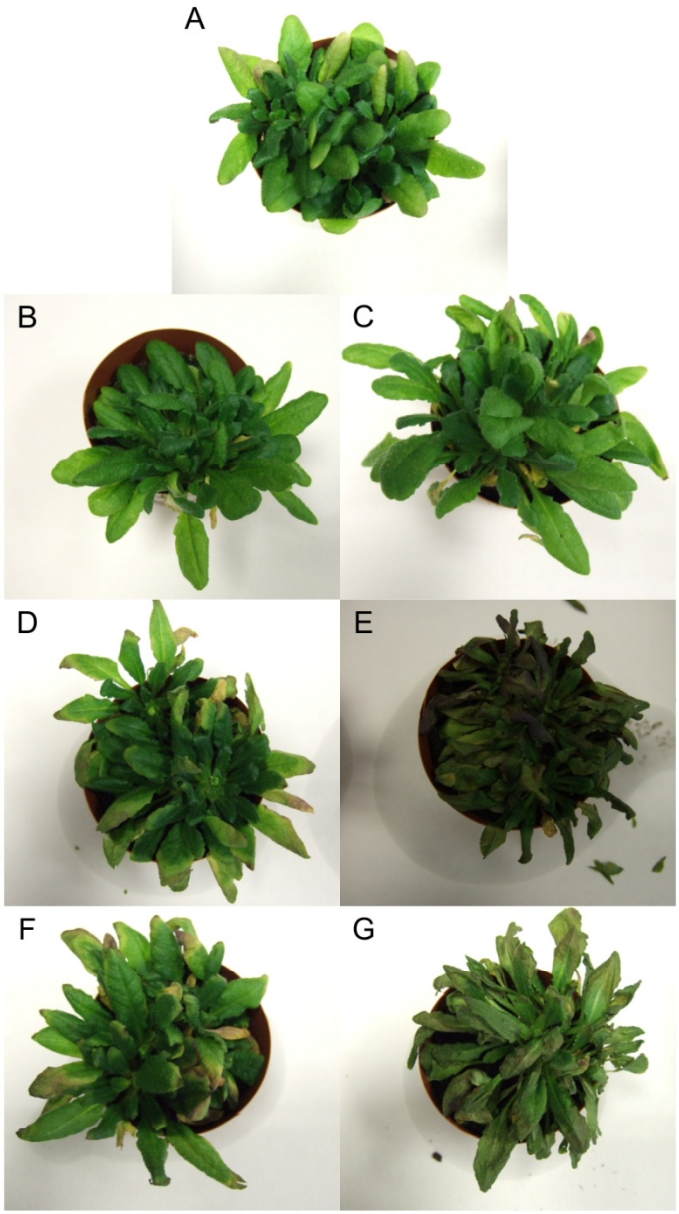

A - No gold or NH_4SCN
B - 5 mg / kg gold
C - 50 mg / kg gold
D - 0.5 g / kg NH_4SCN
E - 5 g / kg NH_4SCN
F - 5 mg / kg gold + 0.5 g / kg NH_4SCN
G - 50 mg / kg gold + 5 g / kg NH_4SCN

Figure 3.24 Arabidopsis after growth on soil containing gold
Eight-week-old Arabidopsis plants grown in soil supplemented with 5 or 50 mg/kg gold (as $KAuCl_4$) or with no supplement as noted in the key. Plants were treated with water, 0.5 g/kg or 5 g/kg ammonium thiocyanate as noted in the key. Plants were watered for one week after the thiocyanate treatment.

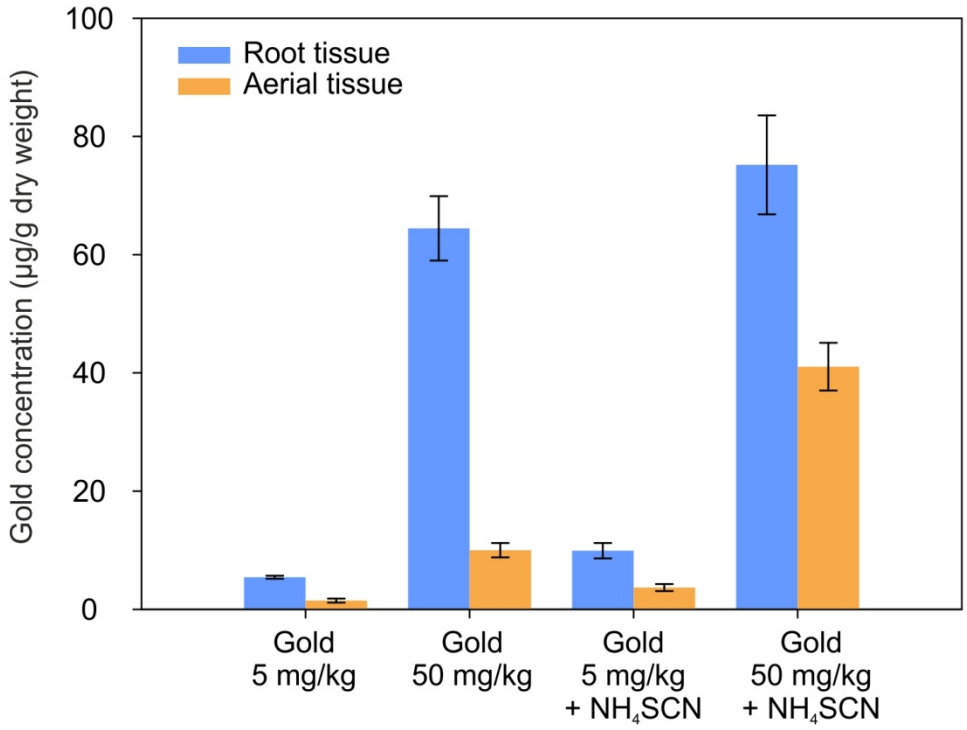

Figure 3.25 Gold uptake from soil
Gold concentration in the root and aerial tissues from eight week old Arabidopsis plants grown in the presence of gold (5 or 50 mg/kg) and subsequently treated with ammonium thiocyanate or water (control). Data are the means from eight replicates and error bars represent the standard error of the mean.

Table 3.5 Gold concentration and root/shoot quotients from soil uptake
Gold concentration (dry weight) in the root and aerial tissues from eight week old Arabidopsis plants grown in the presence of gold (5 or 50 mg/kg) and subsequently treated with ammonium thiocyanate or not. Data are the means from eight replicates.

	Gold concentration (µg/g)		
Treatment	**Root**	**Shoot**	**Root/shoot quotients**
Gold 5 mg/kg	5.4	1.5	3.7
Gold 50 mg/kg	64.5	10.0	6.4
Gold 5 mg/kg + thiocyanate	9.9	3.7	2.7
Gold 50 mg/kg + thiocyanate	75.2	41.1	1.8

3.3.6.2 Electron microscopy of soil grown plants

Aerial tissues from the plants harvested in the above experiment (Section 3.3.6) were analysed via electron microscopy. Sections of the tissue were prepared and viewed as described in Section 2.3 (Figure 3.26). From the analysis of all samples, no gold nanoparticles were visible in the aerial tissues of plants in any of the treatments, consistent with the findings in liquid and transfer experiments (see Sections 3.3.2, 3.3.3.5 and 3.3.5). The electron micrographs (Figure 3.26) show some electron dense bodies in the chloroplasts, however these are not nanoparticles but plastoglobules (see Section 3.3.2.2) and can also be seen in the plants treated without gold. The electron micrographs show that the addition of ammonium thiocyanate damaged the cells and chloroplasts. When ammonium thiocyanate had been added, there were fewer plastoglobules, and the thylakoids appear to have altered structure. There were no visible starch granules in the ammonium thiocyanate treated plants nor were there any when the plants had been treated with gold. Starch granules were only visible when the plants had not been treated with $KAuCl_4$ or ammonium thiocyanate (Figure 3.26a). As all samples were taken at the same time, differences in starch content are due to the treatment. Chloroplast deformity in the thiocyanate treated samples was unsurprising as the plants were visibly affected prior to electron microscopy analysis (see Figure 3.24 and Section 3.3.6).

Although root tissue was harvested for measurement of gold content, small amount of growth substrate which could not be separated from the root tissue meant that the roots were unsuitable for fixing and sectioning.

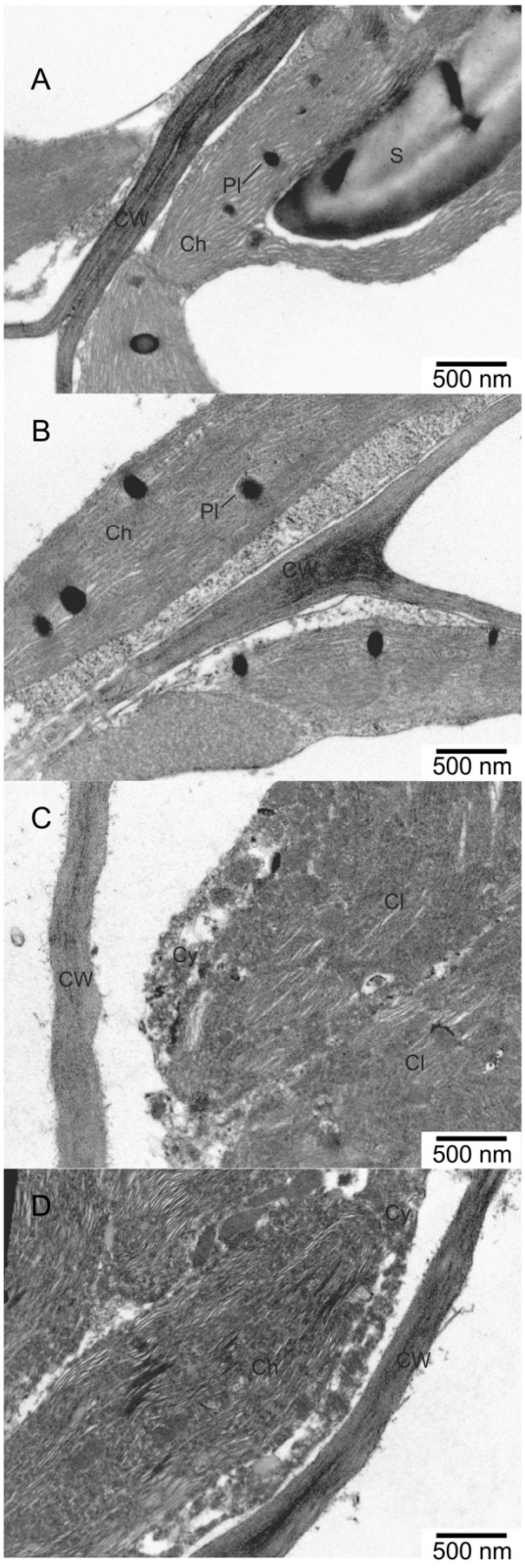

Figure 3.26 Electron micrographs of aerial Arabidopsis tissue from soil grown plants

Transmission electron micrographs of aerial tissue from eight-week-old Arabidopsis plants grown in the presence of gold. A) No gold or thiocyanate. B) 50 mg/kg gold, no thiocyanate. C) No gold, 5 g/kg thiocyanate. D) 50 mg/kg gold, 5 g/kg thiocyanate. Key; Ch, chloroplast; CW, cell wall; Cy, cytoplasm; Pl, plastoglobules; S, starch.

3.3.7 Formation of gold nanoparticles in soil grown alfalfa

As described above (Section 3.3.6), no gold nanoparticles were visible in the aerial tissue of Arabidopsis when the plants were grown in soil containing gold. Previous research has shown that in the presence of gold, alfalfa contains gold nanoparticles in the aerial tissues (Gardea-Torresdey et al. 2002a). To determine whether the results described in Section 3.3.6 were due to species differences between alfalfa and Arabidopsis, or whether differences in the experimental methods used in this work and those used by Gardea-Torresdey et al. (2002a) were the reason nanoparticles were not present in Arabidopsis, alfalfa was grown in the presence of soil, as described in Section 3.2.7 (Figure 3.27). The gold concentration within the root and shoot tissues of the plant were measured (Table 3.6).

Table 3.6 Gold concentration and root/shoot quotients in alfalfa
Gold concentration (dry weight) in the root and aerial tissues from eight-week-old alfalfa plants grown in the presence of 50 mg/kg gold. Data are the means from six replicates.

	Gold concentration (µg/g)		
Treatment	**Root**	**Shoot**	**Root/shoot quotient**
Gold 50 mg/kg	115.0	21.3	5.4

Electron microscopy was carried out on the aerial tissue of the alfalfa plants (Figure 3.28). No gold nanoparticles were visible in the no gold control material (Figure 3.28a). In the plants which were grown in the presence of gold, nanoparticles were visible in both the cell cytoplasm and the cell wall between the cells (Figure 3.28b-d). These nanoparticles had spherical profiles, and ranged from 0.5 nm to 10 nm. Particles were larger in the cytoplasm compared to the cell wall (maximum size of 12 nm compared to 7 nm) although the mean nanoparticle sizes were similar (2.5 nm in the cell wall compared to 4 nm in the cytoplasm). These data suggest that there are differences between the Arabidopsis and alfalfa plants in the formation of gold nanoparticles.

Electron microscopy analysis of the root tissue could not be carried out because of residual growth substrate attached to the roots. This meant that fixing and sectioning was not possible.

Figure 3.27 Growth of alfalfa in the presence of gold
Eight-week-old alfalfa grown in the presence of gold. Seeds were germinated on ½MS(A) for three days prior to transfer to soil.

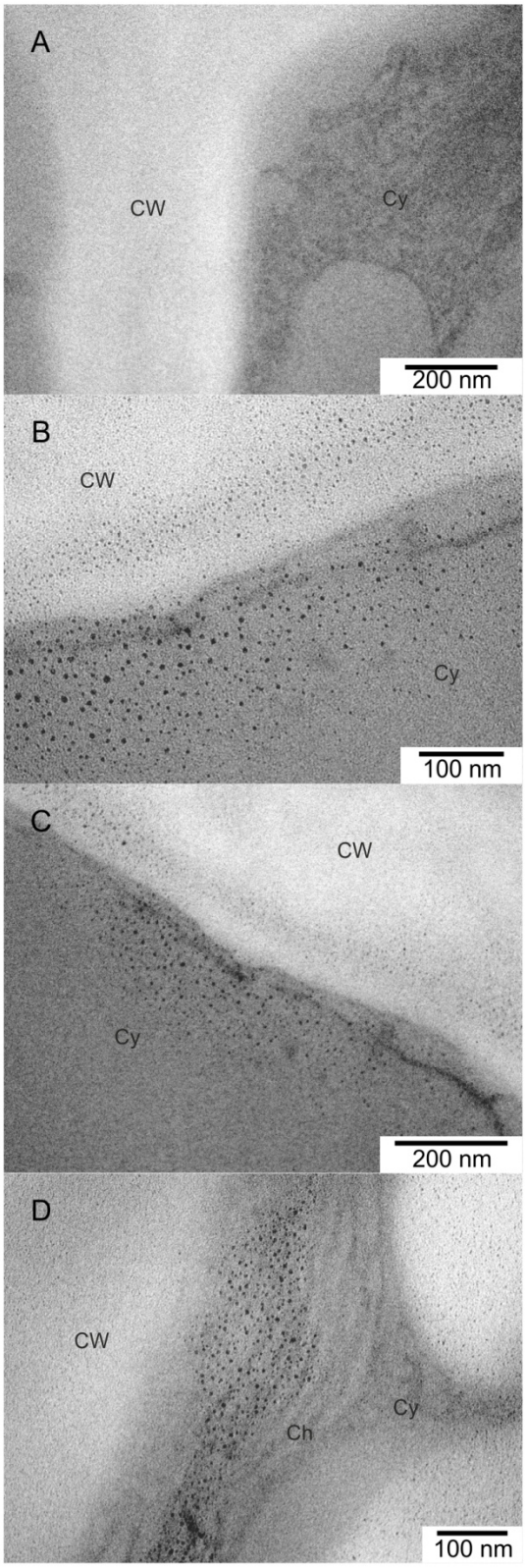

Figure 3.28 Electron micrographs of aerial alfalfa tissue
Transmission electron micrographs of aerial tissue from eight-week-old alfalfa plants grown in compost. A) No gold control B-D) Compost contained 50 mg/kg gold. A-C) Cytoplasm and cell wall of leaf tissue. D) Chloroplast. Samples were fixed and sectioned as described in Section 2.3. Key; Ch, chloroplast; CW, cell wall; Cy, cytoplasm.

3.3.8 Formation of gold nanoparticles

Research published looking at the uptake of gold from solid media by alfalfa (Gardea-Torresdey et al. 2002a) found that gold nanoparticles were present throughout the plant. An hypothesis in the research was that gold(III) is reduced to gold(0) nanoparticles in the growth media and these nanoparticles are subsequently transported into the plant. To test this hypothesis, alfalfa seedlings were treated with gold nanoparticles to study the uptake and distribution within the plant tissues. Five-day-old alfalfa seedlings were transferred to 96 well cell culture plates (see Section 3.2.8).

The nanoparticles were supplied by the manufacturer at 7, 18, 48 and 108 nm. Prior to treating plant samples, the nanoparticles were measured as described in Section 3.2.8 (Figure 3.29 and Figure 3.30). None of the nanoparticles were the sizes stated by the manufacturer, although the sizes were similar. The mean sizes of the four batches were 10, 22, 52 and 118 nm. The sizes determined by the manufacturer are the sizes referred to throughout this section for convenience.

After 24 hours of treatment, seedlings were studied using electron microscopy as described in Section 2.3 (Figure 3.31). No gold nanoparticles were found within the plants treated with water alone. Additionally, nanoparticles were found to be distributed throughout the root of the plants treated with 0.25 mM $KAuCl_4$. However, no nanoparticles were found within the roots of any of the plants treated with gold nanoparticles, therefore showing that the nanoparticles were not taken up. Representative images for all of these treatments are described in Figure 3.31, although only images from the nanoparticle treatments with controlled gold concentration are shown: samples controlled for nanoparticle concentration were identical.

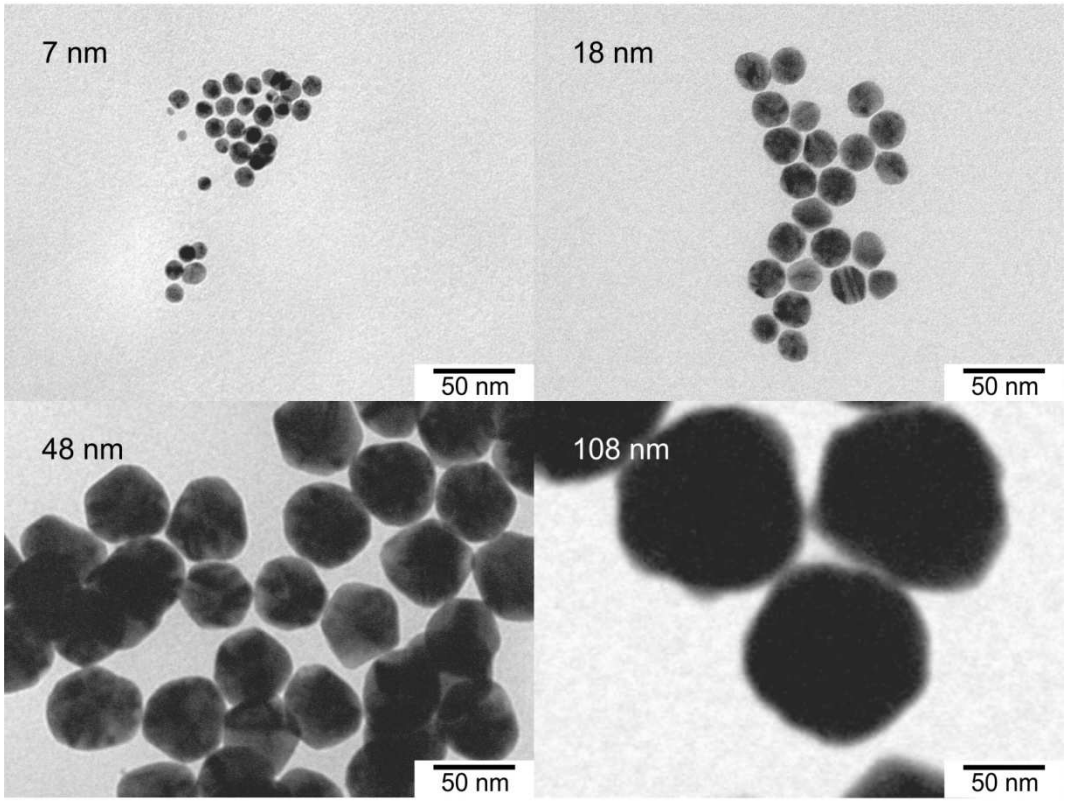

Figure 3.29 Electron micrographs of the nanoparticles in the four treatments

Nanoparticles supplied by Nanopartz and used in the four treatments. Nanoparticles were suspended on a 200 mesh thin-bar Athene grid and viewed using TEM. Images are representative of all of those taken. Sizes noted are those provided by manufacturer.

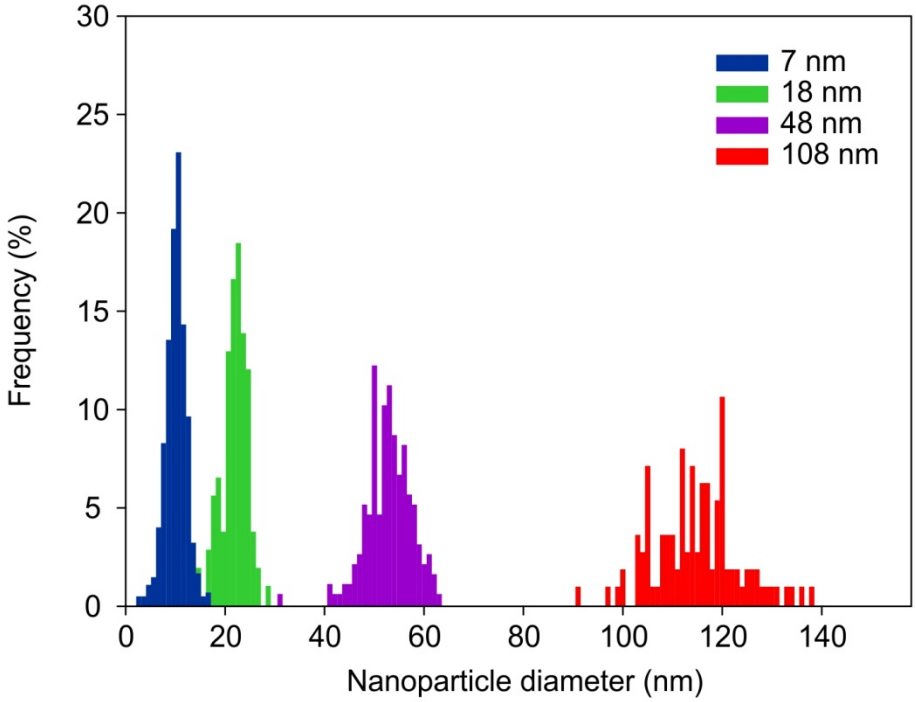

Figure 3.30 Size distribution of the nanoparticles in the four treatments
Frequencies of nanoparticle sizes for the nanoparticles supplied by Nanopartz and used in the uptake experiment. Distributions are presented for nanoparticles supplied at 7, 18, 48 and 108 nm.

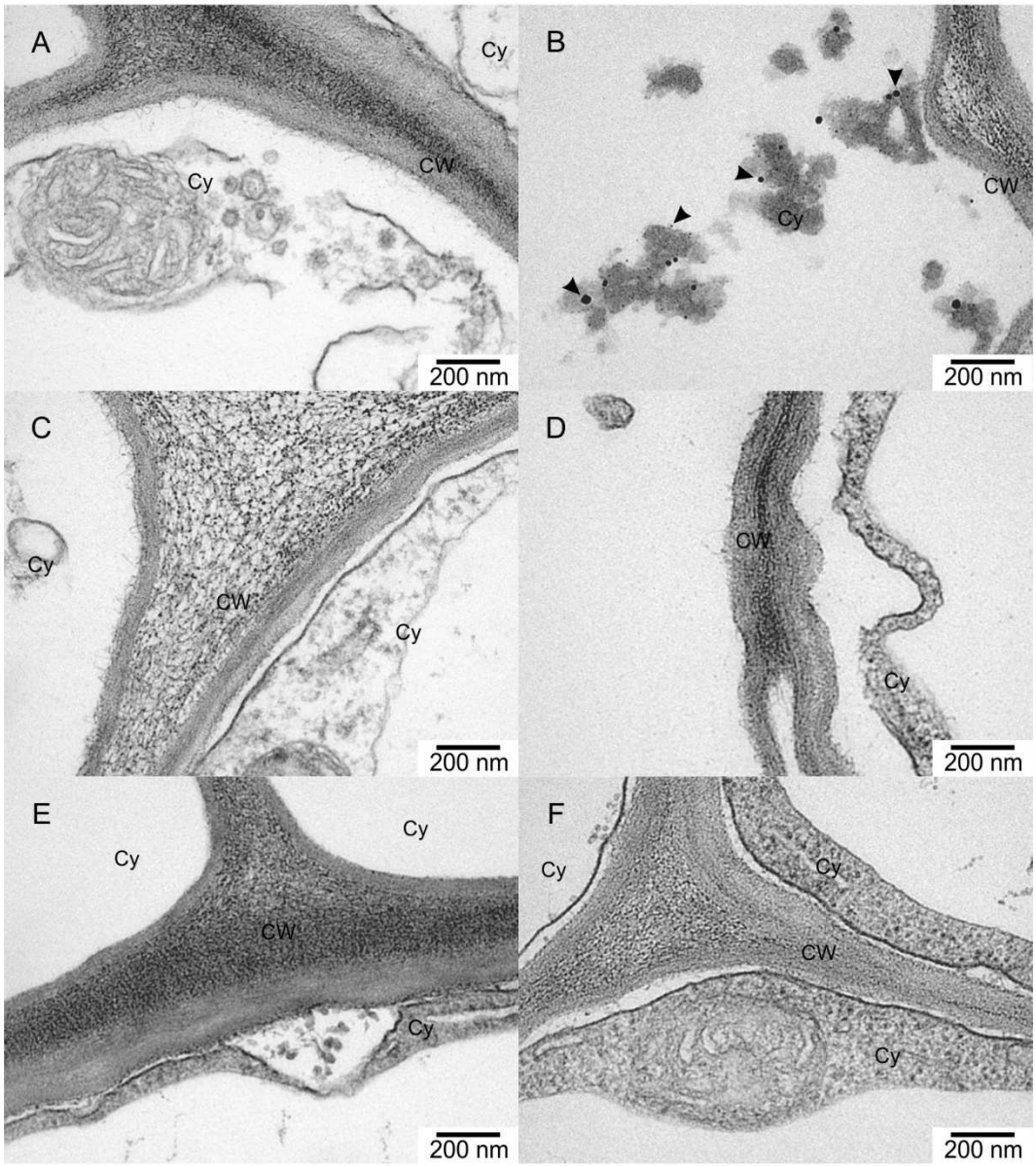

Figure 3.31 Alfalfa epidermal root cells after Nanoparticle treatments
Five-day-old alfalfa seedlings were treated with gold nanoparticles (or a water or 0.5 mM gold control) for 24 hours. These were fixed and sectioned prior to electron microscopy. Images are representative images of the treatments. A) No gold control, B) 0.25 mM $KAuCl_4$, C) 7 nm particles, D)18 nm particles, E) 48 nm particles, F) 108 nm particles. Nanoparticle sizes were those determined by the manufacturer (see text for details of measurement in this work). Nanoparticle treatments were either controlled for gold concentration (0.25 mM) or number of particles (3.65×10^8 particles per mL). Only those with equal gold concentration are described in this figure; results were identical when the number of particles was controlled. Key; CW, cell wall; Cy, cytoplasm. Example nanoparticles are indicated by arrows.

3.4 Discussion

Presented in this Chapter are experiments performed to characterise gold uptake and tolerance in Arabidopsis. Previous work (see Section 3.1.1 and Chapter 1) demonstrated that although plants have been shown to take up gold, no mechanisms had been elucidated. In order to use Arabidopsis to discover mechanisms of gold uptake or response, the physiology of the plant in response to gold had to be studied.

Prior to characterising gold uptake in Arabidopsis, a robust method for measuring gold concentration in plant materials was developed (Section 3.3.1). This is similar to a previously published method for measuring plant gold concentration (Anderson et al. 2005a), but with the following modifications; dry plant material was ashed at 550 ºC, rather than 530 ºC; ashing was carried out for six hours, rather than 14 hours; samples were diluted with water (to 10 mL), rather than 2 M HCl. Results from this method required a slight correction in the measured gold concentration due to evaporation of the aqua regia. The method described is most accurate when measuring the gold concentration in plant tissue above 50 µg/g (dry weight) although the method was suitable for use at concentrations of 5 µg/g with a larger correction.

3.4.1 Toxicity of gold

The data presented in this work show that gold is toxic to Arabidopsis plants when germinated on $KAuCl_4$ (Section 3.3.3). Although germination was not inhibited, in the presence of gold, seedling root growth was inhibited. Additionally, when grown in soil containing gold, the chloroplasts of Arabidopsis contained less starch than the plants grown in soil that did not contain gold. This therefore suggests that photosynthesis was compromised as the plants did not accumulate enough sugar to convert to starch.

It has previously been shown that the roots of some species of plant do not grow as long when grown in the presence of gold ($KAuCl_4$) (Binder et al. 2007; Rodriguez et al. 2007; Sharma et al. 2007; Starnes et al. 2010). The results presented here show that gold inhibited root growth of Arabidopsis seedlings. Further tests determined that gold was the toxic component of the compound added to the growth media. The potassium and chloride components of $KAuCl_4$

were not at high enough concentration to be toxic. Root growth is inhibited by KCl above 100 mM (Zhu et al. 1998) and so root growth was not expected to be inhibited at the concentrations used in this work. Additionally, impurities in $KAuCl_4$ (Table 3.3) were not at toxic concentrations in the media. Although root length growth was inhibited by gold, germination rates were the same as without gold. Gold therefore did not inhibit germination, but inhibited root elongation after germination, a finding consistent with previously published research (Binder et al. 2007). There was a positive correlation between inhibition of root growth and gold concentration in the growth media. At concentrations above 1.5 mM, root elongation was halted completely after radicle emergence and remained this way for the duration of the experiment. The presence of gold in soil-based experiments found that there was no inhibition of growth in either Arabidopsis or alfalfa. This is likely to be due to the reduced bioavailability of the gold within the soil caused by the organic matter within this substrate. Although some research states that below 80 µM, gold acts to stimulate growth (Gardea-Torresdey et al. 2005; Rodriguez et al. 2009) the data presented here and in other studies do not suggest that this is the case.

Previous research has shown that aquaporin function can be inhibited by gold (Niemietz and Tyerman 2002). This is likely to be due to the binding of gold to the sulfhydryl groups of cysteine within the aquaporins (Niemietz and Tyerman 2002). The inhibition of aquaporins could therefore reduce the water permeability of the root cells and so water uptake could decrease. Some maize aquaporins are found to be expressed in areas of root elongation (Chaumont et al. 1998). It is therefore possible that blocking these aquaporins in Arabidopsis could reduce root elongation and be part of the cause of the gold toxicity presented here. This has previously been reported to be a reason for mercury toxicity (Zhang and Tyerman 1999). Further to this, it is thought that gold may oxidise disulfide bonds within proteins and so therefore may act to disrupt proteins key to Arabidopsis root elongation, leading to toxicity (Best and Sadler 1996; Rodriguez et al. 2007). Although little is known of gold toxicity to plants, research with other metals may give clues as to why gold is toxic. It is possible that in addition to disrupting protein structure, gold may displace other essential metals from within proteins, inhibiting protein function and leading to deficiency effects of these metals (Van Assche and Clijsters 1990). The formation of free radicals may also be a problem, causing oxidative stress and possibly inhibiting mitochondrial function (Halliwell and Gutteridge 1984; Messer et al. 2005). Gold tolerance has been

improved by the expression of a mercuric ion reductase from bacteria (Rugh et al. 1996) suggesting that toxicity may have been due to the ionic form of the gold. As gold(III) is likely to be reduced to gold(0) by MerA, it therefore seems that ionic gold is more toxic to plants than gold(0).

It has previously been hypothesised, that because copper is involved in the binding of ethylene to the ETR1 ethylene receptor and that silver ions have been shown to block the action of ethylene in plants, then gold may also inhibit ethylene action (Binder et al. 2007). Gold ions were found to support ethylene binding to ETR1, however, unlike silver, the gold ions did not inhibit the action of ethylene within the plants, even though the presence of the gold reduced plant growth. Therefore, the inhibition of root growth described here is unlikely to be due to disruption of ethylene action.

3.4.2 Gold translocation through Arabidopsis

In both the liquid and soil studies gold was taken up and translocated through Arabidopsis (Sections 3.3.5 and 3.3.6). The majority of the gold was found within the root tissues as this was the point of entry for the gold. Root to shoot ratios from the two experiments show that proportionally more gold was translocated to the aerial tissues in the soil study than in the liquid culture study. In the soil study, the addition of ammonium thiocyanate to the soil increased both the uptake, and translocation of gold to the aerial tissues. This was likely due to the increased availability of the gold.

In the soil uptake experiment, the gold concentration within the roots was similar to the gold concentration of the soil in which the plants grew, although the concentration increased with ammonium thiocyanate treatment. This therefore suggests that gold was not bioconcentrated and that uptake was a passive, rather than an active, process. Other studies have also found low concentrations of gold in the plants similar to the concentration in the soil (Msuya et al. 2000; Piccinin et al. 2007). Upon the addition of ammonium thiocyanate, the gold concentration within the plant increased due to the increased solubility and thus availability of the gold to the plant. Root to shoot translocation also increased with the addition of ammonium thiocyanate. Although in the literature there is large variation in the reported gold concentrations upon the addition of cyanid-based compounds, including ammonium thiocyanate and sodium or potassium cyanide,

the gold concentrations described in this work are consistent with the range described previously (Table 1.4) (Anderson et al. 1998; Msuya et al. 2000; Lamb et al. 2001; Anderson et al. 2005b; Haverkamp et al. 2007; Piccinin et al. 2007). The cellular ultrastructure of the Arabidopsis plants treated with ammonium thiocyanate appeared to be altered, and appeared toxic to the plants when compared to the plants grown on gold alone (Figure 3.24). Ammonium thiocyanate has previously been described as phytotoxic (Hansson et al. 2008) and so is likely to be the cause of the difference in cell ultrastructure.

Hydroponic plant growth experiments (Section 3.3.5) show that some of the gold was bound to the plant material, rather than taken up. Although autoclaved plants had around 80% of the concentration of live plants, the actual amount of binding is likely to be lower than this. Autoclaving the plant material will have increased the surface area of the material by disrupting the plant tissue and so increased the number of sites gold could bind. Other methods of inhibiting gold uptake, such as using dry plant material would also have altered the plant material so that it was not directly comparable to the live tissue. Alternatively, inhibitors of transporters could have been used, although probable interactions with gold and competition for binding sites would have also interfered with the amount of gold binding to the tissue.

3.4.3 Nanoparticle formation

Transmission electron micrographs show electron dense spots which are described throughout this text as nanoparticles. Although not every electron dense spot was tested and shown to be a gold nanoparticle, the lack of these electron dense spots in the controls and the EDX analysis described in Section 3.3.5.3 give confidence that they are gold nanoparticles. The shapes of nanoparticles described in this work are the two-dimensional profile of the nanoparticle as seen in the electron micrographs. Serial sections were not performed to verify the three-dimensional structures.

Gold nanoparticles were found to form in the roots of Arabidopsis seedlings when transferred to growth media containing gold. These nanoparticles were various shapes and sizes with some particles too large to be classed nanoparticles as at least one of the measureable sides was larger than 100 nm (see Section 1.5). The nanoparticle size depended on the pH of the media: nanoparticles were

smaller when the seedlings were transferred to ½MS(A) plus 0.5 mM gold at pH 5.7 compared those transferred to ½MS(A) plus 0.5 mM gold at pH 3.7 (see Table 3.2). In both of these conditions, nanoparticles were found throughout the root tissue, showing that gold was translocated through this tissue and did not only remain in the cells in contact with the treatment. However, the nanoparticles within the epidermis appeared to be more densely distributed than in the root cortex suggesting that there was more gold within the epidermis. Gold nanoparticles were not seen in the aerial parts of the plant, suggesting that the gold was not present as gold(0) or that no gold was present in the aerial tissues. Alternatively, the gold nanoparticles could have been present, but smaller than the resolution of the electron microscope (under 5 nm). The purple colour of the roots found in the transfer experiments (Figure 3.5) suggested that when the pH was lowered, more gold was deposited on the root tissue. As the media the seedlings were transferred to changed colour in a similar manner for both treatment types, the amount of gold available to the plants is unlikely to be different between the treatments, and as such, gold deposition was determined by pH and not gold availability. Previous studies have found that at lower pH, there was more absorption of gold nanoparticles bound externally to dead plant biomass (Armendariz et al. 2004), further suggesting that this was the reason for the difference in colour. In the translocation experiments, root tissue did turn purple, suggesting gold deposition at pH 5.7, although as the gold was in a liquid, the availability for the plant and thus the amount available for deposition on the root surface was increased.

Recently, pH has been shown to have an effect on the size and shape of gold nanoparticles in plants (Starnes et al. 2010). This could go some way in explaining why there were differences in the sizes and shapes of the gold nanoparticle profiles observed. Nanoparticle size has also been shown to be affected by pH in the synthetic production of nanoparticles using citrate reduction (Patungwasa and Hodak 2008) and when nanoparticles were produced using bacteria (Nakajima 2003; He et al. 2007; Deplanche and Macaskie 2008). It would be interesting to further study the effect of pH on intracellular nanoparticle formation by transferring plants to media containing $KAuCl_4$ at a range of pHs including acidic and alkaline conditions. Although the effect of time on gold nanoparticle formation was not studied, previous work has found that the amount of time plants are treated with gold did not have an effect on the size or shape of nanoparticles (Starnes et al. 2010).

In contrast to the results for the transfer experiments, when seeds were germinated on gold, the seedlings did not contain gold nanoparticles in either the roots or shoots (Section 3.3.3). Although the plates were chemically identical to the plates in the transfer experiment, it is unknown why these seedlings did not contain nanoparticles. The results would suggest that the chemistry within the roots between the germinated and transferred plants is different. Additionally, the experimental methods may have affected the formation of gold nanoparticles. Seedlings germinated on ½MS(A) containing gold were exposed to gold for longer compared to the transferred plants and as such had longer to respond to the presence of gold. Although the colours of the plates in both experiments were similar for each concentration, suggesting that the gold available to the plants was the same, this is unlikely to be correct. The ½MS(A) containing gold for the germination experiment was seven days older than that in the transfer experiment at the end of the experiments and as such, it is likely that over this time, less gold was available to the plants. Thus, the availability of gold for the transferred plants would be higher, and so more would be taken up. Nanoparticle formation is therefore more likely if more gold is within the roots.

Nanoparticles formed in the roots of plants transferred to liquid media containing gold (Section 3.3.5). These nanoparticle profiles were various sizes, generally spherical and were distributed throughout the root tissues. Although there was a substantial amount of gold in the aerial tissues (up to 45 µg/g of gold per dry weight) no nanoparticles were visible using transmission electron microscopy, suggesting that the gold present was not gold(0) or that the nanoparticles were too small and thus below the resolution of the Tecnai 12 Bio Twin TEM used. This could be confirmed using X-ray absorption spectroscopy (see below). There could therefore be physiological differences between the root and shoot tissues, leading to the differences in nanoparticle formation observed. As in the liquid culture translocation experiments, no nanoparticles were found in the aerial tissues of Arabidopsis grown on soil containing gold, even though gold had been found in these tissues (Section 3.3.6). This further suggested that Arabidopsis was unable to form nanoparticles in the aerial tissues, even though this has been seen in other plant species (Gardea-Torresdey et al. 2002a; Gardea-Torresdey et al. 2005; Haverkamp et al. 2007; Marshall et al. 2007; Rodriguez et al. 2007; Sharma et al. 2007; Starnes et al. 2010).

It is unknown why nanoparticles were not formed in these aerial tissues. Biochemical differences between the root and shoot tissues is a likely explanation for the differences in nanoparticle formation. In contrast, gold nanoparticles were found in the leaves of alfalfa (Section 3.3.7). The gold concentrations in alfalfa and Arabidopsis were similar. It is there likely that the difference in nanoparticle formation is due to biochemical differences in the aerial tissues between the species. Research in *B. juncea* showed that gold reduction to gold(0) is not a complete process in this species (Marshall et al. 2007). Therefore it is possible that reduction had not occurred at all. The size of nanoparticles is also likely to be dependent on the concentration of gold within the tissues (Rodriguez et al. 2007) and so the lower concentrations seen in aerial tissues may mean that nanoparticles were below the resolution of the TEM used. However this is perhaps unlikely due to the high concentrations of gold seen in the aerial tissues in the translocation experiment (50 mg/g).

Nanoparticle synthesis research hypothesises that cysteine is able to nucleate the formation of gold nanoparticles *in vitro* (Mocanu et al. 2009). Hence, differing cysteine levels in the different tissues may lead to the observed differences in nanoparticle formation. This could be tested by the biochemical analysis of the different tissues to study the cysteine content. Cysteine is effective at reducing gold(III) to nanoparticles due to the reaction of the sulfhydryl group with the gold (Mocanu et al. 2009). Research has indicated that it may not only be cysteine involved in the reduction of gold ions to nanoparticles, carboxyl and amino groups may also contribute to the reduction (Beveridge and Murray 1980; Armendariz et al. 2004), as well as hydroxyl groups (Esumi et al. 2000) and other amino acids and pepsin (Gole et al. 2001). As cysteine is thought to be involved, studying the glutathione content and production in plants may also be informative as to how and where nanoparticles form, especially as glutathione is depleted and glutathione reductase inhibited by various metals (Schutzendubel and Polle 2002).

Although gold nanoparticles have been described in this work, it is unknown whether other oxidation states of gold are present in the plant tissues. For example, even though gold(0) nanoparticles were seen, other oxidation states of gold may have been present alongside these (i.e. gold(I) or gold(III)). In some cases (i.e. the germination experiment and in aerial tissues), gold nanoparticles were not evident, even when gold was present. This may have been due to

nanoparticle size (as described above) or because the gold was present in other oxidation states, hence not in nanoparticle form. To gain further insight into the oxidation states of the gold present in these tissues, X-ray absorption spectroscopy (XAS) could be carried out. Research into the uptake of gold has used two of the components of XAS, X-ray near edge absorption spectroscopy (XANES) and extended X-ray absorption fine structure (EXAFS) to elucidate information about the oxidation state, coordination environment and nearest neighbouring atom of the gold within the plant tissues (Gardea-Torresdey et al. 2002a; Gardea-Torresdey et al. 2005; Lopez et al. 2005b; Marshall et al. 2007; Rodriguez et al. 2007; Sharma et al. 2007; Armendariz et al. 2009). These techniques have also been used to study the formation of gold nanoparticles by bacteria and the formation of silver nanoparticles by plants (Haverkamp and Marshall 2009; Reith et al. 2009). To further elucidate knowledge of gold nanoparticle formation in Arabidopsis, an application was submitted as part of this work to the Diamond Light Source synchrotron facility (Oxford, UK). Although this was unsuccessful, further applications could be submitted in the future.

3.4.4 Uptake of gold nanoparticles

Data presented in this work show that gold can be taken up by Arabidopsis and nanoparticles can form within the tissues in certain conditions. Further to this, alfalfa plants have also been shown to form nanoparticles within aerial tissues when grown in soil containing gold. It is generally thought that gold is taken up and nanoparticles are subsequently formed within the plant tissues (Gardea-Torresdey et al. 2005; Marshall et al. 2007; Rodriguez et al. 2007; Starnes et al. 2010). However, researchers studying gold uptake in alfalfa hypothesised that gold nanoparticles formed in the plant growth media and these were subsequently taken up (Gardea-Torresdey et al. 2002a). Current understanding of gold nanoparticle uptake is further described in Chapter 1 (Section 1.5.4).

In light of this, gold nanoparticle uptake was studied in alfalfa to determine whether gold nanoparticles could be taken up and to determine whether this is the route of nanoparticle deposition within plants as hypothesised by Gardea-Torresdey et al. (2002a). By studying the size and shape of the nanoparticles that the plants were treated with and comparing these to the size and shape of nanoparticles within the plants, it could be determined whether gold is taken up as nanoparticles or as an ion. The data presented as a result of this work show

that gold nanoparticles above 10 nm diameter were not taken up by alfalfa plants. This therefore shows that when gold nanoparticles are seen within plants in this work, ionic gold has been taken up and subsequently been reduced to form gold nanoparticles. However, although no gold nanoparticles could be found within the plants, it is possible that the nanoparticles were too large to be taken up. Alternatively, the nanoparticles could have been dissolved into ionic gold and taken up, forming nanoparticles within the plant tissue that were below the resolution of the electron microscope. Repetition of this experiment with smaller nanoparticles, in the range of 1-10 nm diameter, would further investigate this theory.

Chapter 4 Microarray study of the Arabidopsis response to gold

4.1 Introduction

In Chapter 3, the physiological response of Arabidopsis to gold was studied; the knowledge gained was used as a platform to identify the genetic responses of Arabidopsis using microarray-based expression studies presented in this Chapter. Microarray technology is a powerful tool that has been used to study the genetic response of Arabidopsis to a range of environmental, physiological and developmental conditions. This has led to the accumulation of a vast database of searchable information (www.genevestigator.com) (Hruz et al. 2008); a valuable tool for Arabidopsis research. Examples of gene expression studies using microarrays include biotic stress (Thilmony et al. 2006; Murray et al. 2007), xenobiotics (Gandia-Herrero et al. 2008) and other abiotic stresses including cold, osmotic and salt stress (Kreps et al. 2002).

Microarray analysis is a useful tool to study the genetic responses of Arabidopsis to heavy metal stress. Metals for which the genetic response in Arabidopsis has been studied using this technique include lead, cadmium, silver (as an inhibitor of the ethylene pathway) and aluminium (Herbette et al. 2006; Goda et al. 2008; Kumari et al. 2008; Liu et al. 2009). In addition, the genetic response to deficiency of some essential metals has been studied, including copper, zinc and iron (Thimm et al. 2001; Wintz et al. 2003). These studies have identified various groups of genes involved in metal uptake and tolerance, including genes involved in sulfur accumulation, glutathione metabolism, the oxidative stress pathway, metal transporters, transcription factors and genes involved in common stress responses.

The gene expression profiles between non-hyperaccumulator species such as *Arabidopsis thaliana* and hyperaccumulator species such as *Arabidopsis halleri* have also been compared using microarray technology (Becher et al. 2004; Weber et al. 2004). These studies have been able to identify differences in the metal tolerance and uptake systems, and as such elucidate why some species can hyperaccumulate certain metals. This has included the increased expression of metal transporters in the hyperaccumulating species (outlined in Section 1.2.4).

The Arabidopsis gene expression chip routinely used is ATH1 (Affymetrix). This chip contains tags for 24,000 of the 26,000 genes encoded in the Arabidopsis (Col-0) genome (Redman et al. 2004) (Affymetrix, Data sheet, GeneChip Arabidopsis ATH1 Genome Array, www.affymetrix.com). Potential drawbacks of the ATH1 microarray are that some genes are not present on the array and so expression cannot be measured. Further to this, some genes with closely related sequences are indistinguishable from each other. Additionally, the algorithm chosen to process the data can have an impact on the measured expression (Millenaar et al. 2006).

4.1.1 Transition metal transporters

One of the general aims of this project was to identify any genes potentially involved in gold tolerance and uptake. It is therefore possible that transition metal transporters would have altered regulation in response to gold treatment. The six main families of transition metal transporters outlined in Chapter 1 are described in more detail below and in Figure 4.1.

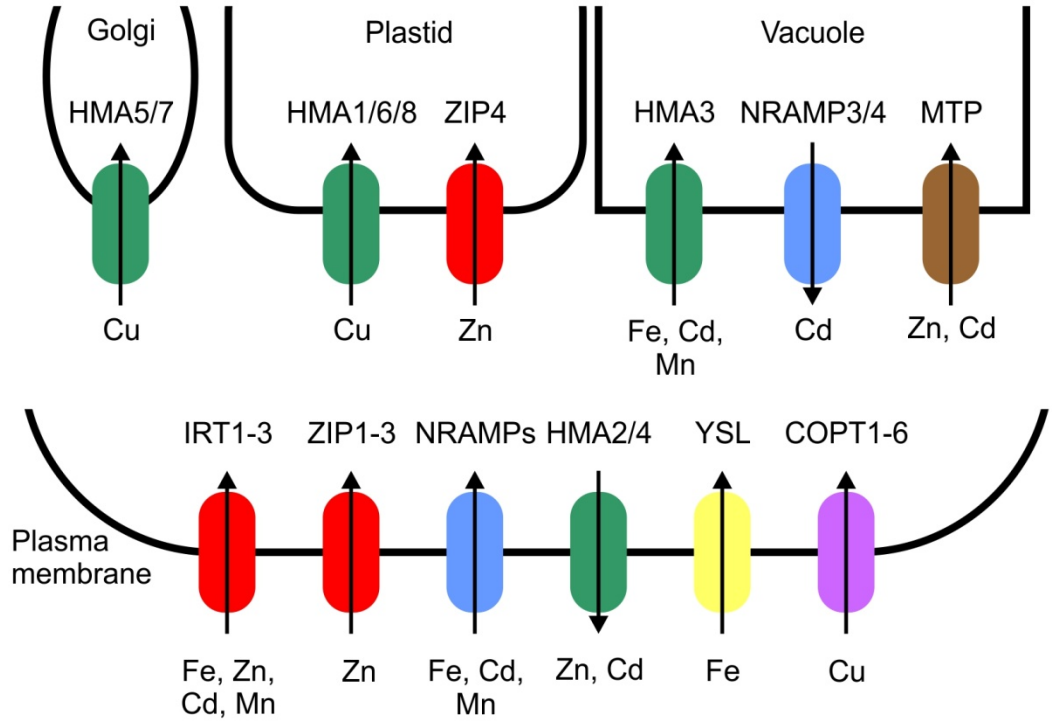

Figure 4.1 Transition metal transporters
The main transporters of transition metals in Arabidopsis are outlined here along with known substrates. These transporters are further discussed in this section. Colours represent different transporter families; green, heavy metal ATPases (HMA); red, zinc-regulated transporter, iron regulated transporter like proteins (ZIP); blue, natural resistance associated macrophage proteins (NRAMP); brown, metal tolerance proteins/cation diffusion facilitators (MTP); yellow, yellow stripe1-like proteins (YSL); purple, copper transporters (COPT).

4.1.1.2 The ZIP family of transporters

The ZIP (ZRT, IRT-like protein) protein family is named after IRT1 (zinc-regulated transporter, iron regulated transporter), the first member of the family to be discovered in *A. thaliana* (Eide et al. 1996; Guerinot 2000). Although predominantly an iron transporter with a preference for iron(II), IRT1 has a broad substrate specificity and is also able to transport zinc, manganese, cadmium, cobalt and possibly copper (Eide et al. 1996; Korshunova et al. 1999; Rogers et al. 2000; Vert et al. 2002). This broad specificity can be altered by replacing individual amino acids (Rogers et al. 2000).

In the roots of *A. thaliana*, iron deficiency leads to high levels of IRT1 expression which is probably controlled at the transcriptional and protein accumulation levels (Connolly et al. 2002; Vert et al. 2002). The transcription factor FIT1 (Fe-

deficiency induced transcription factor 1) is thought to control IRT1 expression (Colangelo and Guerinot 2004). FIT1 is discussed in greater detail in this Chapter..

To date, 15 ZIP transporters have been discovered in *A. thaliana* which may be used to transport different metals across different membranes in different locations (Maser et al. 2001). In addition to those in plants, ZIP proteins have been discovered in various taxa, and fall into four distinct groups (Gaither and Eide 2001). The ZIP transporters of higher plants all fall into one group (Maser et al. 2001) and have been shown to transport heavy metals in various species including rice, alfalfa, maize and tomato (Ramesh et al. 2003; López-Millán et al. 2004; Ishimaru et al. 2005; Chauhan 2006). Although many of the ZIP proteins are zinc transporters, some can be inhibited by treatment with other metals, suggesting that they may have more than one substrate (Grotz et al. 1998; Guerinot 2000; Vert et al. 2001; Wintz et al. 2003).

All of the ZIP proteins characterised to date, including IRT1, have eight transmembrane regions (Eide et al. 1996; Maser et al. 2001). A metal binding site is thought to be present between the third and fourth transmembrane domains and the fourth domain is highly conserved across the ZIP proteins, further indicating the involvement in heavy metal binding (Eng et al. 1998). In addition to this, the main variation in protein size and sequence in the Arabidopsis ZIP proteins is in the region between transmembrane domains three and four, which may explain the variability in specificities for different substrates (Guerinot 2000; Maser et al. 2001). Phylogenetic analysis of the ZIP transporters (Maser et al. 2001) suggests that there has been recent duplication of the genes and so some genetic redundancy is likely.

4.1.1.3 The NRAMP Family

The NRAMP family of transporters (Natural resistance associated macrophage proteins) were first identified in mouse macrophages and are thought to regulate divalent cations (Supek et al. 1997; Hall and Williams 2003). The NRAMP genes have now been found in a wide variety of organisms, including many in plants, with six in Arabidopsis (Maser et al. 2001; Hall and Williams 2003). The NRAMP proteins have 12 membrane spanning regions, and the consensus membrane transport domain is between the eighth and ninth regions (Gunshin et al. 1997;

Curie et al. 2000; Williams et al. 2000). The predicted structure of the conserved hydrophobic core of the NRAMP proteins is similar to those in other transporters and channels (Belouchi et al. 1997).

The Arabidopsis NRAMP1 and NRAMP2 amino acid sequences are closely related to those in rice (Belouchi et al. 1997; Curie et al. 2000). Both proteins can transport iron with NRAMP1 able to functionally complement the yeast *fet3fet4* mutant (Curie et al. 2000). Additionally, Arabidopsis NRAMP1 responds to iron starvation and overexpression increased tolerance to increased iron concentrations, whereas NRAMP2 is down regulated under iron starvation, and highly expressed under normal iron conditions (Curie et al. 2000). In addition to iron, NRAMP2 can transport a wide range of divalent metal ions; Fe^{2+}, Zn^{2+}, Mn^{2+}, Co^{2+}, Cd^{2+}, Cu^{2+}, Ni^{2+} and Pb^{2+} (Gunshin et al. 1997).

NRAMP3 can also transport a wide range of metals including iron, cadmium, zinc and manganese and is likely to be similar in function to NRAMP4 (Thomine et al. 2000; Thomine et al. 2003). Both proteins localise to the vacuole and are thought to be involved in long distance metal transport (Thomine et al. 2003; Lanquar et al. 2005). Expression of these two genes is similar and both are located within the same region of the Arabidopsis genome, suggesting that they derived from a recent duplication event, which is also indicated by phylogenetic analysis (Maser et al. 2001; Thomine et al. 2003; Lanquar et al. 2005). Further to this, single knockouts do not have a phenotype in response to iron whereas the double knockout is hypersensitive to iron (Lanquar et al. 2005).

Although little research has been carried out on the other NRAMPs, it is clear that this group of proteins is able to transport a wide variety of metals and has functions in different membranes.

4.1.1.4 Heavy metal ATPases

The heavy metal ATPases (HMAs) are members of a larger group of P-Type ATPases. This group of proteins is one of the more extensively studied groups of metal transport proteins in Arabidopsis. There are five groups of P-Type ATPases (I-V) which are subdivided into eight smaller families (Palmgren and Axelsen 1998). Of these eight smaller families, the type IB P-Type ATPases are considered to be heavy metal ATPases with early evolution shown by the

distribution in all biological kingdoms (Axelsen and Palmgren 1998). These proteins have eight transmembrane domains and contain an intramembranous cysteine-proline-cysteine/histidine motif (Solioz and Vulpe 1996; Axelsen and Palmgren 1998). Further to this, a heavy-metal binding motif is at the N-terminus of the protein, a feature likely to be essential in heavy metal transport (Solioz and Vulpe 1996). The heavy-metal ATPases are thought to comprise two smaller groups of proteins: those specific for Cu^{+}/Ag^{+} and those specific for $Zn^{2+}/Co^{2+}/Cd^{2+}/Pb^{2+}$ (Axelsen and Palmgren 2001; Hall and Williams 2003).

Forty-five P-Type ATPases were initially discovered in Arabidopsis, of which seven were classified as heavy metal ATPases (Axelsen and Palmgren 2001). This number has subsequently been revised to eight and these were named HMA1-8 (Williams and Mills 2005). Proteins previously known as PAA1, RAN1 and PAA2 have been renamed HMA6, HMA7 and HMA8 respectively to follow the current naming convention. As described below, these eight proteins have different functions within Arabidopsis. HMA1-4 are specific for $Zn^{2+}/Co^{2+}/Cd^{2+}/Pb^{2+}$, whereas HMA5-8 have been classified as Cu^{+}/Ag^{+} transporters (Axelsen and Palmgren 2001; Abdel-Ghany et al. 2005).

HMA1 is localised in the chloroplast envelope where it was initially shown to be important in the transport of copper into this organelle, although cadmium and zinc were also hypothesised as potential substrates (Williams and Mills 2005; Seigneurin-Berny et al. 2006). Recently, it has been confirmed that HMA1 is located in the chloroplast and, under excess zinc, acts to reduce the zinc content of plastids, therefore reducing zinc toxicity (Kim et al. 2009). Further to this, in yeast, expression of Arabidopsis HMA1 increases cadmium tolerance indicating that it is a also a cadmium transporter (Moreno et al. 2008).

HMA2 and HMA4 are closely related and often studied together as they are thought to be redundant (Williams and Mills 2005). Although these proteins have been found to be transporters of zinc and cadmium, both single and double mutants have indicated that HMA2 and 4 are not responsible for metal uptake into the root of the plant (Hussain et al. 2004; Verret et al. 2004; Mills et al. 2005). It is likely that HMA2 and HMA4 are important in the transport of metals from the cytoplasm into the xylem as indicated by reduction in root to shoot translocation (Verret et al. 2004; Williams and Mills 2005; Wong and Cobbett 2009). Studies in the zinc hyperaccumulator *Thlaspi caerulescens* have indicated that HMA4 is

important in zinc and cadmium tolerance in this species and as such, may play a role in the hyperaccumulation of metal by this plant (Papoyan and Kochian 2004).

Although the *hma3* mutant has no obvious phenotype (Hussain et al. 2004), yeast studies have demonstrated that it does act as a functional metal transporter. Cadmium and lead are sequestered into intracellular compartments by HMA3 in yeast (Gravot et al. 2004). Furthermore, HMA3 is localised to the Arabidopsis vacuole, strongly indicating that it is important for the transport of metals from the cytoplasm and into the vacuole (Gravot et al. 2004; Morel et al. 2009). In the Columbia-0 ecotype of Arabidopsis, *HMA3* contains a nonsense mutation which leads to a shorter protein missing the ATPase domain, meaning that it is non functional (Morel et al. 2009).

Expression of *HMA5* is increased Arabidopsis in the presence of excess copper, but not with cadmium, iron, silver and zinc, therefore demonstrating that regulation is copper specific (Andres-Colas et al. 2006). Copper compartmentalisation is partly undertaken by HMA5, and it is thought that HMA5 interacts with copper chaperones to facilitate copper transport (Andres-Colas et al. 2006). Additionally, the importance of HMA5 has been elucidated in Arabidopsis and copper tolerance can vary depending on the sequence of the protein (Kobayashi et al. 2008).

There is similarity in the functions of HMA6 and HMA8. Both proteins have a role in copper delivery to the chloroplasts, with mutants in both genes leading to impaired electron transport in photosynthesis (Shikanai et al. 2003; Abdel-Ghany et al. 2005). However, although the proteins appear to have similar functions, they are located on different membranes with non-redundant functions (Abdel-Ghany et al. 2005).

HMA7 has been shown to be important in the early part of the ethylene signalling pathway and is similar to yeast copper transporter CCC2 (Hirayama et al. 1999). Further to this, HMA7 can complement the yeast *ccc2* mutant further demonstrating this similarity and determining that HMA7 is a copper transporter (Hirayama et al. 1999; Williams and Mills 2005). Additionally, *hma7* mutant plants were partially rescued by copper addition, further demonstrating that HMA7 is important in copper transport (Hirayama et al. 1999). It is also hypothesised that

HMA7 may have roles in cell expansion and copper mobilization (Williams and Mills 2005).

4.1.1.5 The YSL family of proteins

There are eight yellow stripe1-like (YSL) proteins in Arabidopsis (YSL1-8) which were discovered in maize due to an inability to take up Fe(III)-phytosiderophore (Curie et al. 2001; Kim and Guerinot 2007). All eight Arabidopsis proteins complement a yeast iron uptake mutant showing their function as iron transporters (Waters et al. 2006). The YSL transporters are widely distributed in plants, with 19 in rice (Le Jean et al. 2005). The size of YSL proteins varies as they contain between 12 and 15 transmembrane domains (Curie et al. 2001; Schaaf et al. 2004; Walker and Connolly 2008).

Arabidopsis YSL1-3 are thought to be redundant in function. All three have been found to be iron transporters, specifically when bound to nicotianamine (DiDonato et al. 2004; Le Jean et al. 2005; Waters et al. 2006). Evidence suggests that these proteins are important in the movement of iron through the veins of plants (DiDonato et al. 2004; Le Jean et al. 2005; Grotz and Guerinot 2006). Evidence in maize suggests that these proteins have a broad specificity and are able to transport a range of metals in addition to iron, including; zinc, copper, nickel, manganese and cadmium (Schaaf et al. 2004).

4.1.1.6 The CDF Family

The cation diffusion facilitator (CDF) family of proteins was first identified in bacteria (Nies and Silver 1995). CDF proteins have subsequently been discovered in various plants, and were named the metal tolerance proteins (MTPs). Twelve MTPs have been identified in Arabidopsis (Krämer et al. 2007). Each protein has six transmembrane regions and a cation binding domain at the C-terminal (Paulsen and Saier 1997; Maser et al. 2001). The first member of this family to be characterised was ZAT1 (van der Zaal et al. 1999). ZAT1 was later renamed MTP1 (Maser et al. 2001).

The Arabidopsis MTPs are able to transport a variety of metals in a variety of places. For example, MTP1 is a zinc transporter which is expressed throughout Arabidopsis. Mutants are sensitive to increases in zinc, whereas overexpressors have increased tolerance (van der Zaal et al. 1999; Kobae et al. 2004). Evidence

suggests that MTP1 acts to remove zinc from the cytosol by transporting it into the vacuole (Kim et al. 2004a; Kobae et al. 2004). This is also thought to be the case for MTP3, although this is also confers tolerance to cobalt (Arrivault et al. 2006). Not all MTP transporters are zinc transporters. MTP8-11 are thought to be involved in manganese tolerance (Delhaize et al. 2003; Delhaize et al. 2007). These proteins are thought to have redundant functions and mutants of MTP11 are sensitive to increased manganese tolerance.

4.1.1.7 The COPT transporter family

The COPT (Copper Transport) transporters are the plant members of the CTR family of copper transporters which are conserved and distributed throughout eukaryotes. The COPT transporters were first discovered from their ability to complement yeast copper transport mutants (Kampfenkel et al. 1995). Currently, six Arabidopsis COPT transporters have been identified (Sancenon et al. 2003; Puig et al. 2007; Penarrubia et al. 2010). Of these, only COPT1 and COPT5 have been characterised (Sancenon et al. 2004; Garcia-Molina et al. 2011) and the sixth protein is hypothetical and only recently discovered (Puig et al. 2007; Penarrubia et al. 2010).

These proteins have three transmembrane domains. This is low when compared to the transporters described above. However, these proteins have been shown to trimerise in the membrane to produce metal transporting channels (Lee et al. 2002). Important methionine and glycine residues have been identified, and mutations within these regions can impair protein function (Puig et al. 2002; Aller et al. 2004).

The COPT family of transporters is investigated in this thesis. As such, a more comprehensive description of what is known about the Arabidopsis COPT family can be found in Chapter 5.

4.1.2 Aim and strategy

The aim of the experimental work presented in this Chapter was to elucidate the genetic response of Arabidopsis to gold and so identify possible mechanisms for gold uptake and tolerance with a particular emphasis on metal transporters. Studies were focussed on gene expression in the roots of the plants; the site of exposure and uptake. Results described in Chapter 3 have shown that gold nanoparticles form in the roots of Arabidopsis plants yet were not visible in the aerial tissue (Section 3.3.5), suggesting differences in the responses of the root and shoot tissues. For these reasons, microarray studies were carried out on the root tissue only.

As described above, microarrays have previously shown that under metal stress, plants can generally respond to metals. This study was therefore designed so that the results could be compared to other metal stress responses, with the aim of identifying gold specific responses. The response of Arabidopsis to aluminium stress provided a useful comparison as aluminium is also a trivalent, non-essential, metal (Kumari et al. 2008). The methods outlined below are therefore as similar as possible to the methods described in this aluminium study. In order to obtain statistically sound data, experiments were performed with three biological replicates and compared pairwise to the no gold control.

4.2 Methods

4.2.1 Plant growth

For the microarray experiment, Arabidopsis was grown according to the method described by Kumari et al. (2008). Rafts were made from circular lightweight plastic, 75 mm on diameter and 6 mm thick. Approximately 100 holes (3-4 mm diameter) were drilled into each disk. These rafts were sterilised by autoclaving and the holes were plugged with ½MS(A). Sterile Arabidopsis seeds, which had been stratified for two nights in the dark at 4 ºC, were pipetted onto each plugged hole. Rafts were transferred to liquid Richard's medium (pH 5.7). Plants were grown in sealed sterile jars for 14 days at 22 ºC / 19 ºC day / night temperatures on a 16 hour light (80 $\mu mol.m^{-2}.s^{-1}$) / 8 hour dark cycle. For an example setup, see Figure 4.3.

4.2.2 Determination of optimum gold concentration for treatment

To determine the optimum gold concentration for the microarray experiment, 14-day-old plants grown as described above (Section 4.2.1) were treated with 0, 0.125 or 0.25 mM $KAuCl_4$ (pH 5.7). Gold solutions were prepared by adding $KAuCl_4$ to water and adjusting the pH to pH 5.7 using NaOH. Liquid growth medium was replaced by gold solution for six hours in growth room conditions as described in Section 4.2.1. After six hours, roots and shoots were harvested and separated. Samples were snap frozen in liquid nitrogen and stored at -80 ºC prior to RNA extraction and cDNA transcription as described in Sections 2.4.3 and 2.4.4.

Gene expression for six genes; *HMA5*, *HMA7*, *mtLPD1*, *mtLPD2*, *mtHSC1* and *mtHSC2* was determined using qPCR. *ACTIN2* (At3g18780) was used as the endogenously expressed control (Seciton 2.4.5). Primers (Table 4.1) were designed using Primer Express v3.0 (Applied Biosystems).

Table 4.1 Primers used in optimisation of microarray
F and R after the primer names denote the forward and reverse primers respectively.

Gene	Primer Name	Sequence
HMA5	HMA5F	TCTCAAGCGATCGCAAAGC
	HMA5R	ATTCCCTTCCTTGTCCAAACTCA
HMA7	HMA7F	TCAGCCTGGTGATACATTAAAAGTTC
	HMA7R	CCCCACACCACAACACCAT
mtHSC1	mtHSC1F	TCCACCGACTCTAATCCAATCA
	mtHSC1R	CGCAGATACGGAAGCCATTT
mtHSC2	mtHSC2F	CGAAAGTCATTGAAAATGCTGAA
	mtHSC2R	GCTGGTGTACCCACAAGAAGTTC
mtLPD1	mtLPD1F	GCTTCGCCTCATCAGGATCT
	mtLPD1R	GATCGCGGCTACGTAACCA
mtLPD2	mtLPD2F	AATTCTCCCACTGATGCTTTCAG
	mtLPD2R	GACCGCCGCCGATGA
ACTIN2	ACTINF	TACAGTGTCTGGATCGGTGGTT
	ACTINR	CGGCCTTGGAGATCCACAT

4.2.3 Microarray experiment

For the microarray experiment, 14-day-old plants, grown as described in Section 4.2.1, were treated with 0.125 mM gold or with water alone as a control comparison. Plant material was harvested and RNA was extracted as described above (Section 2.4.3). This was tested for integrity using an Aligent 2100 bioanalyser in the Technology Facility (University of York). This is a capillary electrophoresis based separation method, which separates the RNA molecules depending on their size into the three RNA components present; mRNA, tRNA and rRNA.

Following transcription into cDNA and labelling, ATH1 chips (Affymetrix, California, USA) were hybridised to the cDNA by the Technology Facility (University of York). In order to test the quality of the microarray data and determine which genes had altered regulation in response to gold, statistical analysis of the data was performed. This was performed by Naveed Aziz in the Technology Facility at the University of York. An outline of the methods used is described here.

Raw data processing was performed using Affymetrix GCOS 1.2 software. After hybridization and scanning, probe cell intensities were calculated and summarized for the respective probe sets by using the MAS5 algorithm. Expression values of the genes were compared by using global scaling which

resulted in the normalization of the trimmed mean of each chip. Quality control evaluation was carried out on each sample by checking the percentage of probe sets reliably detected (between 40-60 % present call), and optimal hybridization ratios for the constitutively expressed housekeeping genes (e.g. GAPDH), poly(A) spike-in controls, and the prokaryotic controls (bioB, bioC, bioD and cre).

These normalised data were analysed using the GeneSpring GX10 Expression software (Agilent Technologies, USA). Differentially expressed genes were identified by using a two-class t-test ($p < 0.05$ significance level). Genes that were up or downregulated more than 2.0 fold between groups were selected.

4.2.4 Microarray verification

Prior to further analysis, the array data were validated to increase confidence that the genes indicated as differentially regulated were actually differentially regulated, qPCR was carried out. Nine genes with significant expression changes in the presence of gold were chosen to verify the data. These selections were based on genes thought to be involved in general stress responses and genes possibly involved with metal tolerance. These genes and the change in regulation as determined by the microarray experiment are outlined in Table 4.6 and the reasons for choosing them are outlined below. Primers used for the array verification (Table 4.2) were designed using Primer Express v3.0 and tested for efficiency as outlined in Section 2.4.5.

Table 4.2 Primers used for microarray verification qPCR reactions
Forward and reverse primers are represented by F and R at the end of the primer names respectively. ATGSTU12F/R were designed by Helen Sparrow.

Gene	Primer Name	Sequence
ATGSTU12	ATGSTU12F	GATCTTTCCATCCTCCCAACAC
	ATGSTU12R	CAACGAAGTGAGCCCAAAAAC
CYP71A12	CYP71A12F	TGGTAACCTCCACCAGCTTAGC
	CYP71A12R	TGGTCCGTACCGAAGGCTTA
At1g14550	At1g14550F	CTATTCAGGAGCACACACCATAGG
	At1g14550R	TGTCGCTTGAGTTCTCGTAAAGC
UGT73B4	UGT73B4F	CAACAGAATCCGCGGAGAA
	UGT73B4R	GAACAACACAAGGCAAAGGATGA
IRT1	IRT1F	CTTTGATCACGGTTGGACTTCTAA
	IRT1R	AGATCCACGAGTGCCATGTAAA
IRT2	IRT2F	TCTTTTCAGCCGTTACATTTCG
	IRT2R	AGAAGAAAAACATTTGACGATCATGA
MTPA2	MTPA2F	CATAGTTGTAGAAGTCGTTGGAGGAA
	MTPA2R	GCAAAGGCTGCAACATCAGA
TIP2;2	TIP2;2F	TGACCTTTGCTCTGGTCTACACA
	TIP2;2R	TGGTCCCGAGTGAACCTTTC
TIP2;3	TIP2;3F	CCCAGCTGGTCTTGTAGCAATT
	TIP2;3R	TGTTAGCCGCAATGGAAACTC
ACTIN2	ACTINF	TACAGTGTCTGGATCGGTGGTT
	ACTINR	CGGCCTTGGAGATCCACAT

4.2.5 Data analysis

The up and downregulated genes were functionally classified using MapMan software. MapMan is a tool which was used to visualise the microarray data in heat maps which link the genes to the processes in which they are involved (Thimm et al. 2004).

Published microarray data were analysed to determine conditions in which genes were up or downregulated and find where genes were upregulated using Genevestigator (www.genevestigator.com). Genevestigator is an online tool which can be used to investigate the expression patterns and conditions of various genes from published microarray data (Hruz et al. 2008). Data used were all from the ATH1 array.

4.3 Results

4.3.1 Establishing experimental conditions for microarray experiment

To determine optimal conditions for microarray analysis, the expression of seven genes was studied to identify the conditions which caused minimal stress, whilst still causing altered regulation of some genes. Plants were grown as outlined in Section 4.2.1 above for 14 days, after which, the plants were treated with gold for six hours and the tissues were harvested (Section 4.2.1). RNA was extracted and cDNA was synthesised (Sections 2.4.3 and 2.4.4). The expression of the seven genes was subsequently analysed via qPCR.

Previous microarray research in *Cupriavidus metallidurans* (Reith et al. 2009) investigated the expression of genes in the bacterium in response to gold. Of the 332 genes upregulated when *C. metallidurans* was treated with 100 µM gold for ten minutes, the top 25 were analysed (Table 4.3). These 25 genes were used to identify homologues in the Arabidopsis genome. The protein Basic Local Alignment Search Tool (BLASTP) (http://blast.ncbi.nlm.nih.gov/Blast.cgi) was used to probe the Arabidopsis genome using the *C. metallidurans* protein sequences (Altschul et al. 1990). Of the 25 upregulated genes, one had no homology to any proteins in Arabidopsis and eight were hypothetical proteins to which no function could be attached. These nine genes were therefore not suitable for use in establishing experimental conditions. Twelve of the genes returned hits when Arabidopsis was probed, but only small sections of the genes were conserved and therefore these genes were not suitable. Of the remaining genes, Rmet_3524, Rmet_4888 and Rmet_2922 had homologues in Arabidopsis which had previously been shown to be involved in metal homeostasis (highlighted in Table 4.3). Rmet_3524 is homologous to HMA5 (At1g63440), a heavy metal ATPase shown to be a copper transporter involved in copper detoxification (Andres-Colas et al. 2006). Rmet_4888 is a dihydrolipoamide dehydrogenase and the Arabidopsis homologue (mtLPD1, At1g48030) has been shown to respond to metals other than gold, including cadmium (Sarry et al. 2006) and more recently, zinc, copper and cobalt (Tan et al. 2010). Rmet_2922 is a heat shock chaperone protein and the Arabidopsis homologue (mtHSC70-2, At5g09590) has been shown to respond to cadmium (Sarry et al. 2006).

The Arabidopsis homologues of these genes were therefore chosen for analysis in response to gold in Arabidopsis in order to establish suitable experimental conditions for the microarray. In Arabidopsis, there are two members of the *mtLPD* family (Lutziger and Oliver 2001) and two *mtHSC70* genes (Sung et al. 2001). Thus, both members of the *mtLPD* family and both members of the *mtHSC70* family were tested for changes in expression. The *HMA* family comprises eight members (Axelsen and Palmgren 2001; Abdel-Ghany et al. 2005) (see Chapter 1). Of the eight *HMA* genes, *HMA5* and *HMA7* were tested because they are the two genes most closely related to *Rmet_3524*.

Table 4.3 Upregulated genes in *C. metallidurans* in response to gold

The 25 most upregulated genes in *C. metallidurans* in response to gold(III) (Reith et al. 2009). Cells highlighted green are the three genes whose homologues were chosen to study in this work.

Mage ID	Regulation change	Annotation	Arabidopsis Homologues?
Rmet_3525	87.08	copper chaperone, heavy metal ion binding (modular protein)	Homologues but not conserved
Rmet_4187	83.13	hypothetical protein	Hypothetical protein
Rmet_3524	67.73	copper-transporting P-type ATPase CopA	Homologue is copper transporter
Rmet_4888	58.4	dihydrolipoamide dehydrogenase	Conserved protein
Rmet_4685	49.94	hypothetical protein	Hypothetical protein
Rmet_4684	47.39	hypothetical protein	Hypothetical protein
Rmet_4889	36.59	glutaredoxin-like region	Conserved protein
Rmet_4908	34.14	conserved hypothetical protein	Hypothetical protein
Rmet_0332	33.6	putative lactoylglutathione lyase	Homologues but not conserved
Rmet_3620	33.2	multifunctional enzyme (peptidase / oxidoreductase) (degP / mucDlike)	Conserved protein
Rmet_0333	32.02	regulatory protein, ArsR	Homologues but not conserved
Rmet_3523	30.14	DNA-binding transcriptional activator of copper-responsive regulon genes	□omologues but not conserved
Rmet_1959	27.06	protein disaggregation chaperone	Conserved protein
Rmet_4026	25.5	conserved hypothetical protein	Hypothetical protein
Rmet_4102	24.04	putative transcriptional regulator, TetR familiy	Homologues but not conserved
Rmet_3619	23.86	organic hydroperoxide resistance transcriptional regulator, MarR family	Homologues but not conserved
Rmet_4188	23.39	transcriptional regulator, TetR family	Homologues but not conserved
Rmet_2280	22.63	conserved hypothetical protein; putative hemin uptake protein	Homologues but not conserved
Rmet_1951	21.74	alkyl hydroperoxide reductase D	Homologues but not conserved
Rmet_3522	18.4	lysophospholipase	Conserved protein
Rmet_0720	16.83	hypothetical protein	Hypothetical protein
Rmet_3456	15.95	transcriptional regulator, MerR-family	Homologues but not conserved
Rmet_2922	13.78	chaperone Hsp70, co-chaperone with DnaJ	Conserved protein
Rmet_0085	12.81	conserved hypothetical protein	Hypothetical protein
Rmet_4103	12.4	N-ethylmaleimide reductase, FMN-linked	Conserved protein

4.3.1.2 Analysis of gene expression

The cDNA synthesised for the optimisation studies was used to test for the expression of the genes described above (Section 4.3.1). Relative gene expression was calculated for the 0.125 mM and 0.25 mM samples compared to the no gold treatment samples as described in Section 2.4.5 (Figure 4.2). All data were compared to the no gold control, and were normalised using *ACTIN2* as a constitutively expressed control. For the 0.25 mM treatments, all six genes were upregulated. In the 0.125 mM treatments, all except for *HSC1* were upregulated.

The data presented here demonstrate upregulation of Arabidopsis homologues of genes upregulated in *C. metallidurans* in response to gold. From these results 0.125 mM gold was selected for the microarray experiment. Additionally, at this concentration, changes in gene expression as a general stress response are likely to be lower than for 0.25 mM gold.

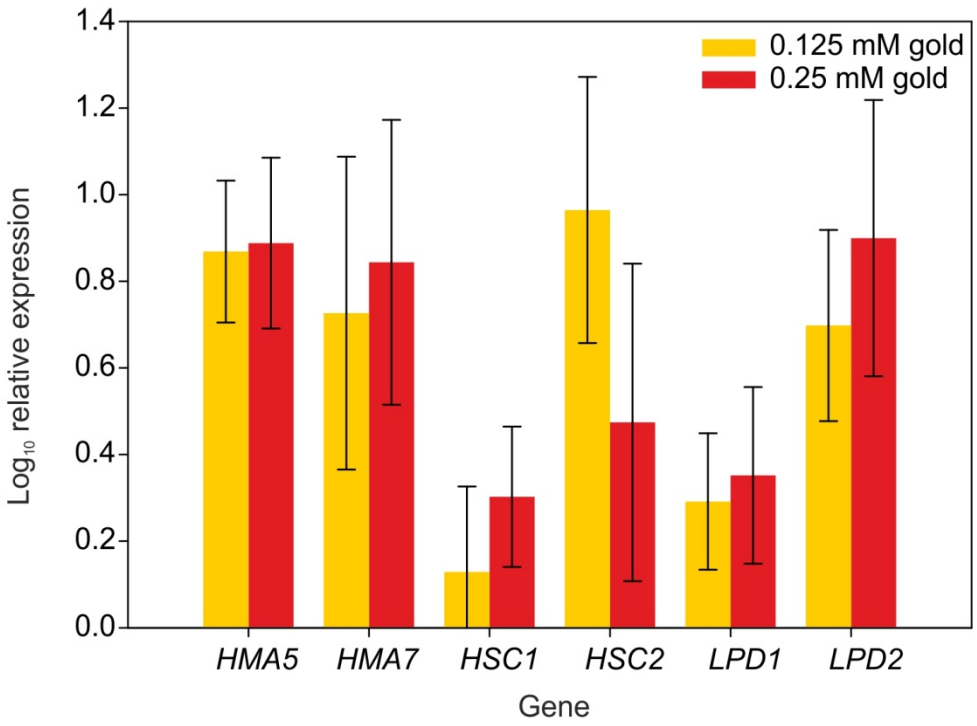

Figure 4.2 Results from qPCR to determine optimum microarray conditions

Changes in gene expression of in Arabidopsis root tissue treated with 0.125 or 0.25 mM gold. Error bars represent the standard error of the mean from four replicates. *ACTIN2* was used as a constitutively expressed control to normalise the data.

4.3.2 Microarray experiment

Arabidopsis seedlings were grown and subsequently treated with gold as described in Section 4.2.3. After six hours of treatment, there was some purple colouration of the root tissues suggesting reduction of gold(III) to gold(0). RNA was extracted from plant tissues and analysed using the bioanalyser system. Six RNA samples were tested for integrity (Figure 4.4). Distinct bands show that the RNA integrity had been kept during the extraction procedure. This was further confirmed by studying the fluorescence of the samples (Figure 4.5). The six samples tested showed good integrity (Figure 4.5a is a representative graph). Had the samples had lower integrity, the RNA would have been more fragmented (Figure 4.5b). The six samples described in Figure 4.4 were subsequently transcribed to cDNA and gene expression was measured using the ATH1 microarray. Statistical analysis of the microarray data was carried out as described in Section 4.2.3 and genes that were up or downregulated more than two-fold were selected.

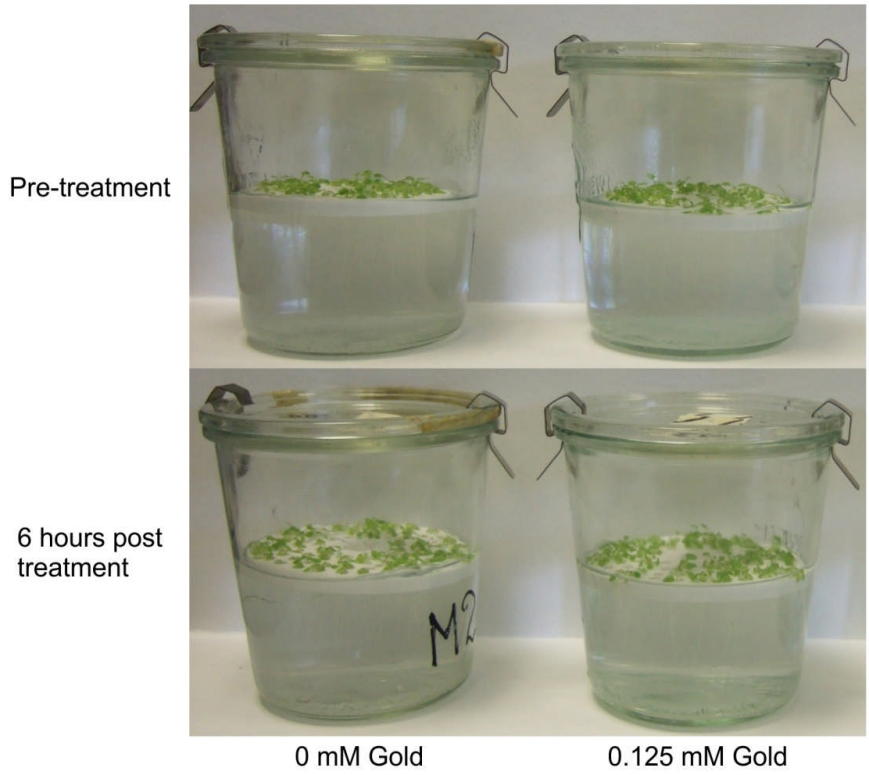

Figure 4.3 Treatment of Arabidopsis plants for the microarray experiment

14-day-old Arabidopsis seedlings both prior to and 6 hours post treatment with either 0 or 0.125 mM $KAuCl_4$. Seedlings were germinated on ½MS(A) plugs and grown into Richard's medium. This medium was changed after two weeks with either water, or $KAuCl_4$ at pH 5.7 for six hours.

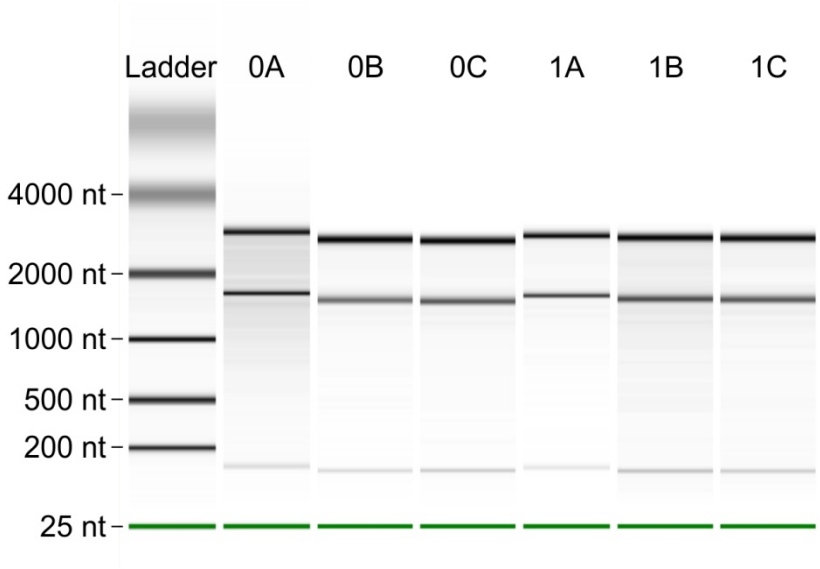

Figure 4.4 Integrity of the RNA used for the microarray experiment
Quality control of RNA extracted from Arabidopsis plants to check for RNA integrity using an Aligent 2100 bioanalyser. No gold control samples are indicated by 0 and 0.125 mM $KAuCl_4$ samples are indicated by 1. Letters indicate separate biological replicates.

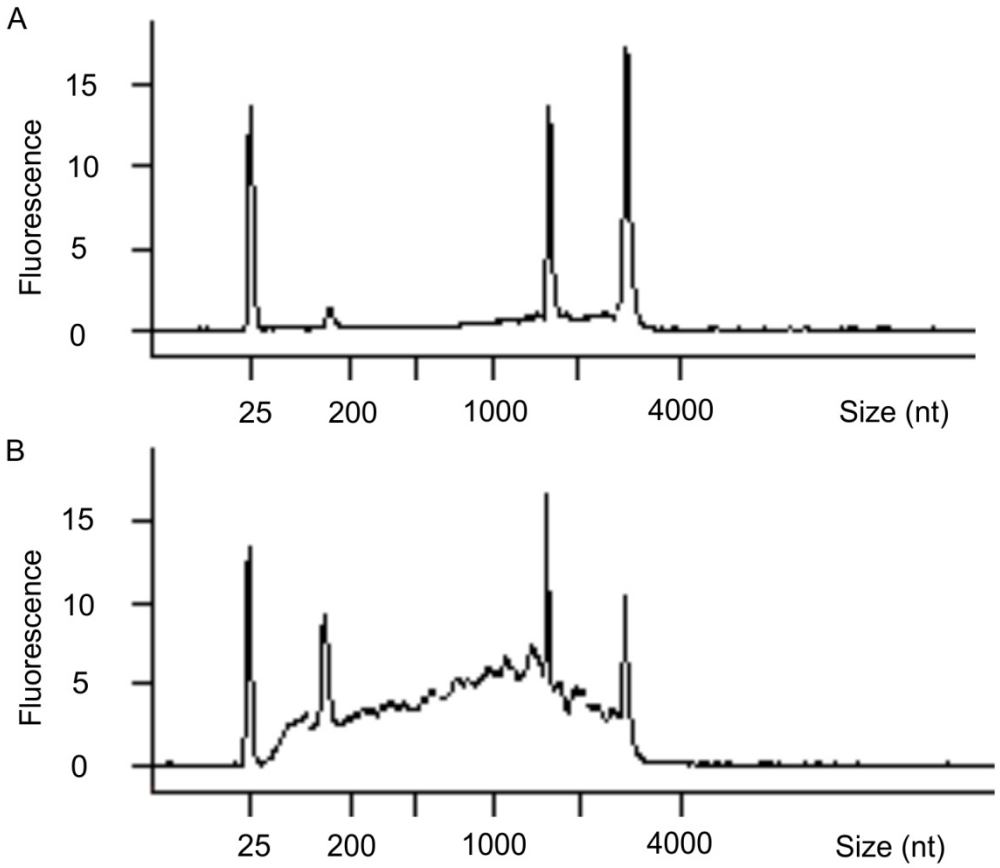

Figure 4.5 Integrity of the RNA used for the microarray experiment
Quality control of RNA extracted from Arabidopsis plants to check for RNA integrity using an Aligent 2100 bioanalyser. A) Good quality RNA. B) RNA with high levels of fragmentation.

4.3.3 Microarray analysis

After the statistical analysis, two data sets were produced outlining the genes up or downregulated more than two-fold. In total, 1720 genes had expression altered by more than two-fold. This represents approximately 7.5 % of the 22 746 Arabidopsis genes tested on the ATH1 microarray (Figure 4.6). The array analysis identified 869 genes which were upregulated (3.8 % of the genes tested) and 851 downregulated (3.7 % of the genes tested). The 25 genes with the largest changes in regulation are outlined in Table 4.4 and Table 4.5. A full list of the genes up and downregulated more than two-fold, along with the change in expression can be found in Appendices A and B respectively.

The fold change in gene expression ranged from 132-fold downregulated to 291-fold upregulated (Figure 4.7). A larger proportion of upregulated genes had more than 20-fold change in expression compared to the downregulated genes. Most

genes with altered expression had between 2 and 10-fold fold change in regulation.

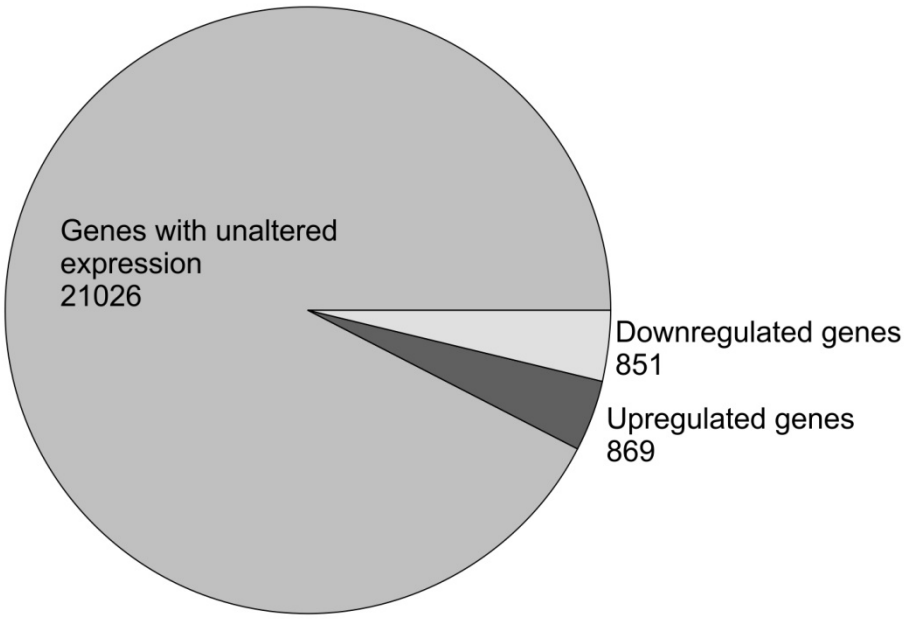

Figure 4.6 Overview of the microarray data
Proportions of genes with expression altered more than two-fold up or down out of a total of 22 746.

Table 4.4 Genes downregulated in response to gold treatment

The 25 most downregulated genes. Fold change describes the result of the microarray. The loci, gene names and descriptions of the gene (and product) were all determined using TAIR (www.arabidopsis.org). For those genes with no gene name, no gene name had been described in TAIR.

Fold change	Locus	Gene name	Description
132.37	At4g19690	*IRT1*	Fe(II) transport protein
106.68	At5g46900		protease inhibitor/seed storage/lipid transfer protein
67.59	At5g04950		nicotianamide synthase
55.75	At1g08090	*ATNRT2:1*	high-affinity nitrate transporter
55.55	At4g12550	*AIR1*	putative cell wall-plasma membrane disconnecting CLCT protein (AIR1A)
43.24	At1g73120		hypothetical protein
38.40	At4g19680	*IRT2*	Fe(II) transport protein
37.15	At3g12900	*MJM20*	oxidoreductase, 2OG-Fe(II) oxygenase family protein
32.79	At3g12820	*AtMYB10*	myb-related protein
32.52	At1g49860	*ATGSTF14*	glutathione S-transferase
30.77	At4g31940	*CYP82C4*	cytochrome P450
26.39	At3g61930		hypothetical protein with unknown function
25.83	At5g04730		hypothetical protein with unknown function
25.63	At3g19430		protein with unknown function; abundant in late embryogenesis
23.60	At3g46900	*COPT2*	copper transport protein
23.40	At3g45710	*T6D9.40*	proton-dependent oligopeptide transport (POT) family protein
23.29	At5g54370		protein with unknown function; abundant in late embryogenesis
23.17	At2g01530	*MLP329*	unknown protein related to major latex proteins, involved in copper binding
22.82	At5g03570	*FPN2*	tonoplast localized nickel transport protein
21.63	At4g22460		putative protease inhibitor/seed storage/lipid transfer protein
21.29	At3g44990	*XTR8*	xyloglucan endo-transglycosylase
19.94	At2g28160	*FIT1*	putative bHLH transcription factor regulating iron uptake responses
19.21	At3g18450		hypothetical protein with unknown function
19.18	At3g50740	*UGT72E1*	UTP-glucose glucosyltransferase
18.98	At1g34760	*GRF11*	encodes a 14-3-3 protein. Binds H+-ATPase in response to blue light

Table 4.5 Genes upregulated in response to gold treatment

The 25 most upregulated genes. Fold change describes the result of the microarray. The loci, gene names and descriptions of the gene (and product) were all determined using TAIR (www.arabidopsis.org). For those genes with no gene name, no gene name had been described in TAIR.

Fold change	Locus	Gene name	Description
291.07	At3g16530		putative lectin
233.89	At1g26380		hypothetical protein containing FAD-binding domain
220.17	At1g69920	*ATGSTU12*	glutathione transferase
133.91	At5g22300	*NIT4*	nitrilase specific for beta-cyano-L-alanine
132.16	At5g40990	*GLIP1*	GDSL-motif lipase
127.24	At2g30750	*CYP71A12*	cytochrome P450
122.02	At2g43000	*ANAC042*	transcription factor with NAC domain
102.81	At1g64160		dirigent protein
93.40	At4g31970	*CYP82C2*	cytochrome P450
88.68	At1g14550		anionic peroxidase
87.57	At1g66690		S-adenosyl-L-methionine:carboxyl methyltransferase family protein
86.87	At2g35980	*YLS9*	similar to harpin-induced protein hin1
85.24	At3g46230	*ATHSP17.4*	small heat shock protein
82.29	At1g69930	*ATGSTU11*	glutathione transferase
78.08	At3g60120	*BGLU27*	beta-glucosidase
76.05	At4g37290		hypothetical protein with unknown function
74.79	At5g39580		putative peroxidase
74.14	At3g26200	*CYP71B22*	cytochrome P450
74.12	At5g12030	*ATHSP17.6A*	small heat shock protein
69.51	At2g26560	*PLP2*	lipid acyl hydrolase
67.74	At2g28210	*ATACA2*	alpha carbonic anhydrase
66.61	At2g15490	*UGT73B4*	glucosyltransferase
63.54	At1g05680	*UGT74E2*	glucosyltransferase
62.31	At1g53540	*ATHSP17.6C*	small heat shock protein
55.43	At3g54150		putative methyltransferase

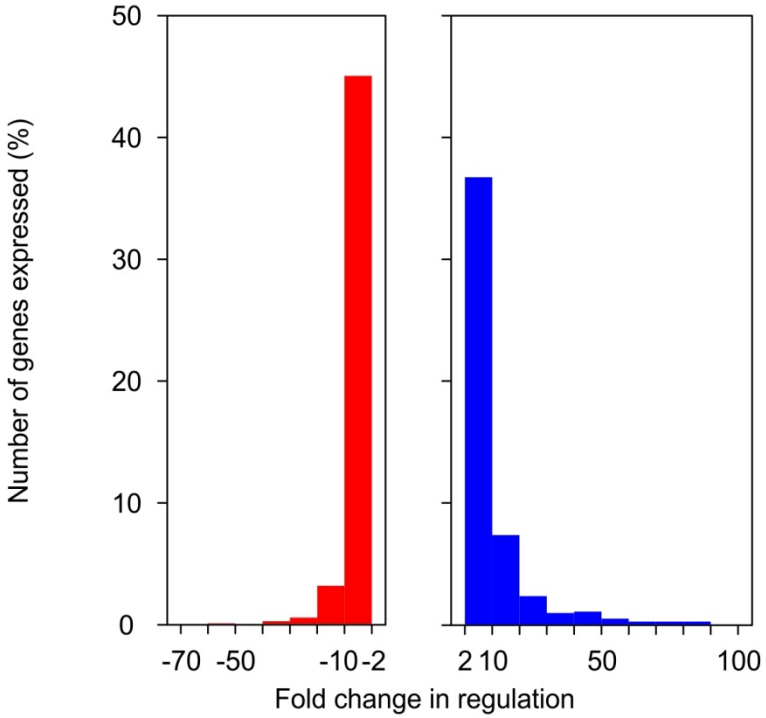

Figure 4.7 Range of regulation change
Proportions of genes with different fold changes in expression. Genes are classified in ten-fold increments from 0. Only two-fold and greater changes in regulation are included in this analysis.

4.3.4 Microarray validation

To verify that the microarray data were accurate, the changes in expression of nine genes were measured using qPCR (Section 4.2.4). The changes in expression measured in the microarray are outlined in (Table 4.6). These genes were chosen because they had some of the largest changes in expression in the microarray and were either thought to be involved in metal transport or stress responses.

IRT1, *IRT2* and *MTPA2* encode metal transporters (as described in Chapter 1 and Section 4.1.1). Glutathione transferases, cytochromes P450, glucosyl transferases and peroxidases are involved in responses to stress (Schuler and Werck-Reichhart 2003; Brazier-Hicks and Edwards 2005; Langlois-Meurinne et al. 2005; Gandia-Herrero et al. 2008; Dixon and Edwards 2010). Additionally, aquaporins transport a number of substances and function has been shown to be inhibited upon gold treatment (see Chapter 1 and Section 4.4.6).

Table 4.6 Genes used to verify the microarray data
Four upregulated and five downregulated genes were chosen to verify the microarray data. Fold changes are from microarray data. Gene titles and descriptions were described by TAIR (www.arabidopsis.org). Gene At1g14550 has not been annotated with a title.

Fold change	Regulation	Gene	Gene title	Description
220.17	Up	At1g69920	*ATGSTU12*	Glutathione transferase
127.24	Up	At2g30750	*CYP71A12*	Cytochrome P450
88.68	Up	At1g14550	*n/a*	Anionic peroxidase
66.61	Up	At2g15490	*UGT73B4*	Glucosyltransferase
132.37	Down	At4g19690	*IRT1*	Fe(II) transport protein
38.4	Down	At4g19680	*IRT2*	Fe(II) transport protein
17.93	Down	At3g58810	*MTPA2*	Zinc transport protein
16.84	Down	At4g17340	*TIP2;2*	Membrane channel like protein
10.79	Down	At5g47450	*TIP2;3*	Membrane channel like protein

To confirm the expression of the genes described in Table 4.6 in response to gold, qPCR was carried out. The primers used for this verification are outlined in Table 4.2 and the primer efficiency was proven using the method outlined in Section 2.4.5. The qPCR reaction was carried out using a subsample of cDNA used in the microarray experiment. The protocol described in Section 2.4.5 was used to run the reaction. The expression of these genes was compared to the microarray results (Figure 4.8). In all cases, the microarray data were qualitatively reliable in that expression measured by qPCR was similar to the expression measured by microarray.

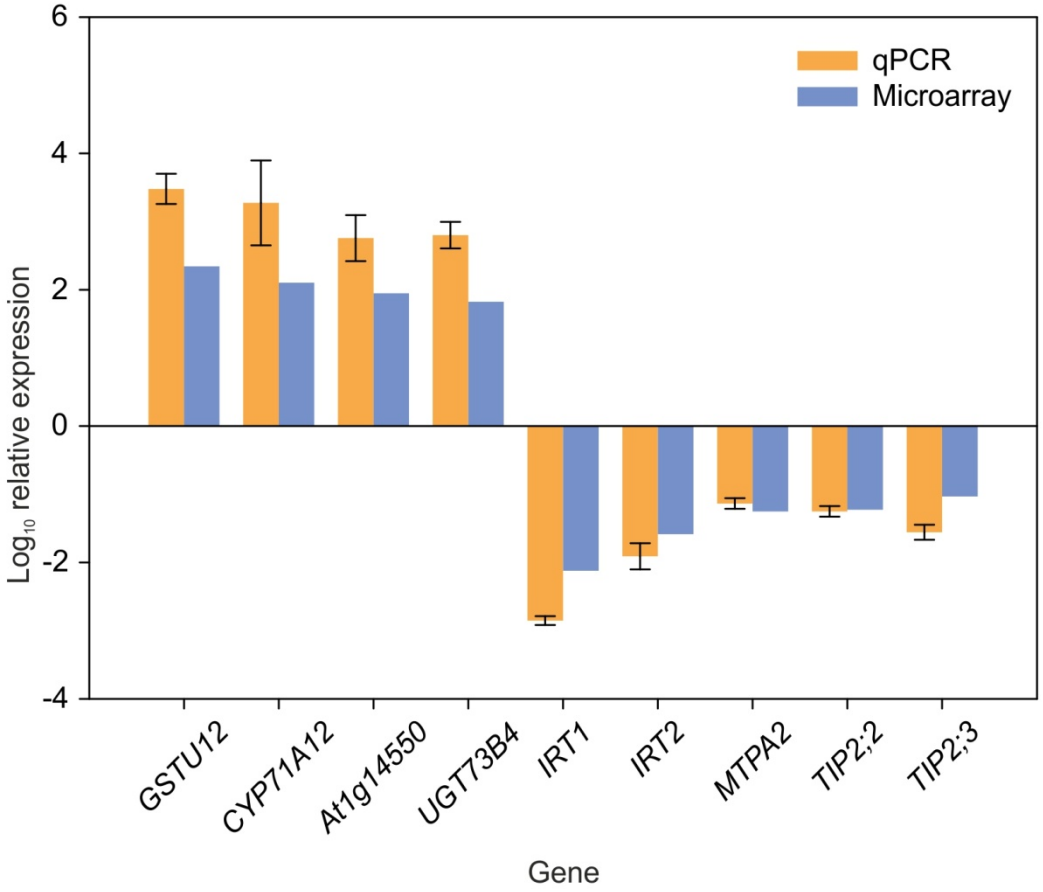

Figure 4.8 Comparison of qPCR and microarray results for verification of microarray data

Relative expression of nine genes in response to the treatment of gold. All values are relative to the expression of the gene in the no gold control. All expression levels were normalised to *ACTIN2*. Orange bars represent the qPCR data with error bars representing the standard error of the mean from three biological replicates. Blue bars represent the data from the microarray experiment.

4.3.5 Functional analysis of the genes with altered regulation

The up and downregulated genes, alongside all genes on the microarray, were analysed for functionality using gene ontology (GO) annotations (Berardini et al. 2004). The proportions of the different classes of up and downregulated genes were determined (Figure 4.9). Some classes of genes appeared to be altered in expression proportionally more than others. When the whole array is studied (Figure 4.9c), the transporters are low in number, however, transporters are the fifth most downregulated class of genes and the seventh most upregulated class. Transferases and kinases also appear to have altered regulation proportionally more than other gene classes compared to the whole genome. Genes involved in nucleic acid binding are lower than the whole genome in both conditions, as are DNA and RNA binding genes.

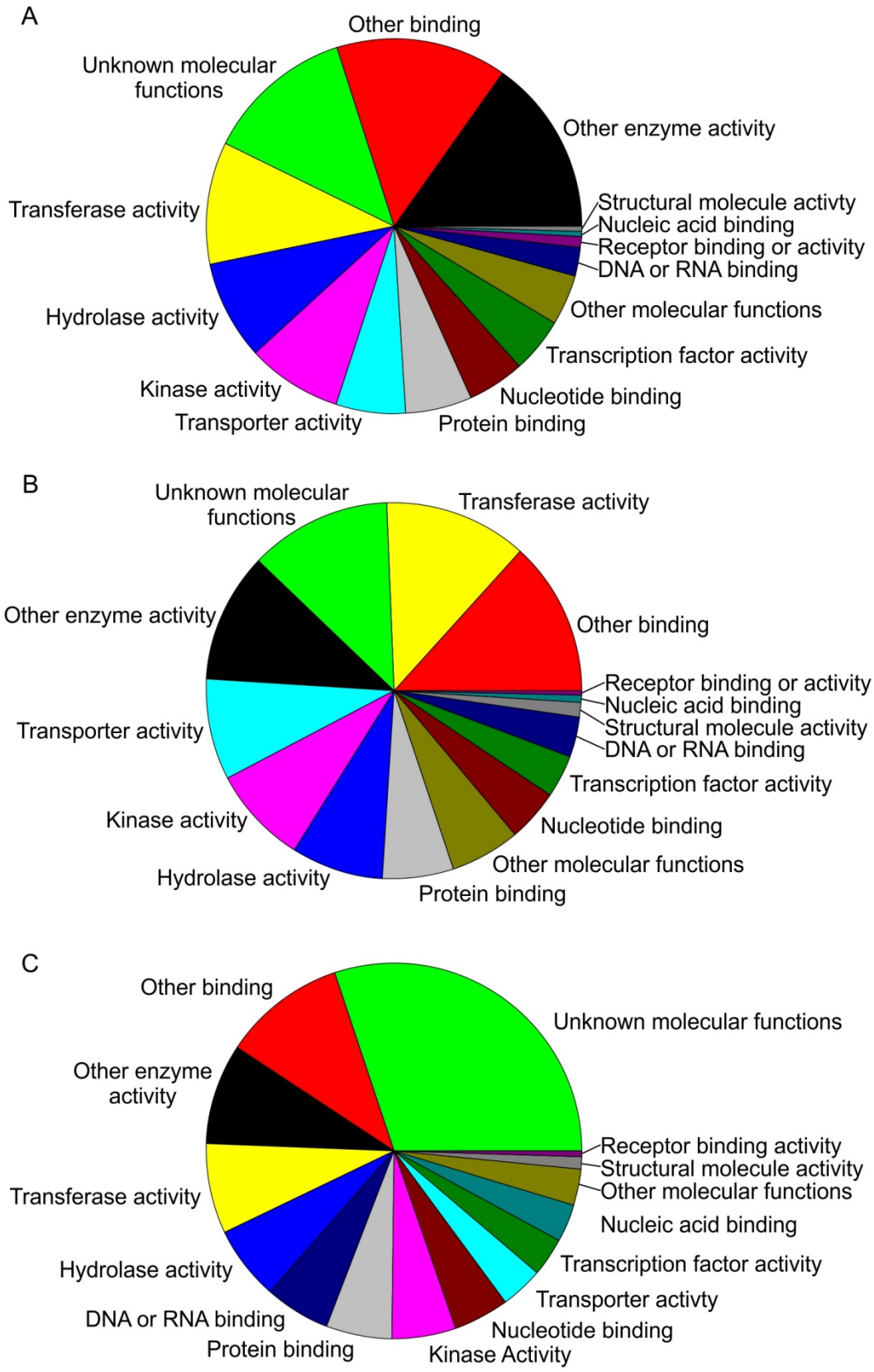

Figure 4.9 Functional analysis of the microarray results
Genes A) upregulated, B) downregulated or C) present on the microarray categorised by function according to gene ontology annotations (Berardini et al. 2004).

4.3.6 Analysis of the most up and downregulated genes

The top 25 most downregulated and the top 25 most upregulated genes were studied for expression locations using Genevestigator. Sixteen of the top 25 genes upregulated in response to gold are normally expressed in the roots (Figure 4.10) although for some of the upregulated genes there is little expression anywhere in the plant.

For the 25 most downregulated genes it is apparent that the majority of these genes are expressed in the root tissues (Figure 4.11). Although the expression of some of these genes seems stronger than others (as indicated by darker colours) and some have low expression, it is evident that they are mainly root expressed genes.

Genevestigator was used to investigate published data to identify the treatment conditions under which the most up and downregulated genes had altered expression. The ten conditions in which each of the fifty genes were most upregulated and the ten in which they were most downregulated were classified into one of nine different groups (Figure 4.12 and Figure 4.13).

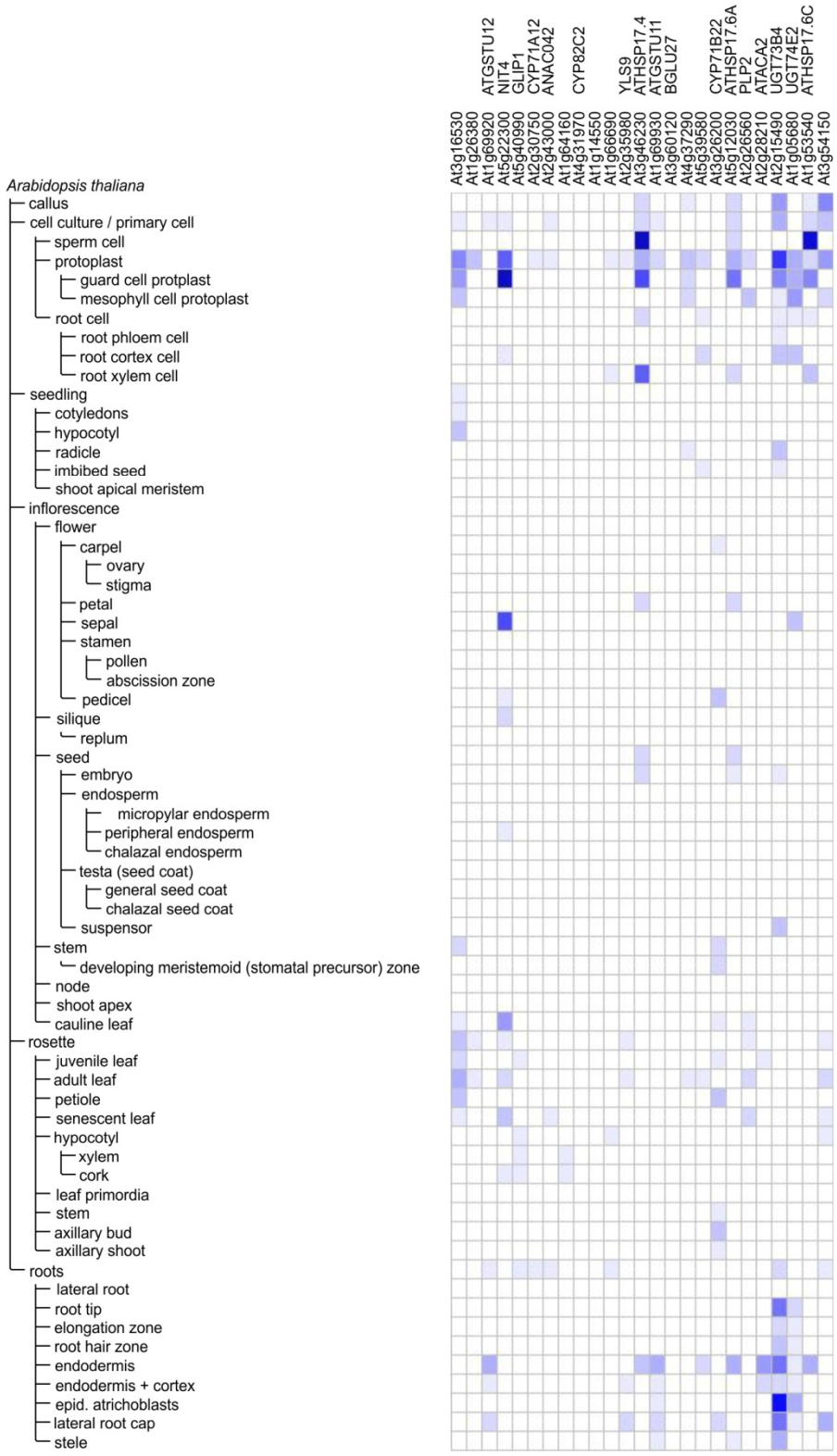

Figure 4.10 Expression patterns of the top 25 most upregulated genes
Darker colours indicate higher levels of expression. Data and figure from Genevestigator (Hruz et al. 2008). Gene names are annotated as in Table 4.5. Genes without annotation had no gene name described in TAIR.

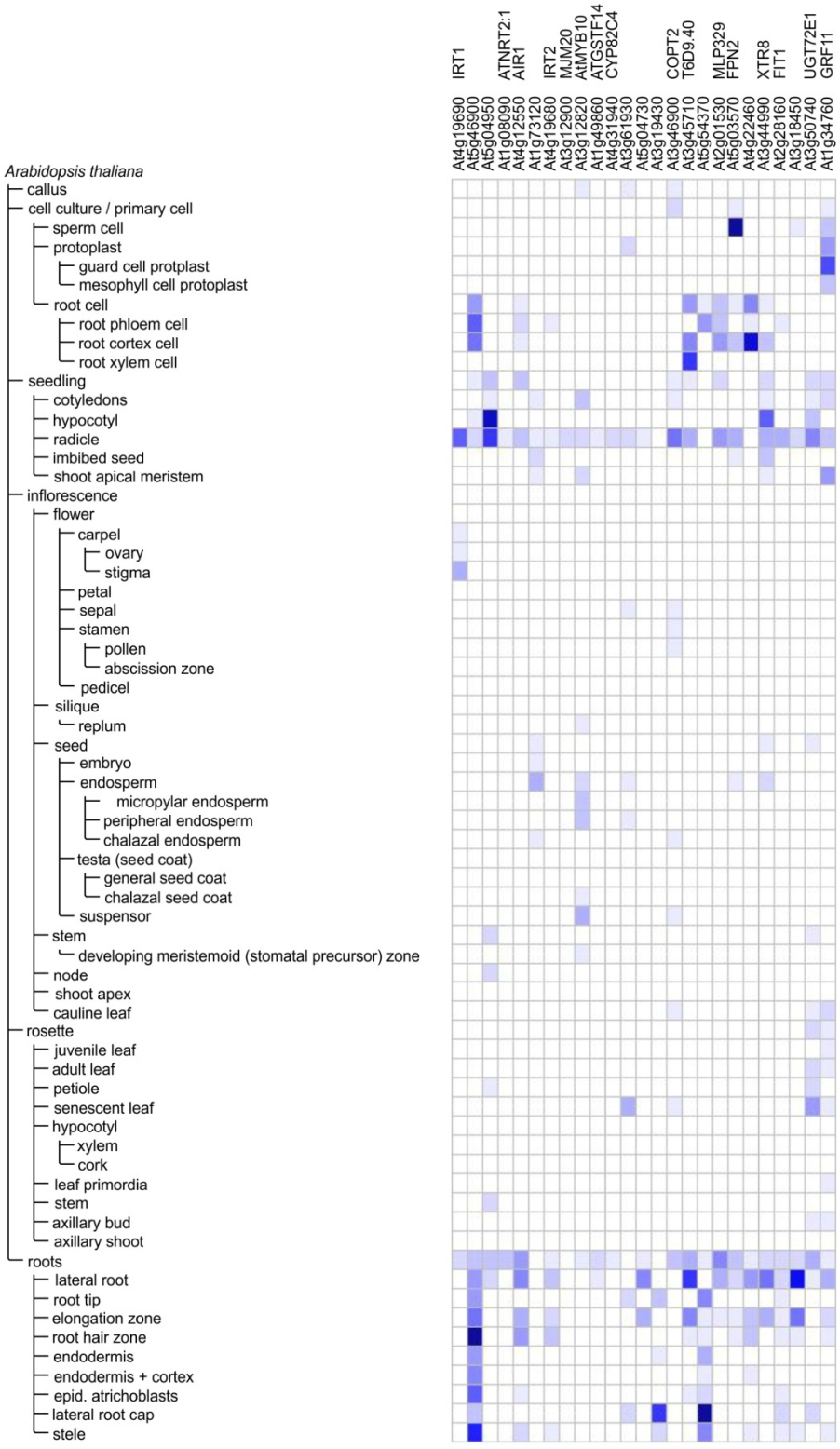

Figure 4.11 Expression patterns of the top 25 most downregulated genes
Darker colours indicate higher levels of expression. Data and figure from Genevestigator (Hruz et al. 2008). Gene names are annotated as in Table 4.4. Genes without annotation had no gene name described in TAIR.

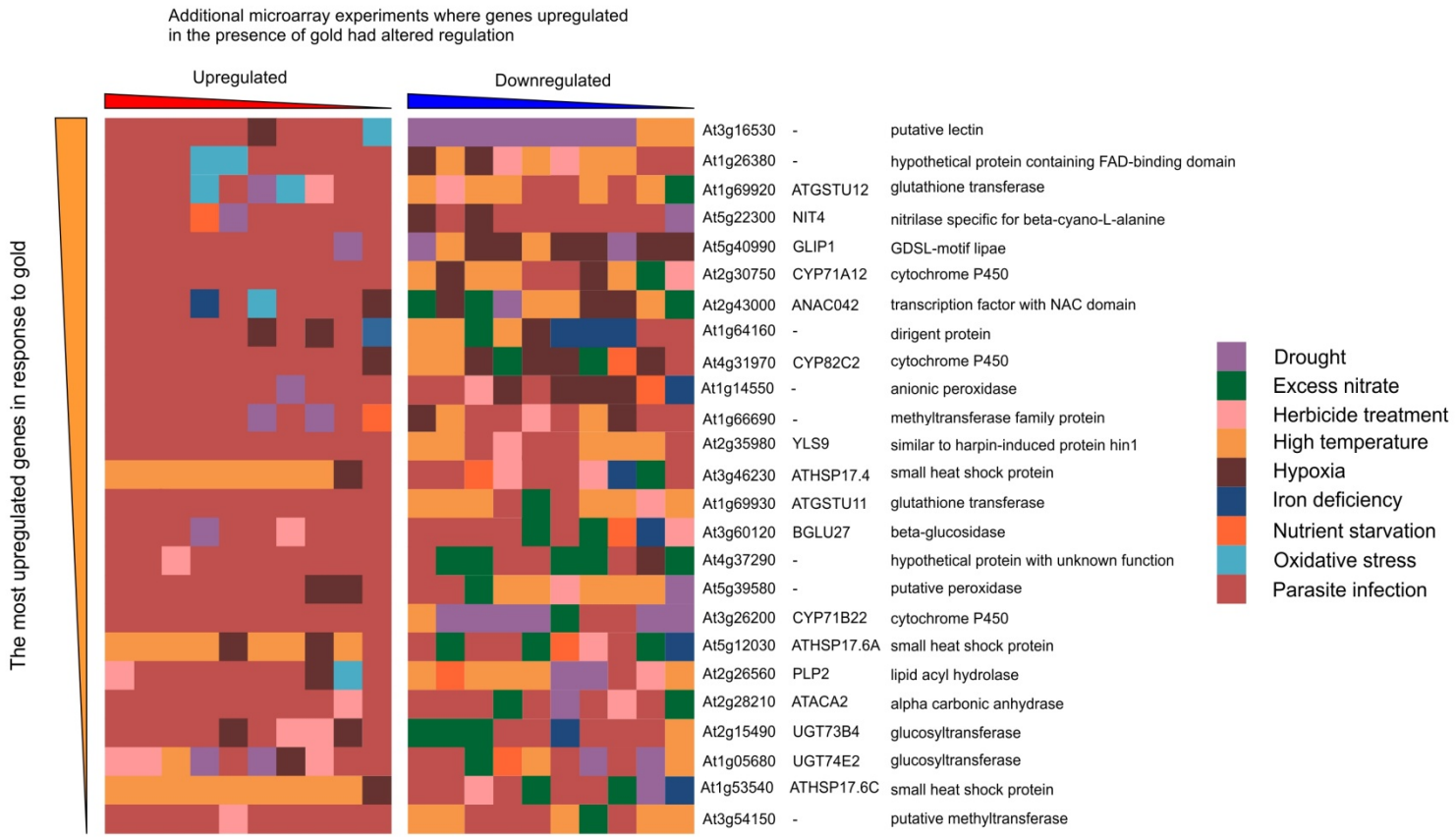

Figure 4.12 Responses of the 25 most upregulated genes to other treatments
The treatments in which the 25 most upregulated genes in the microarray (most upregulated at the top) have the largest changes in regulation. Treatments were clustered into nine different types. Oxidative stress included treatment with hydrogen peroxide or ozone. Herbicides used include cyclohexamide, norflurazon and 2,3,5-triiodobenzoic acid. Experimental data from Genevestigator (Hruz et al. 2008).

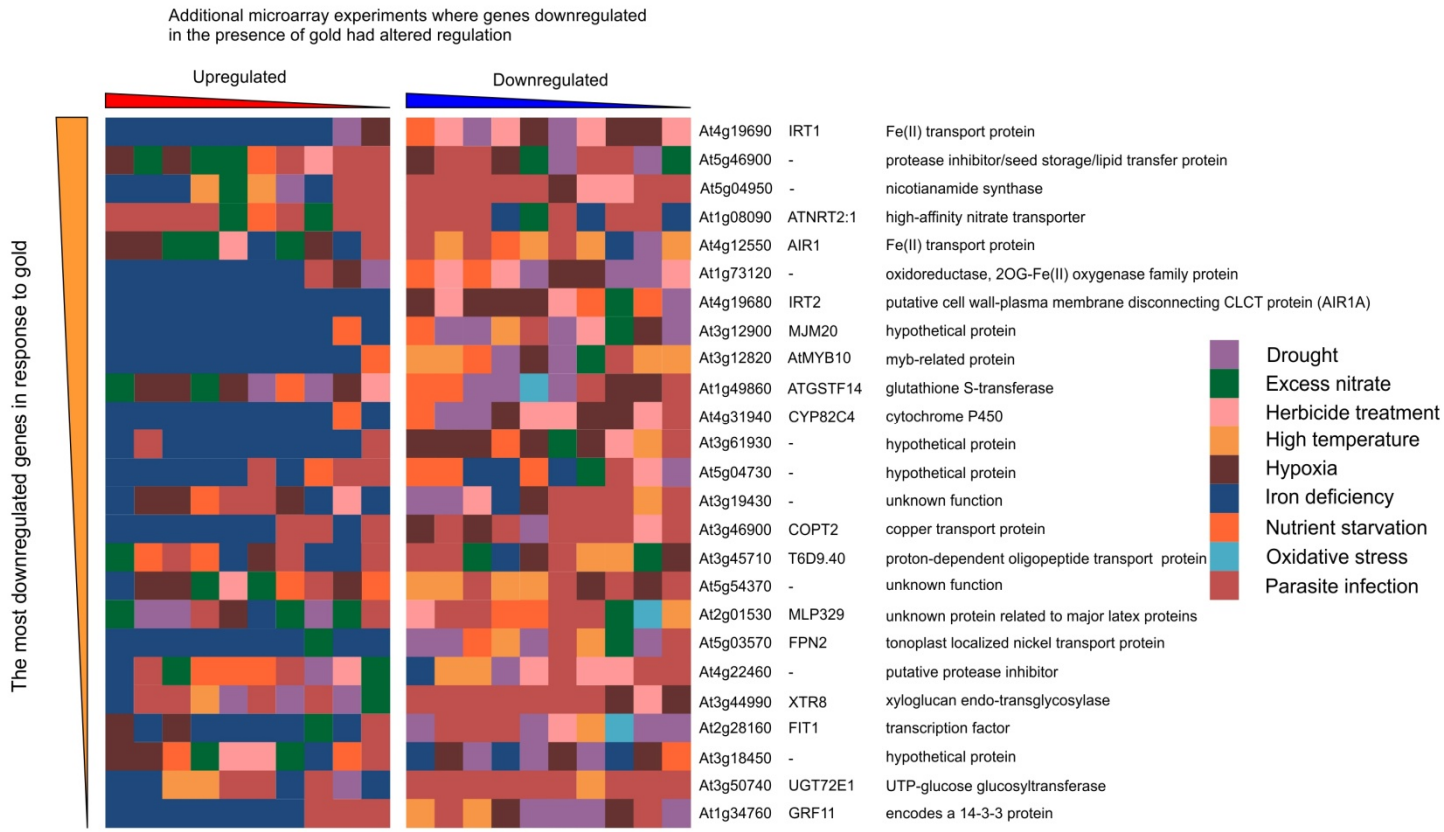

Figure 4.13 Responses of the 25 most downregulated genes to other treatments
The treatments in which the 25 most downregulated genes in the microarray (most downregulated at the top) have the largest changes in regulation. Treatments were clustered into nine different types. Oxidative stress included treatment with hydrogen peroxide or ozone. Herbicides used include cyclohexamide, norflurazon and 2,3,5-triiodobenzoic acid. Experimental data from Genevestigator (Hruz et al. 2008).

4.3.7 Transcription factors

MapMan software as used to determine which groups of transcription factors were altered. One hundred and sixteen transcription factors had more than two-fold altered expression in the presence of gold (Figure 4.14). Although many classes of transcription factor had members with altered expression, two groups in particular stand out as having many members with altered expression: the WRKY and MYB groups of transcription factors.

Eighteen from a total of 148 MYB transcription factors were upregulated in the presence of gold whilst eight were downregulated (Table 4.7). Fourteen of the 72 WRKY genes present in Arabidopsis were upregulated in response to gold and 5 were downregulated (Table 4.8). The scale of regulation change is similar for the two families of transcription factor, although more WRKY genes are upregulated more than ten-fold than the MYBs. The scale of the downregulated MYB genes (32-fold) is greater that of the WRKY genes (four-fold).

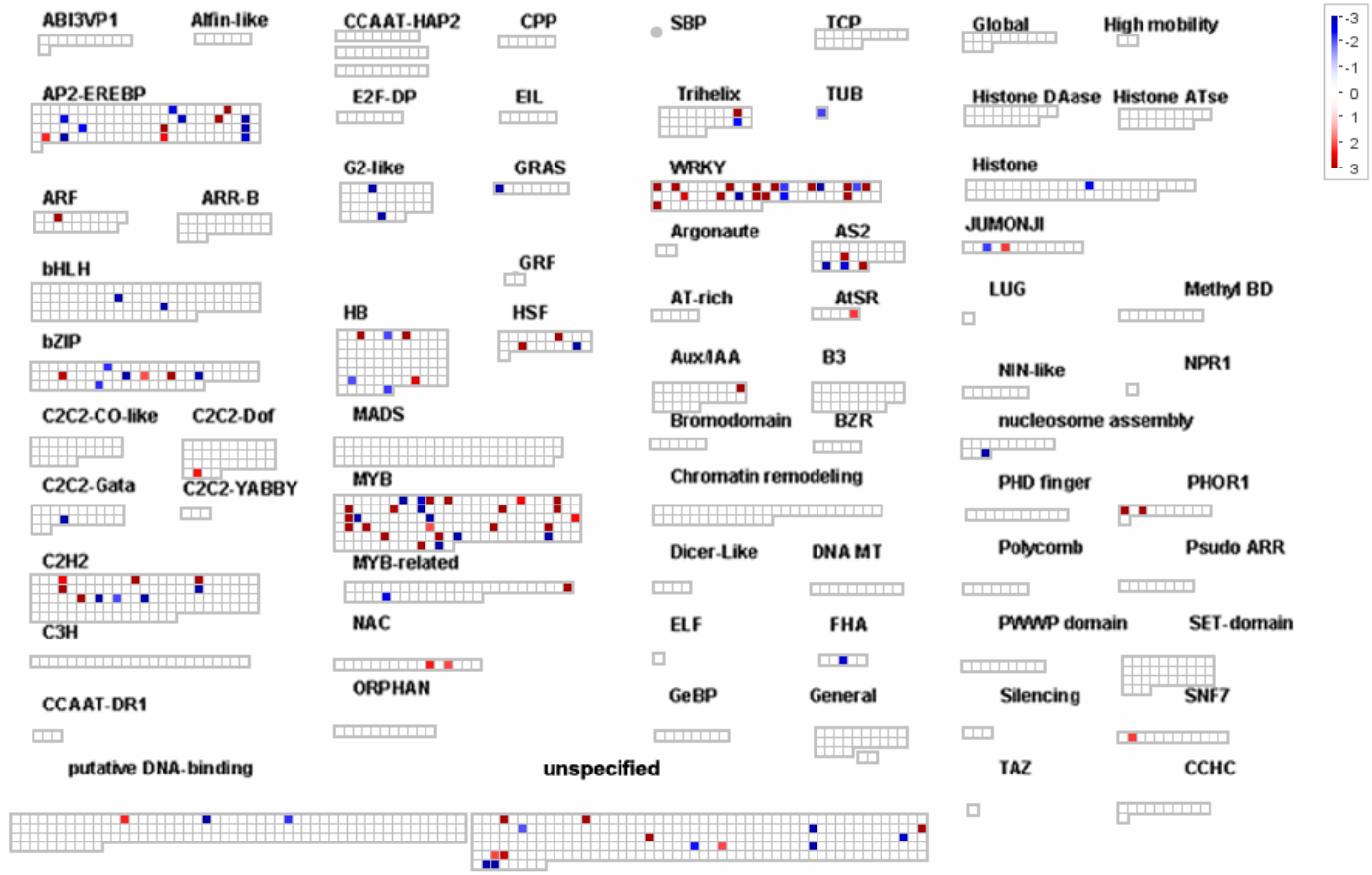

Figure 4.14 MapMan analysis of changes in transcription factor regulation
Overview of the transcription factors with altered regulation after treatment with 0.125 mM $KAuCl_4$. Blue represents downregulated genes, and red represents upregulated genes. All genes tested were included in this analysis, but only those with more than a two-fold change in regulation are coloured on the diagram. Figure was generated using MapMan (Thimm et al. 2004)

Table 4.7 Expression of the MYB transcription factors

The 26 MYB transcription factors with regulation altered more than two-fold in the presence of $KAuCl_4$. Gene descriptions were determined using TAIR.

Locus	Gene	Regulation
At3g23250	*MYB15*	42.64
At1g74080	*MYB122*	22.288
At1g18570	*MYB51*	16.948
At4g17785	*MYB39*	12.907
At1g17950	*MYB52*	9.411
At3g02940	*MYB107*	6.539
At1g48000	*MYB112*	6.051
At5g49620	*MYB78*	6.046
At1g73410	*MYB54*	5.797
At4g28110	*MYB41*	5.542
At1g79180	*MYB63*	5.163
At1g34670	*MYB93*	3.508
At5g65230	*MYB53*	3.234
At3g55730	*MYB109*	2.946
At5g16770	*MYB9*	2.903
At4g34990	*MYB32*	2.428
At5g65790	*MYB68*	2.396
At5g17800	*MYB56*	2.036
At5g52260	*MYB19*	-2.719
At5g59780	*MYB59*	-3.21
At4g01680	*MYB55*	-3.436
At2g47460	*MYB12*	-3.778
At5g61420	*MYB28*	-4.6
At3g46130	*MYB111*	-7.543
At1g56160	*MYB72*	-14.349
At3g12820	*MYB10*	-32.788

Table 4.8 Expression of the WRKY transcription factors
The 14 WRKY transcription factors with regulation altered more than two-fold (up or down) in the presence of $KAuCl_4$. Gene descriptions were determined using TAIR.

Locus	Description	Regulation
At3g01970	*WRKY45*	22.023
At5g13080	*WRKY75*	20.107
At5g46350	*WRKY8*	15.428
At3g56400	*WRKY70*	15.099
At4g18170	*WRKY28*	14.919
At2g46130	*WRKY43*	14.022
At2g38470	*WRKY33*	12.419
At2g46400	*WRKY46*	9.681
At2g40740	*WRKY55*	8.56
At5g49520	*WRKY48*	8.294
At1g62300	*WRKY6*	8.225
At4g22070	*WRKY31*	5.914
At1g64000	*WRKY56*	5.754
At1g29860	*WRKY71*	2.652
At2g25000	*WRKY60*	-2.07
At2g34830	*WRKY35*	-2.157
At3g58710	*WRKY69*	-2.397
At1g30650	*WRKY14*	-3.641
At5g52830	*WRKY27*	-3.964

4.3.8 FIT1

The microarray data showed that a number of the genes downregulated in response to gold are upregulated in response to iron deficiency (Figure 4.13). One of these genes (the 22nd most downregulated) was *FIT1* (Fe-deficient-induced transcription factor 1) and was downregulated almost 20-fold (Table 4.4). *FIT1* is a transcription factor involved in the regulation of 72 genes (Table 4.9) in response to iron, although for some of these genes, the regulation is thought to be partial (Colangelo and Guerinot 2004). Expression of *FIT1* is induced by iron deficiency which suggests that expression would be low when iron is not limited.

Thirty six of the 72 genes thought to be under FIT1 transcriptional control had regulation altered by more than two-fold in the microarray (Table 4.9). Of these, only two were upregulated; an oligopeptide transporter and a hypothetical protein. The other 34 genes were downregulated and included some of the most downregulated genes from the microarray. Of the 25 most downregulated genes in the microarray (Table 4.4), 12 were thought to be under the regulation of FIT1, including *FIT1* itself.

Table 4.9 Genes regulated by the FIT1 transcription factor
This list of genes (in locus order) and gene descriptions were derived from Colangelo and Guerinot (2004). Gene regulation of the 72 genes is as determined by microarray analysis presented in this work. Negative and positive numbers are fold change of downregulated and upregulated genes respectively in response to gold treatment. Where no number is present, the genes did not have regulation altered by more than two-fold in response to gold.

Locus	Description	Regulation
At3g48450	Hypothetical protein	6.0
At4g21680	Oligopeptide transporter (POT) family	5.7
At3g06890	Hypothetical protein	-2.2
At5g06490	C3HC4 RING zinc finger protein-like	-2.2
At4g12910	Ser carboxypeptidase I precursor-like	-2.3
At1g05530	Indole-3-acetate ß-D-glucosyltransferase	-2.4
At3g47040	ß-D-Glucan exohydrolase-like protein	-2.7
At3g54580	Extensin precursor-like protein	-2.9
At1g80830	NRAMP1, metal ion transporter	-3.0
At2g20030	Putative RING zinc finger protein	-3.2
At5g01060	Putative protein kinase, Class 1	-3.2
At1g05700	Putative light repressible receptor kinase	-4.2
At4g30120	HMA3, cadmium-transporting ATPase	-4.4
At3g07720	Unknown protein	-4.6
At1g51860	Receptor-like protein kinase	-5.4
At3g61410	Putative protein protein kinase	-6.0
At5g54790	Unknown protein	-7.3
At5g38820	Amino acid transporter family protein	-7.9
At1g14190	Putative mandelonitrile lyase	-9.5
At2g01880	Putative purple acid phosphatase	-13.1
At3g58060	Putative protein	-13.7
At1g56160	MYB72	-14.3
At3g58810	MTPa2, CDF family	-17.9
At1g34760	14-3-3 Protein	-18.9
At3g50740	UTP-glucose glucosyltransferase-like	-19.2
At2g28160	bHLH29/FIT1	-19.9
At5g03570	FERROPORTIN2, putative Fe transporter	-22.8
At3g46900	COPT2, copper transport protein	-23.6
At3g61930	Hypothetical protein	-26.4
At4g31940	Cytochrome P450-like monooxygenase	-30.8
At3g12820	MYB10	-32.8
At3g12900	Hypothetical, similar to oxidoreductases	-37.1
At4g19680	IRT2, Fe(II) transport protein	-38.4
At1g73120	Hypothetical protein	-43.2
At5g04950	NAS1, nicotianamine synthase	-67.6
At4g19690	IRT1, Fe(II) transport protein	-132.4
At1g09790	Putative phytochelatin synthetase	
At1g18910	Similar to flavonol-induced pollen germ.	
At1g49820	Unknown protein	
At1g60610	Similar to S-ribonuclease binding protein	

Locus	Description	Regulation
At1g77280	Receptor-like protein kinase	
At2g02310	Putative phloem-specific lectin	
At2g05830	Putative translation initiation factor eIF-2B	
At2g19410	Putative protein kinase	
At2g30670	Putative tropinone reductase	
At2g37040	Phe ammonia lyase (PAL1)	
At2g40000	Putative nematode-resistance protein	
At2g46740	Unknown protein	
At3g11750	Putative dihydroneopterin aldolase	
At3g13610	Similarity to DNA binding protein zyxin	
At3g18560	Unknown protein	
At3g21240	Putative 4-coumarate:CoA ligase 2	
At3g31415	Vetispiradiene synthase, putative	
At3g47420	Putative sn-glycerol-3-phosphate permease	
At3g51200	Putative protein	
At3g53280	Cytochrome P450 71B5	
At3g53480	ABC transporter-like protein	
At3g60330	AHA7, plasma membrane H+-ATPase	
At4g02330	Hypothetical, similar to pectinesterase	
At4g09110	Putative RING-H2 zinc finger protein	
At4g10510	Subtilisin-like Ser protease	
At4g14680	ATP-sulfurylase	
At4g19370	Hypothetical protein	
At4g29220	Phosphofructo-1-kinase-like	
At4g31950	Cytochrome P450-like monooxygenase	
At4g33020	ZIP9, Fe(II) and Zn transport protein	
At4g38950	Kinesin-like protein	
At5g02780	Putative protein In2	
At5g35580	Ser/Thr protein kinase-like, Class 1	
At5g36890	ß-Glucosidase	
At5g40590	Putative protein	
At5g47910	RbohD, respiratory burst oxidase protein	

4.3.9 Overview of transporter regulation

One of the aims of this work was to look at the mechanisms and uptake of gold, and therefore regulation of the Arabidopsis transporters was analysed using MapMan software. The resulting analysis (Figure 4.15) shows that in response to the treatment described here, 125 transporter genes had their regulation altered by two-fold or greater. Fifty four of these genes were upregulated and 71 of these genes were downregulated.

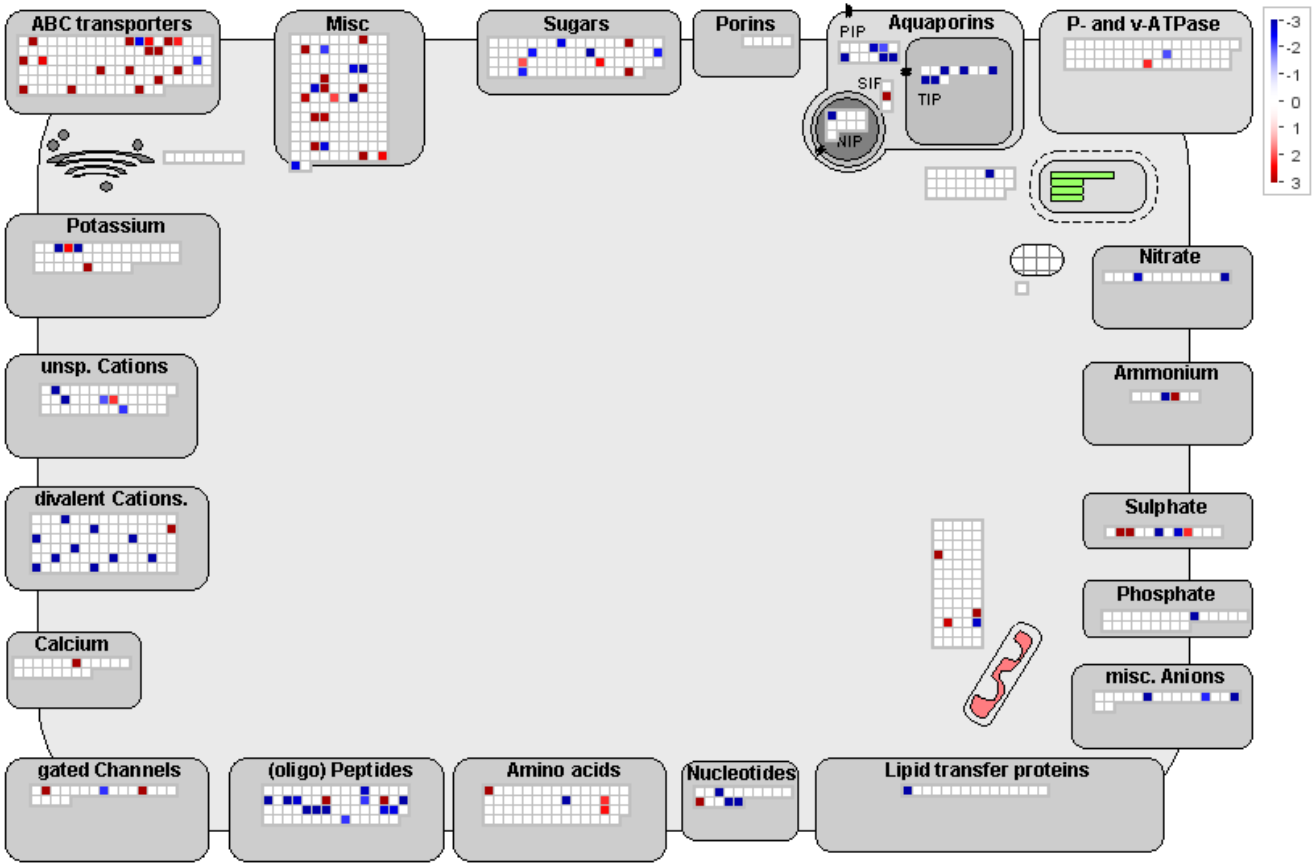

Figure 4.15 MapMan analysis of changes in transporter regulation
Heat map showing the differences in regulation of genes involved in transport within the plant. Only genes with changes in regulation of more than two-fold are displayed. Red represents upregulation with blue representing downregulation. The intensity of the colour shows the level of the regulation. All genes tested in the array were analysed, however only those with more than two-fold changes in regulation are represented by coloured squares. With less than two-fold changes, squares remain white. Figure generated using MapMan (Thimm et al. 2004).

4.3.10 Aquaporin regulation

As shown in Figure 4.15, the aquaporin family of transporters had altered regulation. Eleven aquaporins were downregulated and one was upregulated (Table 4.10). The one upregulated aquaporin was *SIP1;2*. This encodes an endoplasmic reticulum localised protein which functions as a water channel (Ishikawa et al. 2005). Of the 11 downregulated aquaporins, one was a *NIP*, five were *PIP*s and five were *TIP*s. These are described in Section 4.4.6.

The aquaporins with altered regulation in the presence of gold are generally expressed throughout the plant and strongly in the roots (Figure 4.16). The one exception to this is *SIP1;2* which was the only aquaporin upregulated in response to gold. Compared to the other aquaporins described here, *SIP1:2* has low root expression and is instead expressed in the seed and silique.

Table 4.10 Changes in aquaporin regulation
Changes in aquaporin regulation from the microarray experiment. Only genes with regulation altered more than two-fold are described, all other aquaporins did not have a regulation change greater than two-fold.

Fold Change	Regulation	Locus	Gene
13.91	Down	At1g31885	*NIP3;1*
3.55	Down	At3g61430	*PIP1;1*
2.84	Down	At1g01620	*PIP1;3*
9.69	Down	At4g23400	*PIP1;5*
8.03	Down	At5g60660	*PIP2;4*
2.04	Down	At4g35100	*PIP2;7*
7.12	Up	At5g18290	*SIP1;2*
5.39	Down	At2g36830	*TIP1;1*
5.79	Down	At3g26520	*TIP1;2*
8.94	Down	At3g16240	*TIP2;1*
16.84	Down	At4g17340	*TIP2;2*
10.79	Down	At5g47450	*TIP2;3*

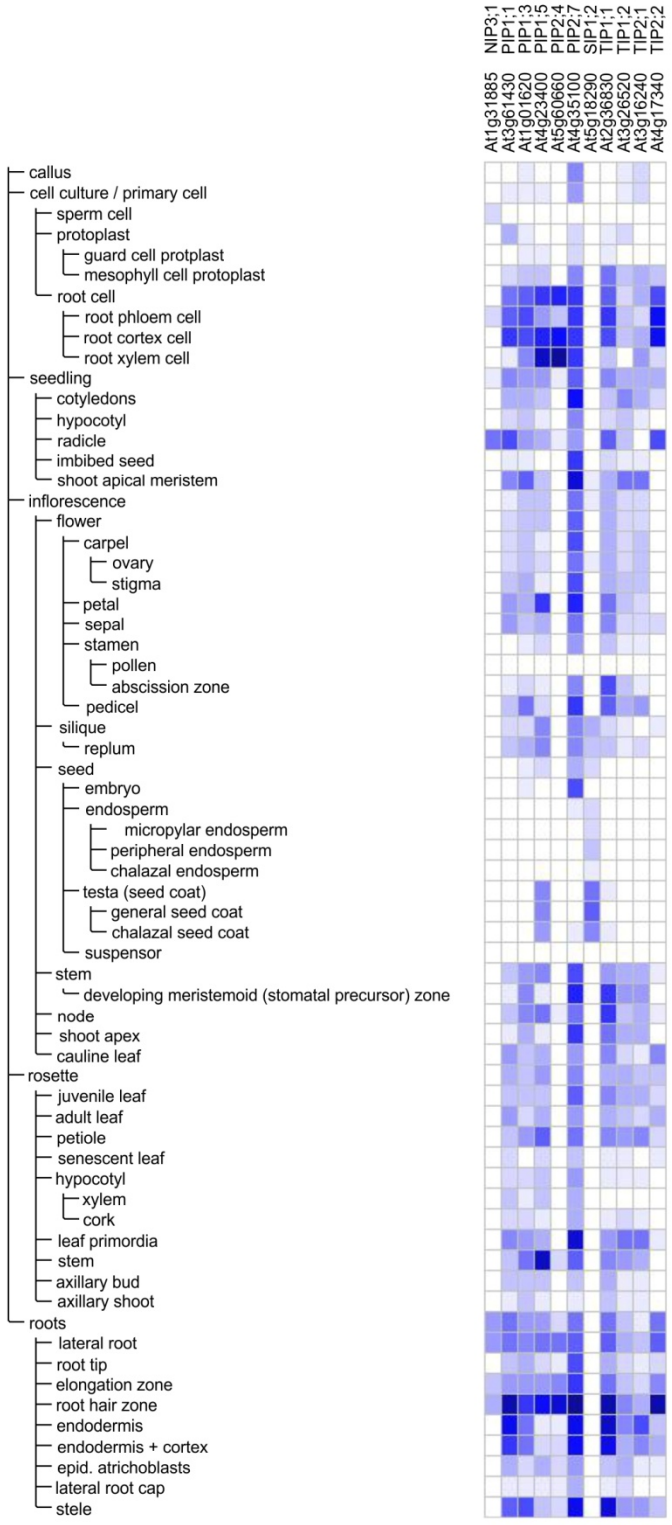

Figure 4.16 Aquaporin expression patterns
Spacial expression patterns of the aquaporins with greater than two-fold changes in expression in response to $KAuCl_4$ (see Table 4.10). Data and Figure generated using Genevestigator (Hruz et al. 2008).

4.3.11 Regulation of cation transporters

MapMan analysis of the transporters in Arabidopsis determined that 11 metal transporters had altered regulation in response to gold treatment (Table 4.11). *CAX3*, a transporter involved in Ca^{2+} regulation (Shigaki and Hirschi 2000; Shigaki et al. 2002) was the only divalent cation transporter found to be upregulated in the microarray analysis. Ten divalent cation transporters were downregulated more than two-fold in the presence of gold. One of these is a sodium hydrogen antiporter and the others have all been implicated in the transport of transition metals.

Expression profiles of the eleven genes encoding for divalent metal transporters with altered regulation in the presence of gold shows that the majority of the genes are normally expressed in the root tissues (Figure 4.17). Most of the genes also appear to be expressed in the radicle. Genevestigator analysis found that root expression for MTPc3, HMA3 or ATIREG3 was lower than the other genes investigated, although there was some expression. Root expression of these genes demonstrates that they could be important in metal tolerance, uptake or detoxification in the immediate presence of gold. Some of these genes (*IRT1*, *IRT2*, *COPT2* and *ATIREG2*) were within the most altered (more than 20-fold change in expression) in the microarray data and may therefore be important in gold tolerance or transport.

Table 4.11 Changes in regulation of divalent cation transporters
These data are the changes in regulation of those divalent cation transporters found to have altered regulation in response to gold treatment. Negative numbers show downregulation and positive numbers represent upregulation. Only genes with more than two-fold changes in regulation are shown.

Fold change	Locus	Gene	Description
-132.367	At4g19690	*IRT1*	Cadmium, copper, iron, manganese and zinc transporter
-38.405	At4g19680	*IRT2*	Iron and zinc transporter
-23.599	At3g46900	*COPT2*	Copper transmembrane transporter
-22.824	At5g03570	*ATIREG2*	Nickel transmembrane transporter
-17.925	At3g58810	*MTPA2*	Zinc ion transmembrane transporter
-13.743	At3g58060	*MTPc3*	Cation efflux family protein
-4.464	At4g30120	*HMA3*	Heavy metal ATPase 3
-3.243	At1g64170	*ATCHX16*	Sodium: hydrogen antiporter
-3.075	At5g26820	*ATIREG3*	Iron regulated protein 3
-3.012	At1g80830	*NRAMP1*	Manganese transmembrane transporter
4.648	At3g51860	*CAX3*	Calcium cation antiporter

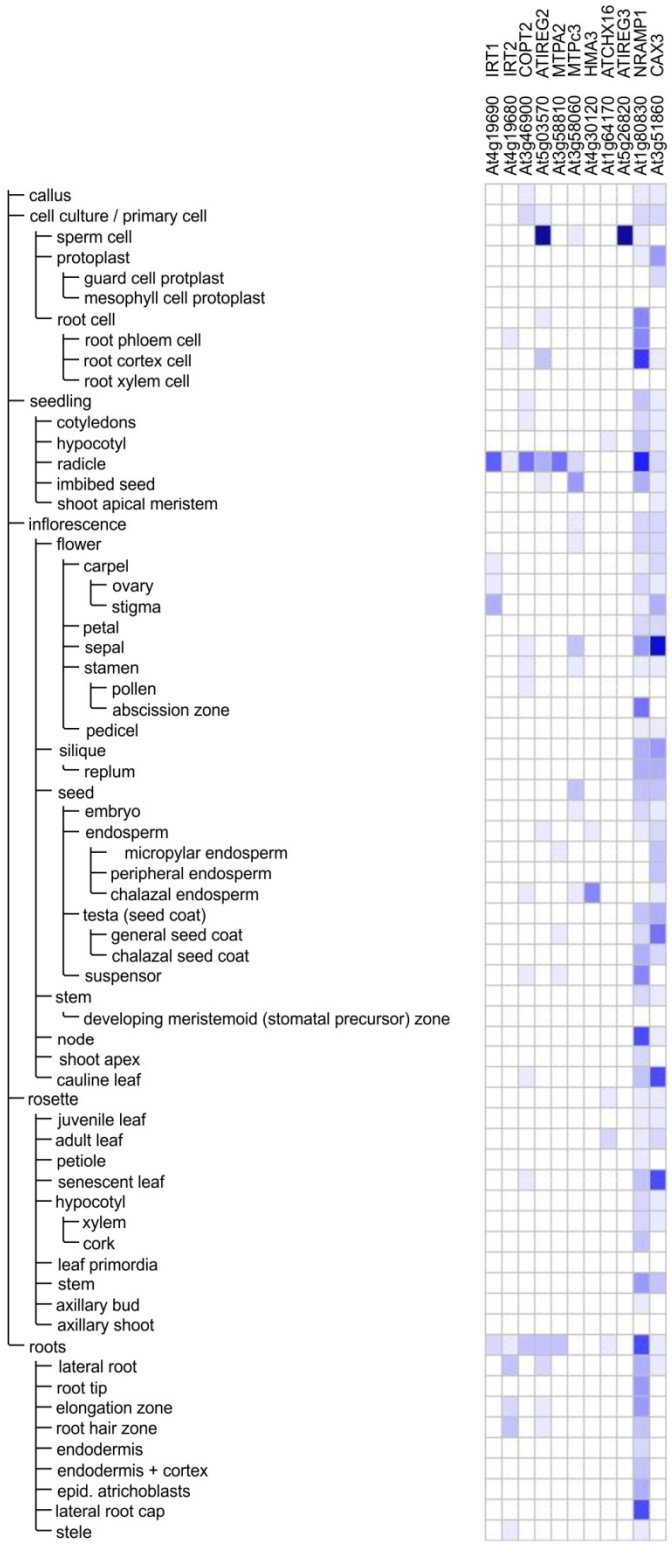

Figure 4.17 Expression patterns of the metal transporters with altered regulation in this work

Spacial expression patterns of the divalent metal transporters with greater than two-fold changes in expression in response to $KAuCl_4$ (see Table 4.11). Data and Figure generated using Genevestigator (Hruz et al. 2008).

4.3.12 Responses of other gene families

Many genes from families which have a large number of members were upregulated in the presence of gold (Figure 4.18). From this analysis, three groups of genes appear to be most altered with gold: cytochromes P450, glutathione-S-transferases (GSTs) and peroxidases. Members of these families have been shown to respond to various stresses. Cytochromes P450 are involved in the stress response to various treatments including hormones, pathogens, and copper (Narusaka et al. 2004). The GSTs have previously been shown to be induced by both abiotic and biotic stress (reviewed in Dixon and Edwards (2010) and Marrs (1996)), therefore the large number of upregulated GSTs could indicate that they are upregulated as a general response to stress. Peroxidases have also been shown to respond to various stresses and stimulants, including infection, drought, cold and metal stress (Schenk et al. 2000; Thimm et al. 2001; Seki et al. 2002; Miao et al. 2006).

Of the cytochromes P450, 18 were upregulated and 19 were downregulated out of a total of 272 (14 %) (Figure 4.18). Some of these genes were strongly upregulated (up to 127-fold). There was no pattern seen within those P450s with altered regulation. Twenty seven of 54 GSTs (Dixon and Edwards 2010) had altered regulation (47 %) of which only six were downregulated. Ten of the upregulated genes had greater than 15-fold upregulation. The most upregulated GST was altered by 220-fold and was one of the most upregulated genes in the microarray. Of the downregulated genes, the lowest was 32-fold downregulation. Fifteen peroxidases were upregulated and eight were downregulated out of a total of 73. The most upregulated was increased by 73-fold and the lowest, was downregulated 14-fold.

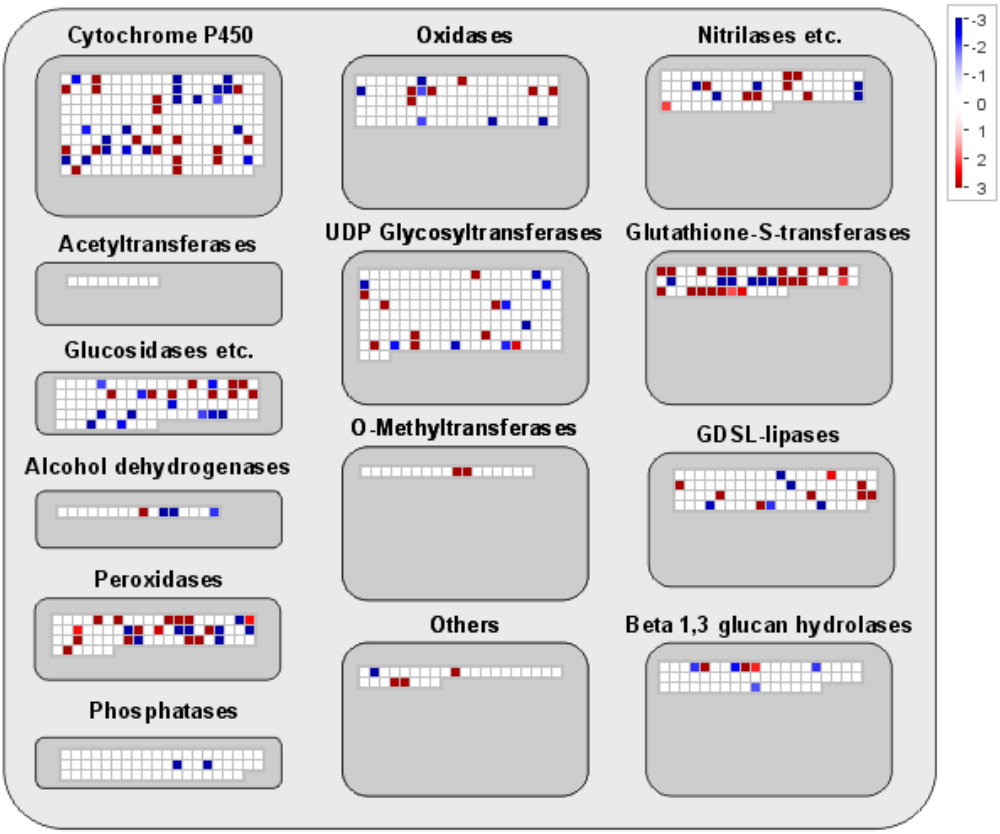

Figure 4.18 MapMan analysis of the changes in expression of large enzyme families

Overview of the members of various enzyme families with altered regulation after treatment with 0.125 mM $KAuCl_4$. Blue represents downregulated genes, and red represents upregulated genes. All genes tested were included in this analysis, but only those with more than a two-fold change in regulation are coloured on the diagram. Figure was generated using MapMan (Thimm et al. 2004).

4.4 Discussion

In this Chapter, microarray technology was used to identify Arabidopsis genes with altered regulation in the presence of gold, with the aim of beginning to determine how plants respond to this stress. Previous research into the response of Arabidopsis to aluminium formed the basis for the microarray experiments presented here (Kumari et al. 2008). Preliminary experiments based on this work determined that 14-day-old Arabidopsis seedlings would be treated with 0.125 mM $KAuCl_4$ for six hours. Microarray experiments were therefore carried out using RNA from the roots of plants treated in this way. The results were validated by carrying out qPCR on a selection of genes, showing that the microarray data could be used to identify which genes were up and downregulated in response to gold. These results also demonstrate that the microarray data can be used to give an idea of the scale of the changes in regulation compared the change in regulation of other genes.

Root tissue is exposed to the gold treatment and so was most likely to show a response to gold exposure. Additionally, nanoparticles were found within Arabidopsis roots and the root growth was inhibited by gold treatment, demonstrating that the roots are important in gold tolerance (see Chapter 3). The microarray experiment performed here was therefore performed using RNA from root tissues only.

There are no published studies of the genetic analysis of gold tolerance or uptake in plants and consequently, comparison of the results presented here with similar studies using gold is impossible. However, microarray analyses using other metals have been carried out. The treatment conditions data from some of these arrays are summarized in Table 4.12. It is evident that there are differences between the treatment conditions in the different experiments (for example treatment time and plant age), therefore direct comparisons are difficult to make. Comparisons of data from microarrays performed using $AgNO_3$ (silver is closely related to gold in the periodic table), are not simple because of the significant effects that will have been due to the nitrate within $AgNO_3$.

Table 4.12 Summary of microarray data for metal stress experiments

Summary of up and downregulated genes from different microarray experiments using different heavy metal treatments. Experimental methods and results are all determined from the literature and published results. All experiments were carried out using the Col-0 Arabidopsis ecotype. References refer to 1. Kumari et al. (2008), 2. Herbette et al. (2006), 3. Liu et al. (2009), 4. Goda et al. (2008).

Treatment	Plant age	Tissue	Time (hours)	Up	Down	Genes Tested	Reference
$AlCl_3$ 25 µM	14 days	Roots	6	111	110	23686	1
$AlCl_3$ 25 µM	14 days	Roots	48	464	343	23686	1
$CdSO_4$ 5 µM	3-4 weeks	Roots	6	42	101	21612	2
$CdSO_4$ 50 µM	3-4 weeks	Roots	6	75	58	21612	2
$KAuCl_4$ 125 µM	14 days	Roots	6	869	851	22746	This work
$Pb(NO_3)_2$ 1 µM	20 days	Whole	3	111	176	6120	3
$Pb(NO_3)_2$ 10 µM	20 days	Whole	3	75	238	6120	3
$Pb(NO_3)_2$ 100 µM	20 days	Whole	3	160	189	6120	3
$AgNO_3$ 10µM	7 days	Whole	3	1784	2878	21095	4

4.4.2 General microarray results and comparisons

Of all measured genes in this work, 7.5% (1720) had altered expression greater than two-fold in response to treatment with $KAuCl_4$. These were distributed approximately equally between the up and downregulated genes (869 and 851 respectively), as was the case for most of the treatments described in Table 4.12 (10 µM lead treatment is the exception). The number of genes with altered expression of greater than two-fold in the presence of gold was approximately nine times greater than had been demonstrated for six hours treatment with aluminium and twice as much for the 24 hour treatment with aluminium (Kumari et al. 2008). The numbers were also greater than those for cadmium, and lead treatment, although for lead, the expression of fewer genes was tested (approximately 6 000 compared to over 20 000) (Herbette et al. 2006; Liu et al. 2009). Comparing the data presented here to the silver microarray demonstrates a similar number of genes with altered regulation (Goda et al. 2008). This is perhaps unsurprising because gold and silver share periodicity, whereas aluminium, cadmium and lead are less similar and are therefore unlikely to elicit a similar response.

When the expression of all up and downregulated genes was studied (Section 4.3.5), some classes of genes were proportionally altered in regulation more than others, suggesting an important role in gold tolerance. Genes encoding transporters were overrepresented as a proportion of the downregulated genes. It is assumed that there are two general categories of metal transporters; those that transport metal into the cell, and those that transport metal out of the cell. It would be expected that transporters responsible for the influx of metal into the cell would be downregulated in response to excess of that metal to reduce the amount of metal getting into the cell. Conversely, those that are responsible for efflux of metal would be upregulated to remove excess metal from the cytoplasm. The GO annotations do not classify the transporters into those which are responsible for influx or efflux of metals, or indeed which are responsible for metal transport at all. The regulation of specific transporters would therefore have to be studied individually. Some metal transport proteins are discussed in further detail below (Section 4.4.5).

The 25 most upregulated and 25 most downregulated genes in the microarray performed in this work were studied using Genevestigator to determine the

conditions in which they have been found to have altered regulation. Studies of the upregulated genes found that the majority are upregulated in response to infection, but also high temperatures and other stresses, such as drought and hypoxia. These data suggest that the genes upregulated by the largest amount were upregulated as a general response to stress.

Evaluating the expression of the 25 most downregulated genes found that 20 of these genes were upregulated in iron deficient conditions (Figure 4.13). This therefore suggests that they would be downregulated in the presence of excess iron although no microarray data are available to investigate this hypothesis. It appears that the downregulation of these genes may have been due to a response to excess metal, specifically the interaction of gold within the iron tolerance pathway. A number of the genes appear to be under the control of the FIT1 transcription factor, a hypothesis which is explored below (Section 4.4.4).

Studying large families identified many genes which were either up or downregulated in response to gold. These included cytochromes P450, peroxidises and glutathione-S-transferases. These data further suggest that many of the changes in gene regulation were due to a general response to stress rather than due to gold specifically. The characterisation of the effects of gold on Arabidopsis described in Chapter 3 demonstrated the toxicity of gold and so at the gold concentrations used in the microarray experiment, it is unsurprising that a large general stress response was observed.

The most upregulated gene with a known function was *ATGSTU12*, which is a member of the tau class of glutathione transferases (GSTs). Members of the GST family are generally known to be upregulated in response to stress as reviewed by Dixon and Edwards (2010). *CYP71A12* encodes a cytochrome P450, a group of proteins upregulated in response to stress and also peroxides as reviewed by Schuler and Werck-Reichhart (2003). An increase in peroxide would also explain the upregulation of *At1g14550*. This gene is thought to be a peroxidase and therefore could be involved in the elimination of peroxides. The fourth upregulated gene used to verify the microarray was *UGT73B4*; a glucosyl transferase (GT). The GTs have been shown to be upregulated in response to various stresses including TNT and pathogens and have been shown to be important in xenobiotic metabolism (Brazier-Hicks and Edwards 2005; Langlois-Meurinne et al. 2005; Gandia-Herrero et al. 2008).

Of the downregulated genes, *IRT1*, *IRT2* and *MTPA2* (or *MTP3*) were three of the most downregulated genes. As described in Chapter 1, the IRT proteins are membrane transporters shown to have high affinity to iron but can also interact with other metals (Eide et al. 1996; Korshunova et al. 1999; Rogers et al. 2000; Vert et al. 2002) and the MTP3 protein has been shown to be involved in the zinc tolerance pathway (Arrivault et al. 2006). It is therefore likely that these genes are involved in response to gold.

4.4.3 Transcription factors

Members of several groups of transcription factors had altered expression after treatment with gold (Figure 4.14). The main two transcription factor families with a large number of members with altered expression were the WRKY and the MYB families. These two families have previously been found to be involved in response to different biotic and abiotic stresses. The WRKY transcription factors are a large family of transcription factors in plants and are distributed throughout the eukaryotes (Zhang and Wang 2005). These proteins are involved in a wide range of plant processes and stress responses. WRKY transcription factors play a role in the defence responses and senescence (Eulgem et al. 2000) and many WRKY genes are upregulated in response to pathogens (Dong et al. 2003). *Pseudomonas syringae* and a human pathogen have both been shown to cause the upregulation of several WRKY genes (Thilmony et al. 2006; Murray et al. 2007). In addition to this, salicylic and abscisic acid lead to WRKY upregulation (Kalde et al. 2003; Chen et al. 2011) and published evidence demonstrates that WRKY genes can occur under drought stress and metal deficiency (Ricachenevsky et al. 2010). This indicates the wide diversity of function of the WRKY transcription factors.

The MYB family of transcription factors also has a wide range of functions and is involved in the response to various biotic and abiotic stresses. As with the WRKY transcription factors, members of the MYB family are involved in the response to pathogens by initiating a cell death response and promoting salicylic acid synthesis (Raffaele et al. 2008; Froidure et al. 2010; Seo and Park 2010). MYB transcription factors have also been shown to be involved in drought tolerance and osmotic stress as well as freezing tolerance and responses to plant hormones (Agarwal et al. 2006; Jung et al. 2008; Ding et al. 2009; Li et al. 2009; Lippold et al. 2009; Seo and Park 2010). There therefore appears to be overlap

in the conditions in which the MYB and WRKY transcription factors are overexpressed, however, the theme that unites the two is that they are generally expressed in response to different stresses.

Fourteen of the 72 WRKY genes were upregulated in response to gold; 5 were downregulated. The upregulation of these is indicative of a general stress response in response to gold. As mentioned above, WRKY genes are activated by a number of different stresses and it appears likely that the upregulation of the WRKY proteins seen here is due to a general stress response, rather than specifically in response to gold.

Generally, the WRKY genes that were upregulated in response to gold, were also (with some exceptions) upregulated in response to silver nitrate (Goda et al. 2008). Those that were not upregulated, tended to be those that were least altered in the gold treatment. Most of the downregulated WRKY genes were not altered in the silver treatment and those that were had low levels of down regulation (approximately two-fold). This contrasts with the results for the aluminium and cadmium microarrays. The expression of most of the genes with altered regulation in the presence of gold was not observed in the aluminium or cadmium studies. For the cadmium study, none of the genes with altered regulation in response to gold were altered by cadmium treatment. In the aluminium study, none of the genes with altered regulation in response to gold were upregulated. Most had no change in regulation and the rest were downregulated. These results suggest that upregulation of the *WRKY* genes in response to gold was not a general response to metals but was a response to gold and similar metals (i.e. silver). *WRKY* genes were also upregulated in response to lead although the data from the study have not been made publically available, so it is not possible to determine which genes these were.

Eighteen of 148 MYB transcription factors were upregulated in response to gold; eight were downregulated. The four MYB genes with the largest increase in expression in the presence of gold were also increased in the presence of silver suggesting that they are important in the response to general metal stress. However, the gene with the fifth largest increase in expression in this study was downregulated in the presence of silver. The majority of the other genes with altered regulation in response to gold did not have altered expression in the presence of silver although two genes downregulated in response to gold were

also downregulated in the presence of silver. As with the WRKY genes, most of the MYB genes were not tested in the aluminium or cadmium microarray experiments. Of those that were, none of those with altered regulation in response to gold were altered in response to cadmium and only two had altered regulation when treated with aluminium. One of these had a high change in expression (increase of approximately 260-fold). Although the lead microarray data are not publically available, the researchers note that *MYB39*, *MYB63* and *MYB93* were increased during lead treatment (Liu et al. 2009). These were also upregulated in response to gold.

The results presented here imply that although there are differences in the regulation of transcription factors between gold and the other metals mentioned, there are also similarities. These similarities appear greatest between gold and silver, which is not surprising due to the similarities in the chemical nature of the two elements. It could be proposed that the responses of the MYB and WRKY transcription factors to gold are specific to gold and not a general response to stress. However, previous research suggests diversity in the functions of WRKY and MYB transcription factors, and some of these genes have altered regulation in response to metals. It is therefore likely that the altered regulation of the WRKY and MYB transcription factors described here is a general response to stress. However, the suggestion that the change in expression of one or more of these transcription factors is in specific response to gold or similar metals, should not be discounted.

4.4.4 The FIT1 transcription factor

The expression of two families of transcription factors is described above (MYB and WRKY families). However, these were not the only transcription factors with altered expression. One of these other transcription factors is FIT1 (At2g28160). The microarray data described here demonstrate that *FIT1* was downregulated almost 20-fold. This was one of the most downregulated genes on the microarray. FIT1 is a basic helix-loop-helix (bHLH) transcription factor upregulated in iron deficient conditions and as such increases the transcription of the genes it controls (Colangelo and Guerinot 2004; Jakoby et al. 2004; Yuan et al. 2005). In conditions of excess iron, FIT1 is downregulated (Colangelo and Guerinot 2004). It has been demonstrated that for some of its functions, FIT1 interacts with other bHLH proteins Notably AtbHLH38 and AtbHLH39, which are

functionally redundant, can bind FIT1 and the interaction regulates IRT1 and FRO2 expression (Yuan et al. 2008). The expression of bHLH38 was not measured as it was not present of the microarray, and bHLH39 did not have more than two-fold change in expression.

The regulation of a large number of the most downregulated genes is thought to be carried out by FIT1. As described in Table 4.9, 34 of the genes thought to be regulated by FIT1 were downregulated in the presence of gold including FIT1 itself. Thus, the data presented here show that in the presence of gold, FIT1 was downregulated, which led to the downregulation of a number of other genes under its control. It would therefore appear that gold interacts in some way with FIT1 itself or with an iron regulatory and sensing system within the plant. The interactions described do not appear to be as strong as those for iron in that not all of the genes under the regulation of FIT1 were downregulated. It is possible that the regulation of these genes only occurs in iron deficient conditions or that the regulation of these genes requires FIT1 interaction with another protein which has unaltered expression.

The regulation of *FIT1* was not changed in the presence of silver (Goda et al. 2008) and only ten of the 34 FIT1 regulated genes downregulated in the presence of gold were downregulated in the presence of silver. This suggests that gold and silver interact with FIT1 in different ways. *COPT2* was downregulated by both silver and gold, suggesting that they both acted similarly on the expression of *COPT2* and that this interaction was independent of FIT1. This may also be the case for *IRT2* expression, which was downregulated in both the presence of silver and gold. Although *FIT1* was downregulated in roots in the presence of aluminium, the data reveal that the downregulation was less than two-fold (-1.59-fold) but was classified as downregulation as the researchers used a 1.5-fold threshold (Kumari et al. 2008). *FIT1* expression was not altered by the cadmium treatment (Herbette et al. 2006). Thus it appears that compared to aluminium, cadmium and silver, gold elicits different responses and as such the *FIT1* downregulation observed in this microarray was due to the presence of gold, rather than the presence of metal in general. It is not the case that the changes in FIT1 regulation (and that of the genes under its control) have altered expression due to a reduction in iron uptake because the regulation of these genes is the opposite of what would be expected (i.e. upregulation would be expected).

The data presented here also suggest that the iron regulatory system, including the FIT1 transcription factor is not specific to iron and may also be induced by other heavy transition metals. This could be tested by studying expression in the presence of other metals in a similar part of the periodic table to gold, such as mercury, platinum, copper or palladium. Other metals more closely related to iron could also be tested, such as manganese or cobalt.

To further investigate the effects of gold on the control of FIT1 and the associated genes, *fit1* mutant plants could be studied in their response to gold. Grown in the presence of gold, these plants could be affected more if the downregulation of all of the genes described in this chapter leads to reduced tolerance to gold. Mutants unable to express *FIT1* would therefore have decreased expression of these genes and so tolerance would be reduced. Alternatively, the converse of this may be true. If the altered regulation observed is important in gold tolerance, then *FIT1* mutants could have increased tolerance to gold due to the reduced expression of these genes (for example if downregulation reduces the amount of gold entering the plant). However, homozygous *fit1* T-DNA insertion mutants are lethal and must be supplemented with excess iron because *IRT1* is not expressed in *fit1* mutants and as such, iron uptake is reduced (Colangelo and Guerinot 2004). It would therefore not be possible to carry out studies in iron deficient conditions.

To investigate the interaction of gold within the iron regulatory system, the response of the genes downregulated in response to gold could be studied in iron deficient conditions with supplemental gold added. Depending on how gold is interacting with the iron response system, those which genes are upregulated in iron deficient conditions may be downregulated or expressed at “normal” levels when grown in iron deficient conditions and subsequently treated with gold. The reverse experiment is not possible as gold is not essential to the plants and so gold deficient conditions are impossible to engineer.

4.4.5 Metal transporters

Characterisation of gold uptake in Arabidopsis described in Chapter 1 found that gold is taken up and translocated through the plant. It was therefore interesting to look at the microarray data to determine whether any metal transporters had altered regulation. Analysis found 11 metal transporters with altered regulation in

response to gold treatment, ten of which were downregulated and included some of the most downregulated genes in the experiment (see Section 4.3.11). The downregulated genes were interesting because downregulation of these genes could mean that the plant was responding to the uptake of gold by inhibiting uptake. This therefore raises the possibility that one or more of the downregulated transporters are able to transport gold. An alternative hypothesis would be that the gold is interacting with the sensing and tolerance mechanism for another metal. This hypothesis has been discussed for the FIT1 regulation of iron uptake as described above.

The most downregulated gene in response to gold was *IRT1* (At4g19690) with an approximately 130-fold decrease in expression. IRT1 is an iron regulated transporter with preference for Fe(II) (Eide et al. 1996). However, IRT1 is also able to transport cadmium, cobalt, manganese, zinc and possibly copper (Eide et al. 1996; Korshunova et al. 1999; Rogers et al. 2000; Vert et al. 2002). With this wide specificity, it is therefore possible that IRT1 is also able to transport gold. *IRT1* expression is thought to be under the control of the FIT1 transcription factor as described above. *IRT2* was also downregulated in the presence of gold (38-fold), which is perhaps unsurprising considering that the two genes are closely related (see Chapter 1). IRT2 is also thought to be under partial FIT1 control and the expression change in response to gold could be due to the alteration of *FIT1* expression. It is again possible that the IRT2 transporter is able to transport gold.

One of the most downregulated genes in the microarray experiment was *COPT2* (approximately 23-fold). COPT2 is one of six members of the COPT family of copper transporters, the first member of which has been shown to transport copper into cells (Kampfenkel et al. 1995; Sancenon et al. 2003). Due to the chemical similarities of copper and gold (they share periodicity) and because COPT2 is highly likely to be a copper transporter, COPT2 was studied in relation to gold uptake and gold tolerance. This research is described in Chapter 5. Although *COPT2* expression is possibly controlled by FIT1, the control is only thought to be partial and it is likely that more than one factor was involved in the suppression of *COPT2* expression in response to gold (Colangelo and Guerinot 2004).

In addition to *IRT1*, *IRT2* and *COPT2*, other genes encoding transition metal transporters were downregulated; ATIREG2, which transports nickel (Schaaf et

al. 2006); ATIREG3 which putitatively transports nickel (Schaaf et al. 2006); MTPA2, a zinc transporter (Arrivault et al. 2006); MTPC2, potentially involved in manganese detoxification (Yang et al. 2010); ATCHX16, a cation antiporter (Cellier et al. 2004) NRAMP1, an iron transporter (Curie et al. 2000) and HMA3, which is discussed in detail below.

The HMA family of metal transport proteins, which are described in Chapter 1 and Section 4.1.1, is involved in metal efflux from the cytoplasm, either out of the root, or into the vacuole or xylem (Puig et al. 2007). If gold were to have an effect on the transcription of the *HMA* genes, it may have been expected that there would be upregulation of these genes as a response to excess metal. The microarray data presented here showed that the transcription of only one member of the *HMA* family was altered in the presence of gold. *HMA3* was downregulated in the presence of gold (4.5-fold). However, in the Columbia ecotype of *A. thaliana* (which was used in this work), *HMA3* contains a nonsense mutation which leads to the translation of a truncated protein, missing key parts required for metal transport (Gravot et al. 2004; Verret et al. 2004; Williams and Mills 2005). The change in *HMA3* expression will therefore have no effect on the plant tolerance to gold. The results presented here show that the HMA family of metal transporters is unlikely to be involved in the Arabidopsis response to gold. It is possible that HMA3 is involved in other Arabidopsis ecotypes, and that in Col-0, although the function has been lost, *HMA3* expression control has not.

Although the COPT family was studied in this work, an obvious future direction would be to study the other metal transporters with altered regulation in response to gold. The obvious candidates to study first would be the two *IRT* genes which were two of the most downregulated genes in the microarray. As these two proteins are members of a much larger family (the ZIP family, see Chapter 1), expression of these and their possible function in gold uptake could also be studied.

4.4.6 Aquaporins

The aquaporins are a group of 35 proteins in Arabidopsis (Quigley et al. 2002). These 35 proteins have been classified into four groups, the plasma membrane intrinsic proteins (PIPs), tonoplast intrinsic proteins (TIPs), and nodulin-26-like membrane proteins, of which there are two groups, NIPs and SIPs (Johanson et

al. 2001). Although the names of the protein groups suggest that they localise to specific intracellular organelles, this is not the case, and the groups are present in multiple cellular locations with multiple functions (reviewed in Maurel et al. (2008)). Aquaporins have also been shown to be expressed in different tissues throughout plants (Quigley et al. 2002) and transport a range of compounds including arsenic, boron and ammonia as well as various other small molecules (Loque et al. 2005; Takano et al. 2006; Isayenkov and Maathuis 2008).

Of the 35 aquaporin genes in the Arabidopsis genome, 11 were downregulated and one was upregulated. Those which were altered represented all four groups of proteins. Only those from the TIP group of the proteins were closely related, with all three of the TIP2 proteins downregulated. The upregulated aquaporin was SIP1;2, a water channel located on the endoplasmic reticulum and is therefore unlikely to be involved in water uptake (Ishikawa et al. 2005).

Gold has previously been shown to inhibit aquaporin function (Niemietz and Tyerman 2002) and is hypothesised to contribute to the toxicity of gold outlined in Chapter 3. Aquaporin inhibition is likely to be a similar mechanism to mercury inhibition of aquaporins with covalent modification of cysteine residues (Preston et al. 1993; Niemietz and Tyerman 2002). As aquaporin function is likely to be inhibited by gold treatment, water uptake would decrease. It would therefore be logical to predict that aquaporin expression would increase in the presence of gold to counteract the reduced water uptake. However, this is not what the data presented here show. Gold treatment was followed by the downregulation of aquaporins (with the exception of SIP1;2).

Evidence in the literature supports the results presented here. Stress conditions have been shown to lead to a reduction in water uptake by the downregulation of aquaporins (reviewed by Javot and Maurel (2002)) including , drought stress and high salt concentrations (Smart et al. 2001; Maathuis et al. 2003). It therefore appears that the downregulation of aquaporins observed in this study was a general response to stress and not in response to the gold. The upregulation of SIP1;2 observed here was also upregulated after aluminium and silver treatments, further suggesting a general stress response. However the downregulation of the aquaporins was not observed in any of the other published microarray data discussed here. It therefore appears that gold elicits a different response in aquaporin regulation compared to other metals.

4.4.7 Microarray conclusions

In this Chapter, microarray data have been presented which describe the genetic response of Arabidopsis to gold. The treatment with gold brings about a large general stress response due to the toxicity of the gold that was described in Chapter 3. There are, however, many interesting responses that appear to be due to the gold treatment, rather than a general stress response. Comparisons of results with microarray data from studies with non essential metals has identified some genes which appear to respond to gold rather than general stress. Interestingly, this included a number of metal transporters, one of which was further studied in Chapter 5. Gold also appears to strongly influence the iron deficiency pathway: many genes that are normally upregulated in iron deficienct conditions (under the control of the transcription factor FIT1) were downregulated in response to gold. This suggests that gold and FIT1 interact leading the some of the changes observed in this study.

Chapter 5 The COPT family of metal transporters

5.1 Introduction

5.1.1 The COPT family of transporters

The Arabidopsis Copper Transport (COPT) family is a member of the copper transport (CTR) family which is conserved and distributed throughout many eukaryotes. The first member to be discovered in Arabidopsis was COPT1. This was found when an Arabidopsis cDNA library was screened for genes able to complement the yeast *ctr1-3* mutant, which is defective in copper uptake (Kampfenkel et al. 1995). Four more Arabidopsis COPT proteins were subsequently discovered by both sequence homology and complementation studies with the yeast *ctr1-3* mutant (Sancenon et al. 2003). These four proteins were named COPT2 to COPT5. It has been suggested, after more recent annotation of the Arabidopsis genome, that there is a sixth member of the COPT family (Puig et al. 2007; Penarrubia et al. 2010). These six genes are distributed throughout the Arabidopsis genome with *COPT1* and *COPT3* adjacent to each other on chromosome five (Figure 5.1).

The CTR proteins are a group of small proteins with three transmembrane domains (Figure 5.2) (Dancis et al. 1994; Puig et al. 2002; Klomp et al. 2003). These proteins trimerise in the membrane, becoming cone shaped pores as indicated in Figure 5.2 (Peña et al. 2000; Lee et al. 2002; De Feo et al. 2009). The MxxxM domain (two methionine residues separated by any three amino acids) within the second of the three transmembrane domains is likely to be the most important domain for trimerisation, although the GxxxG motif within the third domain is also important (Puig et al. 2002; Aller et al. 2004).

Other important residues within CTR proteins include methionine rich regions prior to the first transmembrane domain (Figure 5.2 and Figure 5.3) (Puig et al. 2002). CTR proteins with mutations of these methionine residues, or in those within the second transmembrane domain, exhibit copper transport inhibition, indicating that these methionine rich regions are essential for metal transport (Puig et al. 2002; De Feo et al. 2009).

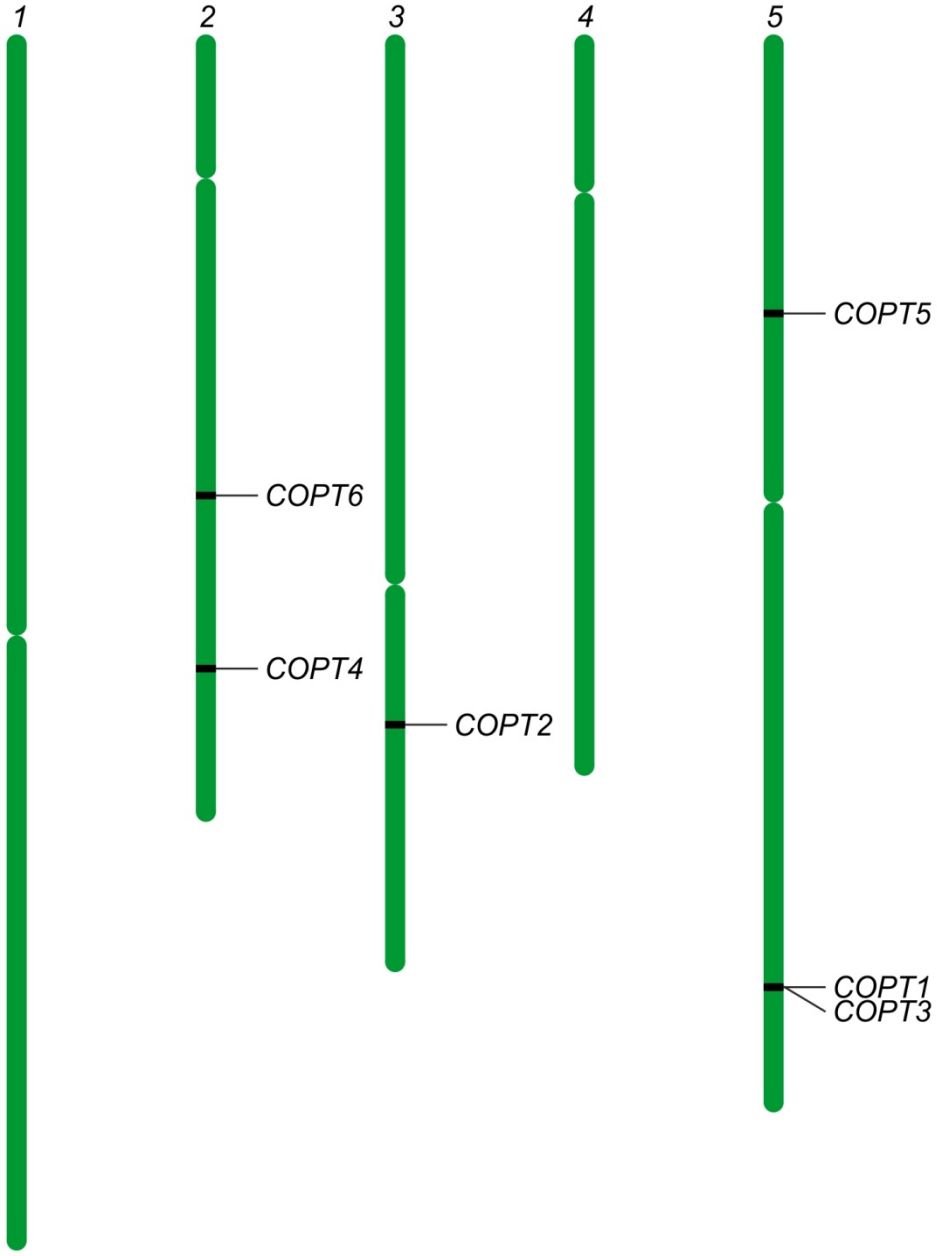

Figure 5.1 Chromosomal locations of the *COPT* genes within the Arabidopsis genome

COPT1 – At5g59030, *COPT2* – At3g46900, *COPT3* – At5g59040, *COPT4* – At2g37925, *COPT5* – At5g20650 and *COPT6* – At2g26975. Figure produced using the TAIR chromosome map tool (http://www.arabidopsis.org/jsp/ChromosomeMap/tool.jsp) (Rhee et al. 2003).

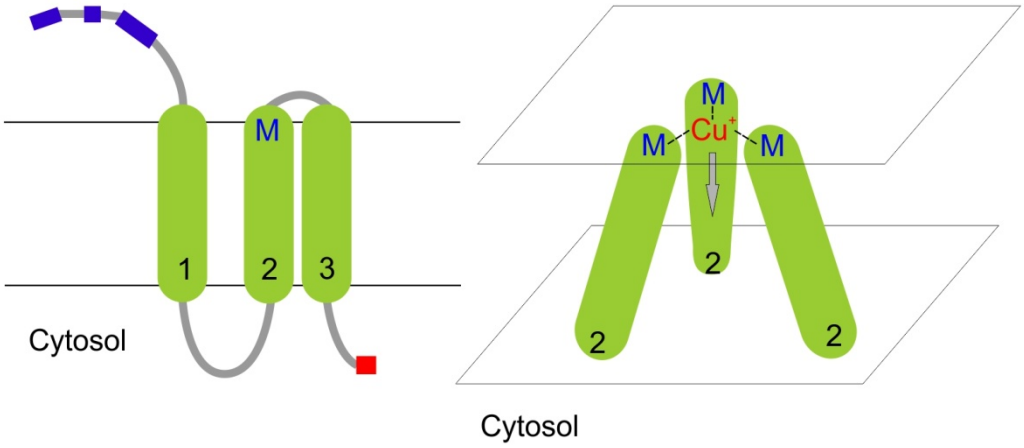

Figure 5.2 Structure of the COPT/CTR proteins
The structure of the CTR proteins demonstrating a cross section through the membrane (left) and the trimeric structure of the pore with only the second transmembrane domains identified (right). Transmembrane domains 1-3 are coloured green. Methionine rich regions before the first transmembrane domain are blue and the CxC motif at the end of some proteins is indicated in red. The methionine residue thought to be involved in copper binding is indicated in blue. Figure adapted from Penarrubia et al. (2010).

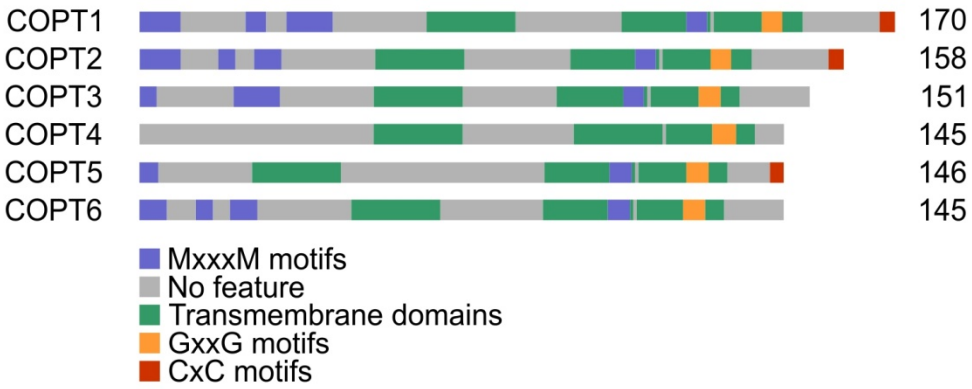

Figure 5.3 Structural features of the six Arabidopsis COPT proteins
Transmembrane domains are green and methionine rich regions are indicated in blue. The orange regions are conserved GxxxG domains and the CxC motif at the end of some proteins is indicated in red. Numbers refer to the amino acid length of each protein. Adapted from Penarrubia et al. (2010).

The COPT1 protein is highly hydrophobic with three transmembrane domains and as such was likely to be a membrane transporter (Kampfenkel et al. 1995). Subsequently, COPT1 has been further characterised and identified as a plasma membrane located protein (Sancenon et al. 2004; Andres-Colas et al. 2010).

COPT1 was found to be important in copper uptake in Arabidopsis. Antisense mutants take up approximately half of the copper that wild-type plants take up, and mutants have reduced root lengths when grown in copper deficient conditions (Sancenon et al. 2004). Additionally, plants overexpressing *COPT1* have been found to take up approximately 1.5 times more copper than wild-type plants and *COPT1* overexpressing plants are sensitive to excess copper (Andres-Colas et al. 2010). When antisense plants were grown in unlimiting copper, genes which are usually upregulated in response to copper deficiency (*CCH* and *COPT2*) were upregulated (Sancenon et al. 2004). When yeast cells expressing Arabidopsis COPT1 were treated with silver, copper uptake was reduced, suggesting that silver is a competitive inhibitor of copper uptake by COPT1 (Sancenon et al. 2003).

Expression of *COPT1* was found to be high in root tips as well as pollen, but was highest in the leaves (Figure 5.4) (Sancenon et al. 2003; Sancenon et al. 2004). In the presence of excess copper, expression was reduced, and in copper limiting conditions, *COPT1* expression increased (Sancenon et al. 2004; del Pozo et al. 2010).

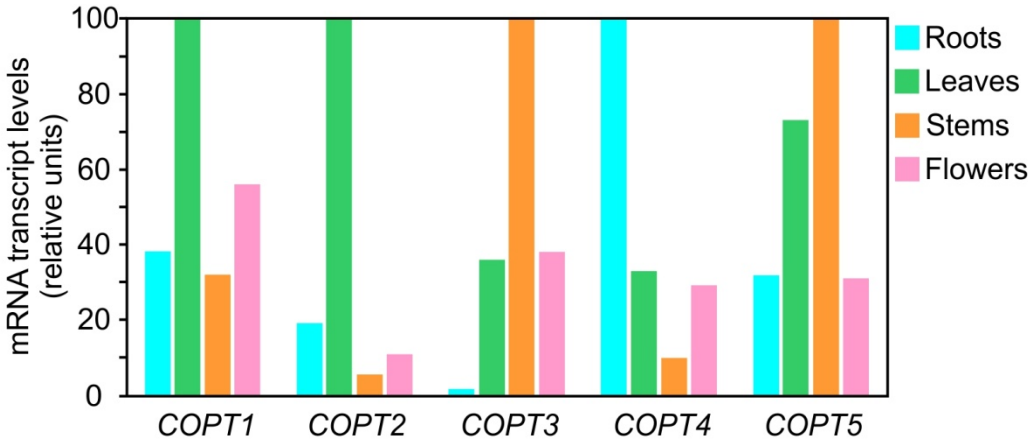

Figure 5.4 Expression of *COPT1-5* in different tissues
Relative expression of *COPT1-5* in roots, leaves, stems and flowers data from Sancenon et al. (2003). Relative values are compared to the highest expression levels in each tissue.

Arabidopsis COPT2 has not been extensively characterised. However, it has been reported that COPT2 is the protein most similar to COPT1 (Sancenon et al. 2003), therefore implying that they are functionally similar. Indeed, Arabidopsis COPT2 was able to fully rescue the ctr1 yeast copper uptake mutant (Sancenon et al. 2003). In Arabidopsis, COPT2 is upregulated in copper limiting conditions and downregulated to low levels in the presence of excess copper (Sancenon et al. 2003; Penarrubia et al. 2010). It was initially found to be expressed at highest levels in plant leaves although it is also expressed in root tissues (Sancenon et al. 2003).

As with COPT2, little is known about Arabidopsis COPT3. The gene is located adjacent to *COPT1* in the Arabidopsis genome indicating that it may have arisen by a duplication event (Figure 5.1). However, there is considerable variation in sequence (Sancenon et al. 2003). Expression of *COPT3* is mainly within the stems with low levels of expression in the roots (Figure 5.4) and in yeast complementation studies, Arabidopsis COPT3 only partially rescued the copper uptake deficient strain and suggesting that COPT3 may be involved in intracellular copper transport rather than plasma membrane uptake (Sancenon et al. 2003; Puig et al. 2007). However, overexpression of *COPT3* in Arabidopsis has demonstrated increased copper content, showing that *COPT3* is important in the uptake of external copper, either directly, or through increased copper translocation (Andres-Colas et al. 2010).

The role of COPT4 is uncharacterised. Although it is structurally similar to the other COPT transporters, there are no conserved methionine residues either preceding the first transmembrane domain or within the second transmembrane domain (Figure 5.3). COPT4 was not expressed into yeast, possibly due to the toxicity of the protein; it is therefore unknown whether it is capable of complementing the copper transport mutants of yeast (Sancenon et al. 2003). Evidence is conflicting as to whether *COPT4* transcript levels are reduced in response to excess copper. *COPT4* expression was initially thought to be unaltered in response to excess copper (Sancenon et al. 2003), however recent research shows *COPT4* downregulation in excess copper, implying a role in copper uptake (del Pozo et al. 2010).

Recently, the COPT5 protein has been studied in detail (Garcia-Molina et al. 2011). Initial research hypothesised that, like COPT3, COPT5 is an intracellular

copper transporter because of the partial ability to rescue yeast copper transport mutants (Sancenon et al. 2003; Puig et al. 2007). This hypothesis was supported by the recent characterisation (Garcia-Molina et al. 2011). *COPT5* is most strongly expressed in root tissue compared to aerial tissue, with expression in the aerial tissues restricted to vascular organs (Garcia-Molina et al. 2011). Expression was not affected by the levels of copper the plant was exposed to, suggesting that the protein is involved in the translocation of copper throughout the plant, rather than copper uptake (Garcia-Molina et al. 2011). When *copt5* mutants were grown on a copper sufficient medium, they were not phenotypically different to wild-type seedlings, however *copt5* seedling roots were shorter in length when plants were grown in copper deficient conditions (Garcia-Molina et al. 2011). This phenotype was restored by the addition of copper, and interestingly also by silver. It is therefore possible that silver shares the copper uptake and transport pathway.

A sixth member of the *COPT* family has now been identified (Puig et al. 2007; Penarrubia et al. 2010). However, no expression data are available for *COPT6* and plants with altered *COPT6* expression have not been studied.

Potential mechanisms of the regulation of *COPT* expresssion have been investigated. In copper deficient conditions, SQUAMOSA Promoter Binding Protein–Like7 (SPL7) may be upregulated. In turn, this is likely to be responsible for the upregulation of a number of genes involved in copper deficiency responses, including *COPT1* and *COPT2* (Yamasaki et al. 2009). This may form part of a regulatory feedback loop, with *COPT2* expression reduced when copper is sufficient (Penarrubia et al. 2010). The basic helix-loop-helix transcription factor FIT1 is also thought to be involved in *COPT2* regulation (Colangelo and Guerinot 2004). *COPT2* expression therefore might be controlled by various factors in various conditions.

In addition to the COPT transporters found in Arabidopsis, homologues have been identified in other plant species. Rice contains seven COPT transporters (Yuan et al. 2010), with some members upregulated in response to pathogen stress; the redistribution of copper therefore might be a pathogen defence response (Yuan et al. 2010).

Phylogenetic analysis of the Arabidopsis and rice COPT proteins, as well as the yeast, human and mouse proteins shows that the plant COPT proteins are more closely related to each other than they are to the CTR proteins from other eukaryotes (Figure 5.5). It is therefore evident that the plant genes diverged after the divergence of plants from other eukaryotes. Although the Arabidopsis and rice proteins are similar, the functions cannot be compared across the two species. For example it is known that Arabidopsis COPT1 is a plasma membrane copper transporter, however it is not possible to determine whether there is a rice COPT with an equivalent function as there are no known proteins that are closely related.

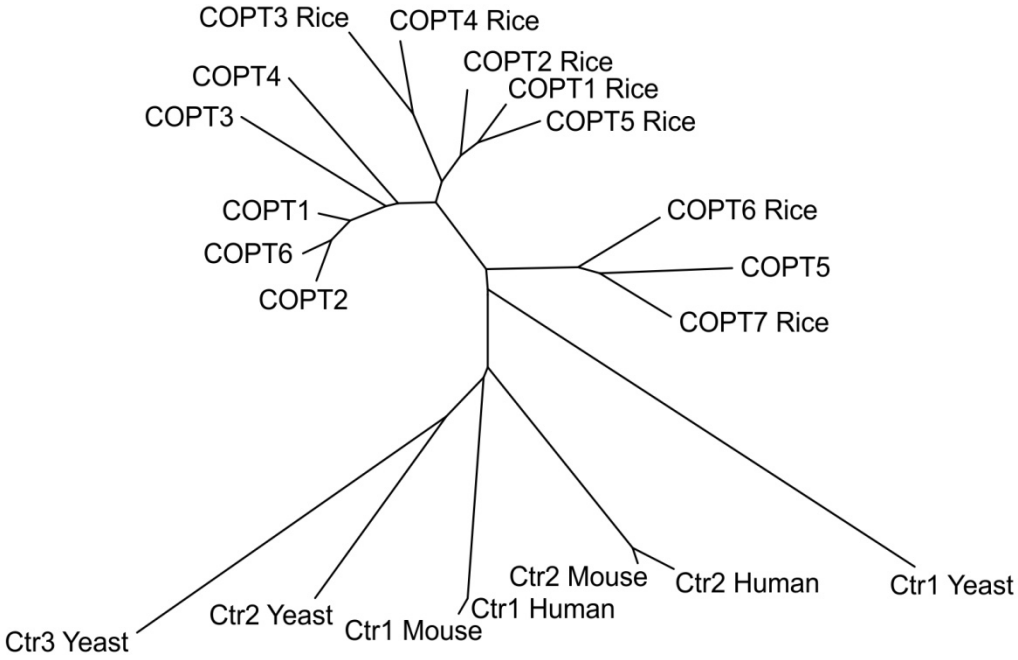

Figure 5.5 Phylogeny of CTR proteins
Phylogenetic relationship between the six Arabidopsis COPT proteins and the seven rice proteins, along with the three proteins identified in yeast, and two each for human and mouse. Protein sequences were aligned using ClustalX2 (Larkin et al. 2007) and the tree was generated using Mega 4.0 (Tamura et al. 2007).

5.1.2 Aims

It has been hypothesised that gold is transported into plants via a transport system which exists for one or more essential metals but is also able to transport gold (Starnes et al. 2010). It is therefore likely that gold uptake would occur through a transporter essential for an element chemically similar to gold. Thus, as gold and copper share periodicity, a copper transporter might be involved in gold transport.

The microarray experiment outlined in Chapter 4 identified *COPT2* as one of the most downregulated genes in response to gold treatment. Given that the COPT family is also known to be involved in copper uptake and translocation and inhibited by silver ions, this small gene family was identified as putatively being involved in gold uptake and translocation. Studies on the COPT family are presented in this chapter.

5.2 Methods

5.2.1 qPCR of the *COPT* genes

The template used for qPCR of the *COPT* genes was the cDNA synthesised for the microarray experiment and the array verification (Section 4.3.2). qPCR was carried out according to Section 2.4.5, using the primers described in Table 5.1. Primers were designed using Primer Express v3.0 and were tested for efficiency as described in Section 2.4.5. For *COPT3*, no efficient primers could be found, therefore *COPT3* primer sequences were taken from research by del Pozo et al. (2010). These primers were also found to be inefficient, but qPCR was carried out using them for completeness. Data were normalised using *ACTIN2* as an endogenously expressed control.

Table 5.1 Primers for qPCR of the COPT genes
F and R at the end of the primer names represent the forward and reverse primers respectively. *COPT3* primers were taken from del Pozo et al. (2010).

Gene	Primer	Sequence
COPT1	COPT1F	CACCGAATGGCTTGCTCAT
	COPT1R	GGCACGATTAGCCGAATCTC
COPT2	COPT2F	TCCTCCTCGCCGTAATTGC
	COPT2R	GCGGCTCGATTGGTTGAG
COPT3	COPT3F	CACCATCATCGTTCTTCCAACA
	COPT3R	CGGCGAGACAGACCCAATAC
COPT4	COPT4F	CTTTCTGGCGTTCTTAGCTGAGT
	COPT4R	TATCGGCACCCTGTTTGATG
COPT5	COPT5F	CCGCGCCTCTTATCCCTAA
	COPT5R	GAAAAGAAGAACCGAAGCAGCTT
COPT6	COPT6F	TGTCCTTTAACGGTGGAGTTTTC
	COPT6R	AGTGCTTCCGAAGAGCATGAA
ACTIN2	ACTINF	TACAGTGTCTGGATCGGTGGTT
	ACTINR	CGGCCTTGGAGATCCACAT

5.2.2 Genotype of *COPT2* insertion line

PCR reactions were designed for genotyping the SALK T-DNA insertion line. Primers were designed which spanned the T-DNA insertion site and a further primer was designed for a location within the insert. Presence of one copy of the T-DNA insert leads to the amplification of two PCR products and so homozygous and heterozygous lines could be detected. This is described in more detail in Section 5.3.5. All lines were compared to a wild-type (Arabidopsis Col-0) control, and after the T_3 generation, a positive control from the T_3 generation was used as

all seeds in this generation were known to contain at least one copy of the T-DNA insert. The primer for the right hand flanking region of the insert was designed using software on the SALK website (http://signal.salk.edu/tdnaprimers.2.html). Multiple primers for the left hand side of the insert sequence were designed by using both the SALK website and Primer3 software (Rozen and Skaletsky 2000) (http://frodo.wi.mit.edu/primer3/). However, none of these primers produced a PCR product when used in conjunction with the right primer (see Section 5.3.5) and as such, no wild-type sequence could be amplified. As the *copt2-1* mutant line was a SALK T-DNA insertion line, the LBb1.3 left border primer was used as described at http://signal.salk.edu. As a positive control to test that the reactions were successful, a reaction for *ACTIN* was carried out. All primers for these reactions are outlined in Table 5.2.

Table 5.2 Primers used for *copt2-1* genotyping
COPT2RP designed using SALK primer design software at http://signal.salk.edu. LBb1.3 is as described at http://signal.salk.edu. Sequences for the *ACTIN* control (ACT2a and ACT2s) were kindly provided by Dr Liz Rylott.

Primer	Sequence
COPT2RP	TCTTGAGTGTGTACACAGCGG
LBb1.3	ATTTTGCCGATTTCGGAAC
ACT2a	CTTACAATTTCCCGCTCTGC
ACT2s	GTTGGGATGAACCAGAAGGA

DNA was extracted, as described in Section 2.4.1, prior to PCR amplification. PCR reactions were carried out using a Px2 Thermal Cycler (Thermo Scientific). Samples were denatured at 94 ºC for three minutes, with thirty subsequent cycles of denaturation, annealing and extension at 94 ºC for one minute, 67 ºC for one minute and 72 ºC for 2 minutes. A final extension at 72 ºC for ten minutes was also performed. The amplifications were subsequently separated by size via gel electrophoresis (see Section 2.4.2).

5.2.3 Sequencing reactions

To determine the sequence of PCR amplified DNA, the product of the reaction was integrated into the pCR2.1-TOPO vector according to the manufacturer's protocol (Invitrogen). After integration into the plasmid, the plasmid was added to chemically competent one shot TOP10 cells and incubated on ice for five minutes, prior to 30 seconds heat shock treatment at 42 ºC. LB was added to the cells (250 µL) and cells were shaken at 37 ºC for one hour. Cells were subsequently spread onto LB agar containing 100 µg/mL kanamycin. After overnight growth, white colonies were selected (due to disruption of the lacZ reporter) and used to inoculate 5 mL of LB containing 100 µg/mL kanamycin. These bacteria were subsequently grown at 37 ºC for 16 hours with shaking at 200 rpm.

Plasmids were purified using the QIAprep Spin Miniprep Kit (QIAGEN) according to the manufacturer's instructions. Plasmid concentration was quantified by measuring the absorbance at 260 nm using a Nanodrop ND-1000 Spectrophotometer (Thermo Scientific). The sequence of the insert was subsequently determined by the Technology Facility (University of York) sequencing service using Sanger sequencing on an ABI 3130 (Applied Biosystems) using the M13rev-26 Primer (GGAAACAGCTATGACCATG).

5.3 Results

5.3.1 Bioinformatic analysis of the COPT family of transporters

As described in Section 5.1.1, there are five known COPT transporters in Arabidopsis (COPT1-5) and one putative transporter (COPT6). The amino acid sequences were obtained from TAIR (The Arabidopsis Information Resource) (http://www.arabidopsis.info) (Rhee et al. 2003) and compared using the Basic Local Alignment Search Tool (BLAST) (Altschul et al. 1990) (Table 5.3). COPT2 and COPT6 are the most identical proteins (77%). COPT1 is also closely related to COPT2 and COPT6 (68 and 66 % respectively). These results indicate that the proteins may be functionally similar.

Table 5.3 Percentage identities of the COPT proteins
Values are percentage identity between the COPT proteins. Values were obtained using the amino acid sequences from TAIR (Rhee et al. 2003) and alignments using BLAST (Altschul et al. 1990).

	COPT1	COPT2	COPT3	COPT4	COPT5	COPT6
COPT1	100					
COPT2	68	100				
COPT3	56	56	100			
COPT4	54	51	48	100		
COPT5	30	33	34	32	100	
COPT6	66	77	56	54	32	100

Amino acid sequences were aligned via ClustalX2 (Larkin et al. 2007) (Figure 5.6). The alignment shows high levels of conservation within some parts of the protein. This is especially obvious in the first transmembrane domain and the sequence spanning the end of the second and the start of the third transmembrane domains (denoted by orange bars). The 20 or so amino acids before the first transmembrane domain are also conserved. Where there are differences, these are in the COPT4 or COPT5 sequences. COPT1-3 and 6 are almost completely conserved in this region. This is also the case for the transmembrane domain sequences where a large number of residues are identical or could be considered to be functionally similar.

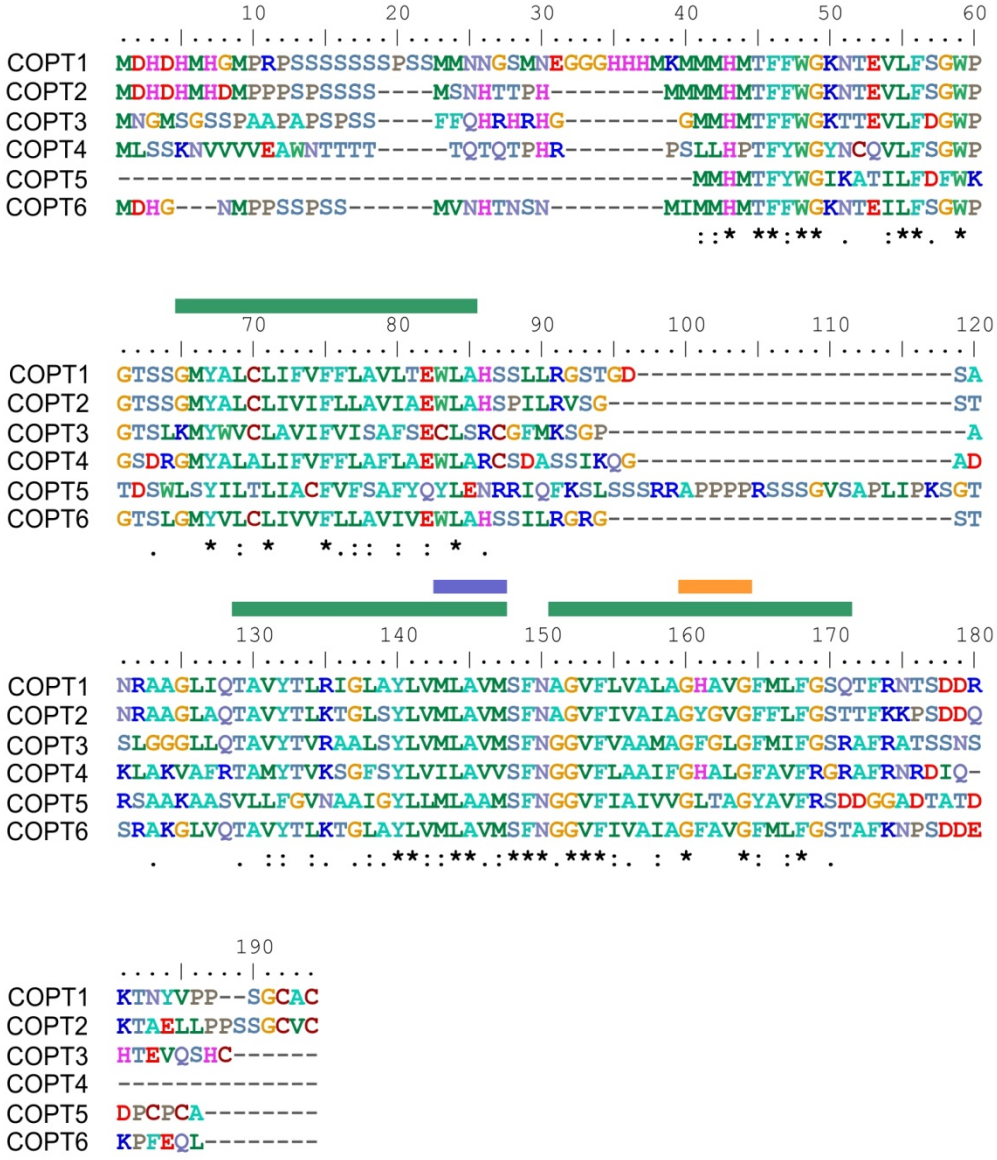

Figure 5.6 Alignment of the COPT protein sequences
Transmembrane domains are indicated by green bars above the sequence and the level of conservation is indicated below the sequences. The blue bar above the sequence represents the MxxxM region and the orange bar represents the GxxxG region. Stars (*) represent fully conserved amino acids, double dots (:) represent strong conservation and single dots (.) represent weaker conservation. Figure generated using ClustalX2 (Larkin et al. 2007) and BioEdit7 (Hall 1999).

The conserved GxxxG domain described in Section 5.1.1 and Figure 5.3 is conserved in all six of the Arabidopsis COPT proteins. Although some of the residues within this domain are not present, others are conserved between some of the proteins and both glycine resides are present in all six proteins.

Methionine residues are absent from the second transmembrane domain of COPT4. These are thought to be involved in trimerisation and also metal

coordination for transport. This supports published data (Puig et al. 2002; Aller et al. 2004) which determined that these residues are crucial for transport, and without them, the protein is unable to function. All five residues within the MxxxM region are conserved within the other five COPT proteins (with the exception of COPT5 in which a valine is replaced with an alanine), highlighting the importance of this region. The analysis in Figure 5.6 demonstrates that the transmembrane domains, along with crucial methionine and glycine residues, are conserved in COPT6. Therefore, COPT6 is likely to function as a copper transporter. The similarity of COPT6 to COPT1 and COPT2 (Table 5.3) suggests that the three proteins have a similar function.

5.3.2 Expression of the *COPT* genes in the presence of gold

The microarray studies described in Chapter 4 showed that the *COPT2* gene was expressed 23.6 fold less when gold was present in the medium. Validation of the microarray experiment (Section 4.3.4) showed that although the data were qualitatively accurate, they were not quantitatively accurate. Thus, the expression of all six members of the *COPT* family was measured using qPCR (Section 5.2.1). The efficiency of the primers for *COPT1*, *COPT2*, *COPT4*, *COPT5* and *COPT6* was confirmed prior to qPCR (Section 2.4.5), however no efficient qPCR primers could be designed for *COPT3*. Previous work was unable to measure *COPT3* expression, and this was probably due to *COPT3* not being transcribed (del Pozo et al. 2010). Other work looking at *COPT3* transcript levels also found low levels of transcript in the roots (Sancenon et al. (2003) and Figure 5.4) therefore suggesting that this was the reason efficient primers could not be designed. Although the efficiency reaction for the *COPT3* primers was not successful, the *COPT3* primers used in previously published work (del Pozo et al. 2010) were used for qPCR for completeness (Table 5.1).

To determine the expression of the six *COPT* genes in response to treatment with gold, qPCR was performed as outlined in Section 5.2.1. Expression of the *COPT* genes was the same as for the microarray experiment (Figure 5.7), although the actual expression levels were different, further validating the microarray results described in Chapter 4. This was the case for *COPT1*, *COPT2* and *COPT5*. *COPT4 and COPT6* were not present on the microarray and so the qPCR result could not be compared to the microarray result. Although *COPT3* expression reactions were carried out, none were successful, which was

unsurprising due to the problems with primer efficiency noted above. Therefore *COPT3* is not discussed further. However, it should be noted that the microarray did not find any alteration of expression for *COPT3*.

For *COPT1*, *COPT4*, *COPT5* and *COPT6*, there was no significant change in expression in the presence of gold (Figure 5.7). The microarray data (Chapter 4) show that *COPT2* was downregulated 23.6-fold in the presence of gold. The result described in Figure 5.7 demonstrates that *COPT2* was downregulated over 1000-fold. It is therefore apparent that *COPT2* expression was almost completely inhibited in the presence of gold.

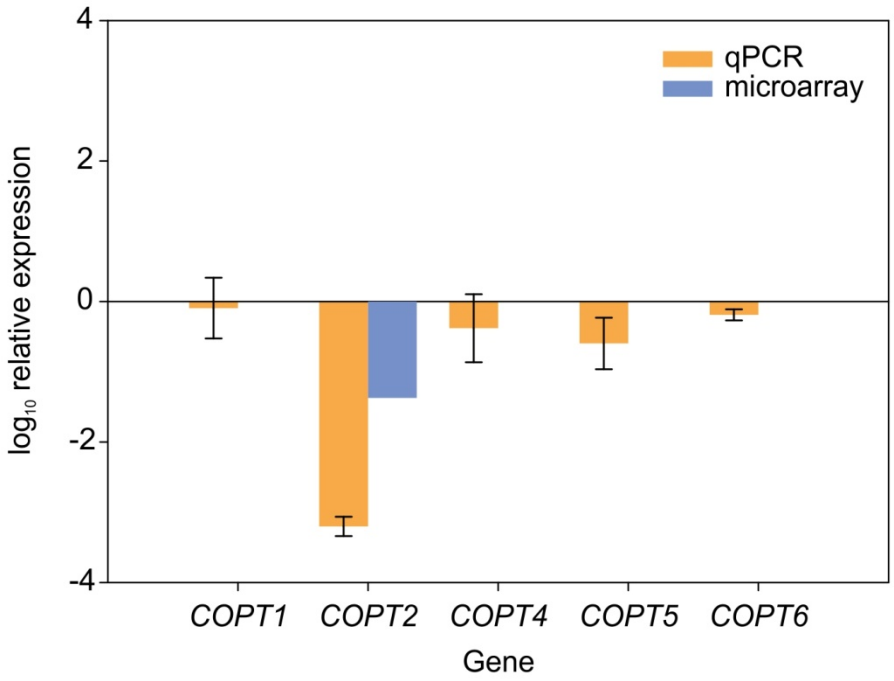

Figure 5.7 Expression of the COPT genes in response to gold
Expression values (orange bars) are relative to the expression when plants were not treated with gold. These values are compared to the microarray data for the genes (blue bars). Only one bar for the array data is shown because *COPT1* and *COPT5* did not show a difference in regulation in the microarray study. *COPT4* and *COPT6* were not on the microarray and so no data are available. As *COPT3* was unable to be amplified via qPCR, *COPT3* data are not shown due to failures in the reaction described in the main text. No changes in *COPT3* expression were noted in the microarray. Error bars represent the standard error of the mean.

5.3.3 General expression of the *COPT* genes

Genevestigator was used to determine the locations of *COPT* expression in Arabidopsis through the analysis of many sets of microarray data. No data for *COPT4* or *COPT6* were available, so the data presented are only for the remaining four of the six genes (Figure 5.8). The data show that expression of *COPT1* is mainly in the pollen and stamen although there is low expression throughout the plant. *COPT2* is expressed at basal levels throughout the plant, with higher levels in the roots and the radical. There does not appear to be any high expression of *COPT3* anywhere in the plant, and expression of *COPT5* appears higher than the other *COPT* genes everywhere in the plant, with slightly higher expression in the roots and in the stem.

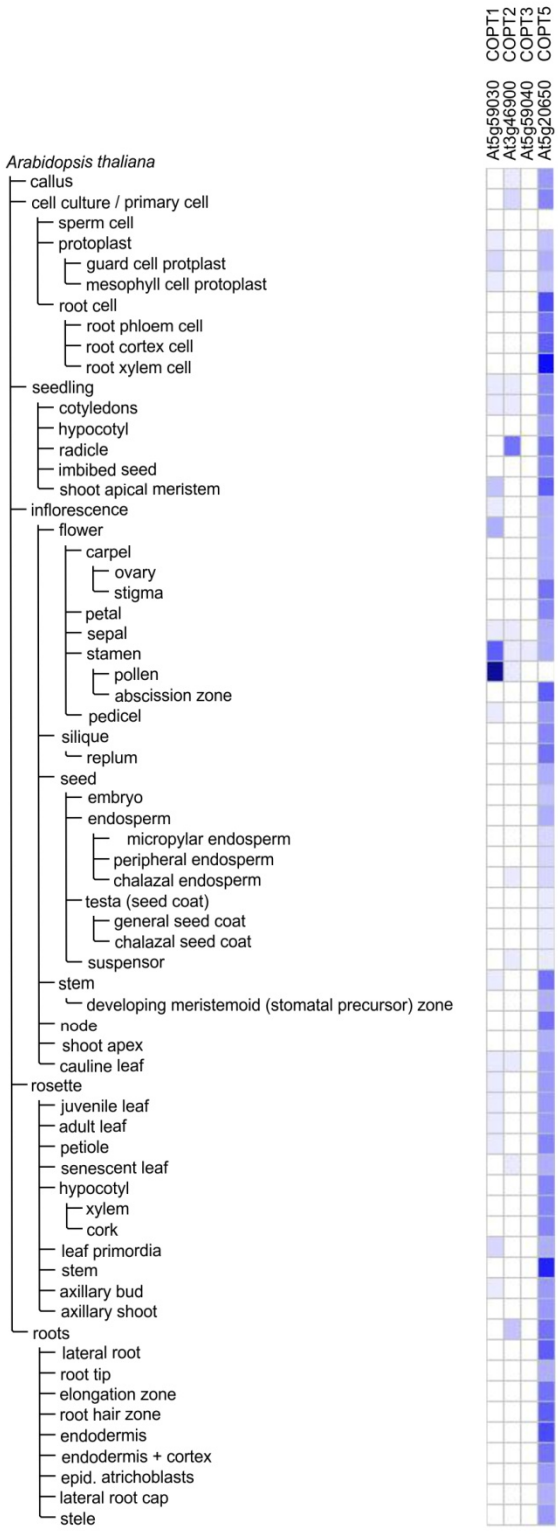

Figure 5.8 *COPT* expression patterns
Spacial expression patterns of *COPT1, 2, 3* and 5. No data were available for *COPT4* or *COPT6*. Darker colours indicate higher levels of expression. Data and Figure generated using Genevestigator (Hruz et al. 2008).

5.3.4 Selection of a *COPT2* knockout line

From the expression studies described above (Section 5.3.2) it was found that *COPT2* is the only one of the six *COPT* genes that has reduced transcript levels in the presence of gold. This infers that *COPT2* is involved in Arabidopsis tolerance to, or uptake of, gold. To study this relationship further, an Arabidopsis *COPT2* knockout line (SALK_147451), hereafter referred to as *copt2-1*, was obtained from the SALK T-DNA insertion library (Alonso et al. 2003a) via the Nottingham Arabidopsis Stock Centre (NASC). *copt2-1* was generated in the Columbia-0 ecotype, and was therefore comparable to the results described throughout this work. Due to the unaltered expression of the other five genes in the *COPT* family, knockout lines in these five genes were not pursued.

5.3.5 Genotyping of knockout lines

Seeds from the T_3 generation of *copt2-1* were provided by NASC and were genotyped to determine whether the line was homozygous for the T-DNA insert. The usual method to determine that SALK T-DNA insertion lines are homozygous is PCR using three primers. One pair is from the insert to a position 3' of the insert location. The second pair uses primers spanning the insertion site. Thus, if the line is heterozygous for the insert, both reactions will take place and there will be two PCR products. If the line is homozygous for the T-DNA insert or lacks the insert, then there will be one PCR product. The identity of the products can therefore be determined and it can be elucidated whether the plant is homozygous for the insert or not.

In order to genotype the *copt2-1* line, primers were designed as described above (Table 5.2). However, a working primer could not be designed for the 5' flanking sequence and therefore the wild-type PCR product (i.e. flanking the insert site) could not be carried out. In the T_3 population, all tested lines contained the T-DNA insert (Figure 5.9), but it was unknown whether these lines were homozygous for the T-DNA insert. As it was not possible to test for the wild-type allele, segregation of the allele was studied in the T_4 generation. Of the seventy T_4 plants tested, 45 contained the insert (data not shown). The T_4 generation was therefore a segregating population from heterozygous parents.

Seeds (T_5) from a parent containing the insert from the T_4 generation were subsequently grown and tested for the insert. Ten plants were tested to

determine the presence of the insert as described above. For two of the lines tested, all plants tested contained the insert, showing that the parent was homozygous (Figure 5.10). Seeds from homozygous T_4 parents (i.e. homozygous T_5 seeds) could then be used in the further experiments described below.

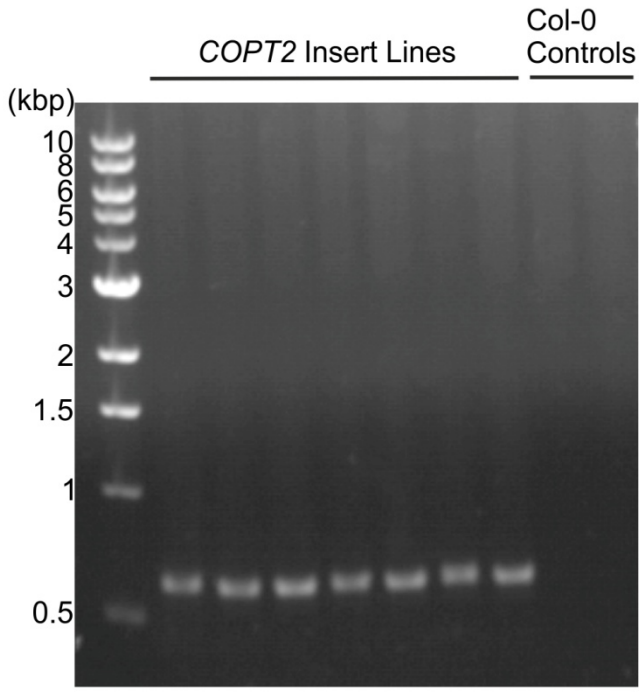

Figure 5.9 T-DNA inserts within the *copt2-1* T_3 generation
DNA electrophoresis gel showing PCR products from the left border to right flanking sequence. DNA ladder was a 1 kb DNA ladder from NEB. Values represent the size of the ladder step in kilobases.

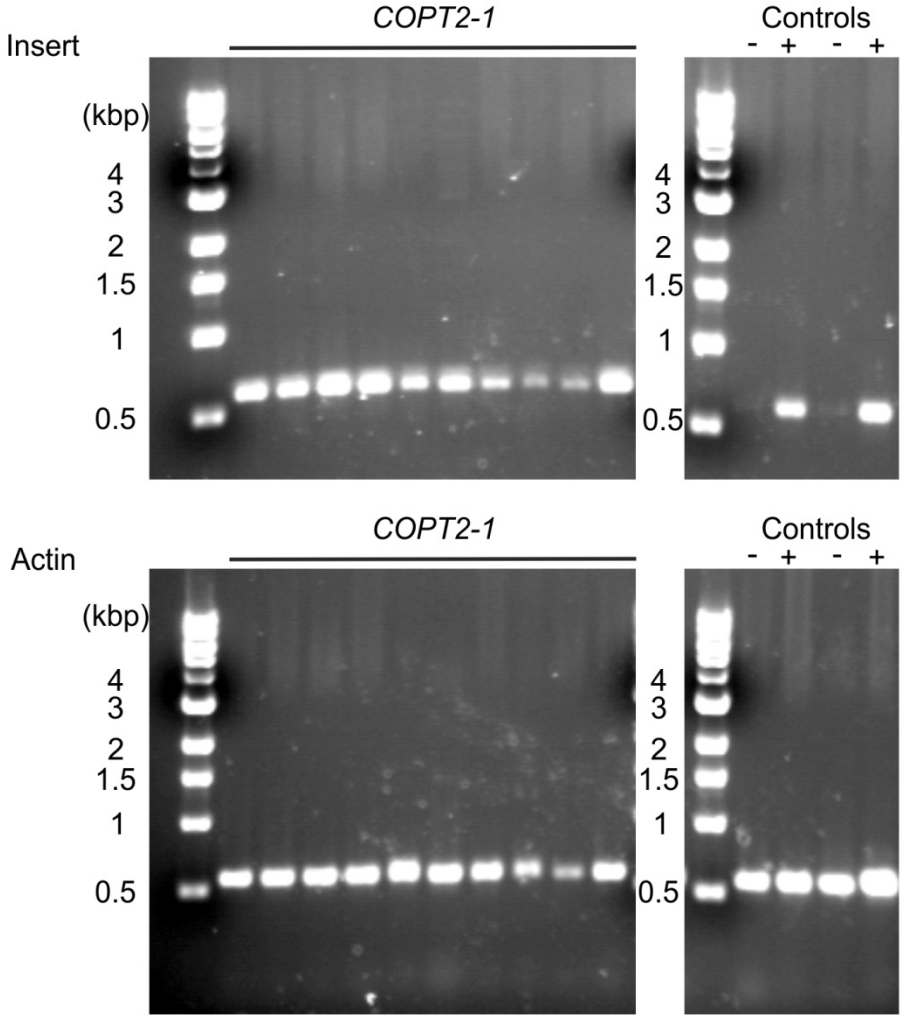

Figure 5.10 T-DNA inserts within the *copt2-1* T_5 generation
DNA electrophoresis gel showing that the insert was present in all of the *copt2-1* plants tested. Insert gels used LBb1.3 and COPT2RP primers. Actin controls used the ACT2a and ACT2s primers. Negative controls were plants known to be wild-type for *COPT2* and positive controls were known to contain the T-DNA insert.

Further to the tests described above, antibiotic resistance was tested to help determine homozygosity. As the T-DNA insert includes a kanamycin resistance marker, plants with the insert would grow in the presence of kanamycin, whereas those without it would not. Seeds from the T_5 generation were tested for segregation on kanamycin by germinating and growing them on ½MS(A) plus kanamycin (50 µg/mL). None of the seeds germinated. It has been found that the SALK lines can lose kanamycin resistance due to silencing effects (Daxinger et al. 2008). It is therefore unsurprising that kanamycin resistance was not observed in the *copt2-1* line.

5.3.6 Location of the T-DNA within *copt2-1*

Seqviewer, a web tool provided by TAIR (http://www.arabidopsis.org/servlets/sv) and the SALK database (http://signal.salk.edu/cgi-bin/tdnaexpress) provided information about the probable location of the T-DNA insertion within the Arabidopsis genome. To confirm the location of the T-DNA insert, the PCR product from the T-DNA to right primer (see Section 5.3.5) was cloned into the TOPO-2.1 vector and sequenced (Section 5.2.3). The sequence of the T-DNA to right primer reaction was compared to the Arabidopsis genome sequence. This analysis showed that the T-DNA is inserted 89 bases upstream of the start codon and 77 bases upstream of the start of the 5' untranslated region (Figure 5.11). This close proximity to the start of *COPT2* means that it is likely that transcription and translocation are disrupted. Production of transcript, using qPCR and protein, monitored by antibody or activity assays were not performed, and thus the line is herein referred to as the putative *copt2-1* mutant.

Figure 5.11 Location of the T-DNA insert in the Arabidopsis genome
Location of the T-DNA insert in *copt2-1* as hypothesised using Seqview and confirmed using the PCR product from the genotyping experiments.

5.3.7 Observations on the phenotype of putative *copt2-1* mutants

Growth and development of the homozygous putative *copt2-1* mutants were compared to those of wild-type plants. No phenotypic differences were observed between wild-type and mutant throughout development. Germination frequency, bolting and flowering times were the same for both mutant and wild-type. Pollen morphology was identical when viewed under a light microscope and the number of seeds per silique remained the same.

5.3.8 Germination of *copt2-1* in different conditions

In order to test the phenotype of putative *copt2-1* mutants in the presence of different metals, seeds were germinated and grown on different media. All media were based on Richard's medium (Section 2.2.2.2) plus agar with altered metal concentrations. Media were either unchanged, supplemented with $KAuCl_4$ (0.25 mM) or $CuSO_4$ (30 µM), or were copper or iron deficient. Element deficient media were produced as in Chapter 2, but with copper or iron left out. Richard's medium was used instead of ½MS(A) as it was simpler to modify for the copper and iron deficient media. As the results below show, the use of Richard's media did not affect the growth of the plants in standard conditions (i.e. without supplemental metals or metals removed). Sterile Col-0 seeds were used as wild-type control and homozygous *copt2-1* mutant seeds (T_5) were used to test growth. Seeds were imbibed and stratified in water for three nights and germinated in growth room conditions (Section 2.2.4). Seedlings were subsequently grown for eight days, and root lengths measured (Figure 5.12).

Germination time and frequency for all of the seed batches were identical in all treatments (i.e. 100 %). The development of putative *copt2-1* embryos was unaffected under the conditions tested and no aberrations in seed development were observed.

As had been seen when wild-type only seeds were tested (Chapter 3), roots were around 20 mm long after eight days on media with no modifications and were shorter when grown on media containing gold. In addition, roots of wild-type seedlings were shorter in the presence of 30 µM copper. These observations were determined to be statistically significant by a one-way ANOVA followed by a test for least significant difference ($p<0.05$). There were no differences in root length for growth in copper or iron deficient conditions. There was no significant difference between the wild-type seeds and this batch of mutant seeds for any treatment showing that the mutation did not have an effect on seedling growth in any of these conditions.

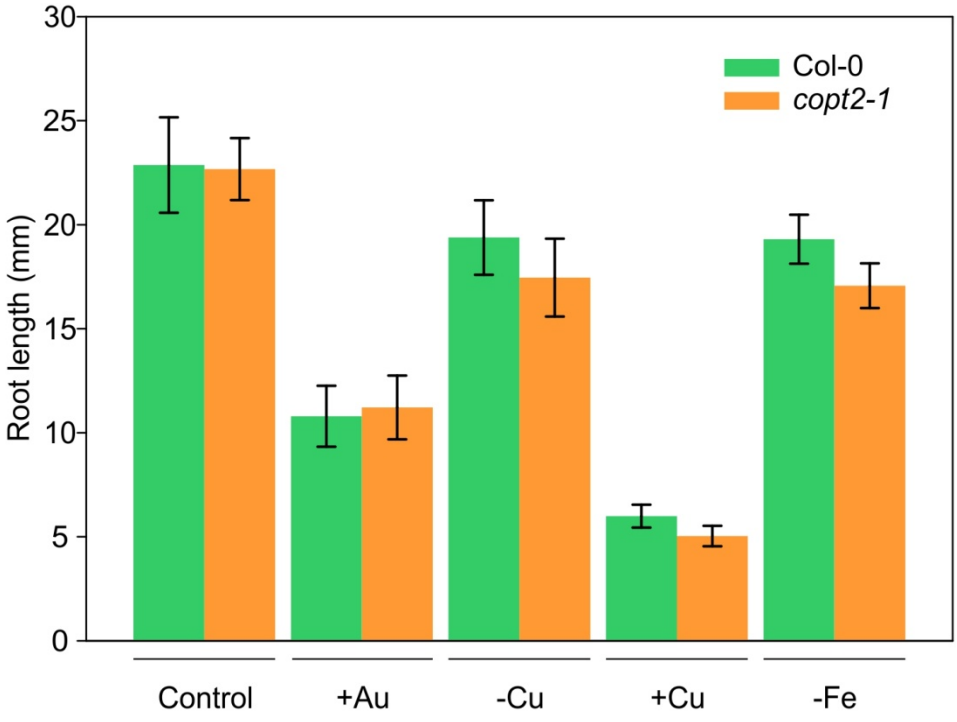

Figure 5.12 Root length of *copt2-1* and Col-0 controls in different treatments

Arabidopsis seeds were imbibed and stratified in water for three nights, prior to germination on Richard's medium with the addition or deficiency of some compounds. These were either a control with no change, the addition of 250 µM $KAuCl_4$, 30 µM $CuSO_4$ or had neither iron nor copper. After eight days of growth, root lengths were measured using ImageJ (http://rsbweb.nih.gov/ij/index.html). Data are the means of at least 30 measurements and error bars represent the standard error of the means.

5.3.9 Growth of *copt2-1* mutants in the presence of gold

In addition to the growth on various substrates as described in Section 5.3.8, the *copt2-1* mutant was also grown in the presence of various gold concentrations to determine whether the mutant was more or less tolerant to gold exposure. To test this, Col-0 seeds and *copt2-1* seeds were germinated on ½MS(A) as described in (Section 3.2.3). These seeds were germinated on ½MS(A) containing $KAuCl_4$ at 0, 0.4, 0.5, 0.6, 0.7, 0.8, 0.9 or 1 mM (pH 5.7) with a total of at least 30 biological replicates. Seedlings were grown for eight days in growth room conditions prior to root measurement (Figure 5.13).

As gold concentration increased, the growth of the plants decreased for both the Col-0 controls, and the *copt2-1* mutants. The root lengths for the plants in this experiment were comparable to those measured in Chapter 3, which also

demonstrated decreased root growth upon increasing gold concentration. One-way ANOVA followed by a test for least significant difference, showed that for all treatments, there was no significant difference between the root lengths of the Col-0 controls and the *copt2-1* mutants. These data therefore show that the *copt2-1* mutant did not have any differences to tolerance to the presence of different concentrations of gold (up to 1 mM).

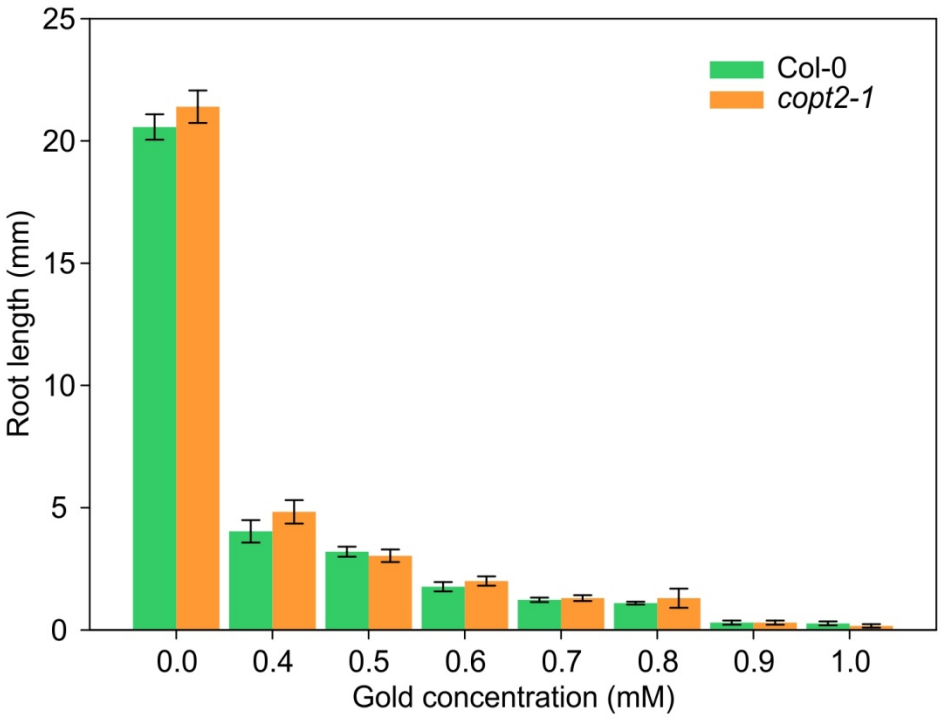

Figure 5.13 Growth of copt2-1 in the presence of gold
Arabidopsis seeds (Col-0 and *copt2-1*) were imbibed and stratified in the dark for three nights at 4 ºC. They were subsequently germinated on ½MS(A) containing $KAuCl_4$ (pH 5.7) at 0, 0.4, 0.5, 0.6, 0.7, 0.8, 0.9 or 1 mM. Plants were grown for eight days prior to measurement with ImageJ software. Error bars represent the standard error of the means from at least 30 biological replicates. Statistical analysis was performed (One-way ANOVA with test for least significant difference) with no significant difference between the growth of the mutant and the growth of the wild-type seedlings.

5.4 Discussion

Presented in this Chapter is a concise analysis of the COPT family of metal transporters, with a more detailed study on the effect of gold on COPT2. The microarray analysis presented in Chapter 4 found that one of the most downregulated genes in response to gold was *COPT2*. The COPT2 protein has been shown to be able to complement a yeast copper transport mutant (Kampfenkel et al. 1995) and because copper and gold share periodicity, COPT2 was studied further.

There are six COPT genes as described in Section 5.1.1, the sixth of which encodes a hypothetical COPT transporter, the function of which has not been elucidated as it has only recently been discovered. In the presence of gold, *COPT2* was downregulated, but the other five *COPT* genes did not have altered expression; this confirms the microarray data presented in Chapter 4. Evidence in the literature shows that *COPT1* and *COPT2* are downregulated to low transcript levels in the presence of copper, with almost no *COPT2* after copper treatment (Sancenon et al. 2003). *COPT3-5* were not altered in the presence of copper (Sancenon et al. 2003) and it appears that they do not respond directly to the metal. It is therefore unsurprising that *COPT4* and *COPT5* do not have altered expression in response to gold.

Although the expression of all *COPT* genes was measured here, efficient primers could not be designed to measure *COPT3* expression. It is likely that this was due to low levels of *COPT3* expression within plant roots as found by Sancenon et al. (2003). This hypothesis is also suggested by (del Pozo et al. 2010) who could not measure *COPT3* expression.

The downregulation of *COPT2* suggests that the response to the treatment with gold was similar to the response to excess copper. However, as there was no change in *COPT1* expression in the presence of gold, the *COPT2* regulatory mechanism is responsive to gold, whereas the *COPT1* mechanism is not. The possible *COPT2* regulatory mechanisms are mentioned in Chapter 4 with the discussion of the FIT1 transcription factor. FIT1 is thought to partially regulate *COPT2* but is not thought to regulate *COPT1*. In combination with the other genes downregulated in the microarray experiment (Section 4.3.8), it appears that the *COPT2* response might be due to the downregulation of *FIT1*. Although

the regulation of *COPT2* is not fully elucidated, and the other components of the regulatory mechanism are unknown, it is likely that the change in regulation of *COPT2* seen here is not due to FIT1 alone. The expression of both *COPT1* and *COPT2* is lower in response to copper exposure (Sancenon et al. 2003), however, the evidence presented here in response to gold suggests that more than one regulatory mechanism is involved, otherwise the two genes would be expected to respond in a similar manner to gold exposure. As such, the changes in *COPT2* expression observed in this work are likely to be regulated by more than one mechanism, including the FIT1 transcription factor.

The downregulation of *COPT2* seen here is likely to be a response to the treatment with gold, rather than a general stress response. Research to stress tolerance in rice has found that general stress can lead to the upregulation of the *COPT* genes (Yuan et al. 2010). Thus, if the response of *COPT2* was a general response, then upregulation of *COPT2* would be predicted, along with upregulation of the other *COPT* genes.

The CTR proteins (including the COPT proteins) are thought to be highly specific for copper (Penarrubia et al. 2010). However, copper transport has been inhibited by competition with silver, showing that silver can also interact with the COPT proteins (Hassett and Kosman 1995; Lee et al. 2002). This has been shown to be true for COPT1 with copper uptake reduced in COPT1-expressing yeast upon treatment with silver (Sancenon et al. 2003). It therefore appears that copper and silver can both interact with the COPT proteins. As copper, silver and gold share periodicity, it is therefore possible that gold can interact with the COPT proteins. This could be tested by determining changes in copper uptake in the COPT1 expressing yeast strain described above in the presence of gold, as carried out with silver by Sancenon et al. (2003). This system is ideal, as the yeast strain is deficient in other copper transporters, and so all copper uptake into the cells is through the COPT1.

5.4.1 Bioinformatic analysis of the COPT family

The bioinformatic analysis in Section 5.3.1 shows that COPT2 and the hypothetical COPT6 are the most closely related of the proteins and these are very similar to COPT1. As COPT1, is the most studied and characterised of the six COPT proteins, many inferences can be drawn about the structure and

function of COPT2. COPT2 is therefore likely to be a plasma membrane transporter involved in copper uptake in Arabidopsis. It therefore follows that as with *COPT1*, *COPT2* overexpressors are likely to have increased copper uptake and likely to be sensitive to excess copper. Mutants would also be expected to be more sensitive to copper deficiency, *copt2* plants are predicted take up less copper.

Although COPT1 and COPT2 are closely related, studies of the expression of the two genes in response to gold and the spatial expression patterns suggests that they do not have fully redundant functions. Genevestigator studies of the COPT1 and *COPT2* expression shows that they are expressed in different places; *COPT2* mainly in the roots and seedling radicle, *COPT1* mainly in the stamen, pollen and roots. In addition to this, *COPT1* was not altered in expression in response to gold, whereas expression of *COTP2* was reduced significantly.

The data presented here confirm that the COPT4 protein is likely to be non-functional. Analysis of the COPT4 sequence shows that the methionine rich residues before the first transmembrane domain, and the MxxxM region within the second transmembrane domain are not present (Figure 5.6). These regions have been shown to be critical in both protein trimerisation within the membrane and metal transport. CTR proteins with the MxxxM domain altered were unable to transport copper (Puig et al. 2002), further indicating that the COPT4 transporter would be non functional.

COPT6 has previously been described as hypothetical because of sequence similarity; however, activity as a transporter has not been demonstrated. The analyses here would suggest that it is a functional protein as it contains all of the features of the other functional proteins. The transmembrane domains are conserved in COPT6, along with crucial methionine and glycine residues. These data would therefore suggest that like COPT2, and also COPT1, COPT6 would transport copper, and if expressed in yeast, would complement the copper uptake mutants. Functionally, COPT6 is likely to be similar to COPT2 because of the sequence similarity. However, lack of microarray data from Genevestigator means that it is not possible to compare expression locations or the conditions in which *COPT6* has altered regulation. The control of the two genes is likely to be different because only *COPT2* had altered regulation in the presence of gold.

5.4.2 The *copt2-1* mutant

The SALK line described here was found to be homozygous for the T-DNA insert, and the insert was found to be very close to the start of the gene, and so it is likely that the gene has been knocked out. However, production of transcript using qPCR and protein production, using antibody assays were not monitored. Thus the *copt2-1* mutant described here is only putative.

As determined in the germination experiments, addition of gold and excess copper to the growth medium reduced the growth of wild-type seedlings whereas copper and iron deficiency did not affect root lengths. For the mutant seeds, the results were identical and there were no significant differences in the growth of roots in any condition tested compared to wild-type Therefore it could be concluded that the mutation in *COPT2* does not increase tolerance to excess copper or gold or deficiency of copper or iron. *copt1* and *copt5* mutants have previously been shown to have reduced root growth in copper deficient conditions (Sancenon et al. 2004; Garcia-Molina et al. 2011), a result not observed in the *copt2-1* mutant described here. Although mean root length was shorter in copper deficient conditions, this was not significantly different to copper sufficient conditions.

It would therefore appear that COPT2 is less important than either COPT1 or COPT5 in the Arabidopsis response to copper deficiency. Alternatively, and possibly more likely, there is redundancy in the functions of COPT1 and COPT2 and thus removal of COPT2 has no effect on the response to copper deficiency. If there was complete redundancy then it could be expected that in the COPT1 mutant, there would be no difference. However, the reduction in growth would imply that the COPT1 transporter is more important in the copper deficiency response or that the two proteins have overlapping but different functions within Arabidopsis.

The growth of Col-0 and *copt2-1* seedlings in the presence of various gold concentrations (Section 5.3.9) demonstrates that the *copt2-1* mutant does not have increased or reduced root lengths in the presence of gold. The mutation therefore did not alter the tolerance of Arabidopsis to gold. These data suggest that the COPT2 protein does not play a role in gold tolerance and that the downregulation of *COPT2* observed is not specifically in response to gold.

However, it is possible that more than one metal transporter is involved in gold tolerance and redundancy between the proteins would hide potential phenotypes.

The similarity in sequence between COPT1 and COPT2 (and COPT6) infers similarity in function as described above. It therefore seems logical to conclude that the lack of difference in growth between Arabidopsis Col-0 and the *copt2-1* may be due to functional redundancy between the proteins. Any function of COPT2 could be replaced entirely by COPT1 and so the physiological response of the plant would be the same. It would be interesting to investigate the copper/gold content of mutant plants to determine whether uptake of these metals is altered. Expression of *COPT1* in *copt2-1* plants could be studied to determine whether it was upregulated in response to a lack of *COPT2*. If copper uptake is reduced due to *COPT2* mutation, then *COPT1* may be upregulated to compensate for this. Another method of testing for redundancy in the COPT1 and COPT2 proteins would be to generate *copt1/2* double knockout mutants to determine whether this would affect growth. However double knockouts might not be viable and might not grow at all. In this case, the use of RNAi (RNA interference) with inducible promoters could be used as the plants would be able to grow prior to inhibition of gene expression. Expression of the zinc transporter MTP1 has previously been inhibited with RNAi under the control of the constitutive CaMV 35s promoter (Desbrosses-Fonrouge et al. 2005).

5.4.3 Future directions

An important direction for future work would not only be to further analyse the *copt2-1* line described in this work, but to find other mutants in *COPT2* or generate RNAi lines. Additionally, *COPT2* overexpressing lines could be produced. Using these lines, further characterisation could be carried out in response to gold treatment. It has been shown here that the *copt2-1* mutant line grows the same way as wild-type Arabidopsis in response to gold treatment but the uptake of gold has not been studied. It would be interesting to characterise *COPT2*-expression-altered lines as was done for wild-type Arabidopsis as presented in Chapter 3. Gold uptake in hydroponic and soil systems could be studied and compared to wild-type plants to determine whether uptake and translocation are altered. In addition to this, nanoparticle formation and distribution could be looked at within these plant lines.

Although the similarity of COPT2 and COPT1 (outlined above) would suggest that COPT2 is a plasma membrane copper transporter which is important in the influx of copper into the cell, the actual subcellular localisation of COPT2 is unknown. This would include determining which membranes the protein is associated with. All four *COPT* genes with available data were found to be upregulated in response to iron deficiency. This was a response that was observed for many of the genes with the largest downregulation in expression in response to gold as discussed in Chapter 4.

To determine whether a transporter is able to transport a particular metal, the transporter could be expressed in a cell type which does not contain it and then look for uptake. As already mentioned, the COPT proteins were initially discovered due to their ability to complement yeast mutants unable to take up copper. Complementation studies are not possible when studying gold uptake because gold is not essential and no gold transporters have so far been identified. One way to study whether COPT2 is able to transport gold is by using *Xenopus* embryos. At an early stage, these embryos contain no membrane transporters. Therefore, if *COPT* is expressed in these embryos and when treated with gold, they accumulate gold, then it can be confirmed that the protein is able to transport the metal. In order to do this, an assay would require development for measuring gold content within the embryos, or alternatively, if gold nanoparticles formed internally, this would be confirmation that gold had been transported across the membrane. This technique has previously been employed in the investigation of the rice arsenic transporter NIP:2;1 (Ma et al. 2008).

Chapter 6 Forward genetic screen

6.1 Introduction

6.1.1 Background

A forward genetic screen interrogates collections of mutations in plants for certain phenotypes. The mutant is subsequently analysed to determine the genetic basis of the phenotype. Forward genetic screens have been used to test for tolerance to a variety of environmental stresses, including cadmium (Wang et al. 2011), arsenic (Lee et al. 2003) and salt stress (Zhu et al. 1998). Additionally, screens have been used to determine biological processes, such as auxin transport (Stirnberg et al. 2002) and the ethylene response pathway (Alonso et al. 2003b).

Two approaches to forward genetic screens in Arabidopsis are to alter the DNA with chemical treatment or to damage the DNA using physical methods. A common method of chemical mutagenesis is the use of ethyl methane sulfonate (EMS). EMS is a base modifying agent, which adds an alkyl group to the hydrogen-bonding oxygen in guanine, causing G/C to A/T transitions (Waugh et al. 2006). Approximately 5 % of EMS mutations in Arabidopsis will result in a change to a stop codon. Further to this, approximately 65 % and 30 % will be missense mutations and silent changes respectively (McCallum et al. 2000). Mutations causing a premature stop codon or a missense translation can lead to loss of function. It is therefore likely that the majority of mutations in an EMS screen will be loss of function mutations rather than gain of function mutations. This can be used to look for genes which confer tolerance or sensitivity to a particular substance by altering sensitivity. An example of this is the discovery of mutants with increased tolerance to aluminium by measuring root lengths in conditions where aluminium inhibits root growth (Larsen et al. 1998). Cadmium sensitive mutants in Arabidopsis have also been isolated by screening EMS mutagenised seeds (Howden and Cobbett 1992).

Fast-neutrons have also been shown to be an effective mutagen (Koornneef et al. 1982). Fast neutron irradiation works by breaking the DNA, thereby introducing deletions (Shirley et al. 1992). This technique has been used to identify genes which confer tolerance of sensitivity to different stresses such as

salt stress (Liu and Zhu 1997), and identify loci within different pathways, such as the ethylene signal transduction pathway (Roman et al. 1995).

6.1.2 Screen aims and strategy

It was demonstrated in Chapter 3 that gold is toxic to Arabidopsis, and when seeds were germinated in the presence of gold, root growth was inhibited. Therefore, to identify potential mechanisms of gold tolerance in Arabidopsis, a genetic screen was carried out. EMS mutagenised seeds were used to identify mutants with increased root growth in the presence of gold.

6.2 Methods

6.2.1 Production of ethyl methane sulfonate (EMS) seeds

In order to screen for genes involved in gold tolerance, an EMS mutant population was produced. Approximately 30 000 Arabidopsis Col-0 seeds were imbibed for two nights at 4 ºC in the dark in three batches of 10 000 seeds. Seeds were treated with 0.2, 0.3 or 0.5 % (v/v) EMS for 16 hours. EMS was removed and seeds were washed. Seeds were subsequently suspended in 0.15 % agar at a density of approximately 100 seeds per 10 mL and then planted on F2 compost and allowed to germinate and grow. Once mature, the resulting seeds were collected and sterilised for the mutant screen.

6.2.2 Screen optimisation

MS agar plates were produced at 0, 0.6, 0.7, 0.8 and 0.9 mM gold. Gold was added as $KAuCl_4$ at pH 5.7 to freshly produced and autoclaved double strength MS agar and diluted with water to give the final gold concentration and full strength MS, which would provide more nutrients and thus improve germination of the mutagenised seed. Twenty Arabidopsis seeds from the F3 generation (wild-type Col-0) or the 0.2 % or 0.3 % EMS seed batches (M2 generation) were germinated on each concentration of gold in triplicate. Seeds were imbibed in water for 5 nights in the dark at 4 ºC to improve germination. Seeds were sown onto agar and germinated at 20 ºC under a 16 / 8 hr light dark cycle. Root lengths of 30 seedlings for each treatment were measured after seven days of growth and the final germination rate from 60 seedlings calculated.

6.2.3 Genetic screen

The mutant M2 seeds produced (Section 6.2.1) were screened for increased tolerance and root length when germinated and grown on media containing gold. EMS mutagenised seeds were sprinkled onto MS agar plates containing 0.6 mM gold, determined as optimal by seedling growth on a variety of gold concentrations. Seeds were produced as described in Section 6.2.1. Seeds were germinated at 20 ºC under a 16 / 8 hr light dark cycle and seedlings grown for seven to ten days. Seeds with increased root length on plates containing gold were transferred to F2 compost and grown to propagate the seed. M3 seed

batches from plants with increased root length were harvested and rescreened on 0.6 mM gold to re-check tolerance to growth on gold.

6.3 Results

6.3.1 Production of EMS seed

Approximately 140 000 EMS mutagenised M2 seed were generated from the M1 parents treated with 0.2 and 0.3 % EMS (Section 6.2.1). Fewer than ten seeds were produced from parent plants treated with 0.5 % EMS and plants were stunted in comparison to the plants from 0.2 and 0.3 % EMS seeds. As such, 0.5 % EMS was deemed too high for successful mutagenesis. Thus, in the subsequent experiments the seeds from the 0.5 % EMS treated plants were not used.

6.3.2 Screen optimisation

Seeds were germinated and grown at 0, 0.6, 0.7, 0.8 and 0.9 mM gold for seven days to determine which of these concentrations would be optimal for the genetic screen of EMS mutants. As with the wild-type seedlings, the presence of gold inhibited the root growth of EMS mutagenised seeds (Figure 6.1). The root lengths at these conditions were similar to those noted in Chapter 3.

Results from the experiments described here showed that the optimum treatment for the screen of EMS seeds was germination and growth for seven days on full strength MS agar plus 0.6 mM gold (pH 5.7) with seeds stratified for 5 nights in the dark at 4 ºC prior to germination at 20 ºC.

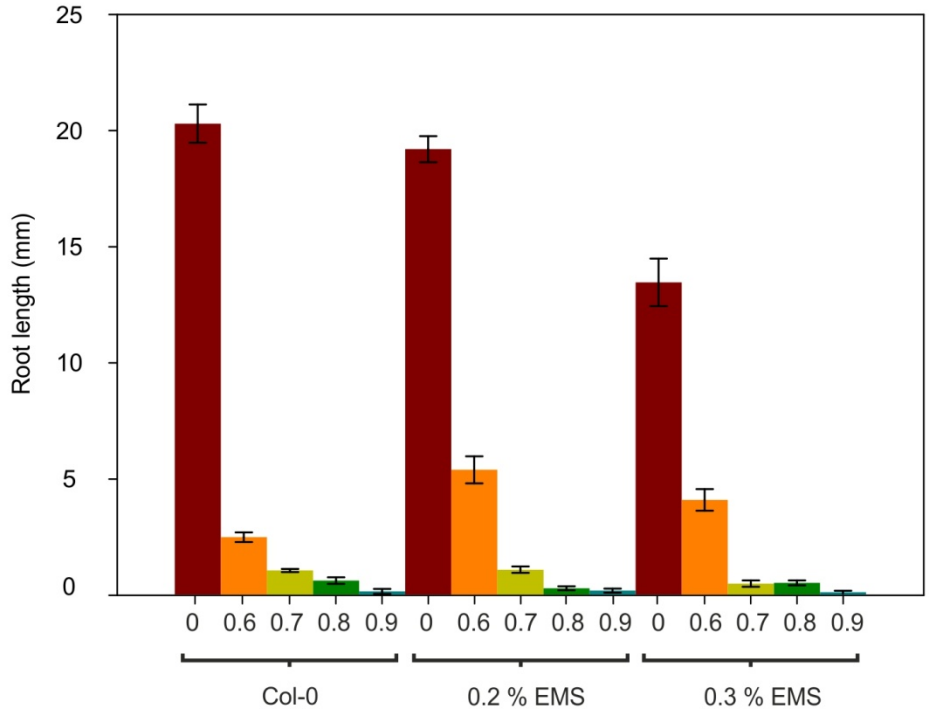

Figure 6.1 Root lengths of EMS seeds on gold
Arabidopsis seeds were imbibed and stratified in water for five nights, prior to germination on ½MS(A) containing 0. 0.6, 0.7, 0.8, or 0.9 mM $KAuCl_4$ (pH 5.7). Seeds were either wild-type Col-0 or the M2 seeds from parents treated with 0.2 or 0.3 % EMS. After eight days of growth, root lengths were measured. Data are the means of at least 30 measurements and error bars represent the standard errors of the means.

In order to determine whether to use seeds from the M1 parents treated with 0.2 % or 0.3 % EMS for the screen, germination frequencies were measured for three batches of seedlings; wild-type, 0.2 % EMS treated and 0.3 % EMS treated. For the EMS seed, it was clear that as the gold concentration increased, germination frequency decreased (Figure 6.2). This change in germination frequency was less for the 0.2 % treated seeds compared to the 0.3%. For the genetic screen described below, the 0.3 % EMS treated seeds were used. It was also noted that the germination times for the seeds varied. Thus, stratification was carried out for 5 days, and plants were grown on MS(A), instead of ½MS(A), in order to reduce variation in germination times.

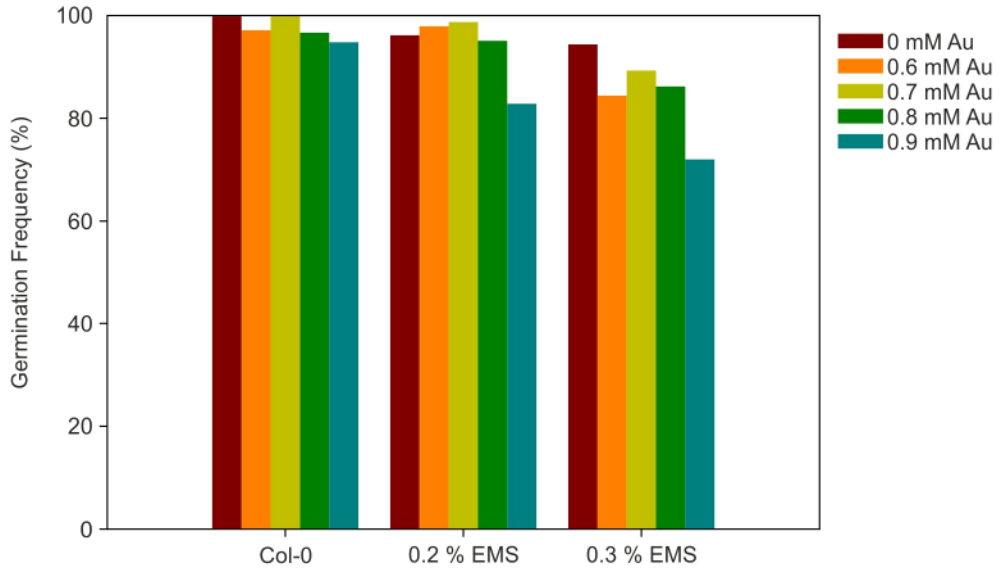

Figure 6.2 Germination frequencies of mutant seed at different gold concentrations

Arabidopsis seeds were imbibed and stratified in water for five nights, prior to germination on ½MS(A) containing 0. 0.6, 0.7, 0.8, or 0.9 mM $KAuCl_4$ (pH 5.7). Seeds were either wild-type Col-0 or the M2 seeds from parents treated with 0.2 or 0.3 % EMS. Germination frequencies were determined as a percentage from 60 seeds.

6.3.3 Selection of mutant phenotypes from a screen of EMS mutant seeds on gold

After the optimisation described above, M2 seeds derived from parents treated with 0.3 % EMS were grown on MS(A) supplemented with 0.6 mM gold for seven days (Figure 6.3). Approximately 140 000 seeds were screened and 30 putative mutants were found with increased root length in the presence of gold. Example mutants are indicated in Figure 6.4. Some of these were from the same pool, suggesting that the mutation was in the same gene, as it is likely that they were from the same plant. This therefore suggests that 22 unique putative mutants were found. Seven-day-old seedlings were transferred to F2 compost and grown to propagate more seeds.

Out of the 140 000 seeds screened, 695 were found to be albino; 0.49 % of all mutants. This was similar to previously seen mutation rates, showing that the EMS treatment had been successful (Tokuhisa et al. 1997).

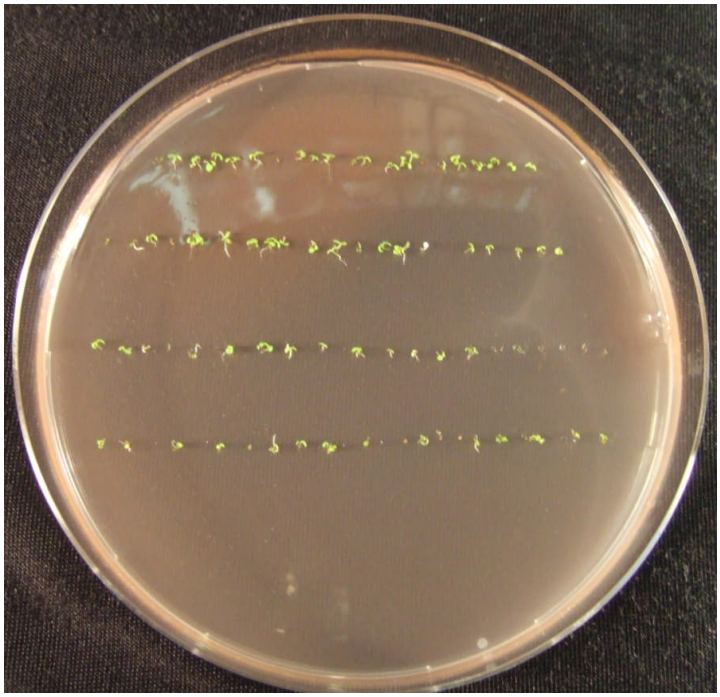

Figure 6.3 Mutant seeds in the presence of gold
Seven-day-old M2 Arabidopsis seedlings after germination and growth in the presence of 0.6 mM gold. M1 seeds were mutagenised with 0.3 % EMS.

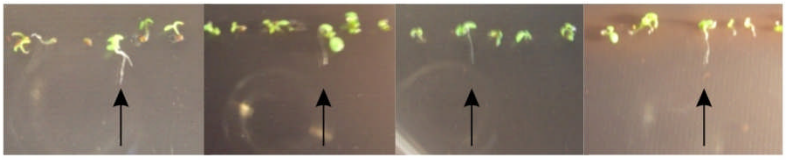

Figure 6.4 A selection of putative mutants
Seven-day-old M2 Arabidopsis seedlings after germination and growth in the presence of 0.6 mM gold. M1 seeds were mutagenised with 0.3 % EMS. Putative mutants are indicated by arrows.

6.3.4 Rescreening of putative mutants

Putative mutants identified as described above (Section 6.3.3) were propagated to collect more seeds. Of the 30 seedlings identified as putative mutants, eleven grew to maturity and produced enough seed to rescreen. Some of the mutants did not grow on F2 compost and for other mutants; fewer than ten seeds were produced and so could not be rescreened. Thus, mature seed from the eleven plants from which seeds could be collected were subsequently rescreened for increased tolerance to gold. Seeds were rescreened on MS media supplemented with or without 0.6 mM gold to determine whether there was increased gold tolerance and to compare how the seedlings grew compared to wild-type.

None of the eleven rescreened seeds had increased root lengths (compared to wild-type) in the presence of gold (Figure 6.5). Some of the seeds had reduced root lengths, and one mutant line did not germinate. Seedlings were also germinated and grown on media without gold as a comparison (data not shown). Those seedlings with reduced root growth when grown in the presence of gold (Figure 6.5) also had smaller roots than wild-type when grown without gold. All other lines had similar root lengths to wild-type, when grown without gold. It was therefore concluded that no mutants were identified with increased tolerance to gold.

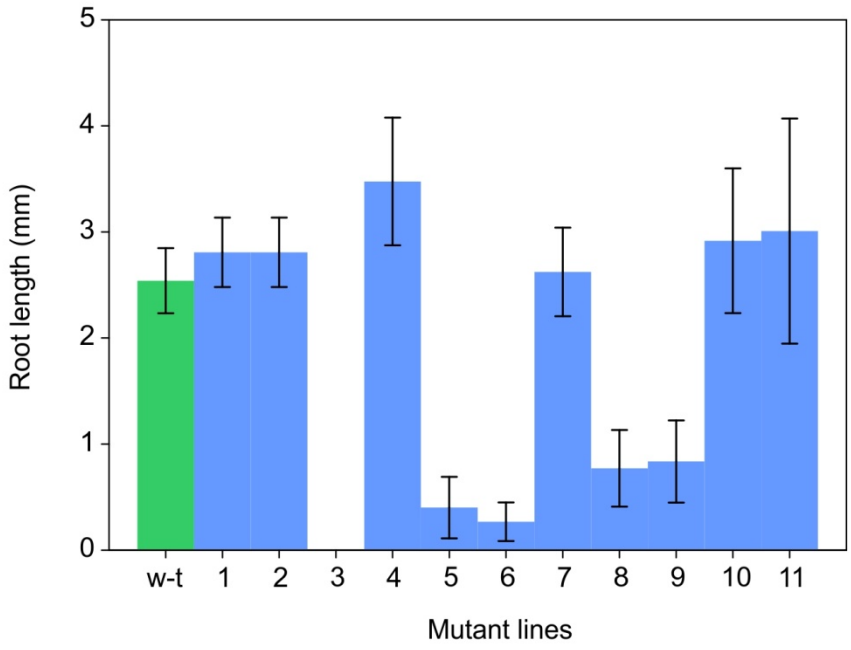

Figure 6.5 Root lengths of putative mutants grown in the presence of gold

Seven-day-old Arabidopsis seedlings after growth on MS(A) containing 0.6 mM gold. Wild-type seedlings are indicated as 'w-t' in the Figure, and putative mutants are indicated numerically. Results are the means from at least 30 biological replicates and error bars represent the standard errors of the means.

6.4 Discussion

The toxicity of gold observed in Chapter 3 was used to design a genetic screen to identify mutants with increased tolerance to growth on gold. The screen was optimised and carried out by germinating and growing Arabidopsis seeds on ½MS(A) containing 0.6 mM gold. EMS mutagenised seeds were produced to carry out the screen. 140 000 seeds were germinated and screened, and 30 putative mutants with increased tolerance to gold were identified. However, on rescreening the M3 progeny, none had increased root lengths in the presence of gold. It is therefore likely that the seedlings identified as putative mutants had longer roots in the initial screen due to natural variation.

Although screening mutant seeds for increased tolerance to metals has been successfully carried out (Larsen et al. 1998), no mutants with increased gold tolerance were identified here. It is possible that there are no EMS induced mutations possible which could increase gold tolerance. If there are no possible EMS induced mutations which could have increased tolerance to growth on gold, this could be because few genes are involved in gold tolerance or uptake. As such, it is possible that none of the genes involved could lead to increased tolerance when expression is inhibited. Any mutations altering the gold tolerance pathway could make the plants more sensitive to gold. Previous studies of cadmium tolerance found mutants with increased sensitivity, suggesting that this may be the case (Howden and Cobbett 1992). Mutants with increased sensitivity to excess copper and aluminium have also been identified (Larsen et al. 1996; Larkin et al. 1999). Using the method outlined here to select for mutants more sensitive to gold would not have been possible because the root lengths were small and as such any reduction in root length would have been difficult to identify. Additionally, there are a number of non-gold related mutations which can inhibit germination and root growth; it would not be possible to distinguish these from mutations which reduce gold tolerance.

Functional redundancy could play a part in why no mutants with increased tolerance were identified. It has been discussed in Chapter 1 that there is much redundancy between metal transporters. Thus, it is possible that inhibiting the function of only one of these would not increase gold tolerance, as, for example, gold uptake would not be inhibited. To get around this problem, expression of more than one gene would have to be knocked out.

It is possible that the fundamental strategy for the screen was flawed, and that, as described above, there are no EMS induced mutations which could confer increased tolerance to gold on Arabidopsis. This could potentially be overcome by screening seeds with increased expression of genes, such as in an activation tagged library. Such a library is generated by inserting promoters, such as the CaMV 35S promoter randomly in the genome and as such, the expression of genes downstream of the promoter (Weigel et al. 2000). This strategy has been successfully employed to find mutants tolerant to arsenic (Sung et al. 2007), and so it is possible that it could be used to find mutants with increased tolerance to gold.

Chapter 7 General discussion

The main aims of this study were to characterise the physiological response to gold in Arabidopsis, and to subsequently investigate the genetic response to gold at the level of transcription. A further aim was to identify and study a gene, or gene family with potential importance in gold tolerance and uptake. These aims were completed using growth studies and gold uptake studies as presented in Chapter 3, to investigate the toxicity of gold, and quantify gold uptake in Arabidopsis. These experiments were carried out alongside studies of *in planta* nanoparticle formation. Subsequently, the genetic response to gold was investigated using microarray technology as described in Chapter 4 and these data used to identify, and produce preliminary characterisation of the COPT family of metal transporters to investigate potential involvement in gold tolerance (Chapter 5).

7.1 Gold nanoparticles

Although initial work in this area was focused on the possible uses of plants to accumulate gold and remediate former gold mines and tailings (Anderson et al. (1998) and Section 1.4.1), more recently, attention has shifted to the mechanisms behind the formation of gold nanoparticles in plants. The electron microscopy studies of plant tissues presented in Chapter 3 demonstrate that gold nanoparticles can be produced in Arabidopsis roots under a variety of conditions. However, nanoparticle formation was not observed in aerial Arabidopsis tissues under the resolution limits of the electron microscope used in this study. Nanoparticles have previously been identified in the aerial tissues of some plant species (Gardea-Torresdey et al. 2002a; Sharma et al. 2007; Bali and Harris 2010) and it was confirmed in this work that gold nanoparticles can form in the aerial tissues of alfalfa plants. This shows that there are physiological differences between Arabidopsis and alfalfa which determine whether formation of gold nanoparticles in aerial tissues takes place.

Gold nanoparticle size and shape in plants has been shown to be dependent on the conditions of the treatment (Starnes et al. 2010). If gold nanoparticles with consistent size and shape could be produced in and extracted from plants, this could offer a low cost and efficient mechanism of nanoparticle production. Nanoparticles are used in many applications, including catalysis and in medical

applications, as described in Chapter 1 (Section 1.5), with nanoparticles between seven and ten nanometres diameter required for the catalytic oxidation of carbon monoxide in fuel cells (Kim et al. 2004b). As an alternative to nanoparticle extraction, plant material could be used in a dried and ground form with liquid reactions carried out in the presence of this catalytic material. Plant material containing nanoparticles has been used successfully to catalyse the reduction of 4-nitrophenol in an aqueous solution, showing that nanoparticle-rich plant material has the potential to be used as a catalyst (Sharma et al. 2007).

With the increased use of gold nanoparticles in industrial applications, the exposure of the environment to gold nanoparticles is expanding. Much research is therefore ongoing into whether plants can take up nanoparticles, and whether these can subsequently be concentrated in the food chain (Judy et al. 2010). It was shown in Chapter 3 that gold nanoparticles were not taken up as nanoparticles by alfalfa roots under the conditions tested, a result with environmental consequences. As nanoparticles were not taken up by alfalfa roots, this elucidates details of gold nanoparticle production in plants. It has been suggested that gold nanoparticles form extracellularly and are subsequently taken up (Gardea-Torresdey et al. 2002a). The data presented here indicate that this is not a correct hypothesis. It is therefore likely that the nanoparticles observed in plant tissues, either in this work, or in other published data (Gardea-Torresdey et al. 2002a; Gardea-Torresdey et al. 2005; Rodriguez et al. 2007; Sharma et al. 2007; Bali and Harris 2010) are formed after gold has been taken up in an ionic form and subsequently reduced to gold(0) in the plant tissues.

7.2 Genetic response of Arabidopsis to gold

In addition to the characterisation of gold uptake and tolerance in Arabidopsis, this project further aimed to understand the genetic responses to gold, an approach not previously published. Microarray technology was used to study the changes in transcription of more than 22 000 genes as described in Chapter 4. Treatment with gold caused the up- and downregulation of a number of genes which would be expected to have altered regulation as a general stress response, including cytochromes P450, GSTs and GTs (Marrs 1996; Schenk et al. 2000; Narusaka et al. 2004). Eleven of the 35 Arabidopsis aquaporins were downregulated in the presence of gold. Aquaporins have previously been implicated in gold toxicity because gold inhibits aquaporin function (Niemietz and

Tyerman 2002). Interestingly, various genes encoding metal transporters were downregulated more than ten-fold, including *IRT1*, *IRT2, COPT2*, *ATIREG2*, *MTPA2* and *MTPc3* (see Table 4.11).

A transcription factor known to be involved in the response to iron deficiency (FIT1) was also downregulated (20-fold). FIT1 regulates a number of genes involved in iron uptake and *fit1* mutants require supplemental iron applications to survive. As a consequence of FIT1 downregulation, many of the genes which FIT1 regulates were also downregulated. These include IRT1, IRT2 and NRAMP1 which are known to be involved in iron uptake (Curie et al. 2000; Vert et al. 2001; Vert et al. 2002). Given the downregulation of *FIT1* in the presence of gold, it is possible that gold interacts with the FIT1 regulatory pathway in place of iron. It would be interesting to study *fit1* mutants or *FIT1* overexpressing plants to determine whether these plants are more or less tolerant to growth in the presence of gold.

The microarray experiment data identified some metal transporters that are possibly involved in gold uptake or tolerance. However, no conclusive evidence exists to suggest that gold is taken up by a specific transporter. One experiment which could be carried out would be to treat plants with gold in combination with one from a range of other metals, including iron, zinc and copper. The gold concentration of these plants could then be measured. If gold can be taken up by metal transporters, then in the treatments with the metal that it shares a transporter with, gold uptake would be reduced. This could potentially narrow down the identification of which transporters are able to transport gold. However, there is considerable redundancy within the Arabidopsis metal transporters characterised so far; for example, transporters IRT1, IRT2 and NRAMP1 all take up iron, and HMA2, HMA4 and MTP1 all transport zinc (see Chapter 1). Thus, if one metal transporter is inhibited in the presence of gold, others might not be, and as such metal uptake would not be inhibited. Alternatively, it could be that gold non-specifically blocks metal transporters which would affect the results of such an experiment. Similar experiments to this were carried out using yeast expressing plant metal transporters to determine which metals the ZIPs (including IRT1), COPTs, and MTP1 transport (Grotz et al. 1998; Korshunova et al. 1999; Sancenon et al. 2003; Kawachi et al. 2008). The interaction of gold with specific metal transporters could therefore be studied, using these yeast strains.

7.3 Genetic screen

In an attempt to identify genes which are involved in gold tolerance, a genetic screen was designed to isolate Arabidopsis mutants with increased tolerance to gold (Chapter 6). However, no mutants with increased tolerance were identified and as such, this work is presented in. One possible reason that no mutants with increased root length in the presence of gold were identified is that the screen strategy was flawed. The screen was carried out using seeds mutagenised with ethyl methane sulfonate (EMS) which causes G/C to A/T point mutations (Waugh et al. 2006). Such mutations are predicted to knock down gene function and as such, it is possible that no mutations are possible which could increase tolerance to gold.

To isolate plants with increased tolerance to growth on gold, a genetic screen as described could be performed using an activation tagged library. In such a library, mutants contain a CaMV 35S promoter to enhance the expression of downstream genes (Weigel et al. 2000). This methodology has been successful in isolating mutants with increased arsenic tolerance (Sung et al. 2007), along with mutants tolerant to other stresses including drought, cold and heat (Kang et al. 2011).

7.4 Gold toxicity to plants

The data presented in this work have demonstrated that gold is toxic to plants. This toxicity was most obvious with the reduced root length when seeds were germinated in the presence of gold. Although germination was not inhibited (suggesting that gold might not penetrate the testa prior to this stage), there was severe inhibition of root growth with increasing gold concentrations. In addition to this, there was reduced starch accumulation in soil grown plants, suggesting that gold compromises photosynthesis. The results from the microarray experiment further demonstrate that gold is toxic. The 25 most upregulated genes have previously been shown to be upregulated in response to other stresses, including high temperature, hypoxia, and parasites. This suggests that these genes are upregulated because of a general stress response, rather than a specific response to gold.

As described in Chapter 3 (Section 3.4.1), toxicity could be due to electrostatic interactions between gold and the root surface or the inhibition of aquaporin function which would reduce water uptake. Additionally, gold could disrupt protein structure, replace the metallic centre of some proteins or lead to the formation of free radicals, causing oxidative stress.

7.5 COPT2

The work described in Chapter 5 describes the response of the *COPT* genes in response to gold. The microarray results showed that in the presence of gold, *COPT2* was downregulated approximately 24-fold. Subsequent qPCR analysis determined that *COPT2* was downregulated approximately 1000-fold, whereas, none of the other five members of the family had altered regulation in the presence of gold. This downregulation is thought to be at least partly due to the altered expression of the FIT1 transcription factor because it is thought that *COPT2* expression is partially regulated by FIT1 (Colangelo and Guerinot 2004). A putative *copt2* mutant, homozygous for a T-DNA insertion 40 bases upstream of the start of *COPT2* was obtained but no phenotypic differences to wild-type in the presence of gold at concentrations between 0.25 and 1 mM were observed. Additionally, the mutant had no phenotypic differences when compared to wild-type in iron or copper deficient conditions or in the presence of excess copper. Further work using reverse transcription PCR or western blot analysis would be required to ascertain that *COPT2* was disrupted. However, these results demonstrate that COPT2 is probably not important in the response of Arabidopsis to gold. It is possible that more than one protein is involved in gold tolerance and thus no difference was observed due to functional redundancy between that protein and COPT2.

7.6 Summary

This work has characterised the physiological and genetic responses of Arabidopsis to gold. The toxicity of gold has been assessed, as has the uptake of gold from various growth substrates. In addition to this, the formation of gold nanoparticles within plant tissues has been studied along with the uptake of gold nanoparticles. Microarray technology was used to analyse the genetic response of Arabidopsis to gold. Many metal transporters were downregulated, some of which were under the control of the FIT1 transcription factor. These results

suggest that gold was interacting with the iron regulatory pathway in Arabidopsis. The microarray results presented here, suggest that the COPT2 copper transport protein plays a role in response to gold. Investigations of the *copt2-1* mutant suggests that this is not the case as the mutant did not have a phenotype different to that of the wild-type plants in the presence of gold, or other metals.

Overall, these results demonstrate the first investigation into the genetic response of plants to gold. The data presented here also provide a further comparison to the physiological responses of plants to gold described in the literature.

Appendix A. List of genes upregulated more than two-fold after treatment with gold

The following list shows the genes found to be upregulated more than two-fold after treatment with gold (as described in Chapter 4). Genes are listed in order of high to low expression compared to untreated plants. The gene titles are those with which the ATH1 microarray chip is annotated and as such, this may be incomplete as recent annotations may not have been included.

Fold change	Gene Title	Gene ID	Target Description
291.07		At3g16530	putative lectin
233.89		At1g26380	hypothetical protein
220.17	ATGSTU12	At1g69920	putative glutathione transferase
133.91	NIT4	At5g22300	nitrilase 4
132.16	GLIP1	At5g40990	GDSL-motif lipase/hydrolase
127.24	CYP71A12	At2g30750	putative cytochrome P450
122.02	ANAC042	At2g43000	NAM-like protein
102.81		At1g64160	dirigent protein
93.40	CYP82C2	At4g31970	cytochrome P450
88.68		At1g14550	anionic peroxidase
87.57	PXMT1	At1g66690	unknown protein
86.87	YLS9	At2g35980	putative harpin-induced protein
85.24	ATHSP17.4	At3g46230	heat shock protein 17
82.29	ATGSTU11	At1g69930	putative glutathione transferase
78.08		At3g60120	beta-glucosidase
76.05		At4g37290	hypothetical protein
74.79		At5g39580	peroxidase ATP24a
74.14	CYP71B22	At3g26200	cytochrome P450
74.12	AT-HSP17.6A	At5g12030	heat shock protein 17.6A
69.51	PLP2	At2g26560	hypothetical latex allergen
67.74		At2g28210	putative carbonic anhydrase
66.61	UGT73B4	At2g15490	putative glucosyltransferase
63.54		At1g05680	putative indole-3-acetate beta-glucosyltransferase
62.31		At1g53540	17.6 kDa heat shock protein (AA 1-156)
55.43		At3g54150	embryonic abundant protein
54.24		At4g10520	subtilisin-like serine protease
52.28	PAD3	At3g26830	putative cytochrome P450
52.22	AOX1D	At1g32350	putative oxidase
51.88	PGIP1	At5g06860	polygalacturonase inhibiting protein 1
51.64	ATGSTU4	At2g29460	putative glutathione S-transferase
50.92	ATGSTU24	At1g17170	putative glutathione transferase
50.88	CCoAMT	At1g67980	putative S-adenosyl-L-methionine:trans-caffeoyl-Coenzyme

			A 3-O-methyltransferase
50.69		At3g02840	unknown protein
49.91		At2g39030	unknown protein
49.35	ATGSTU25	At1g17180	putative glutathione transferase
48.78		At2g29500	putative small heat shock protein
48.26		At1g56060	hypothetical protein
47.80	CYP81F2	At5g57220	cytochrome P450
47.66	CML37	At5g42380	putative protein
46.93	ATBCB	At5g20230	blue copper binding protein
46.67		At5g19880	peroxidase
46.56		At1g57630	putative disease resistance protein RPP1-WsB
45.99	CYP81D8	At4g37370	cytochrome P450
45.87		At1g26390	hypothetical protein
45.37		At5g22530	unknown protein
44.10		At1g79680	wall-associated kinase 3
43.39		At5g38900	frnE protein
42.64	AtMYB15	At3g23250	putative myb-related transcription factor
42.47		At3g18250	hypothetical protein
42.26	CYP706A1	At4g22710	cytochrome P450
40.51	BGLU45	At1g61810	putative beta-glucosidase
40.17		At3g49580	putative protein
38.50	DIN2	At3g60140	putative beta-glucosidase
38.50		At5g37840	putative protein
36.66		At1g26240	hypothetical protein
35.09		At2g32190	unknown protein
34.73		At2g23270	hypothetical protein
34.53		At3g55090	putative ABC transporter
34.39	DIN11	At3g49620	putative SRG1 protein
33.53		At1g14540	putatvie anionic peroxidase
33.25		At3g60420	putative protein prib6
33.07		At1g23730	putative carbonic anhydrase
32.89		At3g53600	zinc finger prtoein
32.44		At2g41380	putative embryo-abundant protein
31.93		At1g22890	unknown protein
31.76		At1g72900	virus resistance protein
31.00	ATERF6	At4g17490	ethylene responsive element binding factor 6
30.31		At1g26420	hypothetical protein
30.30		At2g44460	putative beta-glucosidase
29.81		At5g06730	peroxidase
29.72		At1g66090	disease resistance protein
28.22		At2g39400	putative phospholipase
28.07		At5g52670	putative protein
28.01		At1g33030	putative catechol O-methyltransferase
27.89		At5g14470	putative protein

27.88		At3g09410	putative pectinacetylesterase
27.82		At1g19020	unknown protein
27.46		At3g63380	putative Ca2+-transporting ATPase
27.01		At2g01300	hypothetical protein
26.27		At4g28460	hypothetical protein
26.20	CRK11	At4g23190	serine/threonine kinase
26.07		At5g25260	nodulin
26.06		At5g65600	receptor protein kinase like protein
24.71		At1g35210	hypothetical protein
24.49		At3g03430	pollen allergen Bra r II
23.88		At5g39670	calcium-binding protein
23.23	EXLB3	At2g18660	hypothetical protein
23.16		At5g01380	transcription factor GT-3a
22.84		At1g26410	unknown protein
22.54		At3g61390	putative protein
22.29	MYB122	At1g74080	putative MYB transcription factor
22.16	ATPUP18	At1g57990	unknown protein
22.03		At5g39050	putatvie acyltransferas
22.02	WRKY45	At3g01970	putative WRKY-like transcriptional regulator protein
21.99	ANAC032	At1g77450	GRAB1-like protein
21.66	ATERF-2	At5g47220	ethylene responsive element binding factor 2
21.55		At1g67810	hypothetical protein
21.49		At4g28085	unknown protein
21.39		At5g22270	putative protein
21.08		At3g50930	BCS1 protein
20.97		At3g47480	putative calcium-binding protein
20.84	MSS1	At5g26340	hexose transporter
20.74	AR781	At2g26530	unknown protein
20.62	CP1	At4g36880	cysteine proteinase
20.58	ATDTX1	At2g04040	hypothetical protein
20.42		At2g22880	hypothetical protein
20.34		At5g64870	nodulin-like
20.29	ATMPK11	At1g01560	putative MAP kinase
20.11	WRKY75	At5g13080	putative WRKY DNA binding protein
20.05		At5g67340	putative protein
19.88		At5g66780	putative protein
19.87	CCR2	At1g80820	putative cinnamoyl CoA reductase
19.79		At1g24140	putative metalloproteinase
19.70		At3g56500	putative protein
19.54	PMZ	At3g28210	zinc finger protein (PMZ)
19.50	PROPEP3	At5g64905	unknown protein
19.33		At1g60730	putative auxin-induced protein
19.30	ATTI1	At2g43510	putative trypsin inhibitor
19.25		At2g32210	unknown protein
19.13	AATP1	At5g40010	putative protein

19.01		At1g21120	putative ATPase
19.00		At2g32140	putative disease resistance protein
18.99		At3g21520	hypothetical protein
18.78		At5g44990	putative protein
18.61	ATGSTU10	At1g74590	putative glutathione S-transferase
18.58	LCR67	At1g75830	unknown protein
18.52		At1g21130	putative O-methyltransferase
18.51		At5g35735	unknown protein
18.35		At4g01870	hypothetical protein
18.29	AIG2	At3g28930	AIG2-like protein
18.21		At3g02800	unknown protein
18.18		At1g68620	unknown protein
18.15		At1g74360	putative receptor proein kinase
18.14		At1g55780	hypothetical protein
18.11		At3g59080	putative protein
17.94		At5g22555	unknown protein
17.75	GLP6	At5g39100	germin - like protein GLP6
17.61		At4g14365	unknown protein
17.59		At5g41740	disease resistance protein-like
17.47	CML38	At1g76650	putative calmodulin
17.46	UGT73B5	At2g15480	putative glucosyltransferase
17.43		At1g02850	putative beta-glucosidase
17.19		At4g11480	serine/threonine kinase
17.17	SIB1	At3g56710	SigA binding protein
16.96	ATGSTF7	At1g02930	putative glutathione S-transferase
16.95	MYB51	At1g18570	putative myb factor
16.86		At5g52750	putative protein
16.70		At1g60750	putative auxin-induced protein
16.56	RHL41	At5g59820	zinc finger protein Zat12
16.50		At3g21720	putative isocitrate lyase similar to GB:P25248 from [Brassica napus]
16.37		At1g15010	hypothetical protein
16.35	TCH3	At2g41100	calmodulin-like protein
16.33	AT-AER	At5g16970	quinone oxidoreductase
16.21		At5g64250	2-nitropropane dioxygenase-like protein
15.89	ATGSTU3	At2g29470	putative glutathione S-transferase
15.79		At3g24510	unknown protein
15.72		At2g33710	putative AP2 domain transcription factor
15.62		At4g04540	putative receptor-like protein kinase
15.57		At5g39110	germin -like protein
15.43	WRKY8	At5g46350	putative protein
15.33		At5g59490	putative ripening-related protein
15.33	LAC5	At2g40370	putative laccase (diphenol oxidase)
15.31		At3g28510	hypothetical protein
15.25		At1g71140	hypothetical protein

15.23		At2g18680	unknown protein
15.20	LAC1	At1g18140	laccase,
15.12		At1g61340	late embryogenesis abundant protein
15.10	UGT73C7	At3g53160	glucosyltransferase like protein
15.10	WRKY70	At3g56400	DNA-binding protein
15.03		At1g51920	hypothetical protein
15.01	CRK10	At4g23180	serine/threonine kinase
14.92	WRKY28	At4g18170	DNA binding like SPF1
14.88		At3g55790	putative protein
14.81	ACS6	At4g11280	ACC synthase (AtACS-6)
14.70		At1g30370	putative lipase
14.45	HAK5	At4g13420	potassium transporter
14.26		At3g48850	mitochondrial phosphate transporter
14.26	PBS3	At5g13320	auxin-responsive - like protein
14.09		At2g02990	ribonuclease
14.02	WRKY43	At2g46130	putative WRKY-type DNA binding protein
13.90		At1g33600	hypothetical protein
13.89	PPDK	At4g15530	pyruvate orthophosphate dikinase
13.85		At2g30140	putative glucosyltransferase
13.68	ATCNGC13	At4g01010	cyclic nucleotide gated channel like protein
13.64		At1g28190	hypothetical protein
13.62		At3g01830	hypothetical protein
13.61		At4g13180	short-chain alcohol dehydrogenase
13.44		At5g05340	peroxidase
13.38		At1g76600	unknown protein
13.38		At1g68450	unknown protein
13.29		At5g18470	putative S-receptor kinase PK3 precursor
13.24	FMO1	At1g19250	unknown protein
13.21	CYP72A8	At3g14620	putative cytochrome P454
13.10		At4g26120	regulatory protein NPR1
13.07		At4g28420	tyrosine transaminase
13.00		At4g28350	receptor kinase-like protein
12.91	MYB39	At4g17785	MYB transcription factor like protein
12.60	RHA1A	At4g11370	RING-H2 finger protein
12.59	SKS9	At4g38420	putative pectinesterase
12.47		At3g29670	putatvie anthocyanin 5-aromatic acyltransferase
12.42	WRKY33	At2g38470	putative WRKY-type DNA binding protein
12.35	RAP2.6L	At5g13330	putative protein
12.25		At1g63560	unknown protein
12.22	BGLU46	At1g61820	putative beta-glucosidase
12.11		At5g02230	putative hydrolase
12.08		At1g61550	putative receptor kinase
12.06		At4g20830	reticuline oxidase

11.90		At2g38340	DREB-like AP2 domain transcription factor
11.79		At4g36430	peroxidase like protein
11.79	GLIP4	At3g14225	unknown protein
11.76	ALMT1	At1g08430	hypothetical protein
11.72		At5g47070	protein serine threonine kinase
11.44	ANAC102	At5g63790	putative protein
11.35		At3g28580	hypothetical protein
11.31		At4g15120	hypothetical protein
11.25		At5g66890	putative protein
11.17		At1g33590	hypothetical protein
11.17	EDA39	At4g33050	putative protein
11.14		At1g68850	peroxidase ATP23a
11.12		At2g42360	putative RING zinc finger protein
11.08	AtSerat2;1	At1g55920	serine acetyltransferase
11.08		At5g57510	unknown protein
10.94		At5g49690	putative anthocyanidin-3-glucoside rhamnosyltransferase
10.54		At2g32020	putative alanine acetyl transferase
10.53	ATMRP7	At3g13100	puative ABC transporter similar to AtMRP4
10.53	LOX1	At1g55020	putative lipoxygenase
10.51	BAP1	At3g61190	putative protein
10.50	ATGLR2.5	At5g11210	putative protein
10.43	PBP1	At5g54490	putative protein
10.36	ATCSLE1	At1g55850	putative cellulose synthase catalytic subunit
10.35	ASA1	At5g05730	anthranilate synthase component I-1 precursor
10.35		At1g33110	unknown protein
10.31		At5g13200	ABA-responsive protein
10.18		At1g78410	hypothetical protein
10.08	CYP71B6	At2g24180	putative cytochrome P451
10.01		At1g72920	virus resistance protein
10.00		At2g31945	unknown protein
9.98		At4g18990	xyloglucan endo-transglycosylase
9.97		At1g10700	phosphoribosyl diphosphate synthase
9.94		At1g35910	putative trehalose-phosphatase
9.94	STZ	At1g27730	salt-tolerance zinc finger protein
9.93	OPR1	At1g76690	12-oxophytodienoate reductase (OPR2)
9.88		At1g21520	hypothetical protein
9.84		At1g78820	glycoprotein(EP1)
9.81		At5g14730	putative protein
9.77		At1g66880	putative protein kinase
9.71		At1g13340	hypothetical protein
9.70		At2g43570	endochitinase isolog
9.70	ATERF-1	At4g17500	ethylene responsive element binding

			factor 1
9.68	WRKY46	At2g46400	putative WRKY-type DNA binding protein
9.63	BIP3	At1g09080	putative luminal binding protein
9.61		At4g20000	hypothetical protein
9.61		At3g47540	endochitinase
9.53	MIOX4	At4g26260	putative protein
9.50		At3g16150	putative L-asparaginase
9.41	MYB52	At1g17950	putative myb-like protein
9.40		At5g42830	N-hydroxycinnamoyl benzoyltransferase
9.40	ARK3	At4g21380	receptor-like serine/threonine protein kinase ARK3
9.22		At2g18690	unknown protein
9.17	TRP1	At5g17990	anthranilate phosphoribosyltransferase, chloroplast precursor
9.15	GLIP3	At1g53990	putative lipase
9.13		At4g26270	pyrophosphate-dependent phosphofructo-1-kinase
9.09	ATSBT3.5	At1g32940	subtilisin-like serine protease
9.09		At1g58420	hypothetical protein
9.01		At1g53270	hypothetical protein
9.00		At3g47380	putative protein
8.96	CYP81G1	At5g67310	cytochrome P450
8.93		At3g22910	calmodulin-stimulated calcium-ATPase
8.93		At1g44130	putative nucellin
8.90	AIR12	At3g07390	unknown protein
8.86		At5g13580	putative ABC transporter
8.86	MMP	At1g70170	putative matrix metalloproteinase
8.84		At5g10695	unknown protein
8.82	AGP5	At1g35230	hypothetical protein
8.79	TIR	At1g72930	flax rust resistance protein
8.79		At1g02310	(1-4)-beta-mannan endohydrolase precursor
8.78		At1g12200	unknown protein
8.75		At2g28400	hypothetical protein
8.63	HHP1	At5g20270	putative protein
8.60	THA1	At1g08630	unknown protein
8.58		At1g72940	disease resistance protein
8.58	ANAC092	At5g39610	NAM / CUC2
8.56	WRKY55	At2g40740	putative WRKY-type DNA binding protein
8.50	BAP2	At2g45760	hypothetical protein
8.50	NHL3	At5g06320	harpin-induced protein
8.35	PGP21	At3g62150	P-glycoprotein
8.34		At1g25400	unknown protein
8.29	WRKY48	At5g49520	putative protein

8.22	WRKY6	At1g62300	unknown protein
8.21		At2g23830	unknown protein
8.18	CYP79B2	At4g39950	cytochrome P450
8.15	ADC2	At4g34710	arginine decarboxylase SPE
8.14		At4g39670	putative protein
8.14		At5g25930	putative receptor-like kinase
8.07		At4g14450	hypothetical protein
8.06	UGT73B2	At4g34135	glucosyltransferase like protein
8.03		At3g23110	disease resistance protein
8.00		At2g16900	hypothetical protein
7.97	QRT3	At4g20050	putative protein
7.95		At1g65690	hypothetical protein
7.94	ATGPAT6	At2g38110	unknown protein
7.91		At5g53990	flavonol 3-O-glucosyltransferase-like protein
7.88		At5g48540	33 kDa secretory protein-like
7.88	CYP86B1	At5g23190	cytochrome P450
7.86		At4g18250	receptor serine/threonine kinase
7.86		At2g43590	putative endochitinase
7.81		At2g18140	putative peroxidase
7.81	ATGSTU2	At2g29480	putative glutathione S-transferase
7.79	ATGSTF3	At2g02930	putative glutathione S-transferase
7.76		At5g58120	resistance protein
7.74		At4g35420	putative protein
7.73		At4g08780	peroxidase C2 precursor
7.72	ANAC096	At5g46590	NAM-like
7.70	ATGPAT5	At3g11430	unknown protein
7.69		At1g66160	unknown protein
7.69		At1g08940	unknown protein
7.65		At4g22530	putative protein
7.63		At5g26920	calmodulin-binding
7.61	ATERF#011	At3g50260	putative protein
7.60	SS3	At1g74000	putative strictosidine synthase
7.60	PROPEP2	At5g64890	unknown protein
7.58	SULTR3;4	At3g15990	putative sulfate transporter
7.57		At1g79160	hypothetical protein
7.57		At2g43390	hypothetical protein
7.56		At4g36610	putative protein
7.55	LAC12	At5g05390	laccase (diphenol oxidase)
7.54	NPR3	At5g45110	regulatory protein NPR1-like
7.53		At1g35180	hypothetical protein
7.49		At1g05450	lipid-transfer protein
7.37		At4g35190	putative protein
7.36		At4g11340	putative protein
7.26	ADT4	At3g44720	putative chloroplast prephenate dehydratase
7.19	ATGSTU22	At1g78340	putative glutathione transferase

7.12	SIP1;2	At5g18290	putative protein
7.02		At5g59540	1-aminocyclopropane-1-carboxylate oxidase
6.99		At1g15045	hypothetical protein
6.97		At5g65140	trehalose-6-phosphate phosphatase
6.94		At1g55450	hypothetical protein
6.92		At4g04490	putative receptor-like protein kinase
6.91		At3g50400	putative protein
6.91	ATPP2-A11	At1g63090	unknown protein
6.90		At4g11170	RPP1-WsA-like disease resistance protein
6.89		At2g04400	putative indole-3-glycerol phosphate synthase
6.78		At3g13650	putative dirigent protein
6.75		At3g10340	putative phenylalanine ammonia-lyase
6.71		At1g05880	hypothetical protein
6.67		At1g21550	unknown protein
6.64	ATMRP13	At1g30410	putative ABC transporter
6.59		At1g28600	putative lipase
6.58	IAGLU	At4g15550	glucosyltransferase like protein
6.54	MYB107	At3g02940	putative MYB family transcription factor
6.53		At1g76520	unknown protein
6.49		At1g76700	putative DnaJ
6.48	NDB2	At4g05020	hypothetical protein
6.48	ASN1	At3g47340	glutamine-dependent asparagine synthetase
6.42		At3g44540	acyl CoA reductase
6.42		At5g57890	anthranilate synthase beta chain
6.42	ATGSTU7	At2g29420	putative glutathione S-transferase
6.37	MLO6	At1g61560	putative Mlo protein
6.35		At4g11470	serine/threonine kinase
6.34	TSA1	At3g54640	tryptophan synthase alpha chain
6.32		At1g70810	unknown protein
6.28	CIPK9	At1g01140	putative serine/threonine kinase
6.26		At5g10380	putative protein
6.22		At4g27280	putative protein
6.18		At2g23680	putative cold acclimation protein
6.17		At3g44550	putative acyl CoA reductase
6.14	CYP89A2	At1g64900	putative cytochrome P450
6.12	Apr-03	At4g21990	PRH26 protein
6.12	BON3	At1g08860	hypothetical protein
6.09		At5g52720	putative protein
6.05	MYB112	At1g48000	myb-related transcription factor
6.05	AtMYB78	At5g49620	myb-related transcription factor
6.02		At3g04640	hypothetical protein
6.00		At3g48450	hypothetical protein

5.99		At1g63720	hypothetical protein
5.95	PMI2	At1g66480	hypothetical protein
5.91	WRKY31	At4g22070	putative protein
5.91		At5g09530	periaxin
5.83	ATGSTU8	At3g09270	putative glutathione transferase
5.80		At5g40170	disease resistance protein
5.80	CLE3	At1g06225	CLE3, putative CLAVATA3/ESR-Related 3 (CLE3)
5.80	MYB54	At1g73410	putative myb-like transcription factor
5.79		At5g59530	1-aminocyclopropane-1-carboxylate oxidase
5.77	YLS5	At2g38860	unknown protein
5.77		At5g12930	putative protein
5.76		At3g27270	unknown protein
5.75		At5g12420	putative protein
5.75	WRKY56	At1g64000	putative WRKY DNA binding protein
5.75	ATSBT3.3	At1g32960	subtilisin-like serine protease
5.71		At4g21680	peptide transporter
5.69		At2g43620	putative endochitinase
5.69	WAK5	At1g21230	hypothetical protein
5.69	ATPCA	At3g49120	peroxidase
5.64	NAP	At1g69490	unknown protein
5.64		At1g76470	putative cinnamoyl CoA reductase
5.62		At1g10990	hypothetical protein
5.59	SEC1B	At4g12120	putative protein
5.56	NSL1	At1g28380	unknown protein
5.54	AtMYB41	At4g28110	putative transcription factor MYB41
5.52	ATAMT2	At2g38290	putative ammonium transporter
5.52		At1g64610	hypothetical protein
5.48		At3g22160	unknown protein
5.47	ATBZIP1	At5g49450	putative protein
5.45		At3g46110	putative protein
5.45		At2g42440	hypothetical protein
5.45	AOX1A	At3g22370	alternative oxidase 1a precurso
5.43	ATTAP2	At5g39040	putative ABC transporter
5.37		At5g08350	putative protein
5.36	ATGLR1.2	At5g48400	ligand-gated ion channel protein
5.36	ATCNGC19	At3g17690	hypothetical protein
5.35		At1g54540	hypothetical protein
5.35	COBL8	At3g16860	unknown protein
5.33		At3g53590	receptor kinase-like protein
5.28		At4g17215	unknown protein
5.27		At1g67000	putative receptor-like kinase
5.26		At1g59740	putative oligopeptide transporter
5.25	DIN9	At1g67070	putative phosphomannose isomerase
5.20		At1g62840	hypothetical protein
5.20	ATHCHIB	At3g12500	basic chitinase

5.20		At1g30700	putative reticuline oxidase
5.18	ATFH4	At1g24150	unknown protein
5.16	AtMYB63	At1g79180	putative myb-like transcription factor
5.16		At3g53510	putative ABC transporter
5.15		At5g19410	membrane transporter
5.12		At4g39830	putative L-ascorbate oxidase
5.09		At1g51420	unknown protein
5.07		At1g74010	putative strictosidine synthase
5.07		At5g47050	putative protein
5.06		At1g72680	putative cinnamyl-alcohol dehydrogenase
5.05		At1g68690	putative protein kinase
5.01		At2g44480	putative beta-glucosidase
5.01		At3g13430	unknown protein
5.01	AtRABA1g	At3g15060	ras-related GTP-binding protein
5.00		At1g08050	unknown protein
4.97		At4g19720	putative protein
4.97		At1g76070	hypothetical protein
4.95	ATMP2	At3g48890	putative progesterone-binding protein
4.95		At4g24130	putative protein
4.92	ATCDPK1	At1g18890	calcium-dependent protein kinase
4.90	LAC13	At5g07130	laccase
4.90		At4g39230	NAD(P)H oxidoreductase, isoflavone reductase
4.89		At3g05360	putative disease resistance protein
4.88		At5g22540	putative protein
4.84		At5g19240	putative protein
4.84	TSB2	At4g27070	tryptophan synthase beta-subunit (TSB2)
4.83		At3g09010	putative receptor ser/thr protein kinase
4.80	IAA10	At1g04100	putative IAA1 protein
4.70		At5g41040	N-hydroxycinnamoyl benzoyltransferase
4.70	ATEXLB1	At4g17030	allergen like protein
4.69		At1g67850	hypothetical protein
4.67	LACS7	At5g27600	long-chain-fatty-acid--CoA ligase
4.67		At3g07970	putative polygalacturonase
4.66		At4g25390	receptor kinase-like protein
4.65		At3g16330	unknown protein
4.65	CAX3	At3g51860	putative Ca2+/H+-exchanging protein
4.64		At5g13900	putative protein
4.62		At4g10500	putative Fe(II)/ascorbate oxidase SRG1 protein
4.59		At1g05340	unknown protein
4.59	UGT73D1	At3g53150	glucosyltransferase like protein
4.57		At2g16760	hypothetical protein
4.57	SUS3	At4g02280	putative sucrose synthetase

4.57		At5g07870	N-hydroxycinnamoyl benzoyltransferase
4.54		At3g12700	hypothetical protein
4.50	WRKY59	At2g21900	putative WRKY-type DNA binding protein
4.49		At4g24160	putative protein
4.45	ATMRP2	At2g34660	ABC transporter (AtMRP2)
4.45		At1g14130	dioxygenase-like protein
4.45		At4g20780	calcium-binding protein
4.42		At3g22620	hypothetical protein
4.41		At1g80160	hypothetical protein
4.41	ICS1	At1g74710	isochorismate synthase (icsI)
4.39		At2g47950	hypothetical protein
4.39	GLP4	At1g18970	putative germin
4.39		At2g05940	putative protein kinase
4.37		At5g14230	ankyrin - like protein
4.36	ATGSTU1	At2g29490	putative glutathione S-transferase
4.35		At2g38870	putative protease inhibitor
4.33		At5g06740	lectin-like protein kinase
4.31		At5g54170	membrane related protein
4.30	ATGLR1.3	At5g48410	ligand-gated ion channel protein
4.30		At1g06840	putative receptor kinase-like protein
4.29		At2g23420	unknown protein
4.29		At5g52710	unknown protein
4.29	SYP122	At3g52400	syntaxin-like protein
4.26		At4g15610	hypothetical protein
4.24		At1g67520	putative receptor kinase
4.23	CAT1	At1g20630	hypothetical protein
4.21	JAZ6	At1g72450	unknown protein
4.19		At3g62960	glutaredoxin
4.19	RALFL18	At2g33130	hypothetical protein
4.19	CYP86A2	At4g00360	putative cytochrome P450
4.19		At5g27760	putative protein
4.17		At1g74460	putative lipase/acylhydrolase
4.17		At3g44630	disease resistance protein
4.15		At5g45630	putative protein
4.13		At1g51890	light repressible receptor protein kinase
4.13		At4g27830	putative beta-glucosidase
4.13		At4g18360	glycolate oxidase
4.12		At2g03200	putative chloroplast nucleoid DNA binding protein
4.12		At5g55180	beta-1,3-glucanase-like protein
4.12		At2g43060	unknown protein
4.11	ATNEK5	At3g20860	putative serine/threonine protein kinase
4.11	SCPL28	At2g35770	putative serine carboxypeptidase II
4.10	XLG2	At4g34390	extra-large G-protein

4.08		At1g73480	lysophospholipase homolog
4.08		At1g56120	wall-associated kinase 2
4.08		At5g24090	acidic endochitinase
4.07		At1g67060	hypothetical protein
4.06		At4g34150	putative protein
4.05		At1g69840	unknown protein
4.05		At1g50740	unknown protein
4.03		At1g70930	putative homeobox protein
4.03	LACS2	At1g49430	putative acyl CoA synthetase
4.03		At3g22260	hypothetical protein
4.02	ATGPAT4	At1g01610	hypothetical protein
4.01		At2g37760	putative alcohol dehydrogenase
4.01		At3g43430	putative RING-H2 zinc finger protein ATL4
4.00		At5g09800	putative protein
3.98		At5g20910	ABI3-interacting protein 2
3.96		At3g15760	unknown protein
3.95	BCDH BETA1	At1g55510	branched-chain alpha-keto acid decarboxylase E1 beta subunit
3.94		At2g27080	unknown protein
3.93	ATATH6	At3g47780	ABC-type transport protein
3.92	GGT1	At4g39640	putative gamma-glutamyltransferase
3.91	CYP86A8	At2g45970	putative cytochrome P450
3.91	SCPL5	At1g73290	putative serine carboxypeptidase
3.91		At1g13990	unknown protein
3.91	AT-HSFA8	At1g67970	putative heat shock transcription factor
3.90	ANAC062	At3g49530	NAC2
3.90		At3g23570	unknown protein
3.89		At1g71695	peroxidase ATP4a
3.89	ATMKK9	At1g73500	putative MAP kinase
3.88		At5g14130	peroxidase ATP20a
3.88		At5g52810	putative protein
3.88		At3g50770	calmodulin-like protein
3.86		At4g14440	carnitine racemase like protein
3.84	AKN2	At4g39940	adenosine-5-phosphosulfate-kinase
3.82		At4g05030	hypothetical protein
3.82	CAD5	At4g34230	cinnamyl alcohol dehydrogenase - like protein
3.82		At2g39110	putative protein kinase
3.80	CYP72A13	At3g14660	putative cytochrome P452
3.80		At5g17650	glycine/proline-rich protein
3.79		At1g02360	putative chitinase
3.78	TOM20-1	At3g27070	TOM20
3.78		At5g13190	putative protein
3.77		At4g16000	hypothetical protein
3.73		At5g43760	beta-ketoacyl-CoA synthase

3.72		At1g56320	hypothetical protein
3.72	NIA2	At1g37130	putative nitrate reductase
3.71		At2g44230	hypothetical protein
3.70		At4g38540	monooxygenase 2 (MO2)
3.67		At4g15260	glucosyltransferase
3.67	ATCHIP	At3g07370	hypothetical protein
3.65	FDH	At2g26250	beta-ketoacyl-CoA synthase (FIDDLEHEAD)
3.63		At4g39720	putative protein
3.63		At5g59700	receptor-like protein kinase precursor
3.63	NDA2	At2g29990	putative NADH dehydrogenase (ubiquinone oxidoreductase)
3.62		At3g26470	unknown protein
3.61		At2g23540	putative GDSL-motif lipase/hydrolase
3.61		At5g66070	putative protein
3.60	AtSerat2;2	At3g13110	serine acetyltransferase (Sat-1)
3.60	ATNUDT10	At4g25440	putative protein
3.60		At2g45920	unknown protein
3.57	AST68	At5g10180	sulfate transporter
3.56		At4g21580	putative NADPH quinone oxidoreductase
3.55	ADH1	At1g77120	alcohol dehydrogenase
3.53	IAR3	At1g51780	auxin conjugate hydrolase (ILL5)
3.53	ProT2	At3g55740	proline transporter 2
3.53	MIOX2	At2g19800	unknown protein
3.52		At2g43670	putative beta-1,3-glucanase
3.51	AtMYB93	At1g34670	putative myb-like transcription factor
3.51	CYP72A15	At3g14690	putative cytochrome P453
3.50		At1g69790	putative protein kinase
3.50		At1g50590	pirin
3.50		At4g33540	putative protein
3.50		At1g22180	hypothetical protein
3.49	ZPR1	At2g45450	unknown protein
3.48	ANAC003	At1g02220	NAM (no apical meristem)-like protein
3.48		At1g78860	hypothetical protein
3.47		At5g19440	cinnamyl alcohol dehydrogenase - like protein
3.46		At1g67800	hypothetical protein
3.45		At1g31490	hypothetical protein
3.44	SYP121	At3g11820	putative syntaxin
3.43		At5g54860	putative protein
3.42		At4g08770	peroxidase C2 precursor
3.41		At1g74100	putative flavonol sulfotransferas
3.40	MP	At1g19850	transcription factor
3.39		At3g22600	unknown protein
3.39	FQR1	At5g54500	1,4-benzoquinone reductase-like
3.37	PGP11	At1g02530	hypothetical protein

3.36		At2g46750	unknown protein
3.36		At1g21590	hypothetical protein
3.36		At5g47710	putative protein
3.35		At1g22510	hypothetical protein
3.33	CYP86A4	At1g01600	putative cytochrome P450
3.33	SUS1	At5g20830	sucrose-UDP glucosyltransferase
3.32	LEJ1	At4g34120	putative protein
3.31		At5g01500	putative protein
3.31	CYP79B3	At2g22330	putative cytochrome P450
3.31		At4g19200	putative protein
3.30	AP4.3A	At2g32800	putative protein kinase
3.30		At1g49960	permease
3.27		At5g04760	I-box binding factor
3.26		At1g35190	hyoscyamine 6-dioxygenase hydroxylase
3.26		At1g75170	unknown protein
3.25		At2g02370	hypothetical protein
3.25		At5g01750	putative protein
3.25	ATL6	At3g05200	putative RING-H2 zinc finger protein ATL6
3.24	AAT	At2g22250	putative aspartate aminotransferase
3.23	GPDHC1	At2g41540	glycerol-3-phosphate dehydrogenase
3.23	AtMYB53	At5g65230	transcription factor-like protein
3.23		At5g09520	putative proline-rich protein surface protein
3.22		At3g53540	putative protein
3.22	EDA4	At2g48140	unknown protein
3.21		At1g21320	hypothetical protein
3.20	AT-HSFB3	At2g41690	putative heat shock transcription factor
3.20		At5g61820	putative protein
3.20		At3g13330	hypothetical protein
3.19		At4g19880	putative protein
3.18		At3g03660	hypothetical protein
3.17		At1g80520	hypothetical protein
3.17		At2g17220	putative protein kinase
3.16	ANAC010	At1g28470	putative NAM protein
3.15		At4g37900	putative protein
3.14		At5g48180	putative protein
3.13		At4g25900	possible apospory-associated
3.13	POP2	At3g22200	putative aminotransferase
3.12	ANAC053	At3g10500	unknown protein
3.12		At1g73800	unknown protein
3.11		At5g09480	PEE-rich protein
3.10		At1g42980	hypothetical protein
3.10		At4g33190	hypothetical protein
3.10		At5g46710	putative protein

3.10	ANAC089	At5g22290	NAM (no apical meristem)-like protein
3.10		At1g43910	unknown protein
3.09		At4g01700	putative chitinase
3.07		At1g13910	disease resistance protein
3.07		At5g57910	putative protein
3.07	ACR6	At3g01990	unknown protein
3.06		At4g34890	xanthine dehydrogenase
3.05		At5g37740	putative protein
3.05		At3g04370	hypothetical protein
3.05	SUC2	At1g22710	putative sucrose transport protein SUC2
3.04		At2g31880	putative receptor-like protein kinase
3.04		At3g62950	glutaredoxin
3.03		At1g78780	hypothetical protein
3.03		At1g47890	disease resistance protein
3.01		At1g25275	unknown protein
3.01	LACS9	At1g77590	putative acyl-CoA synthetase
3.01	ATMRP8	At3g13090	puative ABC transporter similar to AtMRP4
3.01	ANAC016	At1g34180	hypothetical protein
3.00	ATERF11	At1g28370	putative ethylene-responsive element binding factor
3.00		At1g19230	respiratory burst oxidase protein
2.99	XTR4	At1g32170	endoxyloglucan transferase
2.98		At4g22590	trehalose-6-phosphate phosphatase
2.98		At1g10690	unknown protein
2.96		At3g44190	putative protein
2.96		At2g23060	putative hookless1 (HLS1) like protein
2.96	NAK	At5g02290	serine/threonine-specific protein kinase NA
2.95	MYB109	At3g55730	MYB transcription factor like protein
2.94	ASP3	At5g11520	aspartate aminotransferase (Asp3)
2.93		At4g33925	unknown protein
2.93		At1g04220	putative beta-ketoacyl-CoA synthase
2.92		At1g15790	unknown protein
2.92		At5g52450	putative protein
2.92	ATGSTZ1	At2g02390	putative glutathione S-transferase
2.91	ACX1	At4g16760	putative acyl-CoA oxidase
2.90	AtMYB9	At5g16770	putative transcription factor MYB9
2.89	ADT6	At1g08250	hypothetical protein
2.88		At3g26070	unknown protein
2.88		At5g11650	lysophospholipase
2.88	LBD33	At5g06080	putative protein
2.87	BRL3	At3g13380	putative brassinosteroid receptor kinase
2.87	ALF5	At3g23560	unknown protein
2.86		At1g51620	putative protein kinase
2.85	GLP9	At4g14630	germin precursor oxalate oxidase

2.85		At3g57750	protein kinase
2.85		At1g14870	unknown protein
2.84		At5g19140	aluminium-induced protein
2.84	ETFQO	At2g43400	putative electron transfer flavoprotein ubiquinone oxidoreductase
2.83	IBR3	At3g06810	acetyl-coA dehydrogenase
2.83	ATEXO70E2	At5g61010	putative protein leucine zipper-containing protein
2.81		At3g48580	endoxyloglucan transferase
2.81	ATBZIP60	At1g42990	putative bZIP transcription factor
2.81	APS1	At3g22890	putative ATP sulfurylase
2.81	ATCLH2	At5g43860	AtCLH2 chlorophyllase
2.81	SPP2	At3g52340	unknown protein
2.80	AtNUDT7	At4g12720	growth factor protein
2.80	GDH1	At5g18170	glutamate dehydrogenase
2.80		At2g36470	unknown protein
2.79		At4g28400	protein phosphatase 2C-
2.79		At1g03220	unknown protein
2.79	ALDH7B4	At1g54100	aldehyde dehydrogenase
2.78		At4g21510	hypothetical protein
2.78	GSH2	At5g27380	glutathione synthetase
2.76	ATCWINV6	At5g11920	fructosidase
2.75	ATGR1	At3g24170	glutathione reductase
2.75		At1g04360	hypothetical protein
2.75		At5g27520	putative protein
2.73		At3g59660	putative protein
2.73		At4g33420	peroxidase ATP17a
2.72	ATSYTC	At5g04220	calcium lipid binding protein
2.72		At5g24810	putative ubiquinone biosyntheis protein AARF
2.72		At5g08240	putative protein
2.72		At5g44810	putative protein
2.71	GDH2	At5g07440	glutamate dehydrogenase 2
2.70	delta-OAT	At5g46180	ornithine aminotransferase
2.69		At1g53560	hypothetical protein
2.68		At1g53970	unknown protein
2.68		At5g17380	2-hydroxyphytanoyl-CoA lyase-like protein
2.66	UGT84B1	At2g23260	putative glucosyltransferase
2.66	J20	At4g13830	DnaJ-like protein
2.65	WRKY71	At1g29860	putative DNA-binding protein
2.64		At1g21010	unknown protein
2.63		At5g23240	putative protein
2.63	GAE5	At4g12250	nucleotide sugar epimerase
2.62		At3g52870	putative protein
2.61	SYP73	At3g61450	putative protein
2.60	SNAP33	At5g61210	snap25a

2.60	HB53	At5g66700	homeodomain transcription factor-like
2.60	FRS2	At2g32250	Mutator-like transposase
2.60		At1g62420	unknown protein
2.60	ATMKK2	At4g29810	MAP kinase kinase 2
2.59		At5g15870	putative protein
2.58	SKIP3	At2g02350	SKP1 interacting partner 3 (SKIP3)
2.57	ATGSTU19	At1g78380	putative glutathione transferase
2.55	ATATH1	At3g47730	ABC-type transport protein
2.54		At1g32520	unknown protein
2.51		At5g25940	nodulin
2.51		At3g47800	aldose 1-epimerase - like protein
2.50	MLO11	At5g53760	putative protein
2.50		At3g11210	unknown protein
2.49		At1g15170	hypothetical protein
2.49		At4g31960	hypothetical protein
2.49		At3g27880	hypothetical protein
2.48		At3g14780	hypothetical protein
2.47	ZFP5	At1g10480	zinc finger protein 5
2.46		At4g23880	hypothetical protein
2.46	ATOFP16	At2g32100	hypothetical protein
2.46	ABA3	At1g16540	hypothetical protein
2.46		At5g44550	putative protein
2.45		At2g37360	putative ABC transporter
2.44	ATKT1	At2g30070	high affinity K+ transporter (AtKUP1/AtKT1p)
2.44		At4g16640	proteinase
2.44		At3g54200	putative protein
2.43		At4g38080	putative protein
2.43	AtMYB32	At4g34990	MYB-like protein
2.41	DUR	At5g44480	putative protein
2.40		At5g17430	ovule development protein aintegumenta
2.40	ERD6	At1g08930	zinc finger protein ATZF1
2.40		At3g60450	putative protein prib5
2.40		At4g39540	shikimate kinase
2.40	MYB68	At5g65790	transcription factor-like protein
2.39		At4g37530	peroxidase
2.38		At5g41400	RING zinc finger protein
2.37	AAP6	At5g49630	amino acid permease 6
2.36		At2g34140	putative DOF zinc finger protein
2.36		At5g66390	peroxidase
2.35	ALDH3H1	At1g44170	aldehyde dehydrogenase
2.35		At1g28260	hypothetical protein
2.34		At2g47710	unknown protein
2.34		At2g21430	cysteine proteinase
2.33		At4g26240	putative protein
2.33		At2g17760	putative chloroplast nucleoid DNA

			binding protein
2.33	ANAC087	At5g18270	NAM (no apical meristem)-like protein
2.32		At3g28940	AIG2-like protein
2.32	ANAC041	At2g33480	putative NAM (no apical meristem)-like protein
2.31		At4g02550	hypothetical protein
2.31	IQD15	At3g49380	hypothetical SF16 protein
2.31	MEKK1	At4g08500	MEKK1/MAP kinase kinase kinase
2.31		At3g02070	unknown protein
2.31		At1g33490	unknown protein
2.30		At5g44580	unknown protein
2.30	LTI30	At3g50970	dehydrin Xero2
2.29	ATMRP1	At1g30400	glutathione S-conjugate transporting ATPase
2.28		At3g19200	hypothetical protein
2.27		At4g09670	AX110P -like protein
2.27		At3g05050	putative cyclin-dependent protein kinase
2.27		At2g33700	putative protein
2.27		At3g06780	hypothetical protein
2.27		At3g48020	hypothetical protein
2.27		At1g26450	hypothetical protein
2.27		At4g04800	putative transcriptional repressor
2.27		At1g76150	hypothetical protein
2.26	AIL6	At5g10510	ovule development protein
2.25	BIGYIN	At3g57090	hypothetical protein
2.25	DHAR2	At1g75270	putative GSH-dependent dehydroascorbate reductase 1
2.25		At1g17860	putative lemir (miraculin)
2.25	SULTR4;1	At5g13550	sulfate transporter
2.24	NFD4	At1g31470	hypothetical protein
2.24	AHA4	At3g47950	H+-transporting ATPase
2.24	AGP2	At2g22470	unknown protein
2.24		At4g21865	putative protein
2.24	CRCK3	At2g11520	putative protein kinase
2.24		At5g47530	putative protein
2.24	LPAT4	At1g75020	putative acyl-CoA:1-acylglycerol-3-phosphate acyltransferase
2.23		At1g23390	unknown protein
2.23	CSY2	At3g58750	citrate synthase
2.22		At1g26930	unknown protein
2.22		At5g50350	unknown protein
2.21		At1g14890	unknown protein
2.21	LHT1	At5g40780	amino acid permease
2.21		At1g48320	hypothetical protein
2.21		At2g48130	unknown protein
2.20	AtRABH1a	At5g64990	GTP binding protein-like
2.19		At4g39190	hypothetical protein

2.18		At1g10140	unknown protein
2.18		At1g79610	hypothetical protein
2.18		At4g24610	putative protein
2.18	AOC3	At3g25780	unknown protein
2.17		At2g29250	putative protein kinase
2.17	ATSTE14B	At5g08335	unknown protein
2.17		At3g14990	4-methyl-5(b-hydroxyethyl)-thiazole monophosphate biosynthesis protein
2.17		At1g65520	hypothetical protein
2.17	PR4	At3g04720	hevein-like protein precursor (PR-4)
2.17	ATMAMI	At5g54110	membrane associated protein
2.16		At1g48120	serine/threonine phosphatase PP7
2.15		At3g53180	nodulin / glutamate-ammonia ligase
2.15		At2g22300	unknown protein
2.15	VPS60.1	At3g10640	unknown protein
2.15		At1g78280	unknown protein
2.14		At4g33940	hypothetical protein
2.13	AtRABA1e	At4g18430	membrane-bound small GTP-binding protein
2.13		At5g25910	disease resistance protein
2.13		At3g03610	hypothetical protein
2.13	CPK29	At1g76040	putative calcium-dependent protein kinase
2.12		At3g12790	unknown protein
2.12		At3g02740	putative aspartyl protease
2.11	LRP1	At5g12330	lateral root primordia (LRP1)
2.11	ATGSTU13	At1g27130	glutathione transferase
2.11		At5g10300	alpha-hydroxynitrile lyase-like protein
2.10	PIL2	At3g62090	putative protein
2.10		At1g70520	putative protein kinase
2.09		At5g10830	embryonic abundant protein
2.09		At2g36440	hypothetical protein
2.09		At2g24200	putative leucine aminopeptidase
2.08		At1g04960	unknown protein
2.08		At1g09920	unknown protein
2.08		At5g45350	unknown protein
2.08		At3g03020	unknown protein
2.08		At5g52330	putative protein
2.07		At2g17500	unknown protein
2.07		At3g03150	unknown protein
2.07	RGLG2	At5g14420	putative protein copine I
2.07		At5g45280	pectin acetylesterase
2.06		At1g11200	hypothetical protein
2.06	ANAC047	At3g04070	NAM-like protein
2.06	PYK10	At3g03870	hypothetical protein
2.06		At3g56580	hypothetical protein
2.06		At4g23850	acyl-CoA synthetase

2.05		At2g37110	unknown protein
2.05	ANAC048	At3g04420	hypothetical protein
2.05		At5g48370	putative protein
2.05		At1g61080	hypothetical protein
2.05		At1g58842	virus resistance protein
2.04		At3g16220	hypothetical protein
2.04		At1g22900	putative disease resistance response protein
2.04	ADC1	At2g16500	arginine decarboxylase
2.04	AtMYB56	At5g17800	MYB factor family member
2.04	BT5	At4g37610	putative protein SPOP
2.03		At4g26910	putative dihydrolipoamide succinyltransferase
2.03	ATNUDT5	At2g04430	putative mutT domain protein
2.03	GBF6	At4g34590	bZIP transcription factor ATB2
2.03	ATGSTZ2	At2g02380	putative glutathione S-transferase
2.02		At1g02750	hypothetical protein
2.01	ZIF1	At5g13740	transporter-like protein
2.01		At1g47480	hypothetical protein
2.01		At3g22530	unknown protein

Appendix B. List of genes downregulated more than two-fold after treatment with gold

The following list shows the genes found to be downregulated more than two-fold after treatment with gold (as described in Chapter 4). Genes are listed in order of most to least downregulation compared to untreated plants. The gene titles are those with which the ATH1 microarray chip is annotated and as such, this may be incomplete as recent annotations may not have been included.

Fold change	Gene Title	Gene ID	Target Description
132.37	IRT1	At4g19690	Fe(II) transport protein
106.68		At5g46900	extA
67.59		At5g04950	nicotianamine synthase
55.75	ATNRT2:1	At1g08090	high-affinity nitrate transporter
55.55	AIR1	At4g12550	putative cell wall-plasma membrane disconnecting CLCT protein
43.24		At1g73120	hypothetical protein
38.4	IRT2	At4g19680	putative Fe(II) transport protein
37.15		At3g12900	hypothetical protein
32.79	AtMYB10	At3g12820	myb-related protein
32.52	ATGSTF14	At1g49860	putative glutathione S-transferase
30.77	CYP82C4	At4g31940	cytochrome P450
26.39		At3g61930	hypothetical protein
25.83		At5g04730	putative protein
25.63		At3g19430	putative late embryogenesis abundant protein
23.6	COPT2	At3g46900	copper transport protein
23.4		At3g45710	putative transport protein
23.29		At5g54370	root cap protein
23.17	MLP329	At2g01530	unknown protein
22.82		At5g03570	putative protein
21.63		At4g22460	extensin like protein
21.29	XTR8	At3g44990	xyloglucan endotransglycosylase
19.94	ATBHLH029	At2g28160	putative bHLH transcription factor
19.21		At3g18450	hypothetical protein
19.18	UGT72E1	At3g50740	UTP-glucose glucosyltransferase
18.98	GRF11	At1g34760	14-3-3 protein GF14omicron (grf11)
18.26		At3g24290	putative ammonium transporter
17.93	MTPA2	At3g58810	zinc transporter
16.84	DELTA-TIP2	At4g17340	membrane channel like protein
16.46		At1g33840	unknown protein
16.22		At5g19970	putative protein
15.33		At3g01260	putative aldose 1-epimerase
15.13		At1g52050	putative jasmonate inducible protein

14.96		At1g44050	unknown protein
14.84	FLA13	At5g44130	putative protein
14.78		At4g25790	putative pathogenesis-related protein
14.44		At5g15180	prx10 peroxidase
14.42		At1g32450	peptide transporter
14.4		At1g19900	unknown protein
14.35	AtMYB72	At1g56160	Myb-family transcription factor
14.29		At1g52060	putative jasmonate inducible protein
13.91		At2g21020	putative major intrinsic (channel) protein
13.8		At1g07560	putative protein kinase
13.74		At3g58060	putative protein
13.58		At5g47950	acetyl-CoA:benzylalcohol acetyltranferase
13.54		At5g60530	late embryonic abundant protein
13.44	CLC-B	At3g27170	CLC-b chloride channel protein
13.29	XTR9	At4g25820	putative xyloglucan endo-1,4-beta-D-glucanase
13.11	ATPAP7	At2g01880	putative purple acid phosphatase
13.03	GASA5	At3g02885	gibberellin-regulated family protein
13.01	SKS15	At4g37160	pectinesterase
13		At2g33790	putative proline-rich protein
12.65		At4g02270	hypothetical protein
12.55		At4g25250	putative protein
12.45		At5g35190	extensin like protein
12.38		At2g19970	putative pathogenesis-related protein
12.15	CYP71B2	At1g13080	putative cytochrome P450 monooxygenase
12		At5g57530	xyloglucan endotransglycosylase
11.69	ACPT	At2g23410	hypothetical protein
11.64	ATPT1	At5g43370	inorganic phosphate transporter
11.64		At5g67400	peroxidase
11.56		At5g62420	aldose reductase
11.56		At4g00680	putative actin-depolymerizing factor
11.48		At4g11190	putative disease resistance response protein
11.37	PAP8	At2g01890	putative purple acid phosphatase
11.36		At1g22500	RING-H2 zinc finger protein
11.22	MRH6	At2g03720	unknown protein
11.21		At1g74760	hypothetical protein
11.04	CKX4	At4g29740	cytokinin oxidase
11.01		At3g06460	unknown protein
10.88	ATGSTU20	At1g78370	glutathione S-transferase
10.79	AtTIP2;3	At5g47450	membrane channel protein-like
10.74		At3g59370	putative protein
10.6		At1g65570	putative polygalacturonase
10.47		At5g54040	CHP-rich zinc finger protein-like
10.25	PRP3	At3g62680	proline-rich protein

10.11		At1g05250	putative peroxidase
9.69	PIP1;5	At4g23400	PIP-like protein
9.63	AGP3	At4g40090	arabinogalactan-protein
9.61	MAM1	At5g23010	2-isopropylmalate synthase
9.58		At2g39040	putative peroxidase
9.56		At5g57540	xyloglucan endotransglycosylase
9.55		At5g58784	dehydrodolichyl diphosphate synthase
9.48		At5g59680	serine/threonine-specific protein kinase
9.47		At1g14190	putative mandelonitrile lyase
9.45		At5g51520	ripening-related protein
9.41	RAB7	At1g22740	RAS-related protein
9.4	ATCSLB05	At4g15290	cellulose synthase like protein
9.37		At3g14060	unknown protein
9.32		At5g37450	receptor protein kinase
9.31		At1g72200	RING-H2 zinc finger protein
9.28	CYP705A5	At5g47990	cytochrome P450
9.2		At1g50050	putative pathogenesis-related protein 1b precursor
9.15	RALFL27	At3g29780	unknown protein
9.12		At4g07820	putative pathogenesis-related protein
8.99		At3g49190	putative protein
8.94	DELTA-TIP	At3g16240	delta tonoplast integral protein (delta-TIP) i
8.92		At4g04460	putative aspartic protease
8.71	GH3.17	At1g28130	putative auxin-regulated GH3 protein
8.67		At1g34040	putative allinase
8.67		At5g19800	proline-rich protein extensins
8.62	CYP735A2	At1g67110	putative cytochrome P450
8.42		At3g51350	putative protein
8.37	TNY	At5g25810	transcription factor TINY
8.26	ATCEL5	At1g22880	putative endo-1,4-beta-D-glucanase
8.24		At3g01190	putative peroxidase
8.2		At5g26270	putative protein
8.17		At4g11210	putative disease resistance response protein
8.15	SKOR	At3g02850	stelar K+ outward rectifying channel
8.11		At3g21340	putative serine/threonine-specific protein kinase
8.08	HMT3	At3g22740	putative selenocysteine methyltransferase
8.04		At4g28850	xyloglucan endotransglycosylase
8.03	PIP2;4	At5g60660	membrane channel like protein
7.97		At1g51830	putative light repressible receptor protein kinase
7.96		At1g06120	putative delta 9 desaturase
7.96		At1g78260	RNA recognition motif
7.91		At5g38820	transporter -like protein

7.86		At4g11310	cysteine proteinase
7.85		At4g34580	putative protein
7.83	GLIP2	At1g53940	lipase
7.81	CYP83A1	At4g13770	cytochrome P450 monooxygenase
7.6		At2g43600	putative endochitinase
7.54	MYB111	At3g46130	Myb DNA binding protein
7.32		At3g20160	geranyl geranyl pyrophosphate synthase
7.29		At5g54790	unknown protein
7.2		At4g15390	HSR201 like protein
7.18	SCPL2	At1g73300	putative serine carboxypeptidase
7.16		At4g12510	pEARLI 1-like protein
7.16		At2g01900	putative inositol polyphosphate-5-phosphatase
7.13		At4g37150	hydroxynitrile lyase
7.13		At3g23800	selenium binding protein
7.02		At2g18800	putative xyloglucan endo-transglycosylase
7.02		At1g47600	putative thioglucosidase
6.98		At4g35030	protein kinase
6.97	CYP708A2	At5g48000	cytochrome P450
6.97		At3g29250	putative short-chain alcohol dehydrogenase
6.94	AGP22	At5g53250	putative protein
6.94		At5g01740	putative protein
6.89	AGP13	At4g26320	putative protein
6.81		At2g37540	putative oxidoreductase
6.79	SP1L4	At5g15600	nitrilase associated protein
6.77	ATGSTF11	At3g03190	glutathione S-transferase
6.75	ATPP2-A6	At5g45080	putative protein
6.73		At1g49310	hypothetical protein
6.59	PSAK	At1g30380	photosystem I subunit X precursor
6.54		At5g24410	6-phosphogluconolactonase
6.5		At3g51360	putative protein
6.48		At1g51850	putative light repressible receptor protein kinase
6.46		At3g61400	1-aminocyclopropane-1-carboxylate oxidase
6.46		At2g40230	putative anthranilate N-hydroxycinnamoyl/benzoyltransferase
6.44		At2g23620	putative acetone-cyanohydrin lyase
6.37		At2g28780	hypothetical protein
6.34		At3g46270	putative protein
6.33		At5g05500	unknown protein
6.29	ATCSLB01	At2g32610	putative cellulose synthase
6.25		At5g06630	putative protein
6.24	JAZ4	At1g48500	hypothetical protein
6.24	PSBR	At1g79040	putative photosystem II polypeptide

6.18		At3g45070	sulfotransferase-like protein
6.17	AGL79	At1g30260	hypothetical protein
6.14	ATCSLB02	At2g32620	putative cellulose synthase
6.08		At1g22550	peptide transporter
6.08		At1g49030	unknown protein
6.07		At1g14960	putative major latex protein
6.06		At2g37700	CER1-like protein
6.03		At1g49500	unknown protein
5.99		At1g09750	hypothetical protein
5.99		At4g33730	pathogenesis-related protein
5.99		At3g61410	putative protein
5.98		At4g15740	hypothetical protein
5.97		At3g11370	unknown protein
5.94		At2g28990	putative receptor-like protein kinase
5.89		At2g15830	unknown protein
5.85		At5g47980	acetyl-CoA:benzylalcohol acetyltranferase
5.83		At5g58010	putative protein
5.8	ATGSTU28	At1g53680	putative glutathione transferase
5.8		At5g06270	putative protein
5.79	TIP2	At3g26520	tonoplast intrinsic protein
5.77		At1g22335	putative glycine-rich RNA-binding protein
5.76		At1g30870	putative peroxidase
5.76		At4g20450	receptor protein kinase
5.76		At1g62560	unknown protein
5.75		At4g23890	putative protein
5.75		At4g27400	putative protein
5.74	SCPL34	At5g23210	serine carboxypeptidase II
5.71		At3g10710	putative pectinesterase
5.67		At3g58000	putative protein
5.63		At1g73600	putative phosphoethanolamine N-methyltransferase
5.6	MLO15	At2g44110	unknown protein
5.56		At2g43550	putative trypsin inhibitor
5.46	BCAT4	At3g19710	putative branched-chain amino acid aminotransferase
5.46		At4g08300	nodulin-like protein
5.46		At2g45180	unknown protein
5.39	GAMMA-TIP	At2g36830	putative aquaporin
5.39		At5g59260	receptor-like protein kinase
5.39		At1g51860	putative receptor-like protein kinase
5.36		At3g58990	3-isopropylmalate dehydratase-like protein (small subunit)
5.34		At5g48290	putative ATFP4
5.34		At5g66490	putative protein
5.33	CYP71B34	At3g26300	putative cytochrome P450
5.21		At3g18170	hypothetical protein

5.19	RAP2.11	At5g19790	AP2 domain containing protein RAP2.11
5.18		At1g01750	putative actin depolymerizing factor
5.17		At5g62330	putative protein
5.16		At1g21440	hypothetical protein
5.1	ATOCT3	At1g16390	putative transport protein
5.05		At5g45490	putative protein
5.04		At2g21045	senescence-associated protein
5.02	LAC7	At3g09220	putative laccase
5.01		At4g38970	putative fructose-bisphosphate aldolase
4.99		At1g74470	geranylgeranyl reductase
4.97		At3g56230	putative protein
4.95	ATHRGP1	At3g54590	extensin precursor
4.94	ANAC070	At4g10350	NAM/NAP like protein
4.94		At2g24980	unknown protein
4.93		At2g19060	putative GDSL-motif lipase/hydrolase
4.89		At1g48750	putative lipid transfer protein
4.89		At5g46040	peptide transporter
4.88	AGP24	At5g40730	putative protein
4.87	ATGH9C1	At1g48930	putative endo-1,4-beta-glucanase
4.87		At2g37440	unknown protein
4.87	PGR5	At2g05620	unknown protein
4.82	PSBO-1	At5g66570	33 kDa polypeptide of oxygen-evolving complex (OEC) in photosystem II
4.82		At3g48940	remorin
4.8	ATROPGEF4	At2g45890	hypothetical protein
4.8		At4g20820	reticuline oxidase
4.79	MAM-L	At5g23020	2-isopropylmalate synthase
4.79		At5g24313	unknown protein
4.78		At1g66800	putative cinnamyl alcohol dehydrogenase
4.77	CLE2	At4g18510	putative CLAVATA3/ESR-Related-2 (CLE2)
4.77		At5g27930	protein phosphatase
4.76		At3g01730	hypothetical protein
4.76		At5g24100	receptor-like protein kinase
4.75		At3g46370	receptor-like protein kinase
4.74		At3g29110	putative terpene synthase-related protein
4.74		At2g44380	unknown protein
4.71	SYP123	At4g03330	SYR1-like syntaxin
4.7		At5g44020	vegetative storage protein
4.69		At1g66930	putative receptor-like kinase
4.68	ANNAT3	At2g38760	putative annexin
4.67	XTH33	At1g10550	putative endoxyloglucan transferase
4.67		At5g26280	putative protein

4.65		At3g07720	unknown protein
4.63		At3g55310	beta-ketoacyl-ACP reductase
4.6		At1g07680	hypothetical protein
4.6	AtRABG2	At2g21880	putative RAS superfamily GTP-binding protein
4.6	MYB28	At5g61420	putative transcription factor MYB28
4.6		At3g22570	unknown protein
4.57	GA4H	At1g80340	gibberellin 3 beta-hydroxylase
4.57		At2g02680	hypothetical protein
4.56	ATEBP	At3g16770	AP2 domain containing protein RAP2.3
4.56		At3g45390	receptor-like protein kinase
4.55		At3g12540	hypothetical protein
4.55	CYP718	At2g42850	putative cytochrome P450
4.55	SCPL12	At2g22920	putative serine carboxypeptidase
4.54		At2g43535	unknown protein
4.54	LRX1	At1g12040	putative extensin
4.54		At5g16900	receptor protein kinase
4.53		At5g65320	putative protein
4.53		At5g06640	putative protein
4.52	CALS1	At1g05570	putative glucan synthase
4.52		At3g23730	putative xyloglucan endotransglycosylase
4.46	HMA3	At4g30120	cadmium-transporting ATPase
4.44		At4g30640	F-box protein family
4.44		At4g04840	putative protein
4.43		At5g62360	DC1.2 homologue
4.42		At4g30320	PR-1-like protein gene PR-1 protein - Medicago truncatula,Pir2:S47171
4.4		At3g02120	unknown protein
4.4		At4g21230	receptor kinase
4.38		At5g26010	protein phosphatase
4.37		At3g49930	zinc-finger-like protein
4.35		At5g35940	putative protein
4.34	CYP82F1	At2g25160	putative cytochrome P450
4.32		At5g42500	disease resistance response protein
4.32	HFR1	At1g02340	unknown protein
4.3		At5g58770	dehydrodolichyl diphosphate
4.29		At5g11790	putative protein
4.26		At2g41970	putative protein
4.26	ATRBOHB	At1g09090	putative respiratory burst oxidase protein
4.23	TUB1	At1g75780	tubulin beta-1 chain
4.23	GLTP2	At1g21360	unknown protein
4.22		At2g35585	unknown protein
4.22		At3g14280	unknown protein
4.21		At1g05700	putative light repressible receptor protein kinase

4.19	ATGSTU14	At1g27140	putative glutathione transferase
4.19	AGP14	At5g56540	putative protein
4.18	ATXTH17	At1g65310	putative xyloglucan endotransglycosylase
4.17	MRH1	At4g18640	putative protein
4.16		At1g33900	AIG1-like protein
4.15		At4g12030	putative transport protein
4.14		At3g01860	hypothetical protein
4.13	CYP705A13	At2g14100	putative cytochrome P450
4.11		At1g13300	unknown protein
4.1	ATPP2-A3	At2g26820	unknown protein
4.09	SCPL13	At2g22980	putative serine carboxypeptidase
4.09		At1g73340	steroid 22-alpha-hydroxylase
4.08		At1g11540	hypothetical protein
4.07	CYP709B3	At4g27710	cytochrome P450
4.06	MOT1	At2g25680	hypothetical protein
4.06		At4g29180	putative serine/threonine-specific receptor protein kinase
4.06	AST56	At1g77990	putative sulfate transporter
4.05		At3g07070	putative protein
4.05		At1g29020	unknown protein
4.04		At1g49450	putative En/Spm-like transposon protein
4.01		At1g25450	fatty acid condensing enzyme
4.01		At1g43650	nodulin-like protein
4		At5g06200	putative protein
4		At3g16560	unknown protein
3.99	ATGUS1	At5g61250	putative protein
3.99	GLTP3	At3g21260	unknown protein
3.98	IQD4	At2g26410	putative SF16 protein
3.97		At1g26250	unknown protein
3.96		At1g10810	putative auxin-induced protein
3.96	WRKY27	At5g52830	unknown protein
3.95		At2g27360	putative lipase
3.94		At3g27400	putative pectate lyase
3.93		At4g27030	putative protein
3.93		At4g02850	putative protein
3.91	FLA8	At2g45470	unknown protein
3.9	MLP43	At1g70890	major latex protein
3.9		At2g34810	putative berberine bridge enzyme
3.9		At5g45480	putative protein
3.9		At5g24290	putative protein
3.9	SQD2	At5g01220	putative protein
3.9	FLA6	At2g20520	putative surface protein
3.9	PKS1	At2g02950	unknown protein
3.89	ATSTS	At4g01970	putative raffinose synthase
3.89	AT4G13860	At4g13860	RNA-binding protein

3.88		At3g23190	unknown protein
3.87		At1g74770	hypothetical protein
3.87	LHCA2	At3g61470	Lhca2 protein
3.87	ATGH9B13	At4g02290	putative endo-1,4-beta glucanase
3.87		At1g13930	unknown protein
3.86		At4g25830	unknown protein
3.85		At2g14510	putative receptor-like protein kinase
3.84	GUN5	At5g13630	cobalamin biosynthesis protein
3.83		At4g25090	respiratory burst oxidase
3.82		At1g63450	hypothetical protein
3.82	AGD11	At3g07490	putative calmodulin
3.82		At3g25930	unknown protein
3.79	ATBZIP5	At3g49760	bZIP transcription factor
3.79		At3g27960	hypothetical protein
3.79	PKS2	At1g14280	putative phytochrome kinase substrate 1
3.78	MYB12	At2g47460	putative MYB family transcription factor
3.77		At1g66440	hypothetical protein
3.77	EXGT-A1	At2g06850	putative endoxyloglucan glycosyltransferase
3.75		At3g19030	hypothetical protein
3.75	LHCA3	At1g61520	putative PSI type III chlorophyll a/b-binding protein
3.74	AOP2	At4g03060	putative oxidoreductase
3.73		At1g30110	diadenosine 5,5-P1,P4-tetraphosphate hydrolase
3.73		At4g31840	putative protein
3.72		At1g33320	putative cystathionine gamma-synthase
3.71		At4g04750	putative sugar transporter
3.71		At3g46340	receptor-like protein kinase
3.71		At2g26500	unknown protein
3.69		At4g37550	formamidase
3.69		At5g24880	glutamic acid-rich protein
3.69	PSAF	At1g31330	putative photosystem I subunit III precursor
3.68	ATPC1	At4g04640	ATP synthase
3.67		At4g30420	nodulin-like protein
3.67		At4g38830	receptor-like protein kinase
3.65		At1g08500	unknown protein
3.64	ATGSTF13	At3g62760	glutathione transferase
3.64		At1g09400	putative 12-oxophytodienoate reductase
3.64	WRKY14	At1g30650	putative DNA-binding protein
3.63	PETC	At4g03280	putative component of cytochrome B6-F complex
3.62	AGP4	At5g10430	AtAGP4
3.62		At5g48900	pectate lyase

3.61		At1g65860	flavin-containing monooxygenase
3.61	ATPMEPCRF	At5g53370	pectinesterase
3.61	ATBZIP	At1g68880	putative bZIP transcription factor
3.61	FLA15	At3g52370	unknown protein
3.59	PSAE-2	At2g20260	putative photosystem I reaction center subunit IV
3.54	PIP1A	At3g61430	plasma membrane intrinsic protein
3.54		At3g59930	putative protein
3.53	CYP79F2	At1g16410	putative cytochrome P450
3.5	MT1C	At1g07610	metallothionein-like protein
3.49	ATCLC-A	At5g40890	anion channel protein
3.49		At3g56290	putative protein
3.49		At2g16980	putative tetracycline transporter protein
3.48	AZF1	At5g67450	Cys2/His2-type zinc finger protein 1
3.48		At4g16410	hypothetical protein
3.48	ATGLR2.1	At5g27100	ion channel
3.48	APE2	At5g46110	phosphate/triose-phosphate translocator precursor
3.48	FLA2	At4g12730	putative pollen surface protein
3.47		At5g25090	endosperm specific protein phytocyanin-related protein
3.46	AGP7	At5g65390	unknown protein
3.44		At3g46400	putative protein
3.44	MYB55	At4g01680	putative transcription factor
3.43		At1g57590	pectinacetylesterase precursor
3.42		At5g50140	ankyrin-like protein
3.42	CP12-1	At2g47400	putative chloroplast protein CP12
3.41		At2g42110	hypothetical protein
3.41	DRT112	At1g20340	putative plastocyanin
3.4	ATKC1	At4g32650	potassium channel
3.39	AOP1	At4g03070	putative oxidoreductase
3.38	XTR7	At4g14130	xyloglucan endotransglycosylase
3.37		At2g40480	hypothetical protein
3.36		At5g25830	GATA transcription factor
3.35	GL2	At1g79840	homeobox protein
3.35		At2g36090	hypothetical protein
3.35		At3g02640	unknown protein
3.34		At4g23800	98b like protein
3.34		At2g02620	hypothetical protein
3.34		At2g48080	unknown protein
3.33		At4g26220	caffeoyl-CoA O-methyltransferase
3.33		At3g05900	unknown protein
3.32		At1g11920	pectate lyase
3.31		At2g38320	hypothetical protein
3.31		At1g04610	putative dimethylaniline monooxygenase
3.31		At5g23840	putative protein

3.3	LHCA5	At1g45474	light-harvesting complex
3.3		At4g35060	putative protein
3.29		At2g21830	hypothetical protein
3.27		At4g16985	unknown protein
3.27	ATPP2-A8	At5g45070	putative protein
3.26		At3g50350	hypothetical protein
3.26		At3g07010	putative pectate lyase
3.26		At2g25060	unknown protein
3.26		At3g15950	unknown protein
3.25		At2g29995	unknown protein
3.25		At1g55430	hypothetical protein
3.25		At4g00700	putative phosphoribosylanthranilate transferase
3.24	ATCHX16	At1g64170	hypothetical protein
3.24		At3g16690	MtN3-like protein
3.24	ATPPC3	At3g14940	phosphoenolpyruvate carboxylase
3.24		At5g23750	putative protein
3.24		At1g52910	unknown protein
3.23		At3g23870	unknown protein
3.22		At5g01060	putative protein - kinase
3.22		At2g20030	putative RING zinc finger protein
3.22		At1g49320	unknown protein
3.21		At5g48010	cycloartenol synthase
3.21	MYB59	At5g59780	MYB27 protein
3.21		At1g09170	putative kinesin
3.21		At3g45700	putative transport protein
3.21		At2g17300	unknown protein
3.19	LPAT3	At1g51260	putative acyl-CoA : 1-acylglycerol-3-phosphate acyltransferase
3.19	CYCP4;1	At2g44740	putative PREG1-like negative regulator
3.18		At5g08050	putative protein
3.17		At3g52110	putative protein
3.17		At1g30900	putative vacuolar sorting receptor
3.17		At2g17590	unknown protein
3.16	ATPUP4	At1g30840	hypothetical protein
3.16		At4g11530	serine/threonine kinase
3.15		At4g24670	putative alliin lyase alliin lyase
3.15		At5g22890	putative protein
3.15		At5g07780	putative protein
3.15	SUM3	At5g55170	ubiquitin-like protein
3.14		At2g40150	unknown protein
3.14		At3g25790	unknown protein
3.13		At5g42250	alcohol dehydrogenase
3.13	PIFI	At3g15840	unknown protein
3.12	AT-HSFC1	At3g24520	heat shock transcription factor
3.11		At4g14780	kinase like protein

3.11		At4g23070	putative membrane protein
3.11		At1g51790	receptor protein kinase
3.1		At5g44770	CHP-rich zinc finger protein-like
3.1		At4g40070	putative protein
3.09	BGAL4	At5g56870	beta-galactosidase
3.09	CIPK13	At2g34180	putative protein
3.08	TUB5	At1g20010	putative beta tubulin 1
3.08	PSAD-1	At4g02770	putative photosystem I reaction center subunit II precursor
3.08		At5g26820	putative protein
3.08	ATROPGEF6	At3g55660	putative protein
3.08		At5g14020	unknown protein
3.06		At1g72300	putative leucine-rich receptor-like protein kinase
3.06	WAG2	At3g14370	putative protein
3.05		At4g03500	hypothetical protein
3.05		At1g54500	putative rubredoxin
3.05		At3g62780	shock protein
3.04	HPR	At1g68010	hydroxypyruvate reductase
3.04	ASL9	At1g16530	hypothetical protein
3.04		At1g63100	putative transcription factor SCARECROW
3.03		At3g19320	unknown protein
3.02		At4g13440	hypothetical protein
3.02		At2g37820	hypothetical protein
3.01		At1g02300	cathepsin B-like cysteine protease
3.01	NRAMP1	At1g80830	metal ion transporter
3.01		At5g64110	peroxidase
3.01		At3g07900	putative auxin-independent growth promoter
3.01	ACA4	At2g41560	putative Ca2+-ATPase
3.01		At2g42320	unknown protein
3		At4g30670	unknown protein
3		At1g72120	oligopeptide transporter
3	CYP704A2	At2g45510	putative cytochrome P450
2.99		At5g03555	unknown protein
2.99		At4g27860	putative protein
2.99		At5g55520	putative protein
2.99		At3g04320	putative trypsin inhibitor
2.99	TET12	At5g23030	senescence-associated protein
2.98		At2g22190	putative trehalose-6-phosphate phosphatase
2.97	GAPA	At3g26650	glyceraldehyde 3-phosphate dehydrogenase A subunit
2.97		At5g36270	putative GSH-dependent dehydroascorbate reductase 2
2.97	AtRABH1d	At2g22290	putative GTP-binding protein
2.96		At1g72160	cytosolic factor

2.96		At3g54580	extensin precursor
2.96		At1g34510	peroxidase
2.96		At4g35320	putative protein
2.95	WAK4	At1g21210	hypothetical protein
2.95		At1g62510	unknown protein
2.95	PMI1	At1g42550	unknown protein
2.94		At1g78120	hypothetical protein
2.94	IMK2	At3g51740	putative protein
2.93		At1g23140	unknown protein
2.92	CESA2	At4g39350	cellulose synthase catalytic subunit (Ath-A)
2.92		At1g14345	unknown protein
2.91	LAC8	At5g01040	laccase
2.9		At3g07000	hypothetical protein
2.9	PSBX	At2g06520	hypothetical protein
2.89		At3g46720	glucuronosyl transferase
2.89	PDC3	At5g01320	pyruvate decarboxylase
2.88	LHCB5	At4g10340	chlorophyll a/b-binding protein
2.87		At1g01430	hypothetical protein
2.87		At5g49870	myrosinase binding protein
2.87	TOE1	At2g28550	putative AP2 domain transcription factor
2.87		At3g59340	putative protein
2.87	PLE	At5g51600	putative protein
2.86		At5g64850	putative protein
2.86		At2g16270	unknown protein
2.85		At4g37470	putative protein
2.85		At1g15290	unknown protein
2.84	PIP1C	At1g01620	plasma membrane intrinsic protein
2.83		At1g09390	putative lipase
2.83		At2g28970	putative receptor-like protein kinase
2.83		At3g16180	putative transport protein
2.82	GATL6	At4g02130	putative glycosyl transferase
2.82		At1g16440	putative protein
2.81	GS2	At5g35630	glutamate-ammonia ligase precursor
2.81	RCA	At2g39730	hypothetical protein
2.81		At1g61930	hypothetical protein
2.81		At5g15290	putative protein
2.81		At3g57020	putative protein
2.81		At2g34940	putative vacuolar sorting receptor
2.8	BGAL10	At5g63810	beta-galactosidase
2.8		At1g64910	putative rhamnosyltransferase
2.79		At5g43040	CHP-rich zinc finger protein-like
2.79	ATNRT2.4	At5g60770	high-affinity nitrate transporter
2.78		At2g26360	putative mitochondrial carrier protein
2.77		At4g17870	putative protein
2.77	ATEXO70H1	At3g55150	putative protein

2.77	SULTR1;1	At4g08620	putative sulfate transporter
2.75		At3g47220	1-phosphatidylinositol-4,5-bisphosphate
2.75		At2g36210	hypothetical protein
2.75		At3g51280	MS5-like protein
2.75		At2g39180	putative protein
2.75	SIGE	At5g24120	sigma-like factor
2.75		At1g30690	unknown protein
2.74		At1g64380	AP2-containing DNA-binding protein
2.74	HIK	At1g18370	kinesin heavy chain isolog
2.74		At1g07550	putative protein kinase
2.74		At3g03680	putative phosphoribosylanthranilate transferase
2.74	MEE16	At2g18650	putative RING zinc finger protein
2.74		At1g69080	unknown protein
2.73	LHCA1	At3g54890	chlorophyll a/b-binding protein
2.73	ATGH9B7	At1g75680	putative endo-1,4-beta-glucanase
2.73		At1g24530	hypothetical protein
2.73		At1g68570	peptide transporter
2.73	SCPL4	At1g73310	putative serine carboxypeptidase
2.72	CYC1	At4g37490	cyclin cyc1
2.72	AtMYB19	At5g52260	putative protein
2.71	AK-HSDH	At1g31230	putative aspartate kinase-homoserine dehydrogenase
2.7	BGAL6	At5g63800	beta-galactosidase
2.7		At1g34355	hypothetical protein
2.69	LBD25	At3g27650	hypothetical protein
2.68	ACP4	At4g25050	acyl carrier
2.68		At3g54260	putative protein
2.67		At3g47040	beta-D-glucan exohydrolase
2.67		At3g21190	unknown protein
2.67		At3g06070	unknown protein
2.66	CYP705A25	At1g50560	putative cytochrome P450
2.66	PSBY	At1g67740	F12A21.13 putative photosystem II Core Complex
2.66		At1g06640	putative oxidoreductase
2.66	PATL2	At1g22530	unknown protein
2.65	COR78	At5g52310	low-temperature-induced protein
2.65		At1g20650	putative protein kinase
2.65		At2g21540	putative phosphatidylinositol phophatidylcholine transfer protein
2.65		At2g03370	unknown protein
2.64	CBL8	At1g64480	calcineurin B-like protein
2.64		At1g22570	peptide transporter
2.63	DHAR1	At1g19570	putative GSH-dependent dehydroascorbate reductase 1
2.63		At3g28130	unknown protein
2.62		At3g23510	putative cyclopropane-fatty-acyl-

			phospholipid synthase
2.62	GA4	At1g15550	putative gibberellin 3 beta-hydroxylase
2.62		At1g72250	putative kinesin
2.62		At1g64500	peptide transporter
2.61	COBL9	At5g49270	putative protein
2.61	ATROPGEF11	At1g52240	unknown protein
2.6		At5g08020	replication factor
2.6		At3g20460	putative sugar transporter
2.59	CYP705A4	At4g15380	cytochrome P450
2.59		At3g46710	disease resistance protein
2.59		At2g02020	putative peptide/amino acid transporter
2.59		At3g56080	putative protein
2.59	ATOCT6	At1g16370	putative transport protein
2.58		At4g14980	hypothetical protein
2.58	FLA1	At5g55730	putative protein
2.57	RPS17	At1g79850	30S ribosomal protein S17,
2.57		At1g36060	putative AP2 domain transcription factor
2.57		At2g45590	putative protein
2.57	ATFRO3	At1g23020	putative superoxide-generating NADPH oxidase
2.56	ATPDIL1-3	At3g54960	protein disulfide-isomerase
2.56		At5g03140	receptor like protein kinase
2.55		At1g23560	unknown protein
2.55	MRLK	At3g56100	putative protein
2.55		At3g25290	unknown protein
2.54	ATPDR2	At4g15230	ABC transporter
2.54	ENDO5	At4g21600	putative endonuclease
2.54		At1g01780	LIM domain protein
2.54	FLA16	At2g35860	unknown protein
2.54		At5g04860	unknown protein
2.54		At2g05310	unknown protein
2.53		At3g06990	hypothetical protein
2.53		At1g72360	putative AP2 domain transcription factor
2.53		At4g24580	putative protein
2.52	RPL12-A	At3g27850	50S ribosomal protein L12-C
2.5		At1g07730	disease resistance response protein
2.5	PSBO-2	At3g50820	putative protein
2.49	PPCK2	At3g04530	phosphoenolpyruvate carboxylase kinase
2.49	PSAH-1	At3g16140	photosystem I subunit VI precursor
2.49		At1g73170	putative ATPase
2.49	SRF7	At3g14350	putative leucine-rich repeat transmembrane protein
2.49		At5g01520	putative protein

2.49		At3g46810	putative protein
2.49		At5g45650	subtilisin-like protease
2.48	CYCD3;1	At4g34160	cyclin delta-3
2.48	CYP71A16	At5g42590	cytochrome P450
2.48	EIF-5A	At1g13950	initiation factor
2.48		At5g25020	putative protein
2.47		At5g23400	disease resistance protein
2.47		At1g09200	unknown protein
2.47		At5g05400	NBS/LRR disease resistance protein
2.46		At5g02000	hypothetical protein
2.46	CYCA1;1	At1g44110	putative mitotic cyclin a2-type
2.46		At3g16350	putative MYB family transcription factor
2.46		At1g77630	unknown protein
2.45		At1g74940	hypothetical protein
2.45		At3g12870	hypothetical protein
2.45		At4g09420	putative protein
2.45		At2g35000	putative RING zinc finger protein
2.45		At1g31950	terpene synthase family protein
2.43		At1g70370	putative aromatic rich glycoprotein
2.43		At1g62660	beta-fructosidase
2.43		At4g26770	putative CDP-diacylglycerol synthetase
2.43		At3g11550	unknown protein
2.43		At1g23030	unknown protein
2.42	TOE2	At5g60120	APETALA2 protein
2.42		At1g01300	putative chloroplast nucleoid DNA binding protein
2.42		At2g37780	hypothetical protein
2.42	ATCEL3	At1g71380	putative beta-glucanase
2.41		At3g51540	putative protein
2.41	UGT2	At1g05530	putative UDP-glucose:indole-3-acetate beta-D-glucosyltransferase
2.4	WRKY69	At3g58710	DNA-binding WRKY - like protein
2.4		At1g13830	hypothetical protein
2.4		At1g04900	hypothetical protein
2.4		At3g61380	putative protein
2.39		At2g28460	hypothetical protein
2.39	PYK10	At3g09260	thioglucosidase 3D precursor
2.38		At4g15830	hypothetical protein
2.38	RIC10	At4g04900	hypothetical protein
2.38	GATL3	At1g13250	hypothetical protein
2.38		At5g02370	kinesin
2.38		At2g28960	putative receptor-like protein kinase
2.38		At2g36570	putative receptor-like protein kinase
2.38	GT2	At1g76890	trihelix DNA-binding protein
2.38	ZW9	At1g58270	unknown protein

2.37		At3g27330	hypothetical protein
2.37		At3g15560	hypothetical protein
2.37		At1g51280	hypothetical protein
2.37	ANT	At4g37750	ovule development protein aintegumenta (ANT)
2.36	AGP18	At4g37450	putative protein
2.36		At5g45500	putative protein
2.35		At5g42840	CHP-rich zinc finger protein-like
2.35	ATROPGEF12	At1g79860	hypothetical protein
2.35		At3g54400	nucleoid DNA-binding
2.35	CYCB1;3	At3g11520	putative cyclin
2.35	ATCSLA07	At2g35650	putative glucosyltransferase
2.35		At3g05150	putative sugar transporter
2.35	SCPL20	At4g12910	serine carboxypeptidase I precursor
2.35		At4g10550	subtilisin-like serine protease
2.35	AGP26	At2g47930	unknown protein
2.34		At1g72430	hypothetical protein
2.34		At1g05440	hypothetical protein
2.34		At3g16460	putative lectin
2.34		At3g57780	putative protein
2.34		At5g25820	putative protein
2.34		At4g25160	putative serine/threonine protein kinase
2.34	STR16	At5g66040	senescence-associated protein
2.33		At3g03130	hypothetical protein
2.33	SNRK2-7	At4g40010	putative serine/threonine protein kinase
2.33		At1g48070	unknown protein
2.33		At2g17710	unknown protein
2.32	CYP71B26	At3g26290	putative cytochrome P450
2.32	ANTR2	At4g00370	hypothetical protein
2.32		At1g30850	hypothetical protein
2.32	PFN1	At2g19760	profilin 1
2.31	AMP1	At3g54720	Peptidase
2.31	IAMT1	At5g55250	S-adenosyl-L-methionine:salicylic acid carboxyl methyltransferase
2.31		At3g06750	unknown protein
2.3		At1g60270	putative beta-galactosidase
2.3	STP1	At1g11260	glucose transporter
2.3	PSY	At5g17230	phytoene synthase
2.3		At5g61350	receptor-like protein kinase
2.3		At1g32740	unknown protein
2.29	COR47	At1g20440	hypothetical protein
2.29		At1g76220	hypothetical protein
2.29	ZCF125	At1g59540	kinesin motor protein
2.29	NPH3	At5g64330	non-phototropic hypocotyl 3
2.29	UGT84A2	At3g21560	putative UDP-glucose:indole-3-acetate beta-D-glucosyltransferase

2.29		At1g79910	unknown protein
2.29		At1g56720	unknown protein
2.28		At5g06490	C3HC4-type RING zinc finger protein
2.28	LHCB3	At5g54270	Lhcb3 chlorophyll a/b binding protein
2.27		At5g15900	putative protein
2.27		At3g24190	unknown protein
2.27		At3g01690	unknown protein
2.26		At5g33280	chloride channel-like protein
2.26	MGD2	At5g20410	monogalactosyldiacylglycerol synthase
2.26		At2g37420	putative kinesin heavy chain
2.26		At2g37660	unknown protein
2.25		At3g49360	6-phosphogluconolactonase
2.25		At3g25950	hypothetical protein
2.24	ATCSLD5	At1g02730	hypothetical protein
2.24		At1g14240	putative nucleoside triphosphatase
2.24		At5g16250	putative protein
2.24		At5g16730	putative protein
2.24		At4g34500	putative serine/threonine protein kinase
2.24		At2g29630	putative thiamin biosynthesis protein
2.24		At1g78020	unknown protein
2.23		At5g01530	chlorophyll a/b-binding protein
2.23		At5g42690	putative protein
2.23		At1g08310	unknown protein
2.22	ATATH5	At3g47770	ABC-type transport protein
2.22		At2g33560	hypothetical protein
2.22	SIGF	At2g36990	putative RNA polymerase sigma-70 factor
2.22	CPN60B	At1g55490	Rubisco subunit binding-protein
2.22		At2g12400	unknown protein
2.22	ATMAP65-6	At2g01910	unknown protein
2.22		At2g47440	unknown protein
2.21		At1g03470	hypothetical protein
2.21		At1g08325	putative leucine zipper protein
2.21	SCPL51	At2g27920	putative carboxypeptidase
2.21		At5g03230	putative protein
2.21	TUB6	At5g12250	tubulin beta-6 chain
2.2		At4g35040	putative protein
2.2		At4g18610	putative protein
2.2		At1g76020	unknown protein
2.19	ATCNGC9	At4g30560	cyclic nucleotide and calmodulin-regulated ion channel
2.19		At5g14450	early nodule-specific protein
2.19	ATGLR3.5	At2g32390	putative ligand-gated ion channel subunit
2.18		At4g22110	alcohol dehydrogenase
2.18		At4g14760	centromere protein homolog

2.18		At4g31875	unknown protein
2.18		At2g27660	hypothetical protein
2.18	HKT1	At4g10310	potassium uptake transporter
2.18		At3g58100	putative protein
2.18		At2g45820	remorin
2.18		At2g02960	unknown protein
2.17		At4g29360	beta-1,3-glucanase-like protein
2.17	MVA1	At4g11820	hydroxymethylglutaryl-CoA synthase
2.17	ATBAG1	At5g52060	putative protein
2.17	YSL6	At3g27020	unknown protein
2.17	LYM1	At1g21880	unknown protein
2.16	ATOPT7	At4g10770	putative oligopeptide transporter
2.16	WRKY35	At2g34830	putative WRKY-type DNA binding protein
2.16		At2g22125	unknown protein
2.15		At1g14290	putative acid phosphatase
2.15	CLA1	At4g15560	DEF (CLA1) protein
2.15		At3g06890	hypothetical protein
2.15		At5g49990	permease
2.15		At5g66330	putative protein
2.14	ATHB-16	At4g40060	putative homeodomain protein
2.14	MK	At5g27450	mevalonate kinase
2.14	PSB28	At4g28660	photosystem II protein W
2.14	ATMAP70-5	At4g17220	putative protein
2.14		At1g17970	zinc-finger protein
2.13		At1g31180	putative 3-methyladenine DNA glycosylase
2.13	CIP7	At4g27430	COP1-interacting protein 7 (CIP7)
2.13	CYCB2;4	At1g76310	putative cyclin
2.13		At2g23530	hypothetical protein
2.13	C/VIF2	At5g64620	invertase inhibitor
2.13		At4g38390	putative growth regulator protein
2.13		At4g23870	putative protein
2.13	AIR9	At2g34680	unknown protein
2.13	GASA1	At1g75750	unknown protein
2.12		At3g20810	hypothetical protein
2.12		At3g10310	kinesin
2.12	Sep-01	At4g34190	putative protein
2.12		At1g70460	putative protein
2.12		At1g63050	unknown protein
2.12		At1g54780	unknown protein
2.11		At2g44640	hypothetical protein
2.11	CRB	At1g09340	putative RNA-binding protein
2.11		At1g17100	SOUL-like protein
2.11		At4g26880	STIG1 like protein
2.11	ATXTH20	At5g48070	xyloglucan endo-1,4-beta-D-glucanase

2.1		At4g32260	H+-transporting ATP synthase
2.1		At1g55390	hypothetical protein
2.1	IRE	At5g62310	IRE (root hair elongation)
2.1		At1g31420	putative protein kinase
2.1		At3g51720	putative protein
2.1		At5g49800	unknown protein
2.09	AtGH9B1	At1g70710	endo-1,4-beta-glucanase
2.09		At4g01050	hypothetical protein
2.09	ATPAO5	At4g29720	putative protein
2.09		At2g34330	unknown protein
2.09		At2g35470	unknown protein
2.08		At1g66280	putative beta-galactosidase
2.08	AtTLP8	At1g16070	hypothetical protein
2.08	ATK5	At4g05190	kinesin
2.08		At4g05590	putative protein
2.08		At4g12600	Ribosomal protein
2.07		At1g37607	putative axi 1 protein
2.07		At1g59725	putative chaperone
2.07	PGSIP2	At1g77130	hypothetical protein
2.07	SKS1	At4g25240	Pollen-specific protein precursor
2.07	ATNEK6	At3g44200	protein kinase
2.07	LHCB4.2	At3g08940	putative chlorophyll a/b-binding protein
2.07	WRKY60	At2g25000	putative WRKY-type DNA binding protein
2.06		At3g13470	putative chaperonin 60 beta
2.06	BEL10	At1g19700	putative homeodomain protein
2.06	EMB3012	At5g40480	nuclear pore protein
2.06		At5g19730	pectin methylesterase
2.06		At2g16990	putative tetracycline transporter protein
2.06		At3g45330	receptor-like protein kinase
2.06		At2g29660	unknown protein
2.05		At1g80170	putative polygalacturonase
2.05		At1g27210	unknown protein
2.04	ATPRX Q	At3g26060	putative peroxiredoxin
2.04	PIP2;8	At2g16850	putative plasma membrane intrinsic protein
2.04		At5g04810	putative protein
2.04		At5g16230	stearoyl-acyl carrier protein
2.04	MEE11	At2g01620	unknown protein
2.03	VHA-E3	At1g64200	H+-transporting ATPase
2.03		At3g48080	hypothetical protein
2.03	PLA IIB	At2g39220	unknown protein
2.02		At3g13560	putative glucan endo-1,3-beta-glucosidase precursor
2.02	BLH1	At2g35940	putative homeodomain transcription factor

Appendix B. List of genes downregulated more than two-fold after treatment with gold

2.02	AFR	At2g24540	unknown protein
2.02	ENT1,AT	At1g70330	unknown protein
2.02		At1g30130	unknown protein
2.02		At1g03210	unknown protein
2.01		At5g13840	cell cycle switch protein
2.01	CYP81D4	At4g37330	cytochrome P450
2.01		At4g08400	hydroxyproline-rich glycoprotein precursor
2.01	BAM2	At3g49670	receptor protein kinase
2.01		At1g76450	unknown protein
2.01		At3g15480	unknown protein
2		At4g27700	hypothetical protein
2	ATEXO70C1	At5g13150	putative protein
2		At1g52220	unknown protein
2		At3g06770	unknown protein

Abbreviations

½MS(A)(S)	Murashige and Skoog basal salt medium - half strength (with 8 g/L agar) (with 20 mM sucrose)
AAS	Flame atomic absorption spectroscopy
ANOVA	Analysis of variance
bHLH	Basic helix-loop-helix
BLASTP	Basic local alignment search tool - protein
CaMV 35S	Cauliflower mosaic virus 35S promoter
CDF	Cation diffusion facilitator
cDNA	Complementary cDNA
Col-0	*Arabidopsis thaliana* ecotype Columbia-0
COPT	Copper transport protein
CTR	Copper transport protein
dNTP	Dinucleotide triphosphate
EDTA	Ethylenediaminetetraacetic acid
EDX	Energy-dispersive X-ray spectroscopy
EXAFS	Extended X-ray absorption fine structure
GO	Gene ontology
GST	Glutathione transferase
GT	Glucosyl transferase
HMA	Heavy metal ATPase
ICP-MS	Inductively coupled plasma mass spectroscopy
ICP-OES	Inductively coupled plasma optical emission spectrometry
IRT	Iron regulated transporter
MTP	Metal tolerance proteins
NADH	Nicotinamide adenine dinucleotide
NASC	Nottingham Arabidopsis Stock Centre
NIP	NOD26-like intrinsic proteins
NRAMP	Natural resistance associated macrophage proteins
PCR	Polymerase chain reaction
PIP	Plasma membrane intrinsic protein
qPCR	Real-time (quantitative) PCR
RNA	Ribonucleic acid
SD	Standard deviation
SIP	Small basic intrinsic proteins

TAIR	The Arabidopsis Information Resource
TEM	Transmission electron microscopy
TIP	Tonoplast intrinsic protein
Tris	2-amino-2-hydroxymethyl-1,3-propanediol
XANES	X-ray near edge absorption spectroscopy
XAS	X-ray absorption spectroscopy
YSL	Yellow stripe1-like
ZIP	ZRT, IRT-like protein

References

Abad, A., P. Concepcion, A. Corma and H. Garcia (2005). A collaborative effect between gold and a support induces the selective oxidation of alcohols. *Angewandte Chemie-International Edition* **44**(26): 4066-4069.

Abdel-Ghany, S. E., P. Muller-Moule, K. K. Niyogi, M. Pilon and T. Shikanai (2005). Two p-type ATPases are required for copper delivery in *Arabidopsis thaliana* chloroplasts. *Plant Cell* **17**(4): 1233-1251.

Agarwal, M., Y. J. Hao, A. Kapoor, C. H. Dong, H. Fujii, X. W. Zheng and J. K. Zhu (2006). A R2R3 type MYB transcription factor is involved in the cold regulation of CBF genes and in acquired freezing tolerance. *Journal of Biological Chemistry* **281**(49): 37636-37645.

Ahmad, A., S. Senapati, M. I. Khan, R. Kumar, R. Ramani, V. Srinivas and M. Sastry (2003a). Intracellular synthesis of gold nanoparticles by a novel alkalotolerant actinomycete, *Rhodococcus* species. *Nanotechnology* **14**(7): 824-828.

Ahmad, A., S. Senapati, M. I. Khan, R. Kumar and M. Sastry (2003b). Extracellular biosynthesis of monodisperse gold nanoparticles by a novel extremophilic actinomycete, *Thermomonospora* sp. *Langmuir* **19**(8): 3550-3553.

Aitken, R. J., M. Q. Chaudhry, A. B. A. Boxall and M. Hull (2006). Manufacture and use of nanomaterials: current status in the UK and global trends. *Occupational Medicine* **56**(5): 300-306.

Aller, S. G., E. T. Eng, C. J. De Feo and V. M. Unger (2004). Eukaryotic CTR copper uptake transporters require two faces of the third transmembrane domain for helix packing, oligomerization, and function. *Journal of Biological Chemistry* **279**(51): 53435-53441.

Alonso, J. M., A. N. Stepanova, T. J. Leisse, C. J. Kim, H. M. Chen, P. Shinn, D. K. Stevenson, J. Zimmerman, P. Barajas, R. Cheuk, C. Gadrinab, C. Heller, A. Jeske, E. Koesema, C. C. Meyers, H. Parker, L. Prednis, Y. Ansari, N. Choy, H. Deen, M. Geralt, N. Hazari, E. Hom, M. Karnes, C. Mulholland, R. Ndubaku, I. Schmidt, P. Guzman, L. Aguilar-Henonin, M. Schmid, D. Weigel, D. E. Carter, T. Marchand, E. Risseeuw, D. Brogden, A. Zeko, W. L. Crosby, C. C. Berry and J. R. Ecker (2003a). Genome-wide Insertional mutagenesis of *Arabidopsis thaliana*. *Science* **301**(5633): 653-657.

Alonso, J. M., A. N. Stepanova, R. Solano, E. Wisman, S. Ferrari, F. M. Ausubel and J. R. Ecker (2003b). Five components of the ethylene-response pathway identified in a screen for weak ethylene-insensitive mutants in *Arabidopsis*. *Proceedings of the National Academy of Sciences* **100**(5): 2992-2997.

Altschul, S. F., W. Gish, W. Miller, E. W. Myers and D. J. Lipman (1990). Basic local alignment search tool. *Journal of Molecular Biology* **215**(3): 403-410.

Anderson, C., F. Moreno, F. Geurts, C. Wreesmann, M. Ghomshei and J. Meech (2005a). A comparative analysis of gold-rich plant material using various analytical methods. *Microchemical Journal* **81**(1): 81-85.

Anderson, C., F. Moreno and J. Meech (2005b). A field demonstration of gold phytoextraction technology. *Minerals Engineering* **18**(4): 385-392.

Anderson, C. W. N. (2004). Biogeochemistry of gold: accepted theories and new opportunities. Trace and Ultratrace Elements in Plants and Soil. I. Shtangeeva. Southampton, WIT Press.

Anderson, C. W. N., R. R. Brooks, R. B. Stewart and R. Simcock (1998). Harvesting a crop of gold in plants. *Nature* **395**(6702): 553-554.

Anderson, C. W. N., R. R. Brooks, R. B. Stewart and R. Simcock (1999). Gold uptake by plants. *Gold Bulletin* **32**(2): 48-51.

Andres-Colas, N., A. Perea-Garcia, S. Puig and L. Penaarubia (2010). Deregulated copper transport affects Arabidopsis development especially in the absence of environmental cycles. *Plant Physiology* **153**(1): 170-184.

Andres-Colas, N., V. Sancenon, S. Rodriguez-Navarro, S. Mayo, D. J. Thiele, J. R. Ecker, S. Puig and L. Penarrubia (2006). The Arabidopsis heavy metal P-type ATPase HMA5 interacts with metallochaperones and functions in copper detoxification of roots. *Plant Journal* **45**(2): 225-236.

Armendariz, V., I. Herrera, J. R. Peralta-Videa, M. Jose-Yacaman, H. Troiani, P. Santiago and J. L. Gardea-Torresdey (2004). Size controlled gold nanoparticle formation by *Avena sativa* biomass: use of plants in nanobiotechnology. *Journal of Nanoparticle Research* **6**(4): 377-382.

Armendariz, V., J. G. Parsons, M. L. Lopez, J. R. Peralta-Videa, M. Jose-Yacaman and J. L. Gardea-Torresdey (2009). The extraction of gold nanoparticles from oat and wheat biomasses using sodium citrate and cetyltrimethylammonium bromide, studied by X-ray absorption spectroscopy, high-resolution transmission electron microscopy, and UV-visible spectroscopy. *Nanotechnology* **20**(10): 105607.

Arrivault, S., T. Senger and U. Krämer (2006). The Arabidopsis metal tolerance protein AtMTP3 maintains metal homeostasis by mediating Zn exclusion from the shoot under Fe deficiency and Zn oversupply. *Plant Journal* **46**(5): 861-879.

Asli, S. and P. M. Neumann (2009). Colloidal suspensions of clay or titanium dioxide nanoparticles can inhibit leaf growth and transpiration via physical effects on root water transport. *Plant, Cell & Environment* **32**(5): 577-584.

Axelsen, K. B. and M. G. Palmgren (1998). Evolution of substrate specificities in the P-type ATPase superfamily. *Journal of Molecular Evolution* **46**(1): 84-101.

Axelsen, K. B. and M. G. Palmgren (2001). Inventory of the superfamily of P-type ion pumps in Arabidopsis. *Plant Physiology* **126**(2): 696-706.

Baker, A. J. M., S. P. McGrath, R. D. Reeves and J. A. C. Smith (2000). Metal hyperaccumulator plants: A review of the ecology and physiology of a biochemical resource for phytoremediation of metal-polluted soils. Phytoremediation of Contaminated Soil and Water. N. Terry and G. Bañuelos. Boca Raton, FL, Lewis**:** 85-107.

Bali, R. and A. T. Harris (2010). Biogenic synthesis of Au nanoparticles using vascular plants. *Industrial & Engineering Chemistry Research* **49**(24): 12762-12772.

Bali, R., R. Siegele and A. T. Harris (2010). Phytoextraction of Au: Uptake, accumulation and cellular distribution in *Medicago sativa* and *Brassica juncea*. *Chemical Engineering Journal* **156**(2): 286-297.

Barrena, R., E. Casals, J. Colón, X. Font, A. Sánchez and V. Puntes (2009). Evaluation of the ecotoxicity of model nanoparticles. *Chemosphere* **75**(7): 850-857.

Becher, M., I. N. Talke, L. Krall and U. Krämer (2004). Cross-species microarray transcript profiling reveals high constitutive expression of metal homeostasis genes in shoots of the zinc hyperaccumulator *Arabidopsis halleri*. *Plant Journal* **37**(2): 251-268.

Behmer, S. T., C. M. Lloyd, D. Raubenheimer, J. Stewart-Clark, J. Knight, R. S. Leighton, F. A. Harper and J. A. C. Smith (2005). Metal hyperaccumulation in plants: mechanisms of defence against insect herbivores. *Functional Ecology* **19**(1): 55-66.

Belouchi, A., T. Kwan and P. Gros (1997). Cloning and characterization of the *OsNramp* family from *Oryza sativa*, a new family of membrane proteins possibly implicated in the transport of metal ions. *Plant Molecular Biology* **33**(6): 1085-1092.

Berardini, T. Z., S. Mundodi, L. Reiser, E. Huala, M. Garcia-Hernandez, P. F. Zhang, L. A. Mueller, J. Yoon, A. Doyle, G. Lander, N. Moseyko, D. Yoo, I. Xu, B. Zoeckler, M. Montoya, N. Miller, D. Weems and S. Y. Rhee (2004). Functional annotation of the Arabidopsis genome using controlled vocabularies. *Plant Physiology* **135**(2): 745-755.

Best, S. and P. Sadler (1996). Gold drugs: mechanism of action and toxicity. *Gold Bulletin* **29**: 87-93.

Beveridge, T. J. and R. G. E. Murray (1980). Sites of metal-depostion in the cell-wall of *Bacillus subtilis*. *Journal of Bacteriology* **141**(2): 876-887.

Binder, B. M., F. I. Rodriguez, A. B. Bleecker and S. E. Patterson (2007). The effects of Group 11 transition metals, including gold, on ethylene binding to the ETR1 receptor and growth of *Arabidopsis thaliana*. *FEBS Letters* **581**(26): 5105-5109.

Bizily, S. P., C. L. Rugh and R. B. Meagher (2000). Phytodetoxification of hazardous organomercurials by genetically engineered plants. *Nature Biotechnology* **18**(2): 213-217.

Blaylock, M. J., D. E. Salt, S. Dushenkov, O. Zakharova, C. Gussman, Y. Kapulnik, B. D. Ensley and I. Raskin (1997). Enhanced accumulation of Pb in Indian mustard by soil-applied chelating agents. *Environmental Science & Technology* **31**(3): 860-865.

Bowman, M. C., T. E. Ballard, C. J. Ackerson, D. L. Feldheim, D. M. Margolis and C. Melander (2008). Inhibition of HIV fusion with multivalent gold nanoparticles. *Journal of the American Chemical Society* **130**(22): 6896-6897.

Boyd, R. S. (2007). The defense hypothesis of elemental hyperaccumulation: status, challenges and new directions. *Plant and Soil* **293**(1-2): 153-176.

Brazier-Hicks, M. and R. Edwards (2005). Functional importance of the family 1 glucosyltransferase UGT72B1 in the metabolism of xenobiotics in Arabidopsis thaliana. *The Plant Journal* **42**(4): 556-566.

Brehelin, C., F. Kessler and K. J. van Wijk (2007). Plastoglobules: versatile lipoprotein particles in plastids. *Trends in Plant Science* **12**(6): 260-266.

Brooks, R. R., J. Lee, R. D. Reeves and T. Jaffré (1977). Detection of nickeliferous rocks by analysis of herbarium specimens of indicator plants. *Journal of Geochemical Exploration* **7**(1): 49-57.

Brown, S. L., R. L. Chaney, J. S. Angle and A. J. M. Baker (1995). Zinc and cadmium uptake by hyperaccumulator *Thlaspi caerulescens* and metal tolerant *Silene vulgaris* grown on sludge-amended soils. *Environmental Science & Technology* **29**(6): 1581-1585.

Brust, M., M. Walker, D. Bethell, D. J. Schiffrin and R. Whyman (1994). Synthesis of thiol-derivatised gold nanoparticles in a two-phase Liquid-Liquid system. *Journal of the Chemical Society, Chemical Communications*(7): 801-802.

Cellier, F., G. Conéjéro, L. Ricaud, D. T. Luu, M. Lepetit, F. Gosti and F. Casse (2004). Characterization of AtCHX17, a member of the cation/H+ exchangers, CHX family, from *Arabidopsis thaliana* suggests a role in K+ homeostasis. *The Plant Journal* **39**(6): 834-846.

Chakraborty, N., A. Banerjee, S. Lahiri, A. Panda, A. N. Ghosh and R. Pal (2009). Biorecovery of gold using cyanobacteria and an eukaryotic alga with special reference to nanogold formation - a novel phenomenon. *Journal of Applied Phycology* **21**(1): 145-152.

Chauhan, R. S. (2006). Bioinformatics approach toward identification of candidate genes for zinc and iron transporters in maize. *Current Science* **91**(4): 510-515.

Chaumont, F., F. Barrieu, E. M. Herman and M. J. Chrispeels (1998). Characterization of a maize tonoplast aquaporin expressed in zones of cell division and elongation. *Plant Physiology* **117**(4): 1143-1152.

Checa, S. K., M. Espariz, M. E. P. Audero, P. E. Botta, S. V. Spinelli and F. C. Soncini (2007). Bacterial sensing of and resistance to gold salts. *Molecular Microbiology* **63**(5): 1307-1318.

Chen, H., Z. B. Lai, J. W. Shi, Y. Xiao, Z. X. Chen and X. P. Xu (2011). Roles of arabidopsis WRKY18, WRKY40 and WRKY60 transcription factors in plant responses to abscisic acid and abiotic stress. *BMC Plant Biology* **10**.

Chiang, H. C., J. C. Lo and K. C. Yeh (2006). Genes associated with heavy metal tolerance and accumulation in Zn/Cd hyperaccumulator *Arabidopsis halleri*: A genomic survey with cDNA microarray. *Environmental Science & Technology* **40**(21): 6792-6798.

Chiu, K., Z. Ye and M. Wong (2005). Enhanced uptake of As, Zn, and Cu by *Vetiveria zizanioides* and *Zea mays* using chelating agents. *Chemosphere* **60**(10): 1365-1375.

Colangelo, E. P. and M. L. Guerinot (2004). The essential basic helix-loop-helix protein FIT1 is required for the iron deficiency response. *Plant Cell* **16**(12): 3400-3412.

Colangelo, E. P. and M. L. Guerinot (2006). Put the metal to the petal: metal uptake and transport throughout plants. *Current Opinion in Plant Biology* **9**(3): 322-330.

Coleman, C. M., R. S. Boyd and M. D. Eubanks (2005). Extending the elemental defense hypothesis: Dietary metal concentrations below hyperaccumulator levels could harm herbivores. *Journal of Chemical Ecology* **31**(8): 1669-1681.

Connolly, E. L., J. P. Fett and M. L. Guerinot (2002). Expression of the IRT1 metal transporter is controlled by metals at the levels of transcript and protein accumulation. *Plant Cell* **14**(6): 1347-1357.

Curie, C., J. M. Alonso, M. Le Jean, J. R. Ecker and J. F. Briat (2000). Involvement of NRAMP1 from *Arabidopsis thaliana* in iron transport. *Biochemical Journal* **347**: 749-755.

Curie, C., Z. Panaviene, C. Loulergue, S. L. Dellaporta, J. F. Briat and E. L. Walker (2001). Maize yellow stripe1 encodes a membrane protein directly involved in Fe(III) uptake. *Nature* **409**(6818): 346-349.

Dancis, A., D. S. Yuan, D. Haile, C. Askwith, D. Eide, C. Moehle, J. Kaplan and R. D. Klausner (1994). Molecular characterization of a copper transport protein in *S. cerevisiae*: An unexpected role for copper in iron transport. *Cell* **76**(2): 393-402.

Darnall, D. W., B. Greene, M. T. Henzl, J. M. Hosea, R. A. McPherson, J. Sneddon and M. D. Alexander (1986). Selective recovery of gold and other metal-ions from an algal biomass. *Environmental Science & Technology* **20**(2): 206-208.

Daxinger, L., B. Hunter, M. Sheik, V. Jauvion, V. Gasciolli, H. Vaucheret, M. Matzke and I. Furner (2008). Unexpected silencing effects from T-DNA tags in *Arabidopsis*. *Trends in Plant Science* **13**(1): 4-6.

De Feo, C. J., S. G. Aller, G. S. Siluvai, N. J. Blackburn and V. M. Unger (2009). Three-dimensional structure of the human copper transporter hCTR1. *Proceedings of the National Academy of Sciences of the United States of America* **106**(11): 4237-4242.

De Jong, W. H. and P. J. A. Borm (2008). Drug delivery and nanoparticles: applications and hazards. *International Journal of Nanomedicine* **3**(2): 133.

del Pozo, T., V. Cambiazo and M. Gonzalez (2010). Gene expression profiling analysis of copper homeostasis in *Arabidopsis thaliana*. *Biochemical and Biophysical Research Communications* **393**(2): 248-252.

Delhaize, E., B. D. Gruber, J. K. Pittman, R. G. White, H. Leung, Y. S. Miao, L. W. Jiang, P. R. Ryan and A. E. Richardson (2007). A role for the AtMTP11 gene of Arabidopsis in manganese transport and tolerance. *Plant Journal* **51**(2): 198-210.

Delhaize, E., T. Kataoka, D. M. Hebb, R. G. White and P. R. Ryan (2003). Genes encoding proteins of the cation diffusion facilitator family that confer manganese tolerance. *Plant Cell* **15**(5): 1131-1142.

Demarty, M., C. Morvan and M. Thellier (1984). Calcium and the cell wall. *Plant, Cell & Environment* **7**(6): 441-448.

Deplanche, K. and L. E. Macaskie (2008). Biorecovery of gold by *Escherichia coli* and *Desulfovibrio desulfuricans*. *Biotechnology and Bioengineering* **99**(5): 1055-1064.

Desbrosses-Fonrouge, A.-G., K. Voigt, A. Schröder, S. Arrivault, S. Thomine and U. Krämer (2005). *Arabidopsis thaliana* MTP1 is a Zn transporter in the vacuolar membrane which mediates Zn detoxification and drives leaf Zn accumulation. *Febs Letters* **579**(19): 4165-4174.

Dhankher, O. P., Y. J. Li, B. P. Rosen, J. Shi, D. Salt, J. F. Senecoff, N. A. Sashti and R. B. Meagher (2002). Engineering tolerance and hyperaccumulation of arsenic in plants by combining arsenate reductase and gamma-glutamylcysteine synthetase expression. *Nature Biotechnology* **20**(11): 1140-1145.

DiDonato, R. J., L. A. Roberts, T. Sanderson, R. B. Eisley and E. L. Walker (2004). *Arabidopsis* Yellow Stripe-Like2 (YSL2): a metal-regulated gene encoding a plasma membrane transporter of nicotianamine-metal complexes. *Plant Journal* **39**(3): 403-414.

Ding, Z. H., S. M. Li, X. L. An, X. J. Liu, H. M. Qin and D. Wang (2009). Transgenic expression of MYB15 confers enhanced sensitivity to abscisic acid and improved drought tolerance in *Arabidopsis thaliana*. *Journal of Genetics and Genomics* **36**(1): 17-29.

Dixon, D. P. and R. Edwards (2010). Glutathione Transferases. *The Arabidopsis Book*: e0131.

Dong, J. X., C. H. Chen and Z. X. Chen (2003). Expression profiles of the *Arabidopsis* WRKY gene superfamily during plant defense response. *Plant Molecular Biology* **51**(1): 21-37.

Doshi, R., W. Braida, C. Christodoulatos, M. Wazne and G. O'Connor (2008). Nano-aluminum: Transport through sand columns and environmental effects on plants and soil communities. *Environmental Research* **106**(3): 296-303.

Du, L. W., H. Jiang, X. H. Liu and E. K. Wang (2007). Biosynthesis of gold nanoparticles assisted by *Escherichia coli* DH5 alpha and its application on direct electrochemistry of hemoglobin. *Electrochemistry Communications* **9**(5): 1165-1170.

Eide, D., M. Broderius, J. Fett and M. L. Guerinot (1996). A novel iron-regulated metal transporter from plants identified by functional expression in yeast. *Proceedings of the National Academy of Sciences of the United States of America* **93**(11): 5624-5628.

El-Sayed, I. H., X. H. Huang and M. A. El-Sayed (2005). Surface plasmon resonance scattering and absorption of anti-EGFR antibody conjugated

gold nanoparticles in cancer diagnostics: Applications in oral cancer. *Nano Letters* **5**(5): 829-834.

El-Temsah, Y. S. and E. J. Joner (2010). Impact of Fe and Ag nanoparticles on seed germination and differences in bioavailability during exposure in aqueous suspension and soil. *Environmental Toxicology*: DOI: 10.1002/tox.20610.

Elghanian, R., J. J. Storhoff, R. C. Mucic, R. L. Letsinger and C. A. Mirkin (1997). Selective colorimetric detection of polynucleotides based on the bistance-bependent optical properties of gold nanoparticles. *Science* **277**(5329): 1078-1081.

Eng, B. H., M. L. Guerinot, D. Eide and M. H. Saier (1998). Sequence analyses and phylogenetic characterization of the ZIP family of metal ion transport proteins. *Journal of Membrane Biology* **166**(1): 1-7.

Esumi, K., T. Hosoya, A. Suzuki and K. Torigoe (2000). Spontaneous formation of gold nanoparticles in aqueous solution of sugar-persubstituted poly(amidoamine) dendrimers. *Langmuir* **16**(6): 2978-2980.

Eulgem, T., P. J. Rushton, S. Robatzek and I. E. Somssich (2000). The WRKY superfamily of plant transcription factors. *Trends in Plant Science* **5**(5): 199-206.

Ferry, J. L., P. Craig, C. Hexel, P. Sisco, R. Frey, P. L. Pennington, M. H. Fulton, I. G. Scott, A. W. Decho, S. Kashiwada, C. J. Murphy and T. J. Shaw (2009). Transfer of gold nanoparticles from the water column to the estuarine food web. *Nature Nanotechnology* **4**(7): 441-444.

Franklin, K. A. and G. C. Whitelam (2007). Light-quality regulation of freezing tolerance in *Arabidopsis thaliana*. *Nature Genetics* **39**: 1410-1413.

Frens, G. (1973). Controlled nucleation for regulation of particle-size in monodisperse gold suspensions. *Nature Physical Science* **241**(105): 20-22.

Froidure, S., J. Canonne, X. Daniel, A. Jauneau, C. Briere, D. Roby and S. Rivas (2010). AtsPLA(2)-alpha nuclear relocalization by the Arabidopsis transcription factor AtMYB30 leads to repression of the plant defense response. *Proceedings of the National Academy of Sciences of the United States of America* **107**(34): 15281-15286.

Gaither, L. A. and D. J. Eide (2001). Eukaryotic zinc transporters and their regulation. *Biometals* **14**(3): 251-270.

Gamez, G., J. L. Gardea-Torresdey, K. J. Tiemann, J. Parsons, K. Dokken and M. J. Yacaman (2003). Recovery of gold(III) from multi-elemental solutions by alfalfa biomass. *Advances in Environmental Research* **7**(2): 563-571.

Gandia-Herrero, F., A. Lorenz, T. Larson, I. A. Graham, D. J. Bowles, E. L. Rylott and N. C. Bruce (2008). Detoxification of the explosive 2,4,6-trinitrotoluene in Arabidopsis: discovery of bifunctional O- and C-glucosyltransferases. *Plant Journal* **56**(6): 963-974.

Garcia-Molina, A., N. Andrés-Colás, A. Perea-García, S. del Valle-Tascón, L. Peñarrubia and S. Puig (2011). The intracellular Arabidopsis COPT5 transport protein is required for photosynthetic electron transport under severe copper deficiency. *The Plant Journal* **65**(6): 848-860.

Gardea-Torresdey, J., E. Rodriguez, J. G. Parsons, J. R. Peralta-Videa, G. Meitzner and G. Cruz-Jimenez (2005). Use of ICP and XAS to determine the enhancement of gold phytoextraction by *Chilopsis linearis* using thiocyanate as a complexing agent. *Analytical and Bioanalytical Chemistry* **382**(2): 347-352.

Gardea-Torresdey, J. L., J. G. Parsons, E. Gomez, J. Peralta-Videa, H. E. Troiani, P. Santiago and M. J. Yacaman (2002a). Formation and growth of Au nanoparticles inside live alfalfa plants. *Nano Letters* **2**(4): 397-401.

Gardea-Torresdey, J. L., K. J. Tiemann, G. Gamez, K. Dokken, I. Cano-Aguilera, L. R. Furenlid and M. W. Renner (2000). Reduction and accumulation of gold(III) by *Medicago sativa* alfalfa biomass: X-ray absorption spectroscopy, pH, and temperature dependence. *Environmental Science & Technology* **34**(20): 4392-4396.

Gardea-Torresdey, J. L., K. J. Tiemann, G. Gamez, K. Dokken, S. Tehuacanero and M. José-Yacamán (1999). Gold nanoparticles obtained by bio-precipitation from gold(III) solutions. *Journal of Nanoparticle Research* **1**(3): 397-404.

Gardea-Torresdey, J. L., K. J. Tiemann, J. G. Parsons, G. Gamez and M. J. Yacaman (2002b). Characterization of trace level Au(III) binding to alfalfa biomass (*Medicago sativa*) by GFAAS. *Advances in Environmental Research* **6**(3): 313-323.

Girling, C. A. and P. J. Peterson (1980). Gold in plants. *Gold bulletin* **13**: 151-157.

Gisbert, C., R. Ros, A. De Haro, D. J. Walker, M. Pilar Bernal, R. Serrano and J. Navarro-Aviñó (2003). A plant genetically modified that accumulates Pb is especially promising for phytoremediation. *Biochemical and Biophysical Research Communications* **303**(2): 440-445.

Goda, H., E. Sasaki, K. Akiyama, A. Maruyama-Nakashita, K. Nakabayashi, W. Q. Li, M. Ogawa, Y. Yamauchi, J. Preston, K. Aoki, T. Kiba, S. Takatsuto, S. Fujioka, T. Asami, T. Nakano, H. Kato, T. Mizuno, H. Sakakibara, S. Yamaguchi, E. Nambara, Y. Kamiya, H. Takahashi, M. Y. Hirai, T. Sakurai, K. Shinozaki, K. Saito, S. Yoshida and Y. Shimada (2008). The AtGenExpress hormone and chemical treatment data set: experimental design, data evaluation, model data analysis and data access. *Plant Journal* **55**(3): 526-542.

Gole, A., C. Dash, V. Ramakrishnan, S. R. Sainkar, A. B. Mandale, M. Rao and M. Sastry (2001). Pepsin-gold colloid conjugates: Preparation, characterization, and enzymatic activity. *Langmuir* **17**(5): 1674-1679.

Gravot, A., A. Lieutaud, F. Verret, P. Auroy, A. Vavasseur and P. Richaud (2004). AtHMA3, a plant P-1B-ATPase, functions as a Cd/Pb transporter in yeast. *Febs Letters* **561**(1-3): 22-28.

Greene, B., M. Hosea, R. McPherson, M. Henzl, M. D. Alexander and D. W. Darnall (1986). Interaction of gold(I) and gold(III) complexes with algal biomass. *Environmental Science & Technology* **20**(6): 627-632.

Grotz, N., T. Fox, E. Connolly, W. Park, M. L. Guerinot and D. Eide (1998). Identification of a family of zinc transporter genes from *Arabidopsis* that respond to zinc deficiency. *Proceedings of the National Academy of Sciences of the United States of America* **95**(12): 7220-7224.

Grotz, N. and M. L. Guerinot (2006). Molecular aspects of Cu, Fe and Zn homeostasis in plants. *Biochimica et Biophysica Acta - Molecular Cell Research* **1763**(7): 595-608.

Guerinot, M. L. (2000). The ZIP family of metal transporters. *Biochimica et Biophysica Acta* **1465**(1-2): 190-198.

Gunshin, H., B. Mackenzie, U. V. Berger, Y. Gunshin, M. F. Romero, W. F. Boron, S. Nussberger, J. L. Gollan and M. A. Hediger (1997). Cloning and characterization of a mammalian proton-coupled metal-ion transporter. *Nature* **388**(6641): 482-488.

Hall, J. L. and L. E. Williams (2003). Transition metal transporters in plants. *Journal of Experimental Botany* **54**(393): 2601-2613.

Hall, T. A. (1999). BioEdit: a user-friendly biological sequence alignment editor and analysis program for Windows 95/98/NT. *Nucleic Acids Symposium Series* **41**: 95-98.

Halliwell, B. and J. Gutteridge (1984). Oxygen toxicity, oxygen radicals, transition metals and disease. *Biochemical Journal* **219**(1): 1.

Hammer, D. and C. Keller (2003). Phytoextraction of Cd and Zn with *Thlaspi caerulescens* in field trials. *Soil Use and Management* **19**(2): 144-149.

Hammond, J. P., H. C. Bowen, P. J. White, V. Mills, K. A. Pyke, A. J. M. Baker, S. N. Whiting, S. T. May and M. R. Broadley (2006). A comparison of the *Thlaspi caerulescens* and *Thlaspi arvense* shoot transcriptomes. *New Phytologist* **170**(2): 239-260.

Hänsch, R. and R. R. Mendel (2009). Physiological functions of mineral micronutrients (Cu, Zn, Mn, Fe, Ni, Mo, B, Cl). *Current Opinion in Plant Biology* **12**(3): 259-266.

Hansson, D., M. J. Morra, V. Borek, A. J. Snyder, J. L. Johnson-Maynard and D. C. Thill (2008). Ionic thiocyanate (SCN-) production, fate, and phytotoxicity in soil amended with Brassicaceae seed meals. *Journal of Agricultural and Food Chemistry* **56**(11): 3912-3917.

Harris, A. T. and R. Bali (2008). On the formation and extent of uptake of silver nanoparticles by live plants. *Journal of Nanoparticle Research* **10**(4): 691-695.

Harris, A. T., K. Naidoo, J. Nokes, T. Walker and F. Orton (2009). Indicative assessment of the feasibility of Ni and Au phytomining in Australia. *Journal of Cleaner Production* **17**(2): 194-200.

Hasegawa, I., E. Terada, M. Sunairi, H. Wakita, F. Shinmachi, A. Noguchi, M. Nakajima and J. Yazaki (1997). Genetic improvement of heavy metal tolerance in plants by transfer of the yeast metallothionein gene (*CUP1*). *Plant and Soil* **196**(2): 277-281.

Hashmi, A. S. K. and M. Rudolph (2008). Gold catalysis in total synthesis. *Chemical Society Reviews* **37**(9): 1766-1775.

Hassett, R. and D. J. Kosman (1995). Evidence for Cu(II) reduction as a component of copper uptake by *Saccharomyces cerevisiae*. *Journal of Biological Chemistry* **270**(1): 128-134.

Haughn, G. W. and C. Somerville (1986). Sulfonylurea-resistant mutants of *Arabidopsis thaliana*. *Molecular and General Genetics* **204**(3): 430-434.

Haverkamp, R. G. and A. T. Marshall (2009). The mechanism of metal nanoparticle formation in plants: limits on accumulation. *Journal of Nanoparticle Research* **11**(6): 1453-1463.

Haverkamp, R. G., A. T. Marshall and D. van Agterveld (2007). Pick your carats: nanoparticles of gold-silver-copper alloy produced in vivo. *Journal of Nanoparticle Research* **9**(4): 697-700.

He, S. Y., Z. R. Guo, Y. Zhang, S. Zhang and J. W. N. Gu (2007). Biosynthesis of gold nanoparticles using the bacteria *Rhodopseudomonas capsulata*. *Materials Letters* **61**(18): 3984-3987.

Herbette, S., L. Taconnat, V. Hugouvieux, L. Piette, M. L. M. Magniette, S. Cuine, P. Auroy, P. Richaud, C. Forestier, J. Bourguignon, J. P. Renou, A. Vavasseur and N. Leonhardt (2006). Genome-wide transcriptome profiling of the early cadmium response of *Arabidopsis* roots and shoots. *Biochimie* **88**(11): 1751-1765.

Himmelhaus, M. and H. Takei (2000). Cap-shaped gold nanoparticles for an optical biosensor. *Sensors and Actuators B: Chemical* **63**(1-2): 24-30.

Hirayama, T., J. J. Kieber, N. Hirayama, M. Kogan, P. Guzman, S. Nourizadeh, J. M. Alonso, W. P. Dailey, A. Dancis and J. R. Ecker (1999). Responsive-to-antagonist1, a Menkes/Wilson disease-related copper transporter, is required for ethylene signaling in *Arabidopsis*. *Cell* **97**(3): 383-393.

Hirsch, L. R., R. J. Stafford, J. A. Bankson, S. R. Sershen, B. Rivera, R. E. Price, J. D. Hazle, N. J. Halas and J. L. West (2003). Nanoshell-mediated near-infrared thermal therapy of tumors under magnetic resonance guidance. *Proceedings of the National Academy of Sciences of the United States of America* **100**(23): 13549-13554.

Hosea, M., B. Greene, R. McPherson, M. Henzl, M. D. Alexander and D. W. Darnall (1986). Accumulation of elemental gold on the alga *Chlorella vulgaris*. *Inorganica Chimica Acta* **123**(3): 161-165.

Howden, R. and C. S. Cobbett (1992). Cadmium-sensitive mutants of *Arabidopsis thaliana*. *Plant Physiology* **100**(1): 100.

Hruz, T., O. Laule, G. Szabo, F. Wessendorp, S. Bleuler, L. Oertle, P. Widmayer, W. Gruissem and P. Zimmermann (2008). Genevestigator v3: a reference expression database for the meta-analysis of transcriptomes. *Advances in Bioinformatics* **2008**: 420747.

Huang, J. W., M. J. Blaylock, Y. Kapulnik and B. D. Ensley (1998). Phytoremediation of uranium-contaminated soils: role of organic acids in triggering uranium hyperaccumulation in plants. *Environmental Science & Technology* **32**(13): 2004-2008.

Huang, J. W., J. Chen, W. R. Berti and S. D. Cunningham (1997). Phytoremediation of lead-contaminated soils: Role of synthetic chelates in lead phytoextraction. *Environmental Science & Technology* **31**(3): 800-805.

Hughes, M. D., Y.-J. Xu, P. Jenkins, P. McMorn, P. Landon, D. I. Enache, A. F. Carley, G. A. Attard, G. J. Hutchings, F. King, E. H. Stitt, P. Johnston, K. Griffin and C. J. Kiely (2005). Tunable gold catalysts for selective hydrocarbon oxidation under mild conditions. *Nature* **437**(7062): 1132-1135.

Hussain, D., M. J. Haydon, Y. Wang, E. Wong, S. M. Sherson, J. Young, J. Camakaris, J. F. Harper and C. S. Cobbett (2004). P-type ATPase heavy metal transporters with roles in essential zinc homeostasis in Arabidopsis. *Plant Cell* **16**(5): 1327-1339.

Husseiny, M. I., M. A. El-Aziz, Y. Badr and M. A. Mahmoud (2007). Biosynthesis of gold nanoparticles using *Pseudomonas aeruginosa*. *Spectrochimica Acta Part a* **67**(3-4): 1003-1006.

Isayenkov, S. V. and F. J. M. Maathuis (2008). The *Arabidopsis thaliana* aquaglyceroporin AtNIP7;1 is a pathway for arsenite uptake. *FEBS Letters* **582**(11): 1625-1628.

Ishikawa, F., S. Suga, T. Uemura, M. H. Sato and M. Maeshima (2005). Novel type aquaporin SIPs are mainly localized to the ER membrane and show cell-specific expression in *Arabidopsis thaliana*. *Febs Letters* **579**(25): 5814-5820.

Ishimaru, Y., M. Suzuki, T. Kobayashi, M. Takahashi, H. Nakanishi, S. Mori and N. K. Nishizawa (2005). OsZIP4, a novel zinc-regulated zinc transporter in rice. *Journal of Experimental Botany* **56**(422): 3207-3214.

Jakoby, M., H. Y. Wang, W. Reidt, B. Weisshaar and P. Bauer (2004). FRU (BHLH029) is required for induction of iron mobilization genes in *Arabidopsis thaliana*. *Febs Letters* **577**(3): 528-534.

Javot, H. and C. Maurel (2002). The role of aquaporins in root water uptake. *Annals of Botany* **90**(3): 301-313.

Jhee, E. M., R. S. Boyd, M. D. Eubanks and M. A. Davis (2006). Nickel hyperaccumulation by *Streptanthus polygaloides* protects against the folivore *Plutella xylostella* (Lepidoptera: Plutellidae). *Plant Ecology* **183**(1): 91-104.

Jian, X., E. C. Wasinger, J. V. Lockard, L. X. Chen and C. He (2009). Highly sensitive and selective gold(I) recognition by a metalloregulator in *Ralstonia metallidurans*. *Journal of the American Chemical Society* **131**(31): 10869-10871.

Jiang, R. F., D. Y. Ma, F. J. Zhao and S. P. McGrath (2005). Cadmium hyperaccumulation protects *Thlaspi caerulescens* from leaf feeding

damage by thrips (*Frankliniella occidentalis*). *New Phytologist* **167**(3): 805-814.

Johanson, U., M. Karlsson, I. Johansson, S. Gustavsson, S. Sjovall, L. Fraysse, A. R. Weig and P. Kjellbom (2001). The complete set of genes encoding major intrinsic proteins in arabidopsis provides a framework for a new nomenclature for major intrinsic proteins in plants. *Plant Physiology* **126**(4): 1358-1369.

Judy, J. D., J. M. Unrine and P. M. Bertsch (2010). Evidence for biomagnification of gold nanoparticles within a terrestrial food chain. *Environmental Science & Technology* **45**(2): 776-781.

Jung, C., J. S. Seo, S. W. Han, Y. J. Koo, C. H. Kim, S. I. Song, B. H. Nahm, Y. Do Choi and J. J. Cheong (2008). Overexpression of AtMYB44 enhances stomatal closure to confer abiotic stress tolerance in transgenic Arabidopsis. *Plant Physiology* **146**(2): 623-635.

Kalde, M., M. Barth, I. E. Somssich and B. Lippok (2003). Members of the Arabidopsis WRKY group III transcription factors are part of different plant defense signaling pathways. *Molecular Plant-Microbe Interactions* **16**(4): 295-305.

Kampfenkel, K., S. Kushnir, E. Babiychuk, D. Inze and M. Vanmontagu (1995). Molecular characterization of a putative *Arabidopsis thaliana* copper transporter ad its yeast homolog. *Journal of Biological Chemistry* **270**(47): 28479-28486.

Kang, H.-G., J. Kim, B. Kim, H. Jeong, S. H. Choi, E. K. Kim, H.-Y. Lee and P. O. Lim (2011). Overexpression of FTL1/DDF1, an AP2 transcription factor, enhances tolerance to cold, drought, and heat stresses in *Arabidopsis thaliana*. *Plant Science* **180**(4): 634-641.

Kawachi, M., Y. Kobae, T. Mimura and M. Maeshima (2008). Deletion of a histidine-rich loop of AtMTP1, a vacuolar Zn^{2+}/H^{+} Antiporter of *Arabidopsis thaliana*, stimulates the transport activity. *Journal of Biological Chemistry* **283**(13): 8374-8383.

Kayser, A., K. Wenger, A. Keller, W. Attinger, H. Felix, S. Gupta and R. Schulin (2000). Enhancement of phytoextraction of Zn, Cd, and Cu from calcareous soil: the use of NTA and sulfur amendments. *Environmental Science & Technology* **34**(9): 1778-1783.

Keeling, S. M., R. B. Stewart, C. W. N. Anderson and B. H. Robinson (2003). Nickel and cobalt phytoextraction by the hyperaccumulator *Berkheya coddii*: Implications for polymetallic phytomining and phytoremediation. *International Journal of Phytoremediation* **5**(3): 235 - 244.

Kim, D., J. L. Gustin, B. Lahner, M. W. Persans, D. Baek, D. J. Yun and D. E. Salt (2004a). The plant CDF family member TgMTP1 from the Ni/Zn hyperaccumulator *Thlaspi goesingense* acts to enhance efflux of Zn at the plasma membrane when expressed in *Saccharomyces cerevisiae*. *Plant Journal* **39**(2): 237-251.

Kim, S. A. and M. L. Guerinot (2007). Mining iron: Iron uptake and transport in plants. *FEBS Letters* **581**(12): 2273-2280.

Kim, W. B., T. Voitl, G. J. Rodriguez-Rivera and J. A. Dumesic (2004b). Powering fuel cells with CO via aqueous polyoxometalates and gold catalysts. *Science* **305**(5688): 1280-1283.

Kim, Y. Y., H. Choi, S. Segami, H. T. Cho, E. Martinoia, M. Maeshima and Y. Lee (2009). AtHMA1 contributes to the detoxification of excess Zn(II) in Arabidopsis. *Plant Journal* **58**(5): 737-753.

Klomp, A. E. M., J. A. Juijn, L. T. M. van der Gun, I. E. T. Van Den Berg, R. Berger and L. W. J. Klomp (2003). The N-terminus of the human copper transporter 1 (hCTR1) is localized extracellularly, and interacts with itself. *Biochemical Journal* **370**(Pt 3): 881.

Kobae, Y., T. Uemura, M. H. Sato, M. Ohnishi, T. Mimura, T. Nakagawa and M. Maeshima (2004). Zinc transporter of *Arabidopsis thaliana* AtMTP1 is localized to vacuolar membranes and implicated in zinc homeostasis. *Plant and Cell Physiology* **45**(12): 1749-1758.

Kobayashi, Y., K. Kuroda, K. Kimura, J. L. Southron-Francis, A. Furuzawa, K. Kimura, S. Iuchi, M. Kobayashi, G. J. Taylor and H. Koyama (2008). Amino acid polymorphisms in strictly conserved domains of a P-Type ATPase HMA5 are involved in the mechanism of copper tolerance variation in Arabidopsis. *Plant Physiology* **148**(2): 969-980.

Konishi, Y., T. Tsukiyama, K. Ohno, N. Saitoh, T. Nomura and S. Nagamine (2006). Intracellular recovery of gold by microbial reduction of $AuCl_4^-$ ions using the anaerobic bacterium *Shewanella algae*. *Hydrometallurgy* **81**(1): 24-29.

Koornneef, M., L. W. M. Dellaert and J. H. van der Veen (1982). EMS- and radiation-induced mutation frequencies at individual loci in *Arabidopsis thaliana* (L.) Heynh. *Mutation Research/Fundamental and Molecular Mechanisms of Mutagenesis* **93**(1): 109-123.

Korshunova, Y. O., D. Eide, W. G. Clark, M. L. Guerinot and H. B. Pakrasi (1999). The IRT1 protein from *Arabidopsis thaliana* is a metal transporter with a broad substrate range. *Plant Molecular Biology* **40**(1): 37-44.

Korte, F., M. Spiteller and F. Coulston (2000). The cyanide leaching gold recovery process is a nonsustainable technology with unacceptable impacts on ecosystems and humans: The disaster in Romania. *Ecotoxicology and Environmental Safety* **46**(3): 241-245.

Krämer, U., I. N. Talke and M. Hanikenne (2007). Transition metal transport. *FEBS Letters* **581**(12): 2263-2272.

Kreps, J. A., Y. J. Wu, H. S. Chang, T. Zhu, X. Wang and J. F. Harper (2002). Transcriptome changes for Arabidopsis in response to salt, osmotic, and cold stress. *Plant Physiology* **130**(4): 2129-2141.

Kumari, M., A. Mukherjee and N. Chandrasekaran (2009). Genotoxicity of silver nanoparticles in *Allium cepa*. *Science of the Total Environment* **407**(19): 5243-5246.

Kumari, M., G. J. Taylor and M. K. Deyholos (2008). Transcriptomic responses to aluminum stress in roots of *Arabidopsis thaliana*. *Molecular Genetics and Genomics* **279**(4): 339-357.

LaCoste, C., B. Robinson and R. Brooks (2001). Uptake of thallium by vegetables: Its significance for human health, phytoremediation, and phytomining. *Journal of Plant Nutrition* **24**(8): 1205-1215.

Lamb, A. E., C. W. N. Anderson and R. G. Haverkamp (2001). The induced accumulation of gold in the plants *Brassica juncea*, *Berkheya coddii* and chicory. *Chemistry in New Zealand* **65**(2): 34-36.

Langlois-Meurinne, M., C. M. M. Gachon and P. Saindrenan (2005). Pathogen-responsive expression of glycosyltransferase genes UGT73B3 and UGT73b5 is necessary for resistance to *Pseudomonas syringae* pv *tomato* in Arabidopsis. *Plant Physiology* **139**(4): 1890-1901.

Lanquar, V., F. Lelievre, S. Bolte, C. Hames, C. Alcon, D. Neumann, G. Vansuyt, C. Curie, A. Schroder, U. Krämer, H. Barbier-Brygoo and S. Thomine (2005). Mobilization of vacuolar iron by AtNRAMP3 and AtNRAMP4 is essential for seed germination on low iron. *Embo Journal* **24**(23): 4041-4051.

Larkin, E., S. Dunaway, K. Ellini, M. Rubio, C. Sanchez, M. Sehorn and L. Weiss (1999). An *Arabidopsis thaliana* copper-sensitive mutant. *Bios* **70**(4): 147-157.

Larkin, M. A., G. Blackshields, N. P. Brown, R. Chenna, P. A. McGettigan, H. McWilliam, F. Valentin, I. M. Wallace, A. Wilm, R. Lopez, J. D. Thompson,

T. J. Gibson and D. G. Higgins (2007). Clustal W and clustal X version 2.0. *Bioinformatics* **23**: 2947-2948.

Larsen, P. B., J. Degenhardt, C. Y. Tai, L. M. Stenzler, S. H. Howell and L. V. Kochian (1998). Aluminum-resistant Arabidopsis mutants that exhibit altered patterns of aluminum accumulation and organic acid release from roots. *Plant Physiology* **117**(1): 9.

Larsen, P. B., C. Y. Tai, L. V. Kochian and S. H. Howell (1996). Arabidopsis mutants with increased sensitivity to aluminum. *Plant Physiology* **110**(3): 743-751.

Lasat, M. M., M. Fuhrmann, S. D. Ebbs, J. E. Cornish and L. V. Kochian (1998). Phytoremediation of a radiocesium-contaminated soil: evaluation of cesium-137 bioaccumulation in the shoots of three plant species. *Journal of Environmental Quality* **27**(1): 165-169.

Le Jean, M., A. Schikora, S. Mari, J. F. Briat and C. Curie (2005). A loss-of-function mutation in AtYSL1 reveals its role in iron and nicotianamine seed loading. *Plant Journal* **44**(5): 769-782.

Lee, D. A., A. Chen and J. I. Schroeder (2003). ars1, an Arabidopsis mutant exhibiting increased tolerance to arsenate and increased phosphate uptake. *The Plant Journal* **35**(5): 637-646.

Lee, J., M. M. Pena, Y. Nose and D. J. Thiele (2002). Biochemical characterization of the human copper transporter Ctr1. *J Biol Chem* **277**(6): 4380-4387.

Lee, W.-M., Y.-J. An, H. Yoon and H.-S. Kweon (2008). Toxicity and bioavailability of copper nanoparticles to the terrestrial plants mung bean (*Phaseolus radiatus*) and wheat (*Triticum aestivum*): Plant agar test for water-insoluble nanoparticles. *Environmental Toxicology and Chemistry* **27**(9): 1915-1921.

Lengke, M. F., M. E. Fleet and G. Southam (2006a). Morphology of gold nanoparticles synthesized by filamentous cyanobacteria from gold(I)-thiosulfate and gold(III)-chloride complexes. *Langmuir* **22**(6): 2780-2787.

Lengke, M. F., B. Ravel, M. E. Fleet, G. Wanger, R. A. Gordon and G. Southam (2006b). Mechanisms of gold bioaccumulation by filamentous cyanobacteria from gold(III) - Chloride complex. *Environmental Science & Technology* **40**(20): 6304-6309.

Li, L., X. F. Yu, A. Thompson, M. Guo, S. Yoshida, T. Asami, J. Chory and Y. Yin (2009). Arabidopsis MYB30 is a direct target of BES1 and cooperates with BES1 to regulate brassinosteroid-induced gene expression. *Plant Journal* **58**(2): 275-286.

Li, Y.-M., R. L. Chaney, E. P. Brewer, J. S. Angle and J. Nelkin (2003). Phytoextraction of nickel and cobalt by hyperaccumulator *Alyssum* species grown on nickel-contaminated soils. *Environmental Science & Technology* **37**(7): 1463-1468.

Lin, D. and B. Xing (2007). Phytotoxicity of nanoparticles: Inhibition of seed germination and root growth. *Environmental Pollution* **150**(2): 243-250.

Lin, Z. Y., J. M. Wu, R. Xue and Y. Yang (2005). Spectroscopic characterization of Au^{3+} biosorption by waste biomass of *Saccharomyces cerevisiae*. *Spectrochimica Acta Part a* **61**(4): 761-765.

Lippold, F., D. H. Sanchez, M. Musialak, A. Schlereth, W. R. Scheible, D. K. Hincha and M. K. Udvardi (2009). Atmyb41 regulates transcriptional and metabolic responses to osmotic stress in Arabidopsis. *Plant Physiology* **149**(4): 1761-1772.

Liu, J. and J.-K. Zhu (1997). An Arabidopsis mutant that requires increased calcium for potassium nutrition and salt tolerance. *Proceedings of the National Academy of Sciences of the United States of America* **94**(26): 14960-14964.

Liu, T., S. Y. Liu, H. Guan, L. G. Ma, Z. L. Chen, H. Y. Gu and L. J. Qu (2009). Transcriptional profiling of Arabidopsis seedlings in response to heavy metal lead (Pb). *Environmental and Experimental Botany* **67**(2): 377-386.

Lombi, E., F. Zhao, S. Dunham and S. McGrath (2000). Cadmium accumulation in populations of *Thlaspi caerulescens* and *Thlaspi goesingense*. *New Phytologist* **145**(1): 11-20.

Lombi, E., F. Zhao, S. Dunham and S. McGrath (2001). Phytoremediation of heavy metal-contaminated soils: natural hyperaccumulation versus chemically enhanced phytoextraction. *J. Environ. Qual* **30**(6): 1919–1926.

López-Millán, A.-F., D. Ellis and M. Grusak (2004). Identification and characterization of several new members of the ZIP family of metal ion transporters in *Medicago truncatula*. *Plant Molecular Biology* **54**(4): 583-596.

Lopez, M. L., J. L. Gardea-Torresdey, J. R. Peralta-Videa, G. de la Rosa, V. Armendariz, I. Herrera, H. Troiani and J. Henning (2005a). Gold binding by native and chemically modified hops biomasses. *Bioinorganic Chemistry and Applications* **3**(1-2): 29-41.

Lopez, M. L., J. G. Parsons, J. R. P. Videa and J. L. Gardea-Torresdey (2005b). An XAS study of the binding and reduction of Au(III) by hop biomass. *Microchemical Journal* **81**(1): 50-56.

Loque, D., U. Ludewig, L. X. Yuan and N. von Wiren (2005). Tonoplast intrinsic proteins AtTIP2;1 and AtTIP2;3 facilitate NH3 transport into the vacuole. *Plant Physiology* **137**(2): 671-680.

Lutziger, I. and D. J. Oliver (2001). Characterization of two cDNAs encoding mitochondrial lipoamide dehydrogenase from Arabidopsis. *Plant Physiology* **127**(2): 615-623.

Ma, J. F., N. Yamaji, N. Mitani, X.-Y. Xu, Y.-H. Su, S. P. McGrath and F.-J. Zhao (2008). Transporters of arsenite in rice and their role in arsenic accumulation in rice grain. *Proceedings of the National Academy of Sciences of the United States of America* **105**(29): 9931-9935.

Maathuis, F. J. M., V. Filatov, P. Herzyk, G. C. Krijger, K. B. Axelsen, S. Chen, B. J. Green, Y. Li, K. L. Madagan, R. Sánchez-Fernández, B. G. Forde, M. G. Palmgren, P. A. Rea, L. E. Williams, D. Sanders and A. Amtmann (2003). Transcriptome analysis of root transporters reveals participation of multiple gene families in the response to cation stress. *The Plant Journal* **35**(6): 675-692.

MacCormack, T. J. and G. G. Goss (2008). Identifying and predicting biological risks associated with manufactured nanoparticles in aquatic ecosystems. *Journal of Industrial Ecology* **12**(3): 286-296.

Macnair, M. R., V. Bert, S. B. Huitson, P. Saumitou-Laprade and D. Petit (1999). Zinc tolerance and hyperaccumulation are genetically independent characters. *Proceedings of the Royal Society of London Series B-Biological Sciences* **266**(1434): 2175-2179.

Malik, M., R. L. Chaney, E. P. Brewer, Y.-M. Li and J. S. Angle (2000). Phytoextraction of soil cobalt using hyperaccumulator plants. *International Journal of Phytoremediation* **2**(4): 319 - 329.

Marrs, K. A. (1996). The functions and regulation of glutathione s-transferases in plants. *Annual Review of Plant Physiology and Plant Molecular Biology* **47**(1): 127-158.

Marschner, H. (1995). Mineral nutrition of higher plants. San Diego, Wiley Online Library.

Marshall, A. T., R. G. Haverkamp, C. E. Davies, J. G. Parsons, J. L. Gardea-Torresdey and D. van Agterveld (2007). Accumulation of gold nanoparticles in *Brassic juncea*. *International Journal of Phytoremediation* **9**(1-3): 197-206.

Maser, P., S. Thomine, J. I. Schroeder, J. M. Ward, K. Hirschi, H. Sze, I. N. Talke, A. Amtmann, F. J. M. Maathuis, D. Sanders, J. F. Harper, J. Tchieu, M. Gribskov, M. W. Persans, D. E. Salt, S. A. Kim and M. L. Guerinot (2001). Phylogenetic relationships within cation transporter families of Arabidopsis. *Plant Physiology* **126**(4): 1646-1667.

Massey, A. G., N. R. Thompson, B. F. G. Johnson and R. Davis (1973). The Chemistry of Copper, Silver and Gold, Pergamon Press.

Maurel, C., L. Verdoucq, D. T. Luu and V. Santoni (2008). Plant aquaporins: Membrane channels with multiple integrated functions. *Annual Review of Plant Biology* **59**: 595-624.

McCallum, C. M., L. Comai, E. A. Greene and S. Henikoff (2000). Targeted screening for induced mutations. *Nature Biotechnology* **18**(4): 455-457.

McGrath, S. P., E. Lombi, C. W. Gray, N. Caille, S. J. Dunham and F. J. Zhao (2006). Field evaluation of Cd and Zn phytoextraction potential by the hyperaccumulators *Thlaspi caerulescens* and *Arabidopsis halleri*. *Environmental Pollution* **141**(1): 115-125.

McGrath, S. P. and F. J. Zhao (2003). Phytoextraction of metals and metalloids from contaminated soils. *Current Opinion in Biotechnology* **14**(3): 277-282.

Meers, E., A. Ruttens, M. Hopgood, D. Samson and F. Tack (2005). Comparison of EDTA and EDDS as potential soil amendments for enhanced phytoextraction of heavy metals. *Chemosphere* **58**(8): 1011-1022.

Meinke, D. W., J. M. Cherry, C. Dean, S. D. Rounsley and M. Koornneef (1998). *Arabidopsis thaliana*: A model plant for genome analysis. *Science* **282**(5389): 662-682.

Messer, R. L. W., P. E. Lockwood, W. Y. Tseng, K. Edwards, M. Shaw, G. B. Caughman, J. B. Lewis and J. C. Wataha (2005). Mercury (II) alters mitochondrial activity of monocytes at sublethal doses via oxidative stress mechanisms. *Journal of Biomedical Materials Research Part B: Applied Biomaterials* **75B**(2): 257-263.

Miao, Y. C., D. Lv, P. C. Wang, X. C. Wang, J. Chen, C. Miao and C. P. Song (2006). An Arabidopsis glutathione peroxidase functions as both a redox transducer and a scavenger in abscisic acid and drought stress responses. *Plant Cell* **18**(10): 2749-2766.

Millenaar, F., J. Okyere, S. May, M. van Zanten, L. Voesenek and A. Peeters (2006). How to decide? Different methods of calculating gene expression from short oligonucleotide array data will give different results. *BMC Bioinformatics* **7**(1): 137.

Mills, R. F., A. Francini, P. da Rocha, P. J. Baccarini, M. Aylett, G. C. Krijger and L. E. Williams (2005). The plant P-1B-type ATPase AtHMA4 transports Zn and Cd and plays a role in detoxification of transition metals supplied at elevated levels. *Febs Letters* **579**(3): 783-791.

Misra, S. and L. Gedamu (1989). Heavy metal tolerant transgenic *Brassica napus* L. and *Nicotiana tabacum* L. plants. *TAG Theoretical and Applied Genetics* **78**(2): 161-168.

Mocanu, A., I. Cernica, G. Tomoaia, L. D. Bobos, O. Horovitz and M. Tomoaia-Cotisel (2009). Self-assembly characteristics of gold nanoparticles in the presence of cysteine. *Colloids and Surfaces a-Physicochemical and Engineering Aspects* **338**(1-3): 93-101.

Morel, M., J. Crouzet, A. Gravot, P. Auroy, N. Leonhardt, A. Vavasseur and P. Richaud (2009). AtHMA3, a P1B-ATPase aowing Cd/Zn/Co/Pb vacuolar storage in Arabidopsis. *Plant Physiology* **149**(2): 894-904.

Moreno, I., L. Norambuena, D. Maturana, M. Toro, C. Vergara, A. Orellana, A. Zurita-Silva and V. R. Ordenes (2008). AtHMA1 is a thapsigargin-

sensitive Ca^{2+}/heavy metal pump. *Journal of Biological Chemistry* **283**(15): 9633-9641.

Msuya, F. A., R. R. Brooks and C. W. N. Anderson (2000). Chemically-induced uptake of gold by root crops: Its significance for phytomining. *Gold Bulletin* **33**(4): 134-137.

Mukherjee, P., A. Ahmad, D. Mandal, S. Senapati, S. R. Sainkar, M. I. Khan, R. Ramani, R. Parischa, P. V. Ajayakumar, M. Alam, M. Sastry and R. Kumar (2001). Bioreduction of $AuCl_4^-$ ions by the fungus, Verticillium sp. and surface trapping of the gold nanoparticles formed. *Angewandte Chemie International Edition* **40**(19): 3585-3588.

Mukherjee, P., S. Senapati, D. Mandal, A. Ahmad, M. I. Khan, R. Kumar and M. Sastry (2002). Extracellular synthesis of gold nanoparticles by the fungus *Fusarium oxysporum*. *Chembiochem* **3**(5): 461-463.

Murakami, M., N. Ae and S. Ishikawa (2007). Phytoextraction of cadmium by rice (*Oryza sativa* L.), soybean (*Glycine max* (L.) Merr.), and maize (*Zea mays* L.). *Environmental Pollution* **145**(1): 96-103.

Murashige, T. and F. Skoog (1962). A revised medium for rapid growth and bio assays with tobacco tissue cultures. *Physiologia Plantarum* **15**(3): 473-497.

Murray, S. L., R. A. Ingle, L. N. Petersen and K. J. Denby (2007). Basal resistance against *Pseudomonas syringae* in Arabidopsis involves WRKY53 and a protein with homology to a nematode resistance protein. *Molecular Plant-Microbe Interactions* **20**: 1431-1438.

Musante, C. and J. C. White (2010). Toxicity of silver and copper to *Cucurbita pepo*: Differential effects of nano and bulk-size particles. *Environmental Toxicology*: DOI: 10.1002/tox.20667.

Nakajima, A. (2003). Accumulation of gold by microorganisms. *World Journal of Microbiology & Biotechnology* **19**(4): 369-374.

Narayanan, K. B. and N. Sakthivel (2008). Coriander leaf mediated biosynthesis of gold nanoparticles. *Materials Letters* **62**(30): 4588-4590.

Narusaka, Y., M. Narusaka, M. Seki, T. Umezawa, J. Ishida, M. Nakajima, A. Enju and K. Shinozaki (2004). Crosstalk in the responses to abiotic and biotic stresses in Arabidopsis: Analysis of gene expression in cytochrome P450 gene superfamily by cDNA microarray. *Plant Molecular Biology* **55**(3): 327-342.

Nemutandani, T., D. Dutertre, L. Chimuka, E. Cukrowska and H. Tutu (2006). The potential of *Berkheya coddii* for phytoextraction of nickel, platinum, and palladium contaminated sites. *Toxicological & Environmental Chemistry* **88**(2): 175-185.

Niemietz, C. M. and S. D. Tyerman (2002). New potent inhibitors of aquaporins: silver and gold compounds inhibit aquaporins of plant and human origin. *Febs Letters* **531**(3): 443-447.

Nies, D. H. and S. Silver (1995). Ion efflux systems involved in bacterial metal resistance. *Journal of Industrial Microbiology* **14**(2): 186-199.

Ohnishi, J., U. I. Flügge, H. W. Heldt and R. Kanai (1990). Involvement of Na+ in active uptake of pyruvate in mesophyll chloroplasts of some C4 plants: Na+/pyruvate cotransport. *Plant Physiology* **94**(3): 950.

Palmgren, M. G. and K. B. Axelsen (1998). Evolution of P-type ATPases. *Biochimica et Biophysica Acta* **1365**(1-2): 37-45.

Palomino, M., P. G. Kennedy and E. L. Simms (2007). Nickel hyperaccumulation as an anti-herbivore trait: considering the role of tolerance to damage. *Plant and Soil* **293**(1-2): 189-195.

Pan, A., M. Yang, F. Tie, L. Li, Z. Chen and B. Ru (1994). Expression of mouse metallothionein-I gene confers cadmium resistance in transgenic tobacco plants. *Plant Molecular Biology* **24**(2): 341-351.

Papoyan, A. and L. V. Kochian (2004). Identification of *Thlaspi caerulescens* genes that may be involved in heavy metal hyperaccumulation and tolerance. Characterization of a novel heavy metal transporting ATPase. *Plant Physiology* **136**(3): 3814-3823.

Patungwasa, W. and J. H. Hodak (2008). pH tunable morphology of the gold nanoparticles produced by citrate reduction. *Materials Chemistry and Physics* **108**(1): 45-54.

Paulsen, I. T. and M. H. Saier (1997). A novel family of ubiquitous heavy metal ion transport proteins. *Journal of Membrane Biology* **156**(2): 99-103.

Peña, M. M. O., S. Puig and D. J. Thiele (2000). Characterization of the *Saccharomyces cerevisiae* high affinity copper transporter Ctr3. *Journal of Biological Chemistry* **275**(43): 33244.

Penarrubia, L., N. Andres-Colas, J. Moreno and S. Puig (2010). Regulation of copper transport in *Arabidopsis thaliana*: a biochemical oscillator? *Journal of Biological Inorganic Chemistry* **15**(1): 29-36.

Piccinin, R. C. R., S. D. Ebbs, S. M. Reichman, S. D. Kolev, I. E. Woodrow and A. J. M. Baker (2007). A screen of some native Australian flora and exotic agricultural species for their potential application in cyanide-induced phytoextraction of gold. *Minerals Engineering* **20**(14): 1327-1330.

Pilon-Smits, E. (2005). Phytoremediation. *Annual Review of Plant Biology* **56**: 15-39.

Pilon-Smits, E. A. H., C. F. Quinn, W. Tapken, M. Malagoli and M. Schiavon (2009). Physiological functions of beneficial elements. *Current Opinion in Plant Biology* **12**(3): 267-274.

Pitcairn, I. K., P. E. Warwick, J. A. Milton and D. A. H. Teagle (2006). Method for ultra-low-level analysis of gold in rocks. *Analytical Chemistry* **78**(4): 1290-1295.

Preston, G. M., J. S. Jung, W. B. Guggino and P. Agre (1993). The mercury-sensitive residue at cysteine-189 in the chip28 water channel. *Journal of Biological Chemistry* **268**(1): 17-20.

Puig, S., N. Andres-Colas, A. Garcia-Molina and L. Penarrubia (2007). Copper and iron homeostasis in Arabidopsis: responses to metal deficiencies, interactions and biotechnological applications. *Plant Cell and Environment* **30**(3): 271-290.

Puig, S., J. Lee, M. Lau and D. J. Thiele (2002). Biochemical and genetic analyses of yeast and human high affinity copper transporters suggest a conserved mechanism for copper uptake. *Journal of Biological Chemistry* **277**(29): 26021.

Quigley, F., J. M. Rosenberg, Y. Shachar-Hill and H. J. Bohnert (2002). From genome to function: the Arabidopsis aquaporins. *Genome Biology* **3**(1).

Raffaele, S., F. Vailleau, A. Leger, J. Joubes, O. Miersch, C. Huard, E. Blee, B. Mongrand, F. Domergue and D. Roby (2008). A MYB transcription factor regulates very-long-chain fatty acid biosynthesis for activation of the hypersensitive cell death response in Arabidopsis. *Plant Cell* **20**(3): 752-767.

Ramesh, S. A., R. Shin, D. J. Eide and D. P. Schachtman (2003). Differential metal selectivity and gene expression of two zinc transporters from rice. *Plant Physiology* **133**(1): 126-134.

Redman, J. C., B. J. Haas, G. Tanimoto and C. D. Town (2004). Development and evaluation of an Arabidopsis whole genome Affymetrix probe array. *The Plant Journal* **38**(3): 545-561.

Reith, F., B. Etschmann, C. Grosse, H. Moors, M. A. Benotmane, P. Monsieurs, G. Grass, C. Doonan, S. Vogt, B. Lai, G. Martinez-Criado, G. N. George, D. H. Nies, M. Mergeay, A. Pring, G. Southam and J. Brugger (2009). Mechanisms of gold biomineralization in the bacterium *Cupriavidus*

metallidurans. *Proceedings of the National Academy of Sciences of the United States of America* **106**(42): 17757-17762.

Rhee, S. Y., W. Beavis, T. Z. Berardini, G. H. Chen, D. Dixon, A. Doyle, M. Garcia-Hernandez, E. Huala, G. Lander, M. Montoya, N. Miller, L. A. Mueller, S. Mundodi, L. Reiser, J. Tacklind, D. C. Weems, Y. H. Wu, I. Xu, D. Yoo, J. Yoon and P. F. Zhang (2003). The Arabidopsis Information Resource (TAIR): a model organism database providing a centralized, curated gateway to Arabidopsis biology, research materials and community. *Nucleic Acids Research* **31**(1): 224-228.

Ricachenevsky, F. K., R. A. Sperotto, P. K. Menguer and J. P. Fett (2010). Identification of Fe-excess-induced genes in rice shoots reveals a WRKY transcription factor responsive to Fe, drought and senescence. *Molecular Biology Reports* **37**(8): 3735-3745.

Richards, K. D., E. J. Schott, Y. K. Sharma, K. R. Davis and R. C. Gardner (1998). Aluminum induces oxidative stress genes in *Arabidopsis thaliana*. *Plant Physiology* **116**(1): 409-418.

Rico, C. M., S. Majumdar, M. Duarte-Gardea, J. R. Peralta-Videa and J. L. Gardea-Torresdey (2011). Interaction of nanoparticles with edible plants and their possible implications in the food chain. *Journal of Agricultural and Food Chemistry* **59**(8): 3485-3498.

Robinson, B., R. Brooks and B. Clothier (1999). Soil amendments affecting nickel and cobalt uptake by *Berkheya coddii*: Potential use for phytomining and phytoremediation. *Annals of Botany* **84**(6): 689.

Robinson, B. H., R. R. Brooks, A. W. Howes, J. H. Kirkman and P. E. H. Gregg (1997a). The potential of the high-biomass nickel hyperaccumulator *Berkheya coddii* for phytoremediation and phytomining. *Journal of Geochemical Exploration* **60**(2): 115-126.

Robinson, B. H., A. Chiarucci, R. R. Brooks, D. Petit, J. H. Kirkman, P. E. H. Gregg and V. DeDominicis (1997b). The nickel hyperaccumulator plant *Alyssum bertolonii* as a potential agent for phytoremediation and phytomining of nickel. *Journal of Geochemical Exploration* **59**(2): 75-86.

Rodriguez, E., J. G. Parsons, J. R. Peralta-Videa, G. Cruz-Jimenez, J. Romero-Gonzalez, B. E. Sanchez-Salcido, G. B. Saupe, M. Duarte-Gardea and J. L. Gardea-Torresdey (2007). Potential of *Chilopsis linearis* for gold phytomining: Using XAS to determine gold reduction and nanoparticle formation within plant tissues. *International Journal of Phytoremediation* **9**(1-3): 133-147.

Rodriguez, E., J. R. Peralta-Videa, M. Israr, S. V. Sahi, H. Pelayo, B. Sanchez-Salcido and J. L. Gardea-Torresdey (2009). Effect of mercury and gold on growth, nutrient uptake, and anatomical changes in *Chilopsis linearis*. *Environmental and Experimental Botany* **65**(2-3): 253-262.

Rogers, E. E., D. J. Eide and M. L. Guerinot (2000). Altered selectivity in an Arabidopsis metal transporter. *Proceedings of the National Academy of Sciences of the United States of America* **97**(22): 12356-12360.

Roman, G., B. Lubarsky, J. J. Kieber, M. Rothenberg and J. R. Ecker (1995). Genetic analysis of ethylene signal transduction in *Arabidopsis thaliana*: five novel mutant loci integrated into a stress response pathway. *Genetics* **139**(3): 1393-1409.

Romero-Gonzalez, M. E., C. J. Williams, P. H. E. Gardiner, S. J. Gurman and S. Habesh (2003). Spectroscopic studies of the biosorption of gold(III) by dealginated seaweed waste. *Environmental Science & Technology* **37**(18): 4163-4169.

Rosi, N. L., D. A. Giljohann, C. S. Thaxton, A. K. R. Lytton-Jean, M. S. Han and C. A. Mirkin (2006). Oligonucleotide-modified gold nanoparticles for intracellular gene regulation. *Science* **312**(5776): 1027-1030.

Rozen, S. and H. Skaletsky (2000). Primer3 on the WWW for general users and for biologist programmers. *Methods Mol Biol* **132**: 365-386.

Rugh, C. L., H. D. Wilde, N. M. Stack, D. M. Thompson, A. O. Summers and R. B. Meagher (1996). Mercuric ion reduction and resistance in transgenic *Arabidopsis thaliana* plants expressing a modified bacterial merA gene. *Proceedings of the National Academy of Sciences of the United States of America* **93**(8): 3182-3187.

Sancenon, V., S. Puig, I. Mateu-Andres, E. Dorcey, D. J. Thiele and L. Penarrubia (2004). The Arabidopsis copper transporter COPT1 functions in root elongation and pollen development. *Journal of Biological Chemistry* **279**(15): 15348-15355.

Sancenon, V., S. Puig, H. Mira, D. J. Thiele and L. Penarrubia (2003). Identification of a copper transporter family in *Arabidopsis thaliana*. *Plant Molecular Biology* **51**(4): 577-587.

Sarry, J. E., L. Kuhn, C. Ducruix, A. Lafaye, C. Junot, V. Hugouvieux, A. Jourdain, O. Bastien, J. B. Fievet, D. Vailhen, B. Amekraz, C. Moulin, E. Ezan, J. Garin and J. Bourguignon (2006). The early responses of *Arabidopsis thaliana* cells to cadmium exposure explored by protein and metabolite profiling analyses. *Proteomics* **6**(7): 2180-2198.

Schaaf, G., A. Honsbein, A. R. Meda, S. Kirchner, D. Wipf and N. von Wiren (2006). AtIREG2 encodes a tonoplast transport protein involved in iron-dependent nickel detoxification in *Arabidopsis thaliana* roots. *Journal of Biological Chemistry* **281**(35): 25532-25540.

Schaaf, G., U. Ludewig, B. E. Erenoglu, S. Mori, T. Kitahara and N. von Wiren (2004). ZmYS1 functions as a proton-coupled symporter for phytosiderophore- and nicotianamine-chelated metals. *Journal of Biological Chemistry* **279**(10): 9091-9096.

Schenk, P. M., K. Kazan, I. Wilson, J. P. Anderson, T. Richmond, S. C. Somerville and J. M. Manners (2000). Coordinated plant defense responses in Arabidopsis revealed by microarray analysis. *Proceedings of the National Academy of Sciences of the United States of America* **97**(21): 11655-11660.

Schuler, M. A. and D. Werck-Reichhart (2003). Functional genomics of P450s. *Annual Review of Plant Biology* **54**: 629-667.

Schutzendubel, A. and A. Polle (2002). Plant responses to abiotic stresses: heavy metal-induced oxidative stress and protection by mycorrhization. *Journal of Experimental Botany* **53**(372): 1351-1365.

Schwartz, C., G. Echevarria and J. L. Morel (2003). Phytoextraction of cadmium with *Thlaspi caerulescens*. *Plant and Soil* **249**(1): 27-35.

Seigneurin-Berny, D., A. Gravot, P. Auroy, C. Mazard, A. Kraut, G. Finazzi, D. Grunwald, F. Rappaport, A. Vavasseur, J. Joyard, P. Richaud and N. Rolland (2006). HMA1, a new Cu-ATPase of the chloroplast envelope, is essential for growth under adverse light conditions. *Journal of Biological Chemistry* **281**(5): 2882-2892.

Seki, M., M. Narusaka, J. Ishida, T. Nanjo, M. Fujita, Y. Oono, A. Kamiya, M. Nakajima, A. Enju, T. Sakurai, M. Satou, K. Akiyama, T. Taji, K. Yamaguchi-Shinozaki, P. Carninci, J. Kawai, Y. Hayashizaki and K. Shinozaki (2002). Monitoring the expression profiles of 7000 Arabidopsis genes under drought, cold and high-salinity stresses using a full-length cDNA microarray. *Plant Journal* **31**(3): 279-292.

Seo, P. J. and C. M. Park (2010). MYB96-mediated abscisic acid signals induce pathogen resistance response by promoting salicylic acid biosynthesis in Arabidopsis. *New Phytologist* **186**(2): 471-483.

Shacklette, H. T., H. W. Lakin, A. E. Hubert and G. C. Curtin (1970). Absorption of gold by plants. *Contributions to Geochemistry, US Geological Survey Bulletin* #**1314-B**.

Shah, V. and I. Belozerova (2009). Influence of metal nanoparticles on the soil microbial community and germination of lettuce seeds. *Water, Air, & Soil Pollution* **197**(1): 143-148.

Shankar, S. S., A. Ahmad, R. Pasricha and M. Sastry (2003). Bioreduction of chloroaurate ions by geranium leaves and its endophytic fungus yields gold nanoparticles of different shapes. *Journal of Materials Chemistry* **13**(7): 1822-1826.

Shankar, S. S., A. Rai, A. Ahmad and M. Sastry (2004a). Rapid synthesis of Au, Ag, and bimetallic Au core-Ag shell nanoparticles using Neem (*Azadirachta indica*) leaf broth. *Journal of Colloid and Interface Science* **275**(2): 496-502.

Shankar, S. S., A. Rai, A. Ahmad and M. Sastry (2005). Controlling the optical properties of lemongrass extract synthesized gold nanotriangles and potential application in infrared-absorbing optical coatings. *Chemistry of Materials* **17**(3): 566-572.

Shankar, S. S., A. Rai, B. Ankamwar, A. Singh, A. Ahmad and M. Sastry (2004b). Biological synthesis of triangular gold nanoprisms. *Nat Mater* **3**(7): 482-488.

Sharma, N. C., S. V. Sahi, S. Nath, J. G. Parsons, J. L. Gardea-Torresdey and T. Pal (2007). Synthesis of plant-mediated gold nanoparticles and catalytic role of biomatrix-embedded nanomaterials. *Environmental Science & Technology* **41**(14): 5137-5142.

Sheoran, V., A. S. Sheoran and P. Poonia (2009). Phytomining: A review. *Minerals Engineering* **22**(12): 1007-1019.

Shigaki, T. and K. Hirschi (2000). Characterization of CAX-like genes in plants: implications for functional diversity. *Gene* **257**(2): 291-298.

Shigaki, T., C. Sreevidya and K. D. Hirschi (2002). Analysis of the Ca^{2+} domain in the Arabidopsis H^{+}/Ca^{2+} antiporters CAX1 and CAX3. *Plant Molecular Biology* **50**(3): 475-483.

Shikanai, T., P. Muller-Moule, Y. Munekage, K. K. Niyogi and M. Pilon (2003). PAA1, a P-type ATPase of Arabidopsis, functions in copper transport in chloroplasts. *Plant Cell* **15**(6): 1333-1346.

Shirley, B. W., S. Hanley and H. M. Goodman (1992). Effects of ionizing radiation on a plant genome: Analysis of two Arabidopsis transparent testa mutations. *The Plant Cell Online* **4**(3): 333-347.

Smart, L. B., W. A. Moskal, K. D. Cameron and A. B. Bennett (2001). *MIP* Genes are down-regulated under drought stress in *Nicotiana glauca*. *Plant and Cell Physiology* **42**(7): 686-693.

Solioz, M. and C. Vulpe (1996). CPx-type ATPases: A class of p-type ATPases that pump heavy metals. *Trends in Biochemical Sciences* **21**(7): 237-241.

Somerville, C. and M. Koornneef (2002). A fortunate choice: the history of Arabidopsis as a model plant. *Nature Reviews Genetics* **3**(11): 883-889.

Song, W. Y., E. J. Sohn, E. Martinoia, Y. J. Lee, Y. Y. Yang, M. Jasinski, C. Forestier, I. Hwang and Y. Lee (2003). Engineering tolerance and accumulation of lead and cadmium in transgenic plants. *Nature Biotechnology* **21**(8): 914-919.

Stampoulis, D., S. K. Sinha and J. C. White (2009). Assay-dependent phytotoxicity of nanoparticles to plants. *Environmental Science & Technology* **43**(24): 9473-9479.

Starnes, D. L., A. Jain and S. V. Sahi (2010). In planta engineering of gold nanoparticles of desirable geometries by modulating growth conditions:

an environment-friendly approach. *Environmental Science & Technology* **44**(18): 7110-7115.

Stirnberg, P., K. van de Sande and H. M. O. Leyser (2002). MAX1 and MAX2 control shoot lateral branching in Arabidopsis. *Development* **129**(5): 1131-1141.

Stoyanov, J. V. and N. L. Brown (2003). The *Escherichia coli* copper-responsive copA promoter is activated by gold. *Journal of Biological Chemistry* **278**(3): 1407-1410.

Suelter, C. H. (1970). Enzymes Activated by Monovalent Cations. *Science* **168**(3933): 789-795.

Sung, D.-Y., D. Lee, H. Harris, A. Raab, J. Feldmann, A. Meharg, B. Kumabe, E. A. Komives and J. I. Schroeder (2007). Identification of an arsenic tolerant double mutant with a thiol-mediated component and increased arsenic tolerance in phyA mutants. *The Plant Journal* **49**(6): 1064-1075.

Sung, D. Y., E. Vierling and C. L. Guy (2001). Comprehensive expression profile analysis of the Arabidopsis hsp70 gene family. *Plant Physiology* **126**(2): 789-800.

Supek, F., L. Supekova, H. Nelson and N. Nelson (1997). Function of metal-ion homeostasis in the cell division cycle, mitochondrial protein processing, sensitivity to mycobacterial infection and brain function. *Journal of Experimental Biology* **200**(2): 321-330.

Takahashi, M., Y. Terada, I. Nakai, H. Nakanishi, E. Yoshimura, S. Mori and N. K. Nishizawa (2003). Role of nicotianamine in the intracellular delivery of metals and plant reproductive development. *Plant Cell* **15**(6): 1263-1280.

Takano, J., M. Wada, U. Ludewig, G. Schaaf, N. von Wiren and T. Fujiwara (2006). The Arabidopsis major intrinsic protein NIP5;1 is essential for efficient boron uptake and plant development under boron limitation. *Plant Cell* **18**(6): 1498-1509.

Tamura, K., J. Dudley, M. Nei and S. Kumar (2007). MEGA4: Molecular Evolutionary Genetics Analysis (MEGA) software version 4.0. *Molecular Biology and Evolution* **24**(8): 1596-1599.

Tan, Y. F., N. O'Toole, N. L. Taylor and A. H. Millar (2010). Divalent metal ions in plant mitochondria and their role in interactions with proteins and oxidative stress-induced damage to respiratory function. *Plant Physiology* **152**(2): 747-761.

Thilmony, R., W. Underwood and S. Y. He (2006). Genome-wide transcriptional analysis of the *Arabidopsis thaliana* interaction with the plant pathogen *Pseudomonas syringae pv. tomato* DC3000 and the human pathogen *Escherichia coli* O157 : H7. *Plant Journal* **46**(1): 34-53.

Thimm, O., O. Blasing, Y. Gibon, A. Nagel, S. Meyer, P. Kruger, J. Selbig, L. A. Muller, S. Y. Rhee and M. Stitt (2004). MAPMAN: a user-driven tool to display genomics data sets onto diagrams of metabolic pathways and other biological processes. *Plant Journal* **37**(6): 914-939.

Thimm, O., B. Essigmann, S. Kloska, T. Altmann and T. J. Buckhout (2001). Response of Arabidopsis to iron deficiency stress as revealed by microarray analysis. *Plant Physiology* **127**(3): 1030-1043.

Thomine, S., F. Lelievre, E. Debarbieux, J. I. Schroeder and H. Barbier-Brygoo (2003). AtNRAMP3, a multispecific vacuolar metal transporter involved in plant responses to iron deficiency. *Plant Journal* **34**(5): 685-695.

Thomine, S., R. C. Wang, J. M. Ward, N. M. Crawford and J. I. Schroeder (2000). Cadmium and iron transport by members of a plant metal transporter family in Arabidopsis with homology to Nramp genes. *Proceedings of the National Academy of Sciences of the United States of America* **97**(9): 4991-4996.

Tokuhisa, J. G., K. A. Feldmann, S. T. LaBrie and J. Browse (1997). Mutational analysis of chilling tolerance in plants. *Plant, Cell & Environment* **20**(11): 1391-1400.

Turkevich, J., P. C. Stevenson and J. Hillier (1951). A study of the nucleation and growth processes in the synthesis of colloidal gold. *Discussions of the Faraday Society*(11): 55-75.

Turner, M., V. B. Golovko, O. P. H. Vaughan, P. Abdulkin, A. Berenguer-Murcia, M. S. Tikhov, B. F. G. Johnson and R. M. Lambert (2008). Selective oxidation with dioxygen by gold nanoparticle catalysts derived from 55-atom clusters. *Nature* **454**(7207): 981-983.

Van Assche, F. and H. Clijsters (1990). Effects of metals on enzyme activity in plants. *Plant, Cell & Environment* **13**(3): 195-206.

Van de Mortel, J. E., L. Almar Villanueva, H. Schat, J. Kwekkeboom, S. Coughlan, P. D. Moerland, E. Ver Loren van Themaat, M. Koornneef and M. G. M. Aarts (2006). Large expression differences in genes for iron and zinc homeostasis, stress response, and lignin biosynthesis distinguish roots of *Arabidopsis thaliana* and the related metal hyperaccumulator *Thlaspi caerulescens*. *Plant Physiology* **142**(3): 1127.

van der Zaal, B. J., L. W. Neuteboom, J. E. Pinas, A. N. Chardonnens, H. Schat, J. A. C. Verkleij and P. J. J. Hooykaas (1999). Overexpression of a novel Arabidopsis gene related to putative zinc-transporter genes from animals can lead to enhanced zinc resistance and accumulation. *Plant Physiology* **119**(3): 1047-1055.

Vassil, A. D., Y. Kapulnik, I. Raskin and D. E. Salt (1998). The role of EDTA in lead transport and accumulation by Indian mustard. *Plant Physiology* **117**(2): 447-453.

Verret, F., A. Gravot, P. Auroy, N. Leonhardt, P. David, L. Nussaume, A. Vavasseur and P. Richaud (2004). Overexpression of AtHMA4 enhances root-to-shoot translocation of zinc and cadmium and plant metal tolerance. *FEBS Letters* **576**(3): 306-312.

Vert, G., J. F. Briat and C. Curie (2001). Arabidopsis IRT2 gene encodes a root-periphery iron transporter. *Plant Journal* **26**(2): 181-189.

Vert, G., N. Grotz, F. Dedaldechamp, F. Gaymard, M. L. Guerinot, J. F. Briata and C. Curie (2002). IRT1, an Arabidopsis transporter essential for iron uptake from the soil and for plant growth. *Plant Cell* **14**(6): 1223-1233.

Walker, E. L. and E. L. Connolly (2008). Time to pump iron: iron-deficiency-signaling mechanisms of higher plants. *Current Opinion in Plant Biology* **11**(5): 530-535.

Wan, J. R., X. C. Zhang, D. Neece, K. M. Ramonell, S. Clough, S. Y. Kim, M. G. Stacey and G. Stacey (2008). A LysM receptor-like kinase plays a critical role in chitin signaling and fungal resistance in Arabidopsis. *Plant Cell* **20**(2): 471-481.

Wang, Y., K. Zong, L. Jiang, J. Sun, Y. Ren, Z. Sun, C. Wen, X. Chen and S. Cao (2011). Characterization of an Arabidopsis cadmium-resistant mutant *cdr3-1D* reveals a link between heavy metal resistance as well as seed development and flowering. *Planta* **233**(4): 697-706.

Waters, B. M., H. H. Chu, R. J. DiDonato, L. A. Roberts, R. B. Eisley, B. Lahner, D. E. Salt and E. L. Walker (2006). Mutations in Arabidopsis Yellow Stripe-Like1 and Yellow Stripe-Like3 reveal their roles in metal ion homeostasis and loading of metal ions in seeds. *Plant Physiology* **141**(4): 1446-1458.

Waugh, R., D. J. Leader, N. McCallum and D. Caldwell (2006). Harvesting the potential of induced biological diversity. *Trends in Plant Science* **11**(2): 71-79.

Weber, M., E. Harada, C. Vess, E. von Roepenack-Lahaye and S. Clemens (2004). Comparative microarray analysis of *Arabidopsis thaliana* and *Arabidopsis halleri* roots identifies nicotianamine synthase, a ZIP transporter and other genes as potential metal hyperaccumulation factors. *Plant Journal* **37**(2): 269-281.

Weigel, D., J. H. Ahn, M. A. Blázquez, J. O. Borevitz, S. K. Christensen, C. Fankhauser, C. Ferrándiz, I. Kardailsky, E. J. Malancharuvil and M. M. Neff (2000). Activation tagging in Arabidopsis. *Plant Physiology* **122**(4): 1003.

Williams, L. E. and R. F. Mills (2005). P-1B-ATPases - an ancient family of transition metal pumps with diverse functions in plants. *Trends in Plant Science* **10**(10): 491-502.

Williams, L. E., J. K. Pittman and J. L. Hall (2000). Emerging mechanisms for heavy metal transport in plants. *Biochimica et Biophysica Acta-Biomembranes* **1465**(1-2): 104-126.

Wintz, H., T. Fox, Y. Y. Wu, V. Feng, W. Q. Chen, H. S. Chang, T. Zhu and C. Vulpe (2003). Expression profiles of *Arabidopsis thaliana* in mineral deficiencies reveal novel transporters involved in metal homeostasis. *Journal of Biological Chemistry* **278**(48): 47644-47653.

Wong, C. K. E. and C. S. Cobbett (2009). HMA P-type ATPases are the major mechanism for root-to-shoot Cd translocation in *Arabidopsis thaliana*. *New Phytologist* **181**(1): 71-78.

Yamasaki, H., M. Hayashi, M. Fukazawa, Y. Kobayashi and T. Shikanai (2009). SQUAMOSA Promoter binding protein-like7 is a central regulator for copper homeostasis in *Arabidopsis*. *Plant Cell* **21**(1): 347-361.

Yang, T. J. W., W. D. Lin and W. Schmidt (2010). Transcriptional profiling of the Arabidopsis iron deficiency response reveals conserved transition metal homeostasis networks. *Plant Physiology* **152**(4): 2130-2141.

Yuan, M., Z. Chu, X. Li, C. Xu and S. Wang (2010). The bacterial pathogen *Xanthomonas oryzae* overcomes rice defenses by regulating host copper redistribution. *The Plant Cell Online* **22**(9): 3164-3176.

Yuan, Y. X., H. L. Wu, N. Wang, J. Li, W. N. Zhao, J. Du, D. W. Wang and H. Q. Ling (2008). FIT interacts with AtbHLH38 and AtbHLH39 in regulating iron uptake gene expression for iron homeostasis in Arabidopsis. *Cell Research* **18**(3): 385-397.

Yuan, Y. X., J. Zhang, D. W. Wang and H. Q. Ling (2005). AtbHLH29 of *Arabidopsis thaliana* is a functional ortholog of tomato FER involved in controlling iron acquisition in strategy I plants. *Cell Research* **15**(8): 613-621.

Zhang, W.-H. and S. D. Tyerman (1999). Inhibition of water channels by HgCl2 in intact wheat root cells. *Plant Physiology* **120**(3): 849-858.

Zhang, Y. J. and L. J. Wang (2005). The WRKY transcription factor superfamily: its origin in eukaryotes and expansion in plants. *Bmc Evolutionary Biology* **5**.

Zhao, C.-M. and W.-X. Wang (2010). Biokinetic uptake and efflux of silver nanoparticles in *Daphnia magna*. *Environmental Science & Technology* **44**(19): 7699-7704.

Zhu, J.-K., J. Liu and L. Xiong (1998). Genetic analysis of salt tolerance in Arabidopsis: Evidence for a critical role of potassium nutrition. *The Plant Cell Online* **10**(7): 1181-1192.

Zhu, X. S., J. X. Wang, X. Z. Zhang, Y. Chang and Y. S. Chen (2010). Trophic transfer of TiO2 nanoparticles from daphnia to zebrafish in a simplified freshwater food chain. *Chemosphere* **79**(9): 928-933.